UNIVERSITY OF BIRMINGHAM

PROPERTIES OF ELASTOMERS FOR SMALL-JOINT REPLACEMENTS

by

AZIZA MAHOMED

A thesis submitted to the University of Birmingham for the degree of

DOCTOR OF PHILOSOPHY

School of Metallurgy and Materials

School of Mechanical Engineering

The University of Birmingham

November 2008

ABSTRACT

Silicones are used to manufacture finger and wrist joints. However these joints have fractured prematurely *in vivo*. There is a lack of literature on the mechanical properties of silicones. The aim of this thesis was to investigate the viscoelastic and related properties of elastomers such as silicones and polyurethanes (suggested as a possible substitute for silicones in the implants) and to relate the properties to how an implant may perform *in vivo*. The viscoelastic properties of medical grade silicones and Elast-Eon^{TM} 3 were found to depend on frequency in compression. Above a certain frequency, the silicones appeared to undergo a transition from the rubbery to the glassy state. There is a danger that this could lead to the creation of fracture surfaces. The viscoelastic properties of the silicones were not significantly affected by the temperature; pre-treatment of specimens had no appreciable effect on the results. When the viscoelastic properties were measured in tension, there was a significant difference between the properties measured in tension and compression. Accelerated aging significantly increased the moduli of Elast-Eon^{TM} 3, which is of some concern. The cross-link densities of the silicones were measured using a solvent swelling technique and the Flory-Rehner equation. The results showed that this method is useful as an approximate model.

To Mum, Dad, Mama,

Papa and Anisa

ACKNOWLEDGEMENTS

The work presented in this thesis would not have been possible without the help and guidance of many people. I would like to take this opportunity to acknowledge and thank them.

Firstly, I would like to thank Professor David Hukins and Dr Stephen Kukureka for their excellent supervision throughout my PhD, without which, I would not have achieved what I have. I am extremely grateful for all their time, advice, general support, encouragement, enthusiasm, constructive criticism and funds to attend conferences.

On a more practical side, I would like to thank: Mr Derek Boole, Mr John Lane, and Mr Peter Hinton for help and advice in making the specialist equipment; Mr Carl Hingley and Mr Lee Gantlett for their help in the workshop; Mr Frank Biddlestone for the help with operating the DMTA and TGA equipment.

I would like to thank: the EPSRC for my research studentship; the Arthritis Research Campaign for funds for the testing equipment; IMECHE, IOP, IOM^3, RAE and UKRC for the funding for me to attend conferences in USA and Singapore; Dow Corning Limited for providing free samples of the medical grade silicones; technical staff from Polymer Systems Technology Limited and Wright Medical Technology for information on the mechanical properties and composition of the silicones via e-mails; the Biomedical Research Group in G60 (School of Mechanical Engineering) for a fantastic working and social environment

Finally, I would like to thank my grandparents, parents and sister for their support, sacrifice, encouragement and belief that I could complete this project. They have encouraged and supported me in so many ways throughout my studies and in life in general. What I have achieved until now, I could not have done without them. I hope that I have made them proud and will continue to do so.

TABLE OF CONTENTS

LIST OF FIGURES

LIST OF TABLES

Chapter 1. INTRODUCTION

Healthy natural finger and wrist joints can be destroyed by *rheumatoid arthritis* (Beevers and Seedhom, 1993). This is a painful condition and patients will experience difficulties in carrying out everyday activities (Alderman *et al.*, 2003; Mandl *et al.*, 2002; Yelin *et al.*, 1980). If the disease is at an advanced stage, the only option available to treat the condition is to replace the destroyed joint with an artificial joint (Swanson, 1968). Artificial joints may not restore the full range of motion in the hand of the patients, but will aim to provide the patient with the necessary hand movements to allow them to perform everyday tasks. The most popular artificial joint used to replace arthritic hand joints is a one-piece flexible joint, manufactured from silicone, a synthetic elastomer (Swanson, 1968). Although these joints have been successful, they fracture prematurely *in vivo* (Trail *et al.*, 2004), with fracture rates of up to 82 %, after 5 years, reported (Kay *et al.*, 1978).

To tackle this issue, many different implant designs have been suggested and used (Delaney *et al.*, 2005; Joyce, 2004; Swanson *et al.*, 1997). However, this has not eliminated the fracture problem (Joyce, 2004; Pettersson *et al.*, 2006). More recently, a study (Leslie *et al.*, 2008a) suggested that perhaps the failure of the implant is a materials problem rather than a design problem and went on to investigate the crack growth properties of medical grade silicones. Elast-Eon^{TM}, a material based on polyurethane, has been proposed as an alternative to silicone (Shepherd and Johnstone, 2005). Some authors (Penrose *et al.*, 1997) have suggested that perhaps too little is known about the dynamic behaviour of the implant.

Understanding the dynamic behaviour would be useful when developing or improving the properties of an implant material. This point has previously been made for silicones used in maxillofacial applications (Murata *et al.*, 2003).

The dynamic behaviour of these elastomers will depend on their viscoelastic properties (Ferry, 1961b); therefore, the aim of this thesis is to measure the viscoelastic and related properties of medical grade silicones, to suggest how they might perform in an implant. This has been done by:

- investigating the effect of changing the loading frequency on the storage, *E'*, and loss moduli, *E''*, of medical grade silicones in compression and in tension;
- investigating whether pre-treating the silicones before testing in different environments affects the moduli;
- comparing the effect of accelerated aging on the viscoelastic properties of Elast-Eon™ and on Nagor® medical grade silicone;
- measuring the cross-link density of medical grade silicones by swelling sample pieces in solvents.

Chapter 2 provides the background information required to understand this thesis. It begins by describing rheumatoid arthritis, the main driving force behind the need for silicone finger and wrist implants. It then discusses the various designs of silicone implants that are available on the market and how well they perform *in vivo*. Then the chemistry of silicones and Elast-Eon™ are described, followed by sections on the viscoelastic properties of silicones and polyurethanes. Finally, there is a section discussing the aging process of elastomers.

Previous studies on the properties of elastomers are discussed in the relevant experimental chapters.

Chapter 3 is the Materials and Methods chapter for the whole thesis. It begins by describing the materials used for the experiments in Chapters 4-7. It describes how the silicones and Elast-Eon^{TM} were obtained, processed and how the specimens were prepared for testing or swelling. The specimens used were pre-treated in various environments before testing, and this is discussed next. Following this, is a section describing the specialist equipment that had to be designed and manufactured in order to carry out the experiments in Chapter 4-6. Then the experimental method and setup used for the experiments in Chapter 4-6 are described. The statistics used to analyse the results of my experiments in Chapter 4-7 are discussed next. Finally, there is a section describing the swelling procedure for the swelling experiments in Chapter 7.

Chapter 4 is about determining the storage, *E'*, and loss, *E''*, moduli of short and medium-term implant medical grade silicones in compression, over a wide range of frequencies. Previous studies on the frequency dependence of silicones used in dental liners and for maxillofacial applications are discussed at the beginning of the chapter. Following this, the results from my experiments are reported. These results are discussed and compared to the results from previous studies in the discussion. Some of the experiments on silicones intended for short-term implantation (see § 4.3) were performed, as an undergraduate project, under my supervision, by Ms Nkechi Chidi; this work has already been published (Mahomed *et al.*, 2009).

Chapter 5 is about determining *E'* and *E''* of short-term implant medical grade silicones in tension, over a range of frequencies. Previous studies on the viscoelastic properties of natural rubber and silicones used in dental liners and for maxillofacial applications, measured in tension and compression, are discussed at the beginning of the chapter. Following this, the results from my experiments are reported. Then these results are compared to my previous results measured in compression. The results obtained from my experiments are discussed and compared to the results from previous studies in the discussion.

Chapter 6 is about determining *E'* and *E''* for Elast-Eon ™ 3 and Nagor® medical grade silicone before and after accelerated aging, over a wide range of frequencies. At the beginning of the chapter, previous studies on the effect of aging on the properties of elastomers are discussed. Following this, the results from my experiments are reported. Then these results are discussed and compared to the results from previous studies in the discussion.

Chapter 7 is about determining the cross-link density of short-term implant medical grade silicones using a swelling procedure. Previous studies that have used this method to measure the cross-link density of silicones, used for different applications, are discussed at the beginning of the chapter. Following this, the results from my experiments are reported. These results are discussed and compared to the results from previous studies in the discussion.

Chapter 8 is the final chapter of this thesis. It summarises the results obtained from my experiments in Chapter 4-7 and provides an overall conclusion of the results and how they might be applicable to the performance of silicone or Elast-Eon^{TM} in an implant. Where possible the results obtained from the different chapters are linked to each other. Supplementary information, on a range of topics, appears in the Appendices.

Chapter 2. BACKGROUND

2.1 Chapter overview

This chapter provides the reader the background information needed to understand this thesis. §2.2 discusses rheumatoid arthritis, the disease most commonly associated with the replacement of natural finger joints by artificial implants. §2.3 describes the different types of artificial silicone finger implants and §2.4 discusses the premature fracture of these implants. §2.5 is a review of the chemistry and structure of silicones, the biomaterials currently used to manufacture artificial finger implants; §2.6 is a review of the chemistry and structure of Elast-Eon™, a polyurethane elastomer that has been suggested as a possible substitute for silicones in small-joint replacements. The viscoelastic properties of silicones and polyurethanes is given in §2.7. §2.8 discusses the aging process of elastomers and §2.9 is a chapter summary.

2.2 Rheumatoid arthritis

Rheumatoid arthritis in the hand is one of the main reasons for finger joint replacements (Joyce, 2004). Rheumatoid arthritis is a chronic systemic rheumatic inflammatory disease that can strongly influence the normal biomechanics of finger joints (Alderman *et al.*, 2002; Mandl *et al.*, 2002; McMaster, 1972). In the United Kingdom alone, there are approximately 600 000 individuals affected by rheumatoid arthritis (Trail *et al.*, 2004). It is more common in females than in men (Parkkila *et al.*, 2005; Schmidt *et al.*, 1999b; Trail *et al.*, 2004). There is no known cure for rheumatoid arthritis and it is considered as a remittent, progressive disease that can affect the whole-body (Stanley, 1992).

It can affect and influence various aspects of the sufferers' lives, such as their professional career, family and social life, and psychological status (Katz, 1995). A great reduction in the ability to perform everyday tasks and in the satisfaction of life in general has been reported (Alderman *et al.*, 2003; Goldfarb and Stern, 2003; Katz, 1995; Pincus *et al.*, 1984; Yelin *et al.*, 1980).

The metarcarpophalangel joint (MCP) shown in Figure 2.1 is a key biaxial finger joint, in terms of hand function, allowing the joint to abduct, adduct, flex and extend (Beevers and Seedhom, 1993; Beevers and Seedhom, 1995; Joyce, 2004; Penrose *et al.*, 1997). It is one of the hand joints frequently affected by rheumatoid arthritis (Mandl *et al.*, 2002; Wilson and Carlblom, 1989).

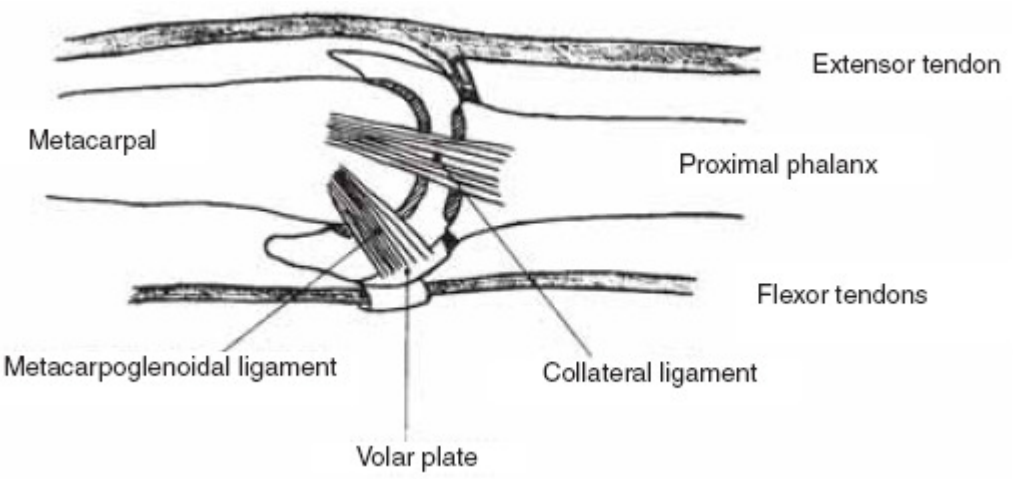

Figure 2.1: The normal MCP joint anatomy (Joyce, 2004). Reproduced with permission from Expert Reviews Ltd.

A rheumatoid arthritic joint is shown in Figure 2.2. Also shown in this figure is an osteoarthritic joint. Osteoarthritis (Gold *et al.*, 1988; MAS, 2004; Pylios and Shepherd, 2007), and post-traumatic osteoarthritis (Beevers and Seedhom, 1995; MAS, 2004; Netscher *et al.*, 2000; Pylios and Shepherd, 2007) can also affect the MCP, but as these conditions are rare in MCP joints (Netscher *et al.*, 2000; Nunez and Citron, 2005; Rettig *et al.*, 2005; Swanson and Swanson, 1985) , they are not discussed further in this thesis.

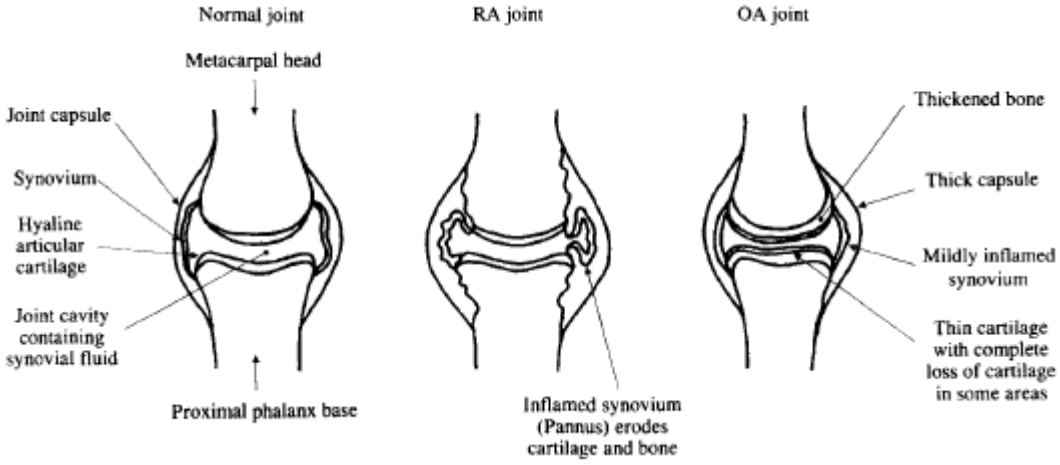

Figure 2.2: A normal, a rheumatoid arthritic (RA) and an osteoarthritic (OA) MCP joint (Beevers and Seedhom, 1993). Reproduced with permission from Professional Engineering Publishing.

The arthritic inflammation destroys the joint, causing severe pain, discomfort, deformity and loss of motion and function to the sufferer (Alderman *et al.*, 2003; Mandl *et al.*, 2002). In severe cases, the MCP joint has to be reconstructed surgically (Mandl *et al.*, 2002), in order to allow these patients with rheumatoid arthritis to restore some form of normality to their lives and provide the necessary range of motions with minimal discomfort (Joyce, 2004; Penrose *et al.*, 1997; Takigawa *et al.*, 2004; Weiss *et al.*, 2004).

The flexible one-piece silicone implant shown in Figure 2.3, which originated from Alfred B. Swanson and was developed in collaboration with Dow Corning Corporation in the 1960s (Foliart, 1995; Hutchinson *et al.*, 1997; Joyce, 2004; Swanson, 1968; Swanson, 1969), is the most popular and widely accepted artificial joint used to replace a rheumatoid arthritic MCP finger joint (Joyce, 2004; Mandl *et al.*, 2002; McMaster, 1972).

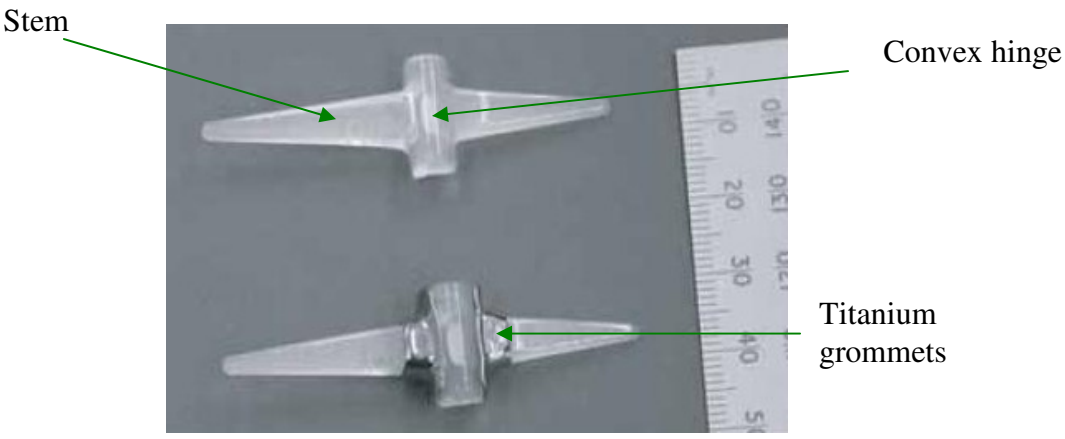

Figure 2.3: A Swanson silicone MCP joint implant without (top) and with titanium grommets (bottom) (Joyce, 2004). Reproduced with permission from Expert Reviews Ltd.

2.3 Silicone implants

The implants were originally manufactured from a conventional high performance (HP) medical grade silicone (Silastic brand; Dow Corning Corporation) (Foliart, 1995; Joyce, 2004; Mandl *et al.*, 2002; Swanson, 1968). They were later manufactured from a silicone with a greater resistance to crack propagation (HP-100 Silastic brand; Dow Corning Corporation) (Goldfarb and Stern, 2003; Joyce, 2004; Linscheid, 2000). They are currently manufactured from FLEXSPAN® (NuSil Technology LLC, Lake Mary, FL 32746, USA) (Biddis *et al.*, 2004; Joyce, 2004; Pylios and Shepherd, 2008b).

Biomedical grade silicones, are currently the material of choice because they are biocompatible, durable, flexible and allow the necessary range of movements (Beevers and Seedhom, 1995; Joyce, 2004; Quinn and Courtney, 1988; Shepherd and Johnstone, 2002; Takigawa *et al.*, 2004; Weiss *et al.*, 2004). The implant itself is manufactured by Wright Medical Technology (Arlington, TN 38002, USA).

Although the Swanson silicone joints are the implants of choice for finger-joint implants (Delaney *et al.*, 2005; Joyce, 2003; Naidu, 2007; Parkkila *et al.*, 2005; Pylios and Shepherd, 2008a), other designs are also available, such as the soft skeletal hand implants (Small Bone Innovations, Inc. Morrisville, PA 19067, USA), formerly known as "Sutter" (Avanta Orthopaedics, Inc., San Diego, CA 92121, USA) and the NeuFlex™ finger joint (DePuy Orthopaedics Inc., Warsaw, IN 46581, USA) shown in Figure 2.4.

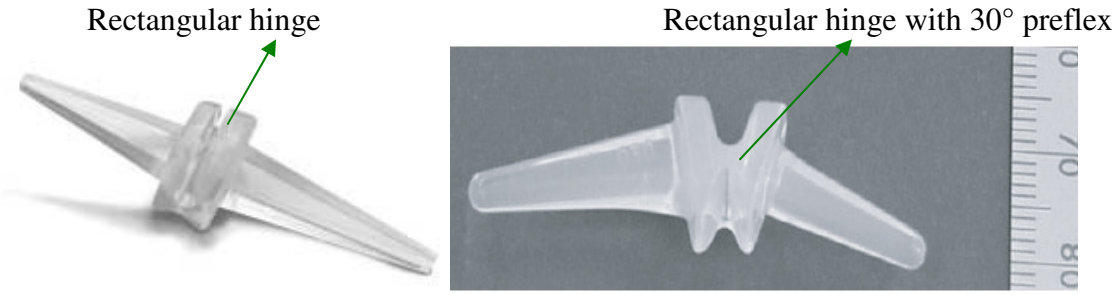

Figure 2.4: Soft skeletal implant (Sutter) (Left hand side) and NeuFlex™ implant (Joyce, 2004). Reproduced with permission from Small Bone Innovations, Inc. (Morrisville, PA 19067, USA) and Expert Reviews Ltd.

X-ray images of a MCP silicone implant are shown in Figure 2.5. Also shown in the X-ray is a proximal interphalangeal (PIP) silicone implant. Rheumatoid arthritis is less common in this joint (Joyce and Unsworth, 2002b; MAS, 2004; Swanson, 1972) and is therefore not discussed further in this thesis.

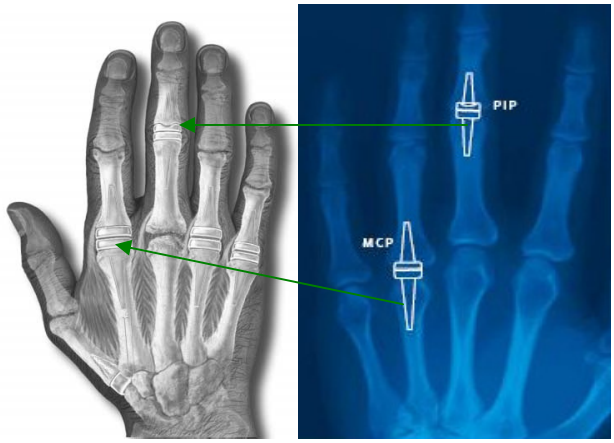

Figure 2.5: X-ray images of a soft skeletal implant (Sutter) in the MCP and PIP joints of the hand Reproduced with permission from Small Bone Innovations, Inc. (Morrisville, PA 19067, USA).

Although all the various silicone implants have enjoyed a degree of success (Trail *et al.*, 2004), there are problems associated with them, the most common being the premature fracture of the stem of the implant (Joyce, 2004; Minamikawa *et al.*, 1994).

2.4 Fracture of silicone implants

The main problem experienced by patients postoperatively with these joints is the fracture of the joint. Varying fracture rates have been reported as shown in Table 2.1, the greatest being 82% after a 5 year follow-up (Kay *et al.*, 1978). Also included in the table are other statistics such as range of motion, ulnar drift (a common deformity) and revision rates postoperatively. The fracture usually occurs at the proximal stem- hinge junction or the distal stem - hinge junction (Jensen *et al.*, 1986; Joyce, 2004; Joyce and Unsworth, 2002a; Kay *et al.*, 1978; Minamikawa *et al.*, 1994; Trail *et al.*, 2004) as shown in Figure 2.6. Hagert *et al.* (1975) reported that fractures across the hinge of the implant are also possible.

Table 2.1 A summary of the fracture rates reported for MCP silicone implants.

Author(s)	**No and type of implant**	**Mean follow-up (years)**	**Fractures rates %**	**Ulnar drift (patients%)**	**Range of motion (°)**	**No. of revisions (%)**
Swanson (1972)	3409 Swanson	5	0.8	1.9	4-57 (53) passive	0.56
Hagert *et al.* (1975)	104 Swanson	3.5	24.0	-	-	
Kay *et al.*(1978)	34 Swanson	5	82.4	66.6	-	
Fleming and Hay (1984)	339 Swanson	4.6	4.1	12	47.4	
Blair *et al.* (1984)	115 Swanson	4.5	20.9	42.6	13-56 (43)	
Bieber *et al.* (1986)	210 Swanson	5.25	0	100.0	22-61(39)	
Wilson *et al.* (1993)	375 Swanson	9.6	3.2	42.9	21-50 (29)	5.9
Gellman *et al.* (1997)	901 Swanson	8	14	-	Improved	7
Hansraj *et al.* (1997)	170 Swanson	2.5	7.1		27	6.5
Kirschenbaum *et al.* (1993)	144 Swanson	8.5	10.4	-	16-59 (43)	2.1
Swanson *et al.* (1997)	139 With grommets	5.8	0.7	-	-	
Schmidt *et al.* (1999a)	57 With grommets	3.5	0	improved	unchanged	
Hagert (1975)	41 Niebauer	3	53.7	-	-	
Beckenbaugh *et al.* (1976)	68 Niebauer	2.7	38.2	44.1	30-65 (35)	
Parkkila *et al.* (2006)	89 Swanson & 126 soft skeletal	4.8	34 and 26 respectively	4.5 Swanson		7 & 4 respectively
Delaney *et al.* (2005)	40 each NeuFlex & Swanson	2	0	No difference between the two groups		
Pettersson *et al.* (2006)	78 each NeuFlex & soft skeletal	1	2.6 and 6.4 respectively		Improved	
Trail *et al.* (2004)	1336 Swanson	17	67 but only 2.9 revised			5.7
Goldfarb and Stern (2003)	148 Swanson & 60 soft skeletal(208)	14	67 and 52 repectively (63 in total)	Improved		
Kimani *et al.* (2009)	237 NeuFlex	5	3	3.0		6.8

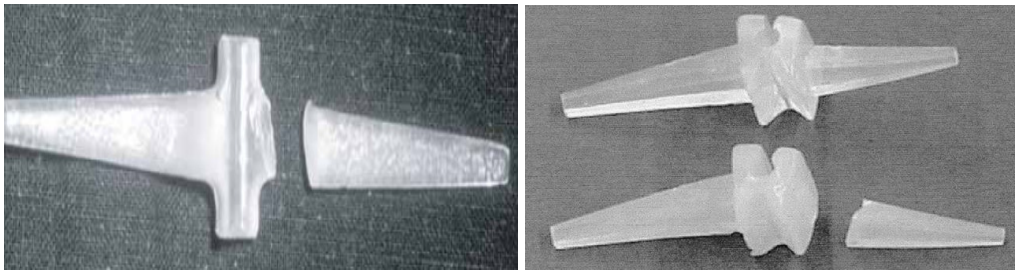

Figure 2.6: Fracture of a Swanson joint (Left hand side) (Joyce, 2004) and fracture of a Soft skeletal (Sutter) implant (Joyce et al., 2003). Reproduced with permission from Expert Reviews Ltd and Elsevier Inc.

Possible initiators of the fractures are listed below.

- Small cuts created by sharp finger bone spurs or by lacerations on the surface of the implant, when the implant are inserted into the patient (Beevers and Seedhom, 1993; Joyce, 2004; Swanson, 1972), can cause a stress concentration region and initiate fractures (Gellman *et al.*, 1997; Jensen *et al.*, 1986; Joyce, 2004; Joyce and Unsworth, 2002a; Kay *et al.*, 1978; Weightman *et al.*, 1972).
- *In vivo* the implant may flex at the interface between the stem and the hinge rather than the hinge itself, during extension and flexion (Beevers and Seedhom, 1993; Gillespie *et al.*, 1979; Joyce and Unsworth, 2002a); therefore, the implant is flexing at a position with a smaller cross sectional area and this can increase the likelihood of a fracture (Joyce and Unsworth, 2002a).

- Silicones are viscoelastic materials i.e. their mechanical properties are time (or frequency) and temperature-dependent (Aklonis and MacKnight, 1983a; Murayama, 1978; Shaw and MacKnight, 2005); therefore, the properties of these silicone finger joints may also be frequency-dependent when mechanically deformed, but there is a danger that this deformation energy will lead to fracture because formation of fracture surfaces then provides a mechanism for dissipating excess deformation energy (Benham *et al.*, 1996; Mahomed *et al.*, 2009); discussed further in Chapter 8 (§8.2).

A fractured implant does not necessarily mean that the patient will experience a loss of function in the MCP joint (Joyce, 2004; Kay *et al.*, 1978; Kirschenbaum *et al.*, 1993). Fractures can remain undetected because the patients are unaware that the implant has fractured and consequently fewer fractured implants will require revision (Beckenbaugh *et al.*, 1976; Beevers and Seedhom, 1993; Kay *et al.*, 1978; Kirschenbaum *et al.*, 1993; Trail *et al.*, 2004).

2.5 Silicones

2.5.1. Introduction

Medical grade silicones are reported (Braley, 1970) as being the most commonly used synthetic polymers for implantable devices. The term medical grade in this case refers to silicones that are manufactured under clean pharmaceutical conditions; have been successfully implanted in animals and humans; and are quality controlled for medical applications (Braley, 1970).

2.5.2. Chemical structure

For justification of the information in this section consult Braley (1970), Brandon *et al.* (2001), Briquet *et al.* (1996), Colas and Curtis (2004a), Colas and Curtis (2004b), Levier *et al.* (1995) and Starch (2002).

Silicones are synthetic polymers with a backbone of repeating silicon and oxygen bonds that have been commercially available since the 1940s from Dow Corning Corporation. The silicon atoms are also bonded to organic groups, the most common being the methyl group. This attachment of the organic groups to inorganic backbones creates unique properties which make them attractive for use in different fields, including aerospace, electronics, health care and building industries. The most common silicone is *polydimethylsiloxane* (PDMS). The chemical structure for PDMS is shown in Figure 2.7.

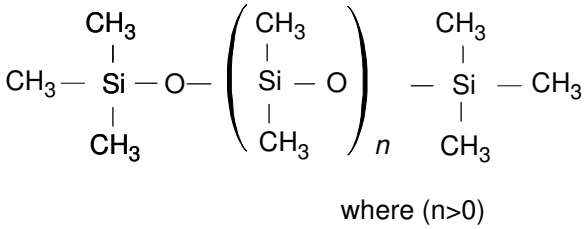

Figure 2.7: Chemical structure for PDMS (Braley, 1970; Colas and Curtis, 2004b; Lewis, 1962).

2.5.3 Cross-linking

Linear silicone polymers with reactive sites along the polymer chains are transformed into three-dimensional networks, via cross-linking reactions that form chemical bonds between adjacent chains (Colas and Curtis, 2004b; Starch, 2002). One form of cross-linking is known as addition curing and requires a catalyst (e.g. platinum) (Colas and Curtis, 2004b). The process of cross-linking the polymer is also known as vulcanisation (Braley, 1970). The cross-link density (defined in §2.5.4.4) is a measure of how highly cross-linked a silicone is. This level of detail of the formulation of the material is not disclosed by the silicone supplier because it is confidential and proprietary. It can be determined experimentally by swelling the silicone in appropriate solvents (Brandon *et al.*, 2003; Brandon *et al.*, 2001; Starch, 2002).

2.5.4 Use of swelling to measure the cross-linking density

2.5.4.1 Introduction

Various natural and synthetic polymers do not swell in water (hydrophobic) but have the ability to swell in suitable low-molecular organic solvents (Treloar, 1958). Swelling occurs because molecules from the solvent are allowed to diffuse into the molecules of the polymers and fill in vacant sites, i.e. areas with no cross-links (Treloar, 1958; Watanabe and Miyauchi, 1973). Softer polymers have a lower cross-link density (i.e. fewer cross-links) compared to a harder polymer, consequently softer polymer swells more when immersed in a solvent (Starch, 2002). The greater the hardness value of the polymer, the greater the number of cross-links, and the lesser the ability it has to swell in a solvent (Starch, 2002).

Therefore, a polymer that is soft and that swells appreciably in a solvent is regarded as having fewer cross-links than a hard polymer that does not swell significantly (Starch, 2002). The amount the polymer swells also depends on the nature of the solvent as different solvents will have different swelling powers (Takahashi, 1983; Treloar, 1958). The greater the swelling ability, the better the solvent. For example, silicone swells appreciably in toluene but not in n-butanol (Andreopoulos *et al.*, 1993). Hence, toluene is considered as a good solvent and has been used in previous studies (Andreopoulos *et al.*, 1993; Boyer and Spencer, 1948; Brandon *et al.*, 2003; Brandon *et al.*, 2001; Favre, 1996) while, n-butanol is considered as a bad solvent for silicones (Andreopoulos *et al.*, 1993). Apart from having a good swelling ability, good solvents should also be compatible (discussed further in §2.5.4.6) with the polymer and should not dissolve the polymer (discussed further in Appendix I (§I.6)) (Diamant and Folman, 1979; Sperling, 1997). The criteria of a good, fair and bad solvent in terms of the polymer-solvent interaction parameter, χ, is discussed in §2.5.4.2 and §2.5.4.8.

2.5.4.2 Thermodynamic and statistical treatment of swelling: the Flory-Huggins equation

The swelling behaviour of the polymer in a solvent can be described by a statistical thermodynamic swelling model; the Flory-Huggins equation proposed in the 1940s (equation 2.2) (Blanks and Prausnitz, 1964; Flory, 1942; Flory, 1953; Huggins, 1942b; Treloar, 1958). This is based on the observation that when a polymer (solute) is immersed in a solvent, the two components mix together and energy is involved in this mixing process and the polymer will swell provided the polymer is not soluble in the solvent (Treloar, 1958).

The free energy available in the mixing process (the Gibbs free energy of mixing or dilution, ΔG_M, for conditions of constant temperature and pressure) is defined as (Rogers and Mayhew, 1994):

$$\Delta G_M = \Delta H_M - T \Delta S_M \tag{2.1}$$

where ΔH_M and ΔS_M are the changes in enthalpy and entropy of mixing, respectively; T is the temperature on the Kelvin scale. Any spontaneous change, at constant temperature and pressure, tends to decrease ΔG_M (Rogers and Mayhew, 1994; Treloar, 1958).

During the swelling process, the entropy will increase but there will be a relatively small change in the internal energy (Treloar, 1958). For the swelling process, the ΔH_M term can be determined from the force fields between the molecules and ΔS_M is calculated in terms of the number of configurations possible for the molecules (Treloar, 1958). Using this, Flory (1942), Huggins (1942a) and Flory and Rehner (1943) derived expressions for ΔH_M (using van Laar's heat of dilution (Hildebrand and Scott, 1950)) and ΔS_M (using the statistical definition of entropy (Treloar, 1958)) and substituted them back into equation (2.1) to give:

$$\Delta G_M = RT\left[\ln(1-\phi_P)+\phi_P+\chi\phi_P^2\right] \tag{2.2}$$

In equation 2.2, χ is the Flory polymer-solvent interaction parameter, (a dimensionless parameter). It is described by Huggins (1943) as being a measure of the preference of a particular molecule to having the same molecule as its neighbour rather than having a different molecule as its neighbour.

It reflects the intermolecular forces or interaction energy between the molecules in a particular polymer-solvent system and is not limited to any theory or model (Barton, 1983; Blanks and Prausnitz, 1964; Favre, 1996; Mulder and Smolders, 1984). ϕ_P is the volume fraction of polymer in the swollen polymer (Flory, 1942). R is the universal gas constant (Rogers and Mayhew, 1994).

2.5.4.3 Swelling of cross-linked polymers: Flory-Rehner equation

The limitation of the Flory-Huggins equation (equation 2.2) is that it is only applicable to uncross- linked polymers. This is because, the expression for ΔS_M derived previously by Flory (1942), which was substituted into equation 2.2 does not consider that the molecules in cross-linked polymers are permanently interconnected (Flory and Rehner, 1943; Treloar, 1958). During swelling the solvent will also mix with the interconnected molecules and expansion of the network will occur. Therefore, there is an extra configurational entropy term of the network to be considered (Flory and Rehner, 1943; Treloar, 1958). For a cross-linked polymer, Flory and Rehner (1943) suggested that ΔG_M is described as:

$$\Delta G_M = \Delta G_{Mm} + \Delta G_{Me} \tag{2.3}$$

where ΔG_{Mm} is the free energy of dilution of the uncross-linked polymer (previously defined by the Flory-Huggins equation (equation 2.2)) and ΔG_{Me} is the free energy change due to the elastic expansion of the polymer network as a result of absorbing one mole of the solvent.

According to Flory and Rehner (1943), ΔG_{Me} is defined as:

$$\Delta G_{Me} = \frac{\rho_p RT}{2M_c} V_S \phi_P^{1/3} \tag{2.4}$$

where the M_c is the molecular weight between cross-links; V_S is the molar volume of the solvent; ρ_p is the density of the polymer (Bueche, 1955b).

Therefore by combining ΔG_{Me} and ΔG_{Mm} (Flory- Huggins equation), ΔG_M for a cross-linked polymer is:

$$\Delta G_M = RT\left[\ln(1-\phi_P)+\phi_P+\chi\varphi_P^2+\left(\frac{\rho_p V_S}{M_c}\right)\left(\phi_P^{1/3}\right)\right] \tag{2.5}$$

Flory (1950) later suggested that the extra configurational entropy term for the network did not take into account fluctuations in entropy and as a result the entropy value was too small. He (Flory, 1950) revised the configurational entropy term and the resulting ΔG_M was:

$$\Delta G_M = RT\left[\ln(1-\phi_P)+\phi_P+\chi\phi_P^2+\left(\frac{\rho_p V_S}{M_c}\right)\left(\phi_P^{1/3}-\frac{\phi_P}{2}\right)\right] \tag{2.6}$$

2.5.4.4 Cross-link density equation

The important concept to consider when swelling a polymer in a solvent is the state of equilibrium swelling between both the polymer and the solvent. When a system is maintained at a constant pressure and temperature, equilibrium is reached when $\Delta G_M = 0$ (Flory and Rehner, 1943; Rogers and Mayhew, 1994; Treloar, 1958).

If $\Delta G_M = 0$, equation 2.6 can be rearranged to give the cross-link density, $\frac{\rho_p}{M_c} = \upsilon_c$ (Brandon *et al.*, 2003; Bueche, 1955b; Flory and Rehner, 1943; Treloar, 1958), where:

$$\frac{\rho_P}{M_c} = \upsilon_c = \frac{-\left[\ln(1-\phi_P)+\phi_P+\chi\phi_P^2\right]}{\left[V_S\left(\phi_P^{1/3}-\frac{\phi_P}{2}\right)\right]} \tag{2.7}$$

2.5.4.5 Determining ϕ_P

Using the definition of ϕ_P in §2.5.4.2 it is possible to derive an equation for ϕ_P (Doty and Zable, 1946; Miller *et al.*, 1998; Muramoto, 1982; Nijhuis *et al.*, 1993), where:

$$\phi_p = \frac{1}{1+\frac{\rho_P}{\rho_s}\left(\frac{m_a}{m_b}\right)-\frac{\rho_P}{\rho_s}} \tag{2.8}$$

where m_b and m_a are the mass before and after swelling respectively; ρ_s and ρ_p are the densities of the solvent and polymer respectively.

2.5.4.6 Determining χ

There are two methods that have been suggested, of determining χ.

1. For equilibrium swelling $\Delta G_M = 0$, therefore equation 2.2 can be rearranged to give (Favre *et al.*, 1996; Orwoll, 1977):

$$\chi = -\left(\frac{\ln(1-\phi_P)+\phi_P}{\phi_P^2}\right) \tag{2.9}$$

where ϕ_P is determined using the method described in §2.5.4.5.

A study (Mulder and Smolders, 1984) suggested that if $\Delta G_M = 0$, and if the last term in equation 2.6 is ignored, then similarly, equation 2.6 can be rearranged to give equation 2.9. It has been implied that equation 2.9 can be used to calculate υ_c (Brandon *et al.*, 2003; Favre, 1996). However, substitution of equation 2.9 into equation 2.6, shows that this method cannot work because it gives a value of $\upsilon_c = 0$. Further evidence of this, will be shown by the results of my swelling experiments reported in Chapter 7.

The theory used to calculate equation 2.9 is unreliable. As discussed previously, equation 2.9 can be calculated from equation 2.6 by applying the equilibrium condition, $\Delta G_M = 0$, and assuming that

$$\left[\left(\frac{\rho_P V_S}{M_c}\right)\left(\phi_P^{1/3} - \frac{\phi_P}{2}\right)\right] = 0 \qquad (2.10)$$

It has been argued that the value of $\frac{\rho_P V_S}{M_c}$ is so small that the left-hand side of equation 2.10 is negligible, when it appears as a term in equation 2.6 (Mulder and Smolders, 1984). However, it makes no physical sense to equate $\frac{\rho_P V_S}{M_c}$ to zero, and so obtain equation 2.9, since equation 2.10 is strictly valid only when

$$\phi = 2\sqrt{2}\,. \qquad (2.11)$$

Equation 2.11 can never be true because, by definition, $\phi \leq 1$.

2. χ can also be determined using Hildebrand's solubility parameter theory (Bristow and Watson, 1958; Flory and Rehner, 1943; Hildebrand and Scott, 1950; Scott, 1945; Treloar, 1958), which states that:

$$\chi = \chi_S + K\frac{V_S}{RT}(\delta_S - \delta_P)^2 \tag{2.12}$$

One of the advantages of equation 2.12, is that it is simple and can therefore be easily used to make numerical calculations (Sperling, 1997). In equation 2.12, χ_s is a constant. It has been shown (Hildebrand and Scott, 1950; Sheehan and Bisio, 1966; Tompa, 1956) from statistical thermodynamics that χ_s is approximately equal to the inverse of the lattice coordination number and is therefore defined as (Blanks and Prausnitz, 1964; Bueche, 1955b; Favre, 1996; Scott, 1945; Scott and Magat, 1945; Tompa, 1956):

$$\chi_S = \frac{1}{Z'} \tag{2.13}$$

where Z' is the effective coordination number (number of nearest neighbour polymer segments); $Z' \approx$ 3-4 (Scott, 1945; Scott and Magat, 1945).

A study (Blanks and Prausnitz, 1964) found the value of χ_s to be 0.34 for three nonpolar polymers in a large number of nonpolar solvents. This value for χ_s has also been suggested in previous studies (Grulke, 1989; Miller *et al.*, 1998; Sheehan and Bisio, 1966). There is a general agreement that the value of χ_s is between 0.3 and 0.5 for cross-linked polymers such as silicone (Bueche, 1955b; Dudek and Bueche, 1964; Favre, 1996; Scott and Magat, 1949).

K is an empirical constant. In general, K=1 for non-polar solvents and K >1 for polar solvents (Scott and Magat, 1949). However, some authors (Bueche, 1955b; Favre, 1996) have suggested that K can be less than 1. V_S is the molar volume of the solvent and δ_S and δ_P are solubility parameters for the solvent and polymer respectively.

The solubility parameters are defined as the square root of the cohesive energy density (i.e. energy per unit volume required to separate the molecules) or the internal pressure of the solvents (Bagley *et al.*, 1970; Bristow and Watson, 1958; Dudek and Bueche, 1964; Hildebrand and Scott, 1950; Orwoll, 1990). δ_S can be obtained from published tabulated values (Barton, 1975; Barton, 1983; Grulke, 1989; Yerrick and Beck, 1964). δ_P can be measured experimentally by swelling the crosslinked polymer until constant mass in various solvents with varying δ_S values (Barton, 1975; Grulke, 1989; Takahashi, 1983; Yerrick and Beck, 1964; Zellers, 1993). δ_P is equated to the δ_S of the solvent in which the polymer swells the most at a constant temperature (Barton, 1975; Grulke, 1989; Takahashi, 1983; Yerrick and Beck, 1964; Zellers, 1993). For example, a study (Yerrick and Beck, 1964) on silicones reported that the samples swelled the most in n-heptane (225 %). Hence, δ_P of the silicones was equated to the δ_S value of n-heptane.

Various values of δ_P for silicone have been suggested from previous studies. For example, two studies (Watanabe and Miyauchi, 1973; Yerrick and Beck, 1964) obtained a value of δ_P = 15.3 $MPa^{½}$, while three other studies by Bueche (1955b), Nijhuis *et al.* (1993) and Hauser *et al.* (1956), suggested using δ_P = 15.8 $MPa^{½}$, 16.2 $MPa^{½}$ and 15.1 $MPa^{½}$, respectively.

It has been discussed (Bueche, 1955b) that errors will propagate when using the swelling method to calculate the solubility parameter of the polymer, δ_P and therefore measuring χ using this method is generally recommended only as a comparison. Other studies (Coleman *et al.*, 1990; Favre, 1996) suggest that to obtain a reasonable prediction of χ, the precision of the δ_P value should be in the range of 0.1 $MPa^{½}$, which is practically impossible to achieve as the precision of the solubility parameter of the solvents used is of the order of 0.2 $MPa^{½}$. It has been suggested that the smaller the difference between the solubility parameters, δ_S and δ_P, the more likely the solvent–polymer system will be compatible (Diamant and Folman, 1979).

2.5.4.7 How the value of χ affects ΔG_M

It has been suggested (Treloar, 1958) that if a value of $\chi < 0.5$ is substituted into the Flory-Huggins equation (equation 2.2), the equation will work well for all values of ϕ_P because $\Delta G_M < 0$ (i.e. it is a possible reaction because it would not violate the second law of thermodynamics (Rogers and Mayhew, 1994); see §2.5.4.2). On the other hand, if $\chi > 0.5$, then for one value of ϕ_P , $\Delta G_M = 0$ (i.e. equilibrium swelling discussed in §2.5.4.4) (Treloar, 1958). It is also possible that if $\chi > 0.5$, ΔG_M is not necessarily less than 0 for all values of ϕ_P. If $\Delta G_M > 0$, this condition is physically impossible. The results of my swelling experiments reported in Chapter 7, will show that this can occur and will yield the physically impossible result of a negative υ_c.

2.5.4.8 Using the value of χ to categorise solvents

The value of χ can also be used to categorise solvents in terms of being good, fair or bad solvents. It has been suggested that for good solvents $\chi \leq 0.5$, for fair or borderline solvents $0.5 < \chi \leq 1$ and $\chi > 1$ for non solvents (Hildebrand and Scott, 1950; Rickles, 1966). However, some authors (Andreopoulos *et al.*, 1993; Favre *et al.*, 1996) have suggested that for good solvents $\chi < 0.7$.

2.5.4.9 Limitations of the Flory- Huggins equation

Some of the limitations of the Flory-Huggins Theory have been discussed previously (Carpenter, 1990; Cowie, 1994; Sheehan and Bisio, 1966; Sperling, 1997; Summers *et al.*, 1972; Takahashi, 1983; Treloar, 1958; Zellers, 1993). These are listed below.

- It assumes no volume change on mixing, i.e. $\Delta V_M=0$, when in fact ΔV_M could be > 0.
- It predicts entropies of mixing that are too positive.
- χ may depend on other factors such as concentration, composition, chain length and temperature, which may not be accounted for.
- Configurational entropy of mixing is used instead of the total entropy of mixing in the Gibbs free energy of mixing equation, but this means that entropic contributions that may arise from the specific interactions between neighbouring solvent and polymer molecules are being neglected, when in fact they should be taken into account.

- It assumes that the solvent and polymer molecules are arranged on a 3-D lattice of sites which can be occupied by either a solvent molecule or by a segment of the polymer chain and the segment-locating process is purely statistical. The assumption of a lattice scheme is not necessarily unreasonable. However, the assumption that the configurations of both the solvent and polymer can be described by the same lattice is more debatable, as it requires the geometry of the two molecular species to be practically identical. If the polymer molecule is a thousand times the size of the solvent molecule, then the assumption of the ability of the molecules of the two species to interchange cannot hold.
- The statistical thermodynamic theory assumes incompressibility of the system, i.e. no small holes are allowed in the lattice.

2.5.5 Filler content

Fillers are material extenders that are used to improve the mechanical properties of silicones (such as mechanical strength and hardness) by reinforcing the cross-linked matrix (Braley, 1970; Brandon *et al.*, 2003; Brandon *et al.*, 2001; Cheremisinoff *et al.*, 1993; Colas and Curtis, 2004b). (Boonstra, 1979) concluded that silica filled silicones are 40 times stronger than unfilled silicones. The properties of a filled polymer such as biomedical grade silicones are dependent on both chemical cross-linking and also on the physical bonding between the filler and the polymer (Brandon *et al.*, 2003) .

Amorphous silica (SiO_2) is the most common filler used in silicones for medical applications (Boonstra *et al.*, 1975; Braley, 1970; Brydson, 1988; Colas, 1990; Colas and Curtis, 2004b; Warrick *et al.*, 1979). Silica consists of small spheroid particles, which fuse irreversibly while in the semi-molten state and create aggregates (Colas and Curtis, 2004b). Silica has a surface area between 180-400 m^2/g, which is equivalent to a diameter between 7-15 nm (Colas and Curtis, 2004b; Lambert, 2006). Some of the supplier's data sheets contain information on the properties of the silica filler used in medical grade silicones, as shown in Chapter 3 (Table 3.2 and Table 3.3). Further information on the equations used to calculate the filler properties is in Appendix A (§A.1).

2.6 Elast-Eon ^{TM}: Introduction and Chemistry

2.6.1 Overview

Synthetic polyurethane elastomers are another family of biomaterials commonly implanted into the body (Gunatillake *et al.*, 2003). Elast-Eon^{TM} (AorTech Biomaterials Pty Ltd, Frenchs Forest, Australia) is the trade name of a more recent thermoplastic segmented polyurethane with soft and hard segments that has been synthesised as an alternative to silicones for surgical implants (Gunatillake *et al.*, 2003; Gunatillake *et al.*, 2000).

Biomedical applications of polyurethane elastomers include reconstructive surgery materials, heart valves, catheters, tubing for medical purposes and implantable drug delivery applications (Gunatillake *et al.*, 2003; Simmons *et al.*, 2008). More recently, Elast-Eon^{TM} has been suggested for use in flexible artificial finger joints (Shepherd and Johnstone, 2005).

2.6.2 Chemical structure

Polyurethane elastomers in general are a class of linear segmented copolymers that have urethane (carbamate) linkages, as shown in Figure 2.8 (Gunatillake *et al.*, 2003; Stokes *et al.*, 1995). Elast-Eon^{TM} is a polyurethane with PDMS, the latter was previously discussed in §2.5.2.

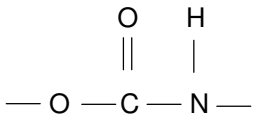

Figure 2.8: Structure of urethane (carbamate) linkages

2.7 Viscoelastic properties of silicones and polyurethanes

2.7.1 Linear viscoelastic behaviour

There is strong dependence of the viscoelastic properties of polymers on time (or frequency) (i.e. how quickly the material is deformed), and temperature, and this can be attributed to the viscoelastic nature of polymers (Aklonis and MacKnight, 1983b; Ferry, 1961b; Murayama, 1978; Shaw and MacKnight, 2005; Ward, 1990a; Ward, 1990b). Viscoelastic materials, such as silicone and polyurethanes have a combination of viscous and elastic properties (Ferry, 1961b; Ward, 1990a).

If a tensile stress is applied to a viscoelastic material, the resulting strain can be determined by solving the differential equation (Ward, 1990b):

$$\sigma = E\varepsilon + \mu\frac{d\varepsilon}{dt} \tag{2.14}$$

where σ is the stress; E is the modulus of elasticity; ε is the strain; μ is related to viscosity; $\frac{d\varepsilon}{dt}$ is the strain rate. E represents the elastic deformation where the energy involved in the process is stored as potential energy and is subsequently used to revert back to its original shape when the tensile stress is removed. μ represents the viscous flow of the system where energy is dissipated as heat when the stress is removed. If E and μ are constants or functions of t (time) only, than equation 2.14 is a linear ordinary differential equation (James, 1993b) (i.e. the material is linear viscoelastic).

For a given $\sigma(t)$ it is possible to find the corresponding $\varepsilon(t)$. Consider that:

$$\sigma(t) = \sigma_o e^{i\omega t} \tag{2.15}$$

where e is a mathematical constant, the base of a natural logarithm (≈ 2.718); ω is the angular frequency; $i = \sqrt{-1}$.

This condition of loading is chosen because any time dependent function can be written as a weighted sum of functions of this form (i.e. Fourier Analysis).

Consider a trial solution of the form:

$$\varepsilon(t) = \varepsilon_o e^{i\omega t} \tag{2.16}$$

Differentiating equation 2.16 gives:

$$\frac{d\varepsilon}{dt} = i\omega\varepsilon_o^{\,i\omega t} \tag{2.17}$$

Substituting equation 2.15, 2.16 and 2.17 into equation 2.14 and rearranging produces a solution of the form:

$$\varepsilon_o = \frac{\sigma_o}{E + i\omega\mu} \tag{2.18}$$

Substituting equation 2.18 and then equation 2.15, into equation 2.16 results in:

$$\varepsilon = \frac{\sigma_o e^{i\omega t}}{E + i\omega\mu} = \frac{\sigma}{E + i\omega\mu} \tag{2.19}$$

The demoninator in equation 2.19 can be expressed in terms of the complex modulus, E^*, which is defined as:

$$E^* = E' + iE'' \tag{2.20}$$

where E' is the storage modulus; E'' is the loss modulus.

Then, in equation 2.19, if E and $\omega\mu$ are replaced with E' and E'', respectively, the equation can be written as:

$$\varepsilon = \frac{\sigma}{E^*} \tag{2.21}$$

The magnitude of E^* is given by:

$$|E^*| = \sqrt{E'^2 + E''^2} \tag{2.22}$$

It can then be used to calculate the deformation.

The phase difference between σ and ε is:

$$\delta = tan^{-1}\left(\frac{E''}{E'}\right) \tag{2.23}$$

2.7.2 Assumptions for linear behaviour

A typical plot of σ against ε for a viscoelastic material (silicone) is shown in Figure 2.9. An approximately linear region (area within the red lines) is identified. It is possible to assume linear behaviour, provided that the experiments are performed within this linear region over a very small deformation (area within the green lines).

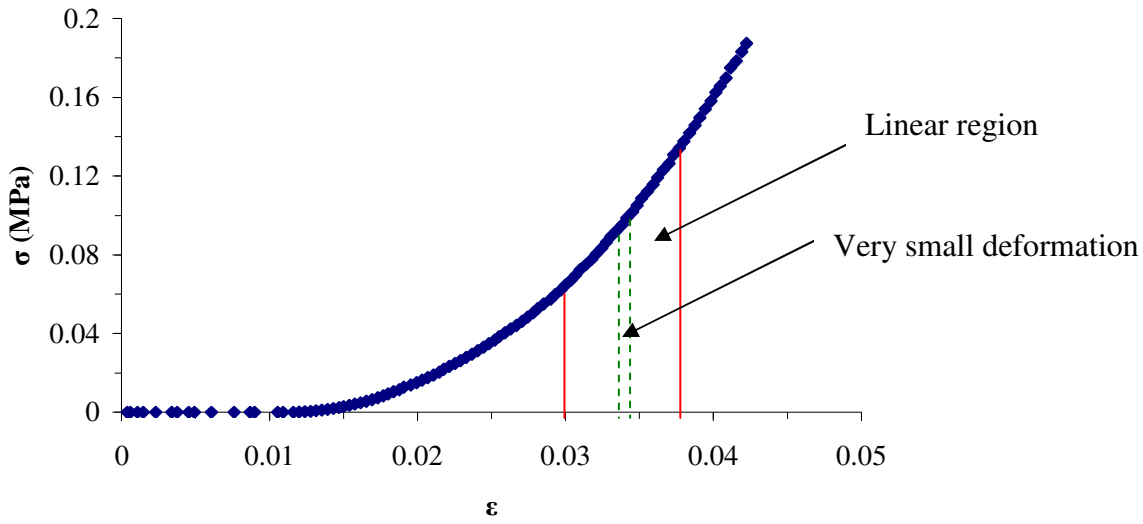

Figure 2.9: Linear viscoelastic behaviour

A previous study (Polyzois, 2000) on silicones for maxillofacial applications has also discussed the concept that the initial portion of a stress-strain curve for silicones is not linear and suggests that the modulus should be measured at a fixed point of strain.

2.7.3 Viscoelastic Creep

If a viscoelastic material is subjected to a constant stress, the strain will increase as a function of time (Ward, 1990b). This phenomenon is knows as creep.

2.7.4 Stress relaxation

If a viscoelastic material is subjected to a constant strain, the stress decreases with time (Ward, 1990b). This phenomenon is knows as stress relaxation.

2.7.5 Hysteresis

When a load is applied to a viscoelastic material, the σ and ε will increase as shown in Figure 2.9. However, when the load is removed, the σ and ε will not follow the same initial path to return to the original position (Benham *et al.*, 1996). This is because some of the energy used to deform the material will be dissipated (viscous behaviour). This phenomenon is knows as hysteresis (Benham *et al.*, 1996) and is shown in Figure 2.10. The area under the red curve is the work per unit volume done in deforming the material. This deformation energy is then either used for recoil or dissipated as heat as shown in Figure 2.10.

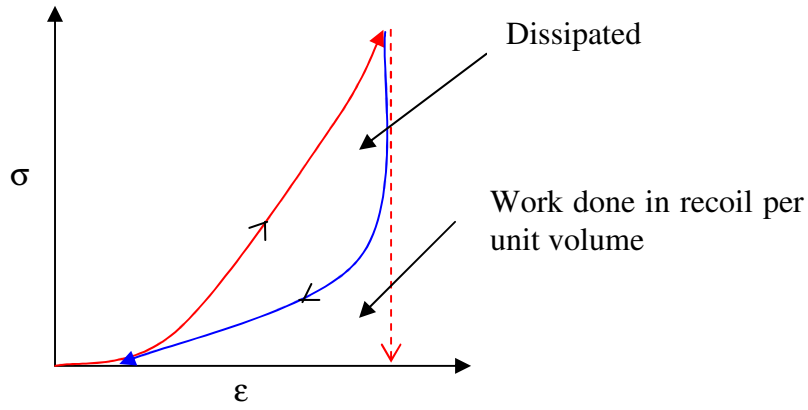

Figure 2.10: Hysteresis in viscoelastic materials

2.7.6 Frequency dependence of a viscoelastic materials

The E' and $\tan\delta$ as a function of frequency for a viscoelastic material are shown in Figure 2.11 (Meakin *et al.*, 2003; Shaw and MacKnight, 2005; Ward, 1990b). The figure shows that at low frequencies the viscoelastic material behaves like a rubber; E' is fairly constant and is independent of frequency (Ward, 1990b; Ward and Sweeney, 2004). Similarly, this frequency independent behaviour also occurs at high frequencies, where the viscoelastic material behaves like a glass (Ward, 1990b; Ward and Sweeney, 2004). However, in the transition zone, the E' becomes dependent on frequency and $\tan\delta$ reaches a maxima in this region (Cheremisinoff *et al.*, 1993; Ward, 1990b; Ward and Sweeney, 2004).

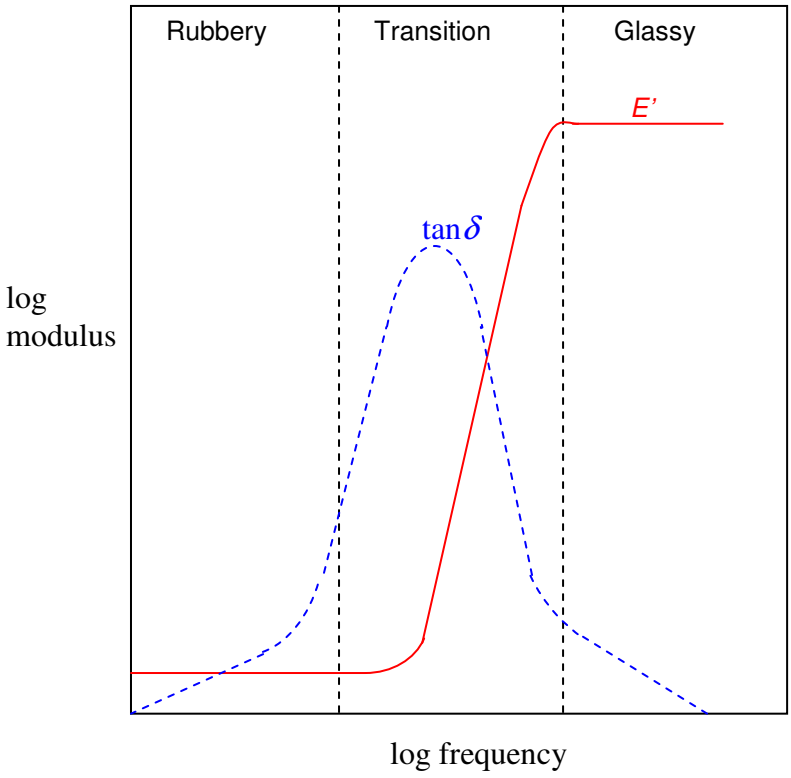

Figure 2.11: E' and $\tan\delta$ as a function frequency (reproduced from (Shaw and MacKnight, 2005; Ward, 1990b). Reproduced with permission from John Wiley & Son Ltd.

2.7.7 Rubber-glass transition

The transition state in Figure 2.11 shows that above a certain frequency, there is a rapid increase in *E'* with frequency; this behaviour is characteristic of a material undergoing a transition from the rubbery to the glassy state (Meakin *et al.*, 2003; Ward, 1990b). Within this transition region, the viscoelastic material will experience a transition at a particular frequency (or its corresponding temperature), corresponding to the exact location where there is a change from the rubbery state to the glassy state (Ward and Sweeney, 2004). This frequency is known as the glass transition frequency, f_g (or its corresponding glass transition temperature, T_g). The T_g is quoted as -123 °C for PDMS (Brydson, 1999; Clarson *et al.*, 1985; Murayama, 1978; Weir *et al.*, 1950).

2.7.8 Time-temperature superposition

There is an equivalence between the modulus measured as a function of time (or frequency) at a constant temperature and the modulus measured as a function of temperature at a constant time (or frequency) (Aklonis and MacKnight, 1983a; Murayama, 1978; Shaw and MacKnight, 2005). Time-temperature superposition implies that the viscoelastic properties at one temperature can be related to that at another temperature by shifting the time scale horizontally by a factor log a_T , where a_T is defined as the shift factor and is a function of temperature (discussed further in §2.7.9) (Aklonis and MacKnight, 1983a; Murayama, 1978; Shaw and MacKnight, 2005). In other words, the viscoelastic properties at one temperature can be superimposed upon data at a different temperatures by shifting the curves horizontally by log a_T (Aklonis and MacKnight, 1983a; Murayama, 1978; Shaw and MacKnight, 2005) .

The viscoelastic properties of polymers at different temperatures can be shifted along a logarithmic axis (such as log time or log frequency), to create a master curve (Murayama, 1978; Ward, 1990b). The value for a_T can be calculated using the Williams-Landel-Ferry (WLF) equation (Ferry, 1961a; Ward, 1990b; Williams *et al.*, 1955); discussed in §2.7.9.

2.7.9 Time-temperature superposition and the WLF equation

The WLF equation (Ferry, 1961a; Ward, 1990b; Williams *et al.*, 1955) is defined as:

$$\log a_T = \frac{C_1(T - T_o)}{C_2 + (T - T_o)} \tag{2.24}$$

where C_1 and C_2 are constants; T is the test temperature; T_o is the reference temperature. For polymers, the WLF equation is often found to work really well within the range T_o - 50ºC ≤ T ≤ T_o + 50ºC (Murayama, 1978; Ward, 1990b).

If $T_o = T_g$, equation 2.21 becomes

$$\log a_T = \frac{C_1^g(T - T_g)}{C_2^g + (T - T_g)} \tag{2.25}$$

where C_1^g and C_2^g are the new constants; T_g is the glass transition temperature (discussed in §2.7.7). In this case, the WLF equation is often found to work really well within the range T_g ≤ T ≤ T_g + 100ºC; where C_1^g = -17.4 and C_2^g =51.6 are the universal constants for the polymer (Aklonis and MacKnight, 1983a; Ferry, 1961a; Huba and Molnár, 2001; Huba *et al.*, 2005; Williams *et al.*, 1955). Above T_g + 100ºC, the equation does not hold extremely well because different systems will show specific properties that are not dominated by the non-specific behaviour associated with supercooling and vitrification (gradual freezing of long-range molecular motions) (Williams *et al.*, 1955).

2.7.10 Measuring the frequency dependent behaviour of silicones indirectly by making use of the WLF equation

It is possible to measure directly the frequency dependent behaviour of the moduli of silicones at a fixed temperature. An alternative method would be to measure the frequency dependence indirectly, by first measuring the temperature dependence of the moduli and then use both the WLF equation (Ferry, 1961a; Meakin *et al.*, 2003; Ward, 1990b) and equation 2.26 to switch from a temperature scale to a frequency scale.

a_T can be defined as (Aklonis and MacKnight, 1983a; Huba and Molnár, 2001):

$$a_T = \frac{f_o}{f} \tag{2.26}$$

where f and f_o are the loading frequency and the reference frequency, respectively. Further information on the use of the WLF equation on silicones is in Appendix B.

2.8 Aging process of elastomers

The properties of materials such as silicones and Elast-Eon^{TM}, that are suitable to be implanted in the body should not deteriorate unacceptably during their shelf-life or while *in vivo*; this is discussed in detail in a paper of which I am a co-author (Hukins *et al.*, 2008). One method that can be used to study the material's aging properties is to implant it into animals (Martin *et al.*, 2000; Simmons *et al.*, 2004; Simmons *et al.*, 2006; Simmons *et al.*, 2008) or from retrieval studies in the human body (Doležel *et al.*, 1989a). However, necessary approval is required for this and the period of implantation used in these studies may not be sufficient.

Another method that can be used to determine whether deterioration is likely to occur over long time scales, is to subject materials to elevated temperatures, known as "accelerated aging" (Hemmerich, 1998; Hukins *et al.*, 2008). This is particularly useful to study the aging of materials that are regarded as potential implant material.

Aging of a material can be accelerated by a factor of (ASTM WK4863, 2005; Hemmerich, 1998; Hukins *et al.*, 2008):

$$f = 2^{\Delta T/10} \tag{2.27}$$

where $\Delta T = T - T_{ref}$. T is the elevated temperature used to accelerate the aging process and T_{ref} is the reference temperature, at which to study the effects of aging. For example, for studies involving materials suitable to be implanted in the body T_{ref} is 37°C (body temperature). Therefore, maintaining a material at 70°C for 38 days is the same as aging it for $38 \times 2^{(70-37)/10} = 380$ days, i.e. aging for ≈ 13 months, at 37°C.

2.9 Chapter summary

This background chapter has highlighted that, although artificial finger implants manufactured from silicone are currently the implant of choice to replace rheumatoid arthritic finger joints, they lack the success of implants in other joints such as the hip and knee (Joyce, 2004). Regardless of their design, their main drawback is that in many cases they fracture prematurely and need to be replaced. Silicones are viscoelastic materials i.e. their properties are time (or frequency) and temperature-dependent (Aklonis and MacKnight, 1983a; Murayama, 1978; Shaw and MacKnight, 2005).

Therefore the properties of these silicone finger joints may also be frequency-dependent when subjected to either a compressive or tensile load. As a first stage in investigating such effects, this thesis is concerned with determining the viscoelastic and related properties of medical grade silicones and Elast-Eon^{TM}. The results reported here provide an indication of the viscoelastic performance of these silicone and polyurethane elastomers *in vitro* and suggest how they might perform *in vivo* as an implant.

Chapter 3. MATERIALS AND METHODS

3.1 Chapter overview

The chapter begins by describing the materials used in the experimental work for this thesis in §3.2. §3.3 describes how the silicone was mixed and how the specimens were prepared, depending on the test for which they would be used. §3.4 discusses the pre-treatment of the specimens prior to testing. §3.5 and §3.6 describes the design of additional parts that were manufactured in order to test the specimens in simulated *in vivo* conditions. §3.7 discusses the experimental method and setup. §3.8 describes how the viscoelastic measurements obtained from the experiments were analysed. §3.9 describes the sample preparation and swelling procedure for the swelling experiments as well as the calculations involved to measure the cross-link density.

3.2 Materials

3.2.1 Silicones

As mentioned in Chapter 2, the Swanson finger implant, the NeuFlex finger implant and the Soft skeletal finger implants are currently manufactured from three medical-grade silicones, sold under the trade name of FLEXSPAN® (NuSil Silicone Technology, Lake Mary, FL 32746, USA), Anasil (DePuy Orthopaedics, Inc, Warsaw, IN 46581, USA) and Silflex II (Small Bone Innovations, Inc, Morrisville, PA 19067, USA), respectively. However, the manufacturers restrict the supply of these silicones. They do, however, supply “restricted” materials intended for short-term (29 day) or medium-term (90 day) implantation.

The medical grade silicones used in this study are listed in Table 3.1, where the prefixes "C6" and "MED" refer to the short-term implantable materials and "Q7" refers to the Silastic® medium-term implantable material.

Table 3.1: Summary of the grades of silicone used in the study

Grade	**Silica Filler content (%) by mass**	**Batch number**	**Supplier**
C6-165	30-60	0002076802	Dow Corning Limited, Allesley, Coventry, CV5 9RG, UK
C6-180	30-60	0002382957	
Q7-4720	15-40	(10)0003082728	
Q7-4735	15-40	(10)0003788771	
Q7-4780	30-60	(10)0003771899	
MED-	40	04080MED0000DM	Polymer Systems Technology Limited*, High Wycombe, Bucks. HP12 3RF, UK
MED-82-5010-80	30	Supplied as a 2 mm thick cured silicone sheet (228.6 x 304.8 mm). LOT NO: 33746	

* UK distributor for NuSil Technology LLC, Lake Mary, FL 32746, USA.

Table 3.2 and Table 3.3 summarise the composition and mechanical properties of both the short and medium-term silicones. The properties of FLEXSPAN (currently used to manufacture the Swanson finger implant) and HP-100 Silastic (formerly used to manufacture the Swanson finger implant) have been included for comparison.

Table 3.2: Mechanical properties for the different silicone grades (Part I) according to the suppliers' data sheets.

Grade	**C6-165**	**C6-180**	**MED-82-5010-80**	**MED-4080**	**HP-100 Silastic**	**FLEXSPAN**
Durometer Hardness (Type A)**	61	77	45-55	73-83	55	52-60
Tear Strength (kN/m)	42.2	39.1	44.1	37.9	52.5	45.5
Tensile Strength (MPa)	8.1	7.2	10	7.9	9.65	7.58
Elongation to failure (%)	940	610	1000	700	600	630
Density, ρ_p (kg/m^3)	1210	1210	1160	1210		1100-1160
Silica filler (%) by mass	30-60	30-60	30	40	Not disclosed by supplier.	
Silica filler surface area (m^2/g)	Within the range of 180-400. Exact value not disclosed by supplier.		200	200		
Silica filler particle diameter ($10^{-9}m$)	Within the range of 7-15. Exact value not disclosed by supplier.		14	14		

** Durometers are commonly used to measure the hardness of an elastomer by applying a force to the material and measuring the resulting indentation depth in the material (ASTM D2240-00; Aziz *et al.*, 2003; BS EN-ISO-868:2003; BS ISO-7619-1:2004; Polyzois *et al.*, 1994). A Type A durometer is used on softer materials such as elastomers (ASTM D2240-00; BS EN-ISO-868:2003; BS- SO-7619-1:2004; Polyzois *et al.*, 1994; Sweeney *et al.*, 1972).

Table 3.3: Mechanical properties for the different silicone grades (Part II) according to the suppliers' data sheets.

Grade	Q7-4720	Q7-4735	Q7-4780
Durometer Hardness (Type A)	23	36	77
Tear Strength (kN/m)	32	36.2	41.7
Tensile Strength (MPa)	9	9.3	7.8
Elongation to failure (%)	1310	1180	660
Density, ρ_p (kg/m^3)	1110	1120	1200
Silica filler (%) by mass	15-40	15-40	30-60
Silica filler surface area (m^2/g)	Within the range of 180-400. Exact value not disclosed by supplier.		
Silica filler particle diameter (nm)	Within the range of 7-15. Exact value not disclosed by supplier		

3.2.2 Elast-Eon™ 3

The Elast-Eon™ 3 used was supplied by the manufacturer (AorTech Biomaterials Pty Ltd, Frenchs Forest, Australia) as cured cylinders of material, for previous work, in 2002 (Shepherd and Johnstone, 2005). The mechanical properties of the material are listed in Table 3.4. It was then stored in air, at room temperature, in the dark, until 2007.

Table 3.4: Summary of the properties of Elast-Eon™ 3 obtained from the supplier. Results were obtained from compression moulded sheets, pre-treated at ambient conditions for a minimum of 7 days.

Property	Result
Durometer Hardness (Type A)	78
Tensile strength (MPa)	18
Tensile Stress at 100% strain (MPa)	5
Tensile Strain at break (%)	630

3.2.3 Nagor ® medium hardness medical grade silicone

This medical grade silicone has a similar hardness to Elast-Eon™ 3, and likely to have similar mechanical properties, hence it was used as a comparison material; see Chapter 6. The silicone was supplied as a cured 17 mm thick carving block with dimensions (70 x 20 mm) by Nagor Limited (Isle of Man, IM99 1AX, British Isles).

3.3 Methods

3.3.1 Silicone mixing

The silicones used in this study were supplied in two parts, Parts A and B (Malczewski *et al.*, 2003). They were prepared by mixing Parts A and B (35 g of each) at room temperature. Following the supplier's instructions, Part B was placed on a Schwabenthan Berlin two-roll-mill (Engelmann & Buckham Ltd, Alton, Hampshire, GU34 1HH, UK), shown in Figure 3.1. After 2 minutes, Part A was fed onto the two-roll mill and allowed to mix into Part B and roll backwards and forwards for two minutes, as shown in Figure 3.2.

Figure 3.1: Schwabenthan Berlin two-roll mill (Engelmann & Buckham Ltd, Alton, Hampshire,UK).

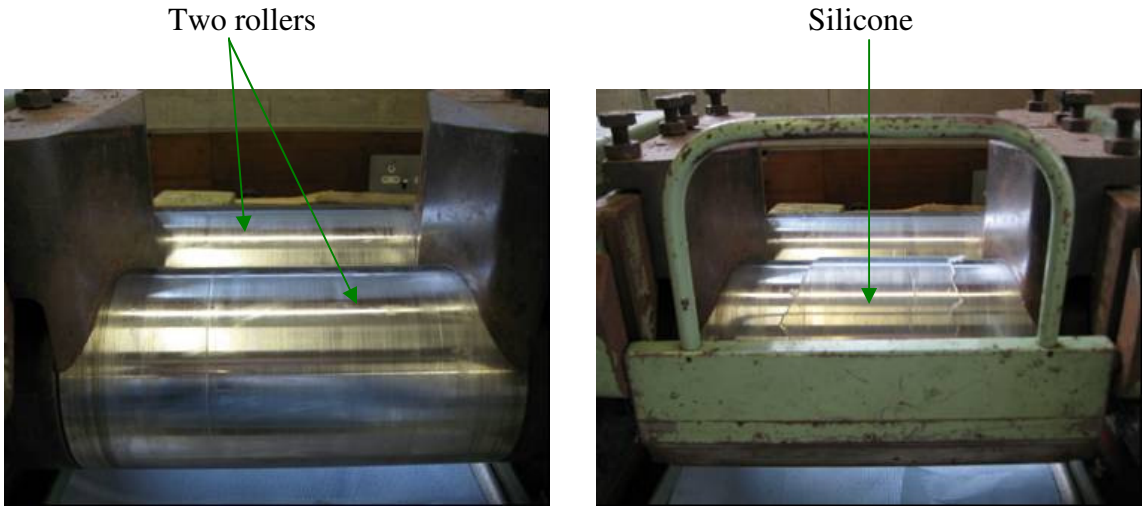

Figure 3.2: A closer view of the two rollers on the two-roll mill before (left hand side) and during (right hand side) the mixing process of the silicone.

The silicone was then removed from the two-roll mill with a pair of tongs and fed immediately back into the two-roll-mill as shown in Figure 3.3 and Figure 3.4. This removal and re-feeding was repeated at one minute interval for ten minutes. The purpose of this was to ensure that Parts A and B were thoroughly blended together.

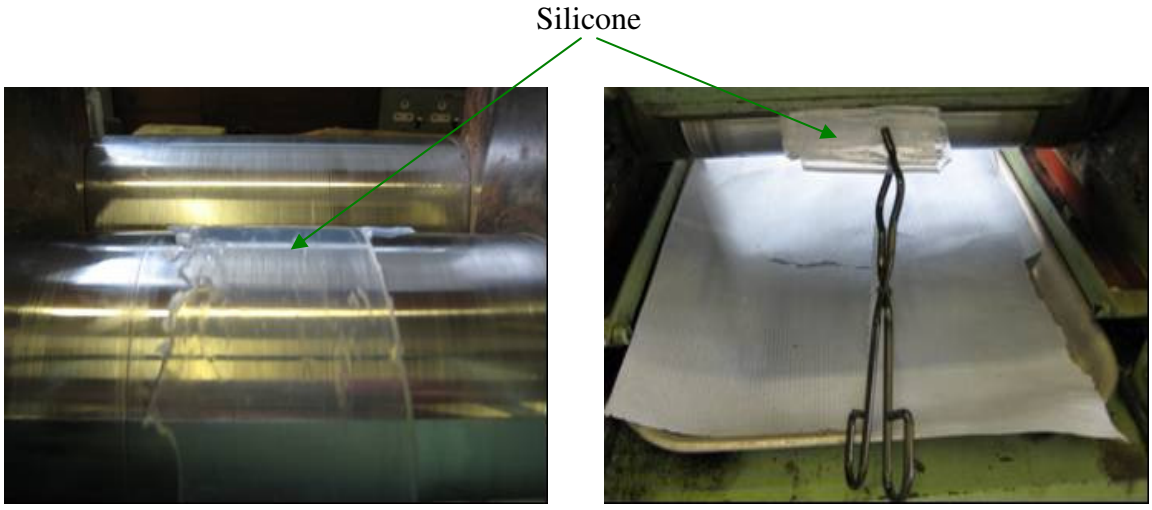

Figure 3.3: Silicone being mixed (left hand side) and removed (right hand side) from the two-roll mill.

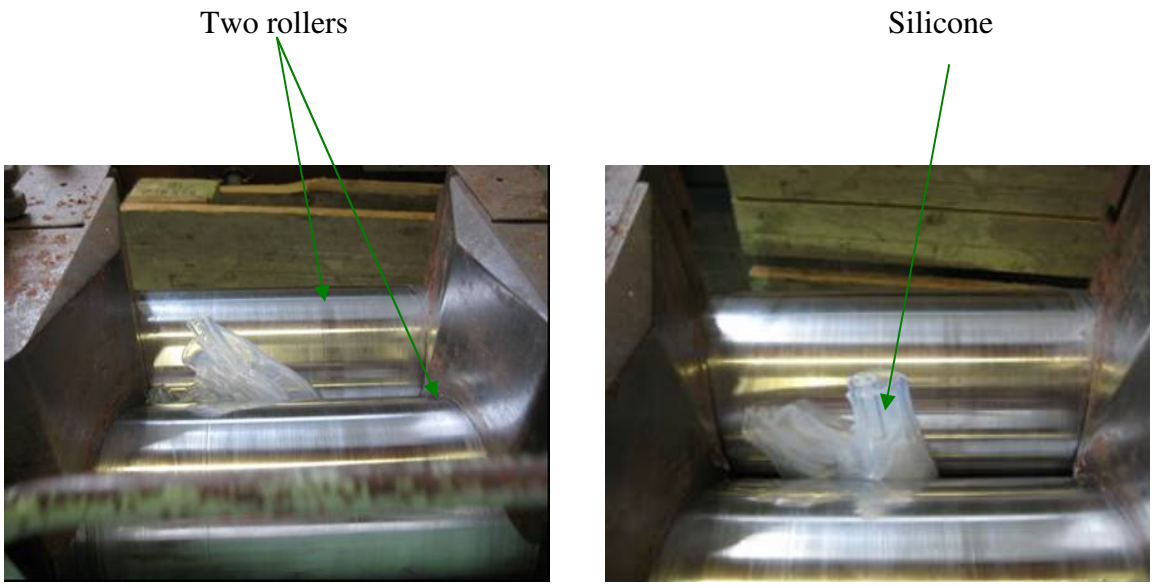

Figure 3.4: Silicone being replaced back into the two-roll mill for further mixing.

Once the mixing was completed, the next stage depended on what test the material was to be used for. The mixed silicone was made into: cylindrical specimens for the compression tests (see §3.3.2); dumb-bells for the tension tests (see §3.3.3); rectangular pieces for solvent swelling experiments (see §3.9).

3.3.2 Silicone cylinders for compression tests

3.3.2.1 Cylindrical moulds

The purpose of making a specimen mould was to ensure that cylindrical specimens of the same size (29 mm in diameter and 13 mm thick) could be produced. The size of the specimens was chosen in order to satisfy the British standard (BS 903-A6:1992). This is important for silicones, because the ratio of the radius to thickness of cylindrical specimens can strongly influence the results (Mahomed *et al.*, 2009; Menard, 1999; O'Sullivan *et al.*, 2003).

I designed and made the specimen mould shown in Figure 3.5 (refer to Appendix C for a CAD drawing with dimensions). It was made from a 13 mm thick PTFE (polytetrafluoroethylene) sheet supplied by RS Components Ltd. (Corby, Northants, NN17 9RS, UK), with overall dimensions of 205 × 85 × 26 mm and consisted of two parts. The top part had ten specimen holes (29 mm diameter and 13 mm thick) and the bottom part was a solid PTFE sheet, screwed against the top part. The purpose of the bottom part was to act as a cover and ensure that, when compressed, the specimen would retain its cylindrical shape and would not stick to the base of the hot press. PTFE was chosen because the silicone does not stick to it, so that the specimens could be easily removed.

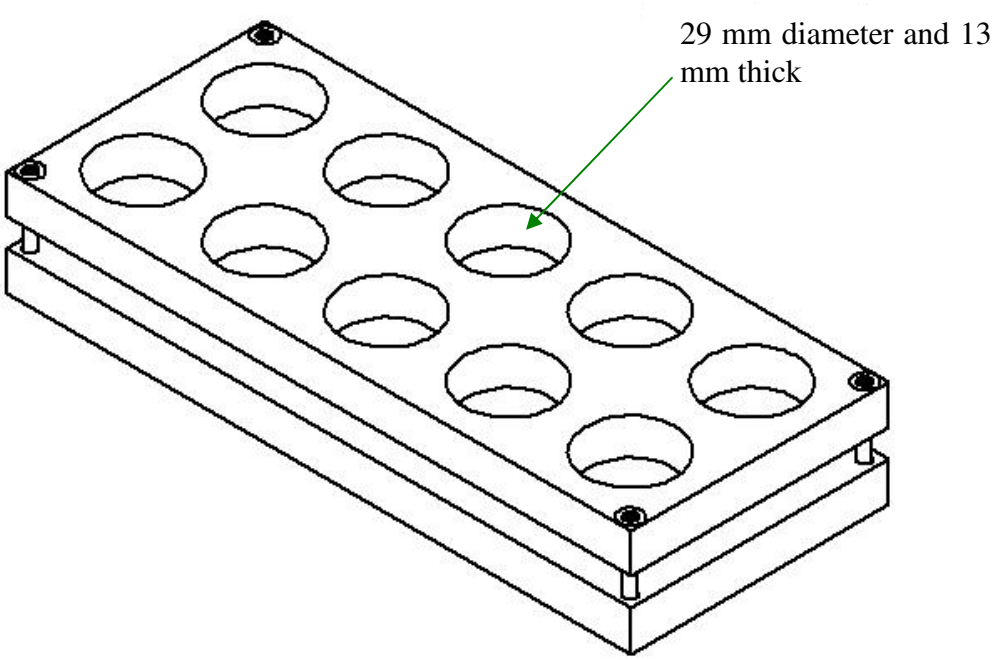

Figure 3.5: PTFE specimen cylindrical mould.

In order to ensure that the moulds and their contents were kept free from dirt and dust particles, the moulds were covered with a PTFE sheet, as shown in Figure 3.6. A steel plate was also placed on top of the PTFE sheet before the curing process.

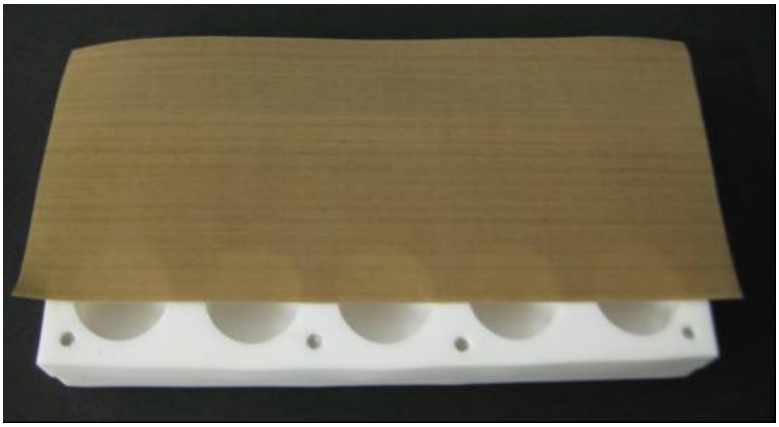

Figure 3.6: Cylindrical mould with PTFE sheet.

3.3.2.2 Curing of specimens

A Moore E1127 hydraulic hot press (George E Moore & Son Ltd, Birmingham, UK), shown in Figure 3.7, was used to cure the specimens. Following the supplier's instructions, the hot press was pre-heated to 116 ºC to ensure even distribution of heat. The mould was then placed on the bottom plate of the hot press and the latter levered upwards towards the top plate. Once the top plate and the mould came into contact with each other, as shown in Figure 3.9, the mould was compressed at a load of 50 kN in order to evenly distribute the silicone. The specimens were then cured for 3 h at 116 ºC. These conditions were recommended by the silicone supplier and have been used in previous silicone research (Leslie *et al.*, 2008a; Leslie *et al.*, 2008b).

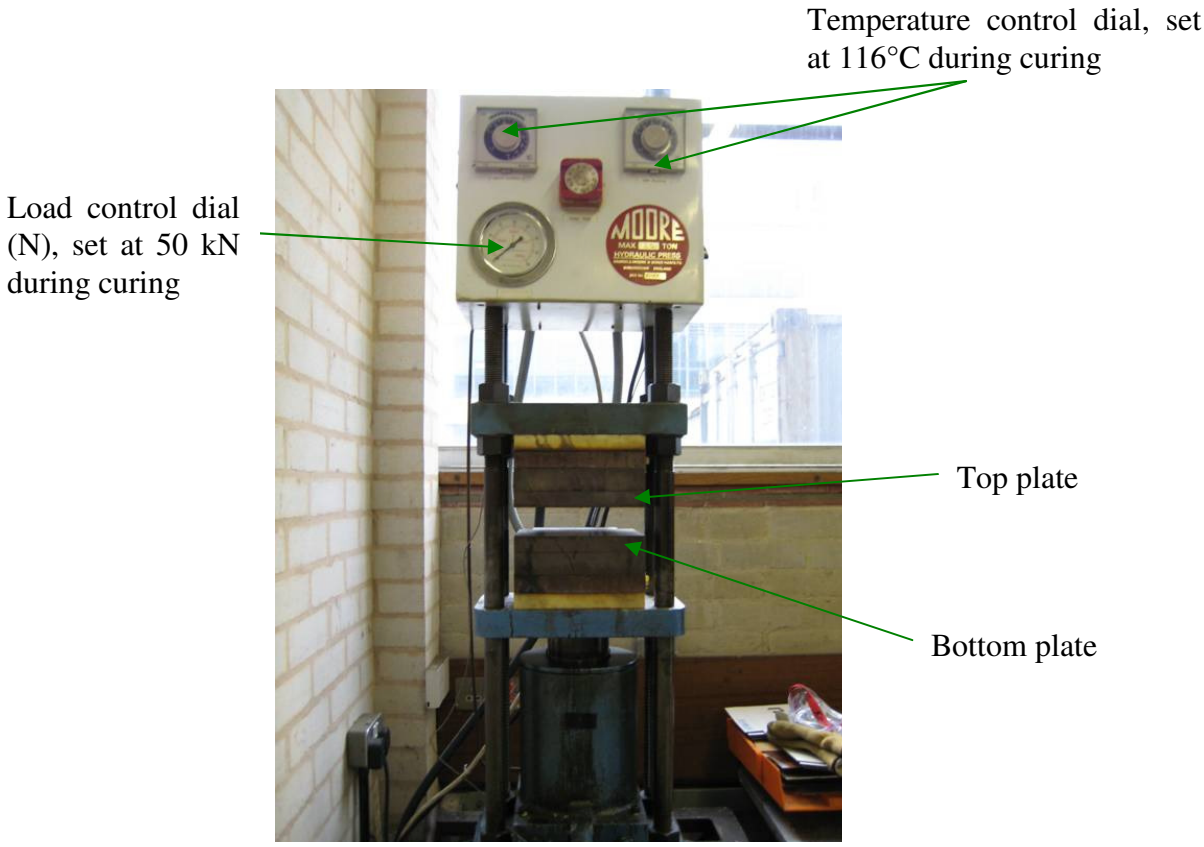

Figure 3.7: The Moore E1127 hydraulic hot press used to cure specimens.

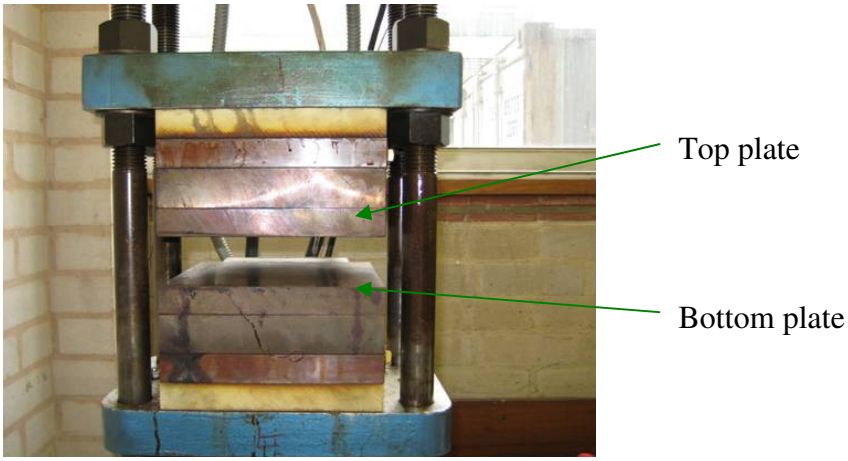

Figure 3.8: Closer view of the plates of the hot press.

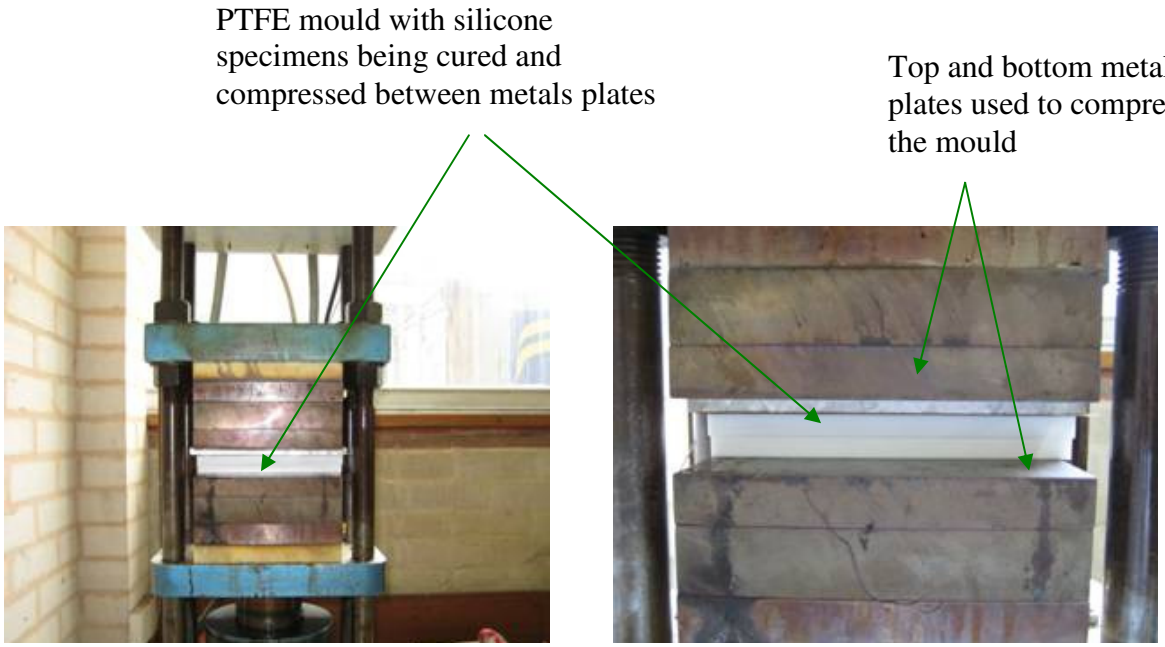

Figure 3.9: Closer views of the contact between the mould and the top plate of the hot press.

Once cured, the batch of specimens was allowed to cool for approximately 24 h and then removed from the mould. Figure 3.10 shows a cured cylindrical silicone specimen. The sizes of the cured specimens were measured using digital callipers. The thickness of all 10 specimens was 12.5 ± 0.5 mm as required by the standard. In some batches, specimens were produced outside this size-range and were discarded.

Each batch of ten specimens, was placed in a resealable bag, given a batch number and dated, so that batches produced at different times could be identified. Specimens were stored in a closed storage cupboard at room temperature under normal atmospheric conditions, until removed for testing.

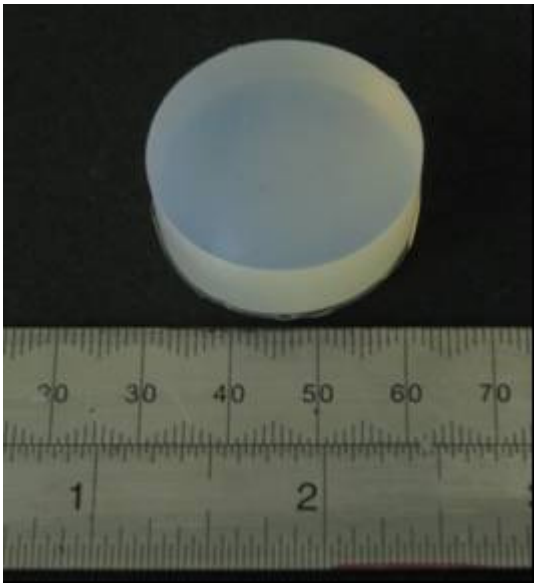

Figure 3.10: Cured cylindrical silicone specimen.

3.3.3 Silicone dumb-bells for tension tests

The mixed silicone in §3.3.1 was placed in a rectangular metal mould measuring 175 × 150 mm and made into 2 mm thick silicone sheets. The mould consisted of a metal mould with an opening of 175 × 150 mm cut into in, sandwiched between two metals plates lined with PTFE sheets, as shown in Figure 3.11.

Figure 3.11: Mould lined with PTFE sheets.

The mould was placed on the bottom plate of a pre-heated (116 ℃) Moore E1127 hot press (George E Moore & Sons Ltd, Birmingham, UK). The bottom plate was levered towards the top plate of the press until there was contact between the mould and the top plate. The mould was then compressed under a 100 kN load in order to evenly distribute the silicone.

Following the supplier's instructions, the silicone sheet was cured at a temperature of 116 ^{o}C for 12 min; the same method has been used previously (Leslie *et al.*, 2008a; Leslie *et al.*, 2008b). Each sheet was allowed to cool, for 1 h and then removed from the mould. After 24 h, six dumb-bells whose dimensions are shown in Figure 3.12 were cut from each sheet using a hand-operated cutter (Wallace Instruments, Kingston, UK). The sizes of the dumb-bells were measured using digital callipers and the dimensions of all the dumb-bells complied with the British standard (BS 903-A2:1995). Each batch of six dumb-bells, were placed in a resealable bag, given a batch number and dated. Dumb-bells were stored in a closed storage cupboard at room temperature under normal atmospheric conditions, until removed for testing.

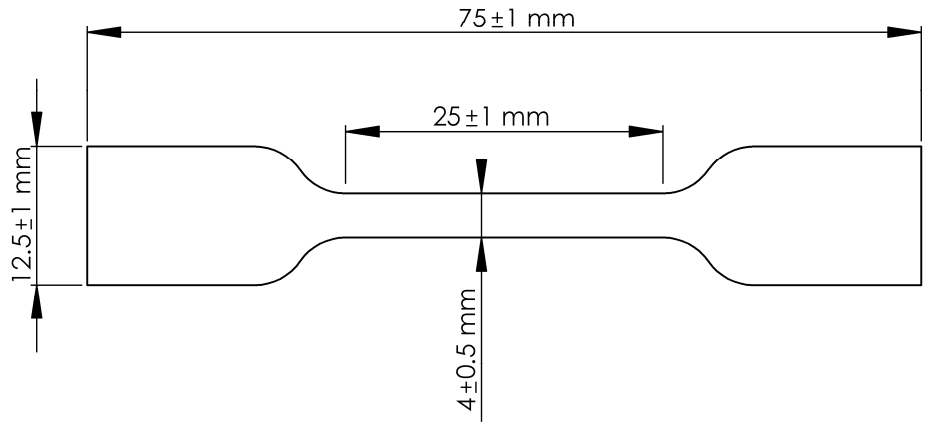

Figure 3.12: Shape and dimensions of a Type 2 dumb-bell test piece. Dimensions satisfy British Standard (BS 903-A2:1995).

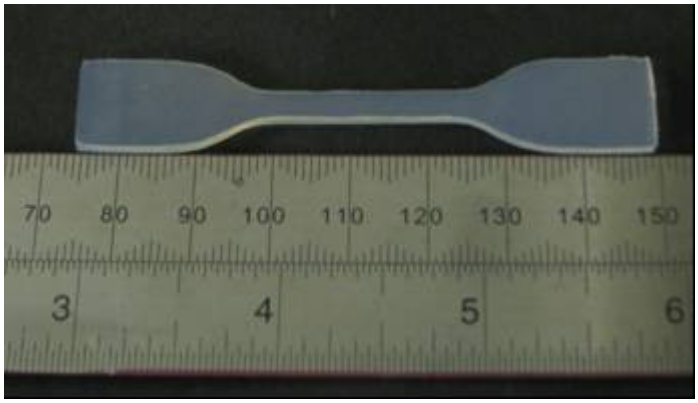

Figure 3.13: Cured silicone Type 2 dumb-bell test piece.

3.3.4 Nagor® silicone carving block

The original carving block was cut into 11 rectangular pieces (70 x 6 x 20 mm). These pieces were held on a Colchester 5*20 Chipmaster lathe (Rockwell Machine Tools Ltd, Redditch, B98 7SY, UK) and were to cut into six cylindrical silicone specimens (15 mm diameter, 6 mm thickness) using a compass with a blade. The resulting test specimens complied with the aspect ratio in the British standard (BS 903-A6:1992) for compression testing of rubber specimens. The cylinders were stored in a closed storage cupboard at room temperature under normal atmospheric conditions, until removed for testing.

3.3.5 Elast-Eon™ 3 cylinder

The original Elast-Eon™ 3 cylinder was cut into six cylindrical specimens (diameter 5 mm, thickness 2.2 ± 0.2 mm) on a Colchester 5*20 Chipmaster lathe (Rockwell Machine Tools Ltd, Redditch ,B98 7SY, UK). The specimen's aspect ratio complied with British standard (BS-903-A6:1992) and the storage conditions of the cylinders were as described in §3.3.4.

3.4 Pre-treatment of cylindrical specimens and dumb-bells before testing

3.4.1 Silicone cylinders and dumb-bells

As the silicones described in this chapter are suitable for use in the human body, it is important that they are exposed to *in vivo* conditions before and during the tests. *In vivo* conditions can be simulated by immersing in physiological saline solution (9.5 $g.L^{-1}$ of sodium chloride in deionised water) at 37°C (body temperature) (Doi *et al.*, 1984; Joyce and Unsworth, 2002a; Kennan *et al.*, 1997; Stokoe *et al.*, 1990). Therefore, six cylindrical specimens and dumb-bells of silicone grades C6-165, C6-180, MED-82-5010-80 (only dumb-bells) and MED-4080, were put into containers (for cylindrical specimens) and test-tubes (for dumb-bells) with saline solution and placed in a Grant JB2 series BAT3042 water bath (Scientific Laboratory Supplies Limited, Wilford, Nottingham, UK) at 37°C for 24 hours and then tested.

It is also possible that the length of time of exposure to *in vivo* conditions affects the properties of the elastomers. Therefore, after the initial testing described above, the specimens were placed back into the bath for 29 days (short-term) and then tested again. Similarly, six cylindrical specimens of Silastic® grades Q7-4720, Q7-4735 and Q7-4780 were also pre-treated in saline solution at 37°C for 90 days (medium–term) and then tested. For comparison, six cylindrical specimens of grade C6-165 and MED-4080 that had not been pre-soaked in saline solution were removed from the storage cupboard and tested.

It is also possible that the temperature of the saline solution affects the properties of the elastomers. Therefore, six cylindrical specimens of grade MED-4080 were placed into containers with saline solution and returned to the storage cupboard. They were only removed from the cupboard at the time of testing and were immersed in saline solution at 23°C (room temperature) during the test.

3.4.2 Nagor® silicone and Elast-Eon ™ 3 cylinders

There is the possibility that exposing the specimens to accelerated aging conditions can affect the material properties. Therefore, six specimens of each material were aged by immersing them in physiological saline solution and placing them in a Carbolite natural convection laboratory oven (Carbolite, Hope Valley, S33 6RB, UK) at 70°C for 38 days, equivalent to aging for a year at 37°C, as described in §2.8. As a control, an Elast-Eon™ 3 specimen was immersed in physiological saline solution and placed in a Grant JB2 series BAT3042 water bath at 37°C for six months. The cylinder was tested three times before and after being in the bath.

3.5 Specialist equipment required for the compression tests

3.5.1 Design criteria of the cylindrical specimen holder

In order to be able to carry out a test, the specimen has to be put into a holder. This holder has to allow the specimen to be compressed and has to be able to store physiological saline solution at 37°C (body temperature). The holder has to be able to fit and be tightly secured onto the testing machine.

3.5.2 Principles to achieve

One possible solution to meet the design criteria is to model the holder as a pot with a water jacket. The water jacket can be connected to a bath at 37°C. This would allow the specimen to be immersed in physiological saline solution while being surrounding by a heated jacket to maintain the temperature of the physiological saline solution at 37°C. An extension is also needed in order to be able to fit the holder onto the testing machine and allow the specimen to be compressed. The diameter of the extension should be greater than that of the specimen being compressed.

3.5.3 Principles of implementation: making the parts

3.5.3.1 Specimen holder

I made the parts described in this section and in §3.6 in the workshop at the School of Metallurgy and Materials with the assistance of the technicians. More detailed CAD drawings with dimensions are in Appendix C.

I chose to make the pot using two Perspex tubes attached to Perspex bases as shown in Figure 3.14. All necessary attachments were made using Perspex glue, Tensol 12 (Bostik Ltd., Common Road, Stafford, Staffordshire, ST16 3EH, UK).

The dimensions of the cylinders were as follows:

- outer cylinder with a 64 mm (inner diameter) and 70 mm (outer diameter) and a height of 150 mm;
- inner cylinder with a 44 mm (inner diameter) and 50 mm (outer diameter) and a height of 90 mm.

A bleed hole (shown in Figure 3.14), was drilled into the holder to allow the air to be bled out. A lid was made to minimise heat loss and evaporation. The lid had a small opening (as shown in Figure 3.14b), where a thermometer could be inserted to monitor the temperature of the physiological saline solution. The other purpose of the opening is to accommodate the extension (described in §3.5.2 and §3.5.3.2), which is required for testing. Holes were drilled onto the base of the holder as shown in Figure 3.14, so that screws could be used to fasten the holder securely to the base of the testing machine.

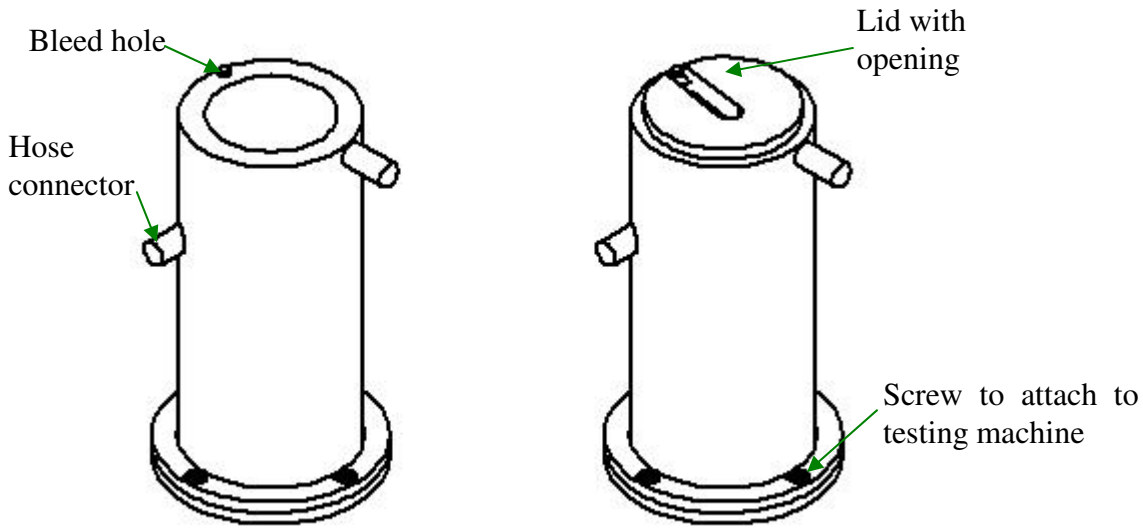

Figure 3.14: a) Specimen holder without a lid (left hand side) and b) with a lid (right hand side).

3.5.3.2 Compression brass extension

The extension was made from brass. Brass was chosen because it is easy to machine and does not corrode in contact with physiological saline solution. A hole was drilled and tapped with a No 10 UNF[1] thread on the top of the extension so that, it could be securely attached to the machine. The dimensions of the extension are shown in Figure 3.15. A CAD drawing with dimensions is in Appendix C.

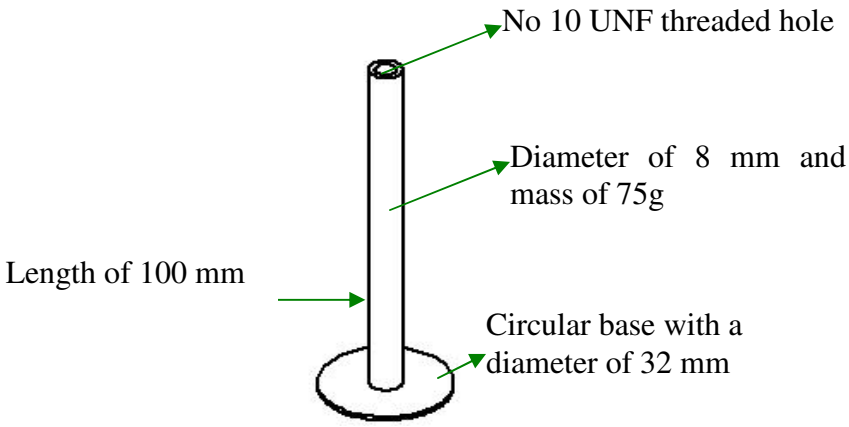

Figure 3.15: Brass extension.

3.5.3.3 Water bath and heating circulator

A water bath with a lid was made from 10 mm thick Perspex sheets. Perspex glue, Tensol 12 (Bostik Ltd., Common Road, Stafford, Staffordshire, ST16 3EH, UK) was used to attach the parts of the bath together. Final dimensions of the bath were 200 x 200 x 200 mm (refer to Appendix C for a CAD drawing with dimensions).

---

[1] Uniform national fine

3.5.4 Principles of implementation: Testing

During a test, the holder was attached to the water bath with a Julabo ED series BAT5300 water heating immersion circulator (supplied by Scientific Laboratory Supplies Limited, Wilford, Nottingham, UK), using silicone hoses and hose connectors. The water in the bath was pumped continuously into the jacket of the holder. The specimen was placed in the inner cylinder of the holder containing physiological saline solution and surrounded by a water jacket stored in the outer cylinder. During the preliminary tests, the temperature of the physiological saline solution in the holder was measured using a digital thermometer. These measurements showed that, because of heat losses, the temperature in the bath had to be set to 40°C, in order to maintain the physiological saline solution in the holder at 37°C. The preliminary tests also showed that, if the temperature of the bath was 40°C, it would take ≈ 30 minutes to heat the saline solution to 37°C from room temperature.

3.6 Specialist equipment required for the tension tests

3.6.1 Design criteria of the dumb-bell holder

The criteria mentioned here is similar to the one discussed in §3.5.1. In order to be able to carry out a test, the dumb-bell has to be put into a holder. This holder has to allow the dumb-bell to be gripped by two stainless steel dumb-bell grips and undergo tensile tests. The holder has to be able to store physiological saline solution at 37°C (body temperature). It has to fit and be tightly secured on to the testing machine.

3.6.2 Principles to achieve

One possible solution to meet the design criteria is to model the holder as a pot with physiological saline solution. The holder can be connected to a bath at 37°C. This would allow the dumb-bell to be immersed in physiological saline solution at 37°C. An extension is also needed in order to be able to fit the holder onto the testing machine and allow the dumb-bell to undergo tension tests.

3.6.3 Principles of implementation: making the parts

I chose to make the dumb-bell holder using a Perspex cylinder attached to a Perspex base as shown in Figure 3.16 (refer to Appendix C for a CAD drawing with dimensions). All necessary attachments were made using Perspex glue, Tensol 12 (Bostik Ltd., Common Road, Stafford, Staffordshire, ST16 3EH, UK). The dimensions of the cylinder were 145 mm (inner diameter) and 150 mm (outer diameter) and a height of 200 mm. A hole was drilled and tapped (No 10 UNF thread) onto the base of the holder to securely attach the bottom dumb-bell grip. An extension was made from brass and holes were drilled and tapped (No 10 UNF thread), at the top and the bottom of the extension, to attach the top grip to the testing machine. The dimension of the extension was a 105 mm (length) rod with a 8 mm diameter.

A lid with a small opening (as shown in Figure 3.16) was made to minimise heat loss and evaporation. The reasons for the opening were discussed in §3.5.3. Holes were drilled onto the base of the holder as shown in Figure 3.16, so that screws could be used to fasten the holder securely to the base of the testing machine. The final design is shown in Figure 3.17.

3.6.4 Principles of implementation: Testing

During a test, the holder was attached to a bath with physiological saline solution and a Julabo ED series BAT5300 water heating immersion circulator (Scientific Laboratory Supplies Limited, Wilford, Nottingham, UK), using silicone hoses and hose connectors. The bath described in §3.5.3.3 was also used for these tests. The physiological saline solution in the bath was pumped continuously into the holder. The grips and then the dumb-bell were put into the holder, as shown in Figure 3.17. Further information on the grips is given in §3.6.5.

During the preliminary tests, the temperature of the physiological saline solution in the holder was measured using a digital thermometer. These measurements showed that, because of heat losses, the temperature in the bath had to be set to 38°C, in order to maintain the physiological saline solution in the holder at 37°C. The preliminary tests also showed that, if the temperature of the bath was 38°C, it would take ≈ 20 minutes to heat the saline solution to 37°C from room temperature.

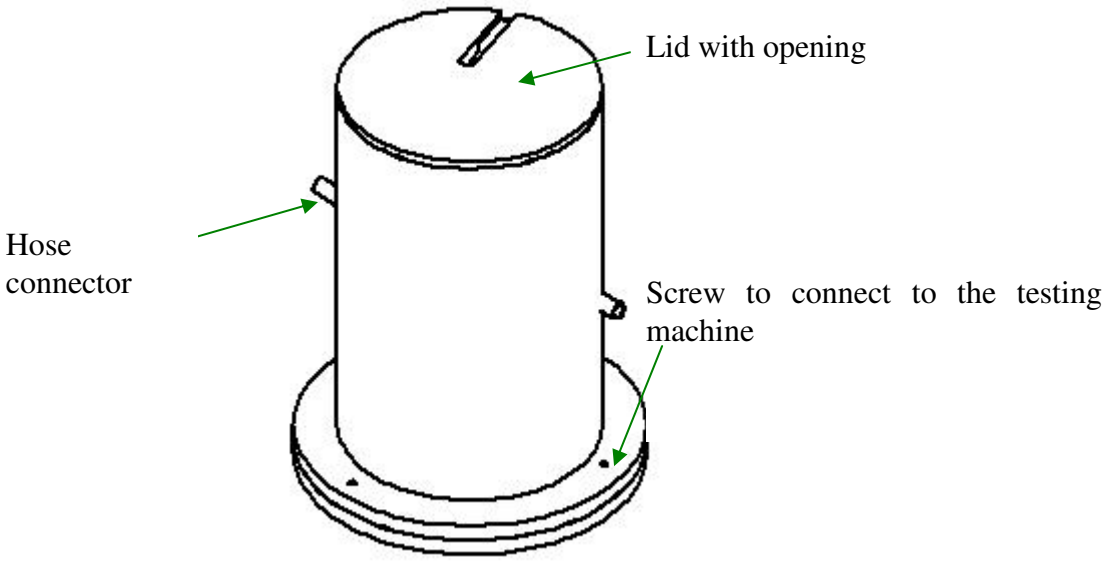

Figure 3.16: Dumb-bell holder with a lid.

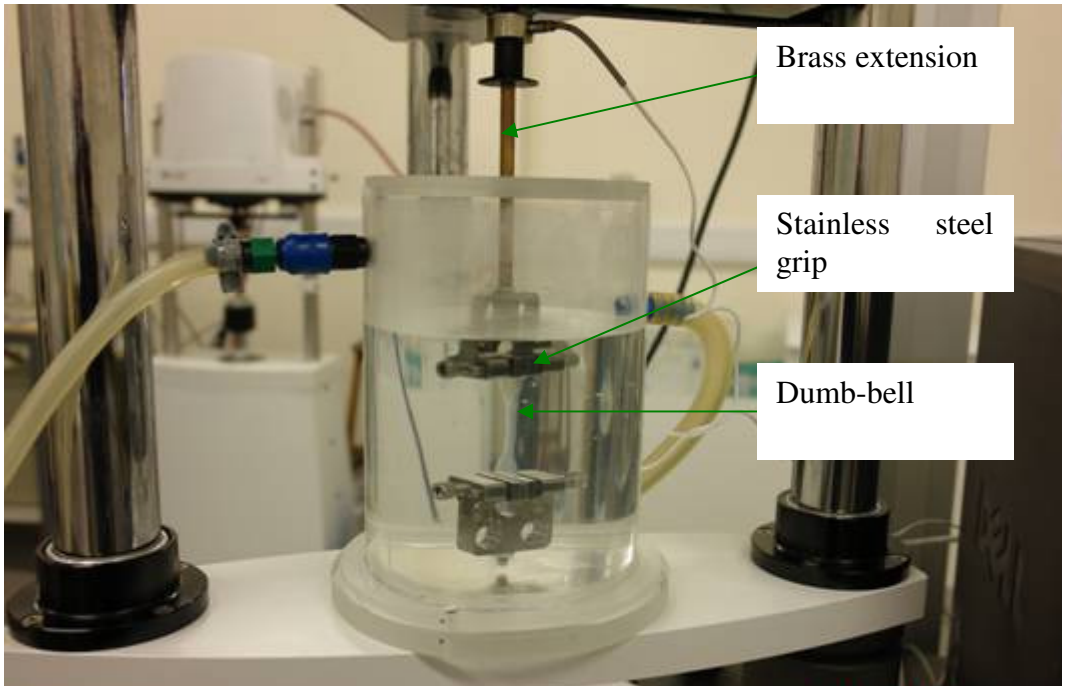

Figure 3.17: Silicone dumb-bell securely attached onto two grips.

3.6.5 Grips

The grips used are intended for use on silicones and were supplied by the testing equipment manufacturer (BOSE Corporation, ElectroForce Systems Group, Minnesota, USA). The area of the grip that grips the dumb-bell have roughened surfaces (shown in Figure 3.18), in order to prevent slippage of the dumb-bell during testing. The screws on both sides of the grip (shown in Figure 3.18) are used to tighten the dumb-bell securely into position.

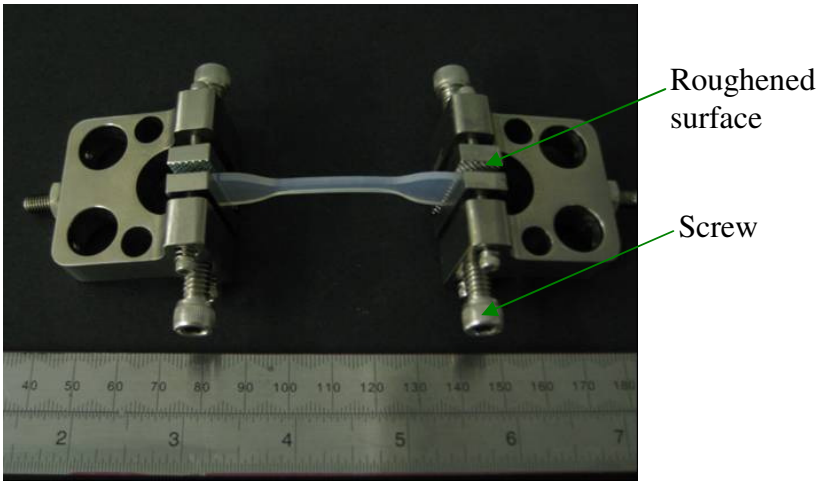

Figure 3.18: Stainless steel grips with dumb-bell.

3.7 Experimental method

3.7.1 Testing equipment

All the measurements of the viscoelastic properties of the elastomers were done on an ELF 3200 (BOSE Corporation, ElectroForce Systems Group, Minnesota, USA) with a 225 N load cell (nominal precision ±0.005 N) and a frame stiffness of > 4000 N/mm (with a standard load cell) or > 8000 N/mm (without a load cell). Based on dimensions given by the manufacturer, the mechanical stability of the frame of the ELF 3200 was calculated as follows: maximum deflection at the centre of the crosshead = 5.44 x 10^{-4} mm; maximum deflection at the centre of the columns = 4.34 x 10^{-4} mm.

3.7.2 Experimental setup and testing for the silicone and Elast-Eon ™ compression cylinders

3.7.2.1 Setup

Figure 3.19 shows the complete experimental set up and equipment for the tests. Figure 3.20 and Figure 3.21 show closer images of the experimental setup.

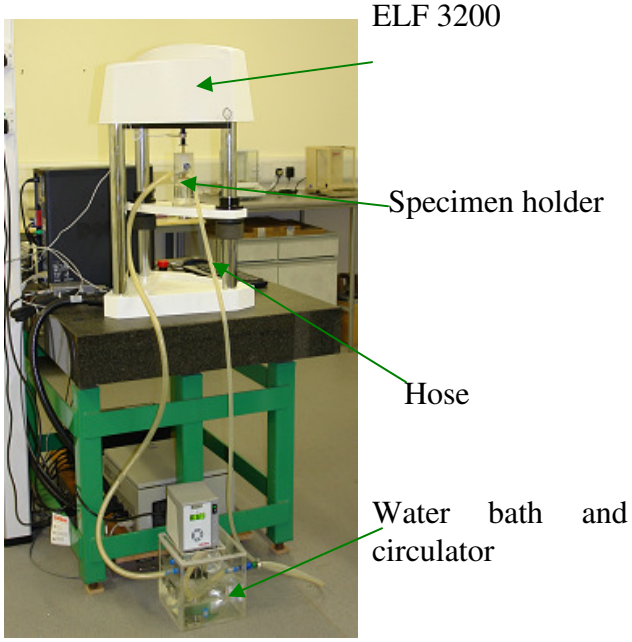

Figure 3.19: Complete experimental setup.

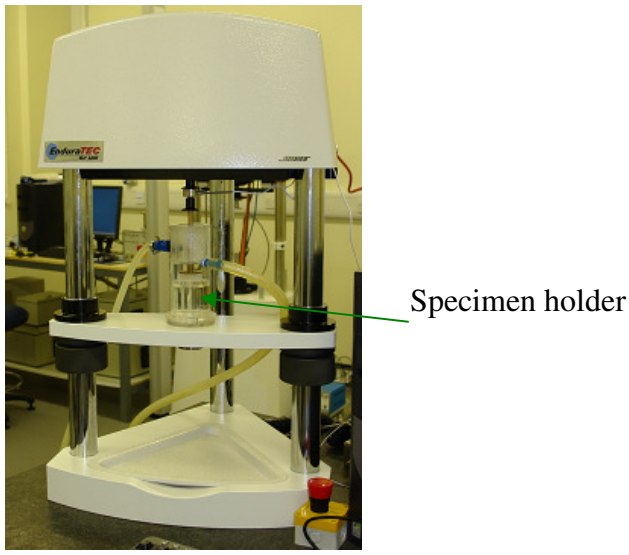

Figure 3.20: Closer view of specimen holder connected to ELF 3200.

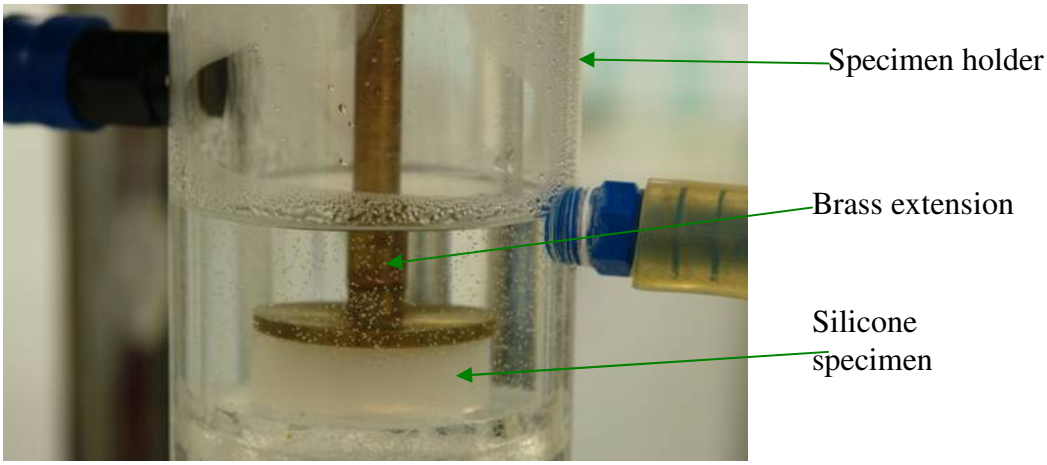

Figure 3.21: Closer view of holder showing the silicone specimen.

3.7.2.2 Measuring the viscoelastic properties

Preliminary quasi-static tests (at a strain rate of 0.004 s^{-1}; equivalent to a rate of 0.05 mm/s) showed that the plot of load against displacement had a linear portion centred around a static load of 40 N as shown in Figure 3.22, for grade C6-165. Similar plots for the other silicone grades and Elast-Eon^{TM} 3 are in Appendix D (§D.1 and §D.2). The assumption of linear behaviour has previously been discussed in Chapter 2 (§2.7.2).

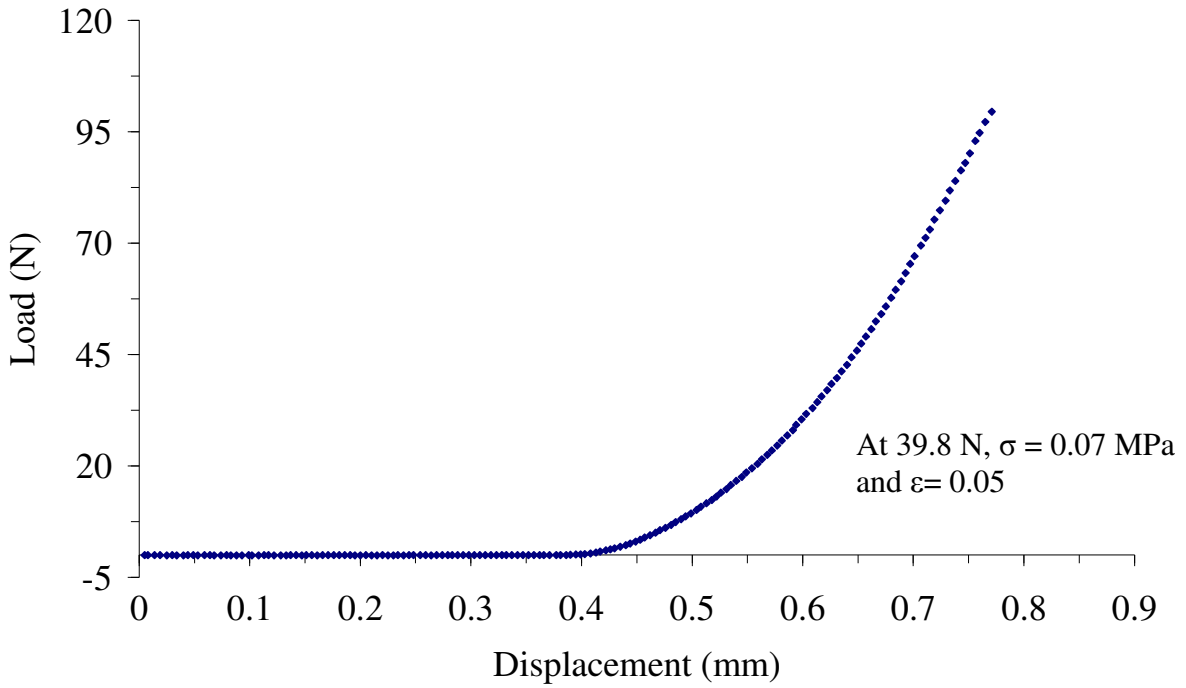

Figure 3.22: Preliminary plot of load against displacement for grade C6-165.

Therefore, six specimens of each grade were subjected to sinusoidal cyclic compression tests, oscillating 5 N either side of a load of 40 N over a frequency range of either 0.02-100 Hz or 0.02- 50 Hz. Preliminary results, suggested using the shorter frequency range for grade Q7-4720 and Q7-4735. Previous studies (Doi *et al.*, 1984; Joyce and Unsworth, 2000; Joyce and Unsworth, 2002b) suggested that frequencies of at least 10 Hz should be used to study finger implants, as under normal conditions, finger joints can operate at frequencies of up to 3 Hz (Joyce and Unsworth, 2002b; Serina *et al.*, 1997). Over the frequency range of 0.02-100 Hz, the loading cycles were applied at 22 different frequencies, which started at 0.02 Hz and gradually increased to 100 Hz. Four sinusoidal cycles were applied between 0.02-0.5 Hz. Above 0.5 Hz the number of cycles increased with the frequency, under the control of the standard machine software, reaching a maximum of 625 cycles at 100 Hz.

Similarly, over the frequency range of 0.02-50 Hz, the loading cycles were applied at 20 different frequencies, from 0.02 Hz to 50 Hz, reaching a maximum of 325 cycles at 50 Hz.

All the tests were controlled using the WinTest DMA software (BOSE Corporation, ElectroForce Systems Group, Minnesota, USA). Once a test started, the system ramped the load to 40 N and held it there for 5 seconds to allow for any creep or relaxation (discussed in §2.7.3 and §2.7.4) to occur before testing. Once the dynamic cycling had begun, the specimen was pre-cycled for 5 seconds to allow for specimen stabilisation before data were taken. Therefore, a 10 second rest period was allowed between each dynamic loading cycle, for the specimen to recover. These times were chosen after preliminary testing showed that they were adequate for the results to be reproducible.

3.7.2.3 Effect of testing at high frequencies

There was a potential problem in that the high frequency used in the tests could have led to an increase in temperature within the specimen. To investigate this potential problem, a Type T thermocouple supplied by RS Components Ltd. (Corby, Northants, NN17 9RS, UK), was inserted into one of the specimens during a test and the internal temperature of the silicone recorded. During the test, the thermocouple readings varied between 37.02°C and 37.15°C, so any internal temperature change was considered to be negligible. A photograph of the experimental setup has been included in Appendix E.

3.7.3 Experimental setup and testing of the dumb-bells

3.7.3.1 Setup

The setup was similar to the one shown in Figure 3.19.

3.7.3.2 Measuring the viscoelastic properties of the silicone dumb-bells

Preliminary quasi-static tests (at a strain rate of 0.004 s^{-1}) showed that the plot of load against displacement had an almost linear region centred around a displacement of 2.5 mm as shown in Figure 3.23, for grade C6-165. Similar plots for the other silicone grades are in Appendix D (§D.3).

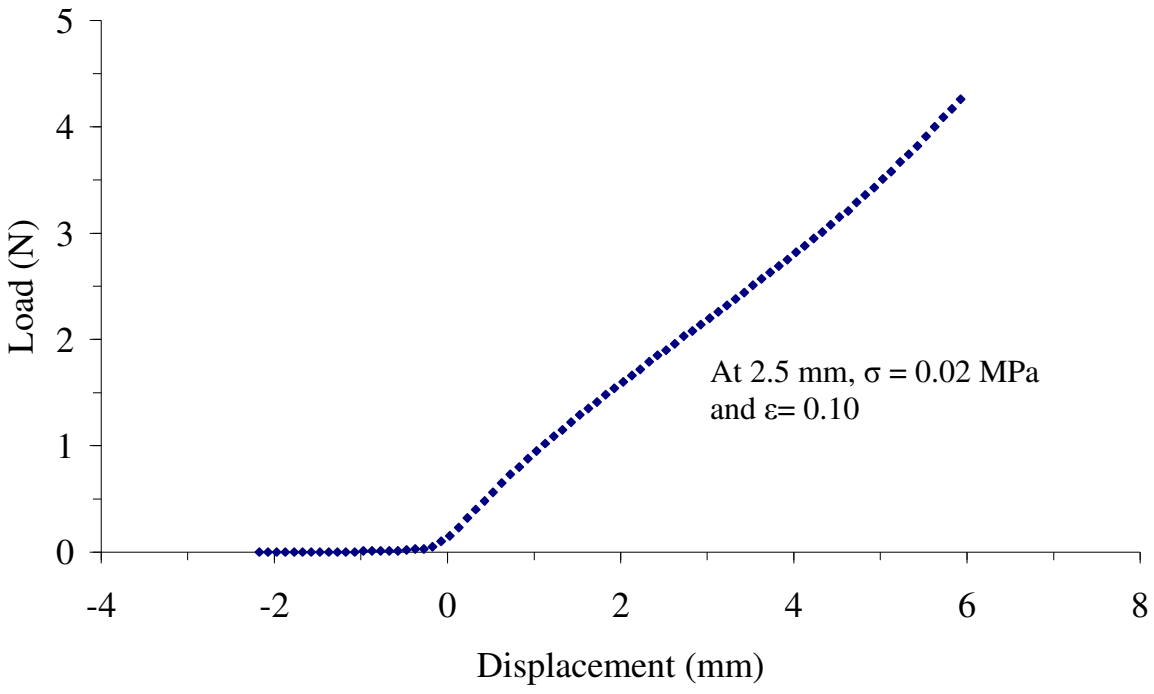

Figure 3.23: Preliminary plot of load against displacement for grade C6-165.

Cyclic tests were performed by subjecting each dumb-bell to an oscillation of 0.5 mm either side of a displacement of 2.5 mm (i.e. under displacement control) over a frequency range of 0.02-2 Hz. Before testing, each specimen was maintained at a constant displacement of 2.5 mm for 5 s, to enable stress relaxation to take place and pre-cycled at the loading frequency for 5 s to allow for specimen stabilisation. A rest period of 10 s was allowed between each testing frequency; these conditions were chosen to give reproducible results. Four sinusoidal cycles were applied at each frequency in the range 0.02-0.5 Hz; above 0.5 Hz, the number of cycles increased with frequency, under the control of the machine software, reaching a maximum of 14 cycles at 2 Hz.

3.7.4 Effect of damping on the experimental set up

3.7.4.1 Problems with Damping

During the preliminary phase of the testing it was noticed that the damping value calculated by the WinTest DMA software could vary from test to test. Results with high values of damping, resulted in unreliable measurements of E^*, E' and E'', while those with lower values of damping produced sensible and reliable measurements. Further information on this has been included in Appendix F.

3.7.4.2 Overcoming excessive damping

After analysing the experimental method, a possible reason for the high damping value was suggested. It was noticed that, after the specimens were inserted into the specimen holder, air bubbles appeared on the surface of the specimen, because the physiological saline solution was heated to 37°C.

This meant that if the experiments were run with these air bubbles on the surface of the specimen, then the machine was sinusoidally exciting the specimen and the air bubbles.

Precautions were taken to reduce the likelihood of air bubbles occurring by:

- allowing sufficient time for the physiological saline solution to stabilise at 37°C and hence allow sufficient time for the air bubbles to disappear from the solution;
- only inserting the specimen just prior to the start of running a test;
- removing any visible air bubbles from the specimen before the start of a test.

In some cases, even these precautions were not adequate and did not eliminate the damping problem. Therefore, the operator had to be aware that the results with high damping values could not be included in the analysis.

3.8 Analysis of the measurements from the experiments

To analyse the results in Chapter 4 and 5, mean values of E^*, E', E'' and $\tan\delta$ were calculated at each loading frequency, *f,* from the six measurements taken for each grade of silicone. The mean values are plotted against the logarithm (base 10) of *f*, measured in Hz. The log scale spreads out the results and makes it easier to see the data trends. In §4.3, the standard deviation of each datum point was calculated and shown as an error bar in the figures; upper bars only are shown for the grade with the highest modulus and lower bars only are shown for the grade with the lowest modulus, to make the graphs clearer.

Since graphs of E^*, E', E'' and $\tan\delta$ against $\log_{10}f$ deviated systematically from a straight line, the results were represented using suitable nth order polynomials of the form (Kreyszig, 2006):

$$E^* = a^*_0 + \sum_{i=1}^{n} a^*_i (\log f)^i \tag{3.1}$$

$$E' = a'_0 + \sum_{i=1}^{n} a'_i (\log f)^i \tag{3.2}$$

$$E'' = a''_0 + \sum_{i=1}^{n} a''_i (\log f)^i \tag{3.3}$$

$$\tan\delta = a_0 + \sum_{i=1}^{n} a_i (\log f)^i \tag{3.4}$$

The lowest order polynomials, which gave a smooth representation of a line through the data points, were chosen. All statistical calculations were performed using a spreadsheet (Excel 2003, Microsoft, Reading, UK). The coefficients of the polynomials plotted through the data points in the figures are also listed in tables. These coefficients can be used to calculate the values of E' and E'' for these silicones, in compression and in tension, over the frequency range: 0.02-50 Hz and 0.02-100 Hz (compression); 0.02-2 Hz (tension). In the tables, R^2 is the square of the correlation coefficient and it shows how well the polynomial curve fits the data (Bland, 2000). When $R^2 = 1$, there is a perfect correlation (Bland, 2000). For the figures in Chapter 8, the p value associated with R^2 is also given, to determine the significance of the result (calculated using Excel 2003, Microsoft, Reading, UK); a result was considered significant when $p < 0.05$ (Bland, 2000).

In Chapter 4 -6 , in order to compare the moduli of the specimens tested under the different conditions, described in §3.4, 95% lower and upper confidence intervals for the mean values were calculated by multiplying the standard error (equation 3.5) associated with each datum point on the graph, by 1.96 (James, 1993a; Kreyszig, 2006). Similarly, in Chapter 7, 95% confidence intervals were also used to compare the swelling measurements.

The standard error, *S*, is defined as (James, 1993a; Kreyszig, 2006):

$$S = \frac{s}{\sqrt{n}} \tag{3.5}$$

where *s* is the standard deviation; *n* is the number of measurements

These confidence intervals represent the regions in which there is a 95% probability of finding the true mean value (Kreyszig, 2006). Therefore, if the regions defined by the 95% confidence intervals for the two sample means overlapped, there was no significant difference between them at the 5% level (James, 1993a). In Chapter 5 and 6, and in some figures in Chapter 7, the error bars shown are the calculated upper and lower 95% confidence interval of each datum point. To avoid confusion, the figure captions state what the error bars represent.

3.9 Experimental method and calculations for the swelling experiments of silicone

3.9.1 Sample preparation and swelling

Sample pieces with dimensions of 10 × 10 × 2 mm, were cut from sheets of silicone grade C6-165, C6-180, MED-4080 and MED-82-5010-80. The method used to prepare the sheets was described in §3.3.1. Each sample was weighed on a digital balance (measurements done to four decimal places), then immersed into a test tube containing 5 ml of solvent and tightly closed, so that no solvent was lost through evaporation. The size of the tubes enabled the silicone samples to be surrounded by the solvent. The test tubes were placed in a Grant JB5 series BAT3046 water bath (Scientific Laboratory Supplies Limited, Wilford, Nottingham, UK) at 25°C.

This storage temperature for the sample and solvent has previously been used in other swelling studies (Andreopoulos *et al.*, 1993; Bueche, 1955b; Doležel *et al.*, 1989b; Orwoll, 1977; Summers *et al.*, 1972). The solvents used to swell the sample are listed in Table 3.5 and were used in previous studies (Favre, 1996; Yerrick and Beck, 1964). They were handled inside a fume cupboard and appropriate protective clothing was used.

Table 3.5: Solvents used for swelling (values from (Barton, 1983; Grulke, 1989; HAZDAT-Chemical-Hazards-Database)). The solubility parameter (δ_s) ***and the molar volume of the solvent (V_S) were discussed in §2.5.4.***

Solvent	Solubility parameter, δ_s ($MPa^{1/2}$)	Molar volume of the solvent, V_S (cm^3/mol)	Density, ρ_s (kg/m^3)
2,2,4-trimethylpentane	14.3	166.1	690
n-heptane	15.3	147.5	680
diisobutyl ketone	15.9	167.3	850
cyclohexane	16.8	108	780
isopropyl acetate	17.2	117.4	870
methyl isobutyl ketone	17.2	125.2	800
toluene	18.2	106.8	862
ethyl acetate	18.6	97.8	895
ethyl methyl ketone	19.0	89.6	803
n-butanol	23.1	91.5	810
ethanol	26.6	59	790

After 24 hours, the swollen samples were removed from the solvent in the test tubes, wiped on tissue to remove any excess solvent, placed in a tightly closed pre-weighed empty test tube and weighed immediately. The solvent in the tubes was discarded and replaced with fresh solvent, which was used for the rest of the swelling procedure. Replenishing with a fresh solvent (Hayes, 1986) is good experimental practice because the initial solvent may become contaminated with materials that might be extracted from the silicone during the approach to equilibrium conditions. The samples were then put back into the test tubes and placed back into the bath.

Once the samples where weighed after the first 24 hours of swelling and the solvent replenished, the samples were only removed from the bath and weighed once a week; preliminary results showed that after the first 24 hours, it took a week for any appreciable swelling. The samples were weighed using the same procedure as described above, until equilibrium (i.e. constant mass) was reached, which took four weeks for these silicones. This process was repeated on three other sample pieces of the same grade of silicone.

3.9.2 Pre-treated samples

Three samples of each silicone grade were also immersed in a container with physiological saline solution and placed in a Grant JB2 series BAT3042 water bath (Scientific Laboratory Supplies Limited, Wilford, Nottingham, UK) at 37°C for 5 months. The samples were then removed from the bath and a sample of each grade was swollen in toluene, ethyl acetate and ethyl methyl ketone, using the same procedure described in §3.9.1. As it was only possible to swell one sample of each grade, the results reported are preliminary and have been relegated to Appendix I (§I.5).

3.9.3 Calculating ϕ_P, χ and the cross-link density (υ_c) using equation 2.8, 2.9 and 2.7 respectively

To analyse the results, values for ϕ_P (the volume fraction of silicone in the swollen silicone; see §2.5.4.2 and equation 2.8 in §2.5.4.5), were calculated for the four swelling measurements taken for each grade of silicone, swollen in the same solvent. The values for ρ_s and ρ_p, required in equation 2.8, are given in Table 3.2 (§3.2.1) and Table 3.5 (§3.9.1), respectively. The mean and standard deviation values for ϕ_P are listed in the tables in Chapter 7.

Only the swelling measurements of the samples swollen in cyclohexane, toluene, ethyl acetate, ethyl methyl ketone and n-butanol, as suggested previously (Andreopoulos et al., 1993; Yerrick and Beck, 1964), were used for this part of the data analysis. The ϕ_P values were substituted into equation 2.9 (see §2.5.4.6) to calculate values for χ (the interaction parameter, see §2.5.4.1 and equation 2.9 in §2.5.4.6). The mean and standard deviation values for χ are listed in the tables in Chapter 7. Finally, the values of χ and ϕ_P were substituted into the Flory-Rehner equation (equation 2.7 in §2.5.4.4) to calculate the cross-link density, υ_c, for each of the four samples swollen in the same solvent. The V_S values required in equation 2.7 are listed in Table 3.5.

3.9.4 Calculating χ and the cross-link density (υ_c) using equation 2.12 and 2.7 respectively

As discussed in §2.5.4.6, in order to be able to use equation 2.12 to calculate χ, it is necessary to know the solubility parameter of the silicones, δ_P, which can be determined using the swelling measurements. The method used to determine δ_P is discussed in the next paragraphs.

The mean and standard deviation values of swelling (as a percentage of the original volume), were calculated from the four measurements taken for each grade of silicone, after swelling until constant mass, in all the solvents listed in Table 3.5. These mean values were plotted against the solubility parameter of the solvent, δ_S (the δ_S values for each of the solvents are listed in Table 3.5), and the standard deviation values are shown as error bars in the figures in Chapter 7 (§7.6) and Appendix I (§I.3).

It will be seen that the swelling plots in §7.6, only have a maximum of eight data points, although the samples were swollen in eleven solvents, as mentioned at the beginning of this section. This is because, it has been suggested (Yerrick and Beck, 1964) and discussed in §7.2 that analysing the results with all the eleven solvents will create a considerable scatter of the data points (this is also shown in the graphs in Appendix I (§I.3)). Therefore, in order to reduce the scatter of data points in the swelling plots, only a selection of solvents and their corresponding swelling measurements were used, as suggested by Yerrick and Beck (1964). The solvents analysed included 2,2,4-trimethylpentane, n-heptane, cyclohexane, toluene, n-butanol and ethanol, as previously suggested by Yerrick and Beck (1964). In addition, the swelling measurements for ethyl acetate and ethyl methyl ketone were also included in the analysis, because including these measurements did not cause the data to scatter considerably.

As discussed in §2.5.4.6, a study (Yerrick and Beck, 1964) used these plots of swelling (as a percentage of the original volume) against δ_S to determine the δ_P of the silicones, by equating the δ_P to the δ_S value of the solvent in which the silicone swelled the most. This method has been used in Chapter 7 (§7.6), but the results will show that this simple process of equating δ_P to the δ_S of the solvent in which the silicone swelled the most, may not be the best method to use. This is because, the maximum point of the curve may not necessarily occur at the δ_S value of the solvent in which the silicone swelled the most. A method that can be used to find the location of the maximum point on a curve is as follows: fit a suitable order polynomial through the data points; differentiate the polynomial and set the derivative equal to zero (James *et al.*, 1996).

However, it will be shown in §7.6, that swelling the silicone in solvents with various δ_S (which is likely to include good, fair and bad solvents; discussed in §2.5.4.1 and §2.5.4.8) and plotting the results (i.e. swelling measurements plotted against δ_S), created a curve with data points at the high, middle and low end of the curve. However, the shape of the curve meant that it was not possible to find a n^{th} ($n \geq 2$) order polynomial that fitted reasonably well through the data points. Therefore, from these curves it was not possible to check whether the δ_S of the solvent in which the silicone swelled the most, did actually occur at the maximum point of the curve. The next paragraph suggests a second method, which appears to be more suitable, to determine the δ_P of the silicones and was also used in Chapter 7 (§7.6).

This second method involved plotting the mean values of swelling (as a percentage of the original volume) against δ_S of a selection of solvents in which the silicone swelled the most (i.e. only consider the good solvents, because the swelling measurements of fair or bad solvents are not necessarily required to identify the maximum point of the curve). Four good solvents were used in this study, as shown in §7.6: 2,2,4-trimethylpentane; n-heptane; cyclohexane; toluene.

A suitable order polynomial was plotted through these data points and the δ_S value at the maximum swelling point was determined by differentiating the polynomial and setting the derivative equal to zero. The δ_P of the silicones was then equated to the δ_S value obtained.

The value of δ_P obtained using both methods were substituted into equation 2.12 to calculate a value for χ, using a value of $\chi_s = 0.34$ and $K = 1$, as in previous work (Blanks and Prausnitz, 1964; Scott and Magat, 1949). The values of χ obtained here and the value of ϕ_P obtained using the swelling method described in §3.9.3 were substituted into the Flory-Rehner equation (equation 2.7; §2.5.4.4), to calculate the cross-link density for each of the four samples swollen in the same solvent. The mean and standard deviation values of the cross-link density were calculated for the four swelling measurements and are listed in the tables in Chapter 7.

As discussed in §2.5.4.6, the value of K, χ_s and δ_P, in equation 2.12 can vary. The form of equation 2.12 shows that, varying these parameters will consequently affect χ. If χ varies, the form of the equation 2.7 shows that this will affect the cross-link density. Therefore, a computed sensitivity analysis on the cross-link density (computed using equation 2.7), as a result of varying K, χ_s and δ_P was also carried out and shown in the figures and tables in Chapter 7 (§7.8).

Chapter 4. DYNAMIC MECHANICAL ANALYSIS OF MEDICAL GRADE SILICONES IN COMPRESSION

4.1 Chapter overview

The chapter reports and discusses the results of the measurements of the viscoelastic properties of the cylindrical silicone specimens in compression; some of these results have already been published (Mahomed *et al.*, 2009). The theoretical background information for this chapter has been discussed in Chapter 2 (§2.7). The materials used, the methods, experimental setup and testing has been described in Chapter 3 (§3.2, §3.3, §3.4, §3.5 and §3.7). §4.2 is an introduction summarising the previous studies on the viscoelastic properties of medical grade silicones used for maxillofacial and dental applications. The weaknesses of these studies are also discussed. §4.3-§4.9 summarises the experimental results. These results have been presented in such a way that they answer the specific questions that are being investigated. The headings of §4.3-§4.9 are these specific questions. §4.10 discusses these results. The main conclusions of the study are summarised in §4.11. The aim of this chapter is to investigate whether the viscoelastic properties of the short and medium-term implant materials (medical grade silicones), are affected by frequency, temperature and pre-treatment.

4.2 Previous studies on the viscoelastic properties of silicones

The dynamic viscoelastic properties of two types of silicones (Molloplast-B and Tokuyama Soft Reclining) used in denture liners were investigated (Murata *et al.*, 2002; Murata *et al.*, 2000). The specimens in the first study (Murata *et al.*, 2000), were stored in distilled water for up to 3 years, except during testing. Testing was carried out at 37 °C and over a frequency range of 0.01-100 Hz. It was reported that the viscoelastic properties were insensitive to frequency and the silicones exhibited elastic behaviour with low values of *E"* and tanδ. *E'* were significantly greater than *E''* and no significant differences were found between the two silicones. Significant changes did not occur to the properties after the silicones were stored for 3 years (Murata *et al.*, 2000). In a later study (Murata *et al.*, 2003), seven other silicones used for maxillofacial applications were also investigated over the same loading frequency range (0.01-100 Hz) and at 23°C and 37°C. It was reported that, all the silicones were sensitive to loading frequency because the values of *E'*, *E"* and tanδ increased at higher frequencies; there was a significant effect of frequency on *E'*, *E"* and tanδ. Hence, the viscoelastic properties of these materials would be affected if impacted at high frequencies (Murata *et al.*, 2003). The viscoelastic properties of the silicones were not sensitive to the changes in temperature. Murata *et al.* (2003) suggested that the temperature-independence could be because of the cross-linked structure of the material. The viscoelastic properties of different grades of silicones may differ because of the differences in the amount of silica, degree of cross-linking and composition of the material (Murata *et al.*, 2003; Murata *et al.*, 2002).

On the other hand, another study (Wright, 1976) investigated the viscoelastic properties of silicones for dental liners at 23 ^{o}C, over the frequency range 0.05-0.5 Hz, and reported that the properties varied slightly with frequency. Studies carried out on three medical grade silicones over the frequency range 0-100 Hz at 20°C concluded that the viscoelastic properties were frequency-dependent (Huba and Molnár, 2001; Huba *et al.*, 2005).

A study (Wagner *et al.*, 1995a) investigated the viscoelastic properties of silicones for denture liners at 23°C and 37°C and at frequencies of 1 Hz, 5 Hz and 10 Hz. It was shown that the properties of some silicones used for this application were only slightly sensitive to frequency at 23^{o}C and 37^{o}C. It was concluded that the effects of increasing the frequency mirrored those of lowering the temperature. Another study (Podnos *et al.*, 2006) studied the mechanical behaviour of silicones at 23^{o}C and 37^{o}C and concluded that the mechanical properties of silicones do not change appreciably.

One study (Waters *et al.*, 1996) tested two types of silicone (Molloplast-B and Flexibase) over the temperature range 30-70^{o}C, at a frequency of 1 Hz, and concluded that the viscoelastic properties were insensitive to temperature. Similarly, another study (Saber-Sheikh *et al.*, 1999b) measured the viscoelastic properties of the same silicones at 1 Hz over the temperature range 15-60^{o}C and also reported that the properties were not temperature-dependent. They suggested that it is possible that the temperature-independence of the silicones is because they have a low glass transition temperature (-123^{o}C) and are functioning in their viscoelastic or rubbery states. In a slightly different study (Ward and Perry, 1981) , the dynamic mechanical properties of medical grade Silastic® silicones that had been immersed in distilled water at 37.5^{o}C and 59^{o}C for up to 4 months was measured.

It was concluded that the *E'* increased by up to 20% over the 4 months at 37.5°C. This increase in *E'* accelerated when the storage temperature increased to 59°C. It was reported that water absorption was not responsible for the increase in *E'*. Naidu *et al.* (1997) measured the viscoelastic properties of unimplanted and retrieved Silastic® HP-100 finger implants, which had been implanted in rabbits for four months. The properties were measured over the temperature range -50°C to 50°C, at a frequency of 1 Hz. It was concluded that the *E'* and *E''* did not change significantly after implantation. The properties of medical grade silicone that had been stored in an environmental chamber at 37°C for 6 months was investigated (Swanson and Lebeau, 1974). The results showed that the tensile strength, elongation to failure and Young's modulus (measured at 200% strain) increased slightly but not significantly after pre-treating for 6 months. They suggested that further research was needed to explain the mechanism responsible for any changes in the properties of the silicone.

In a similar study (Polyzois, 2000), the same properties of a maxillofacial silicone were measured after immersion in perspiration at 37°C for 6 months. The tensile strength, hardness and tensile modulus increased minimally after 6 months. It was suggested (Polyzois, 2000) that it is possible that the cross-link density and consequently the modulus increases after storage in water at 37°C and that this could be explored by measuring the cross-link density by swelling the silicones in solvents. It was also suggested that changes in the surface characteristics after storage in an aqueous environment may also affect the property of the material (Polyzois, 2000). It has also been recognised that different silicones will behave differently and it is possible that, the results reported for maxillofacial silicones may not be applicable to silicones in other applications (Polyzois, 2000).

There seems to be a general agreement from the previous studies that have been carried out that, the viscoelastic properties of silicones for dental and maxillofacial applications, are generally insensitive to temperature changes over the range 23-37^{o}C. However, it is not clear from these studies whether the viscoelastic properties of medical grade silicones depend on loading frequency.

Although these previous studies have made some important conclusions, weaknesses in the study can be identified. For example it is not clear whether some of the studies carried out (Murata *et al.*, 2003; Podnos *et al.*, 2006; Wright, 1976), were done using a suitable simulated body fluid such as physiological saline solution. One of the studies (Murata *et al.*, 2000), mentions that the specimens were stored in distilled water at 37°C prior to the testing only. It would have been better if these studies had been carried out in simulated *in vivo* conditions, in order to be able to use the results to predict the expected behaviour of these silicones *in vivo*. In some studies, the properties of the silicones were not measured over a large frequency range, which is a shortcoming of the work. The results from the studies on silicones for dental liners and maxillofacial (Murata *et al.*, 2003; Murata *et al.*, 2002; Murata *et al.*, 2000), contradict each other, which causes some concern. The previous studies also do not mention whether their specimen dimensions comply with testing standards. As mentioned in §3.3.2.1, a previous study (O'Sullivan *et al.*, 2003) concluded that it is important to control the specimen size.

4.3 Are the viscoelastic properties of the short-term silicones tested frequency-dependent?

The results showed that the viscoelastic properties are frequency-dependent. Figure 4.1 and Figure 4.2, show the dependence of *E'* and *E''* on frequency, *f*, for the three grades of silicones that are classified as being suitable for products intended to be implanted for 29 days. Results are given for C6-165 (▲), C6-180 (■) and MED-4080 (●). Figure 4.3 and Figure 4.4 represent an alternative description of these results in the form of the dependence of $|E^*|$ (equation 2.22) and $\tan\delta$ (equation 2.23) on *f*. The lines shown in the figures are the highest order polynomials that gave the best fit to the data, as discussed in §3.8.

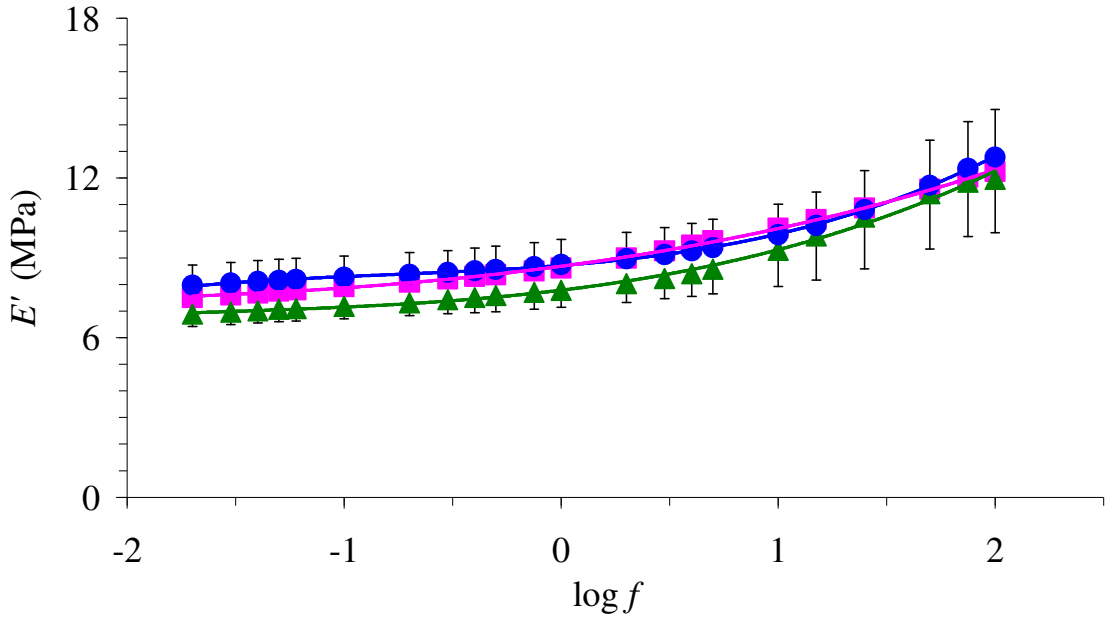

Figure 4.1: Mean values of E' plotted against the $\log_{10}f$ for C6-165 (▲), C6-180 (■) and MED-4080 (●). Error bars represent the standard deviations and the lines shown are third-order polynomials.

The coefficients of the polynomials in Figure 4.1 are given in Table 4.1. The coefficients given here enable the *E''* at a given frequency to be determined, as discussed in §3.8.

Table 4.1: Coefficients of the polynomials fitted to E' plotted against $\log_{10} f$ for each grade of silicone. R^2 is the square of the correlation coefficient and shows how well the polynomial curve fits the data. When $R^2 = 1$, there is a perfect correlation.

Grade	a'_0	a'_1	a'_2	a'_3	R^2
C6-165 *E'*	7.5276	0.7721	0.3712	0.1216	0.9986
C6-180 *E'*	8.6831	1.0834	0.3018	0.03160	0.9994
MED-4080 *E'*	8.7129	0.6389	0.3825	0.1624	0.9997

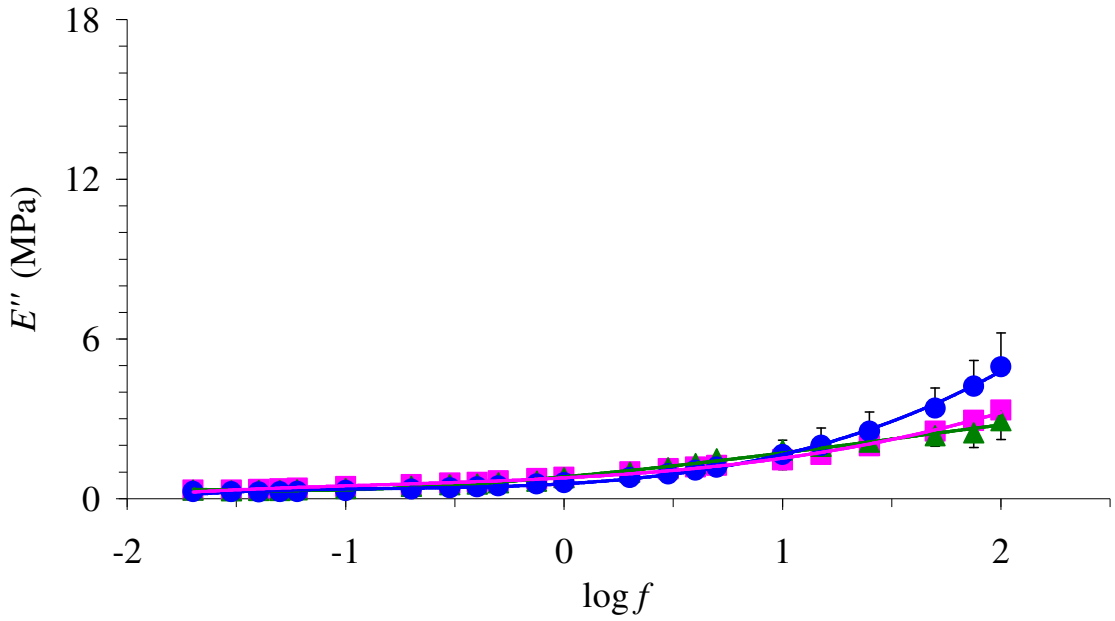

Figure 4.2: Mean values of E'' plotted against the $\log_{10} f$ for C6-165 (▲), C6-180 (■) and MED-4080 (●). Error bars represent the standard deviations and the lines shown are third-order polynomials.

The coefficients of the polynomials in Figure 4.2 are given in Table 4.2. The coefficients given here enable the *E''* at a given frequency to be determined, as discussed in §3.8.

Table 4.2: Coefficients of the polynomials fitted to E'' plotted against $\log_{10} f$ for each grade of silicone. R^2 is the square of the correlation coefficient and shows how well the polynomial curve fits the data. When $R^2 = 1$, there is a perfect correlation.

Grade	a_0''	a_1''	a_2''	a_3''	R^2
C6-165 *E''*	0.6739	0.6302	0.2806	0.0168	0.9957
C6-180 *E''*	0.78	0.4304	0.2204	0.0889	0.9966
MED-4080 *E''*	0.5578	0.4625	0.4527	0.1869	0.9977

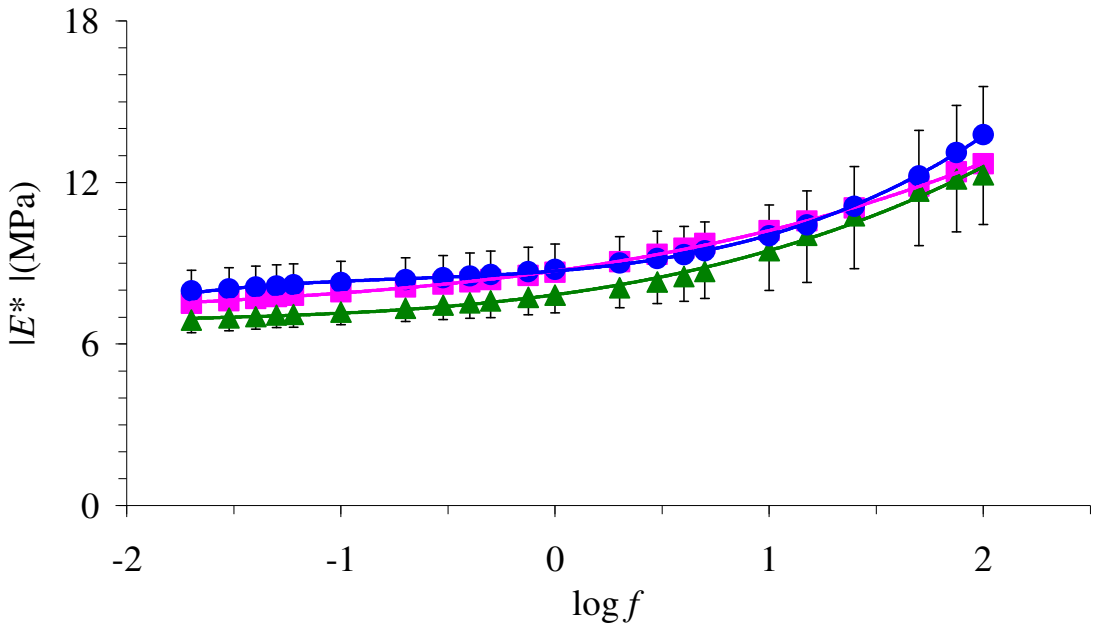

Figure 4.3: Mean values of |E*| plotted against the $\log_{10} f$ for C6-165 (▲), C6-180 (■) and MED-4080 (●). Error bars represent the standard deviations and the lines shown are third-order polynomials.

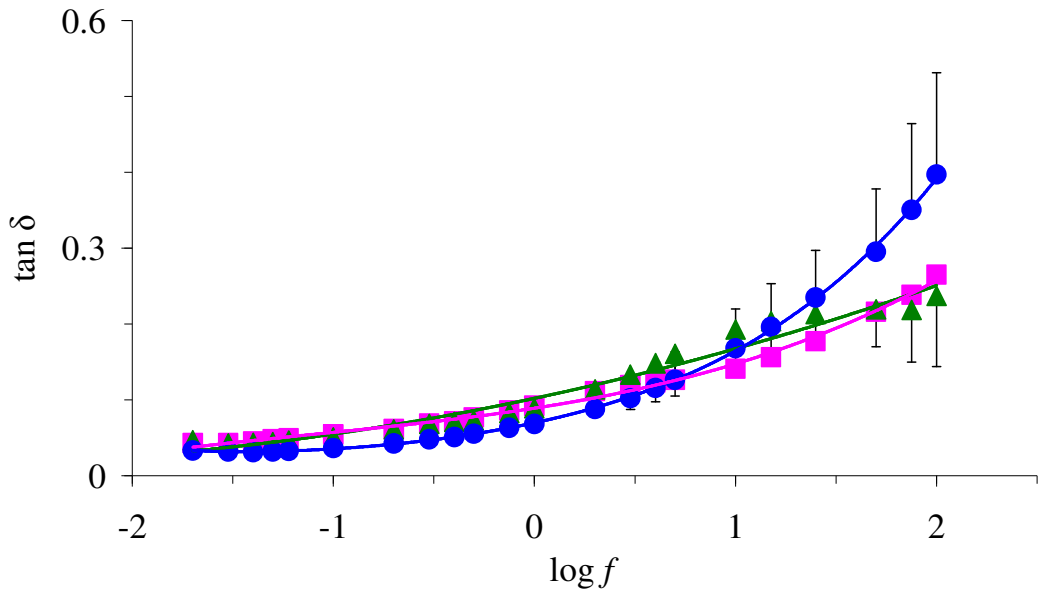

Figure 4.4: Mean values of* tanδ *plotted against the log$_{10}$f for C6-165 (▲), C6-180 (■) and MED-4080 (●). Error bars represent the standard deviations and the lines shown are third-order polynomials.

In Figure 4.1, *E*' increases slowly with frequency from a value between 6-7 MPa, up to a log*f* value of -0.5, which is equivalent to a loading frequency of approximately 0.3 Hz. *E*' then increases slowly until a log*f* value of 0 (equivalent to *f* = 1 Hz). After this point, *E*' increases more steeply and eventually attains a value above about 10 MPa at a log*f* value of 2, which is equivalent to a frequency of 100 Hz. The *E''* and tanδ values (shown in Figure 4.2 and Figure 4.4 respectively), are fairly constant until a log*f* value of -0.5 and then increases rapidly, clearly demonstrating frequency-dependent behaviour. Figure 4.3 shows that |*E**| increases with loading frequency, *f*, especially after a log*f* value of -0.5 or 0.3 Hz.

4.4 Are the viscoelastic properties of the medium -term silicones frequency- dependent?

The results showed that the viscoelastic properties are frequency-dependent. Figure 4.5 and Figure 4.6, show the dependence of *E'* and *E''* on frequency, *f*, for grades of silicones that are classified as being suitable for products intended to be implanted for 90 days. To make the graphs clearer, only results for grades Silastic® Q7-4720 (●) and Silastic® Q7-4735 (■) are shown in this section. The error bars represent the standard deviations and the lines shown are the third-order polynomials, as discussed in §3.8. The frequency-dependent viscoelastic properties for Silastic® Q7-4780 are shown in §4.7 and Appendix G (§G.1). Figure 4.7 and Figure 4.8 represent an alternative description of these results in the form of the dependence of $|E^*|$ (equation 2.22) and $\tan\delta$ (equation 2.23) on log*f*. The lines shown in the figures are the highest order polynomials that gave the best fit to the data, as discussed in §3.8.

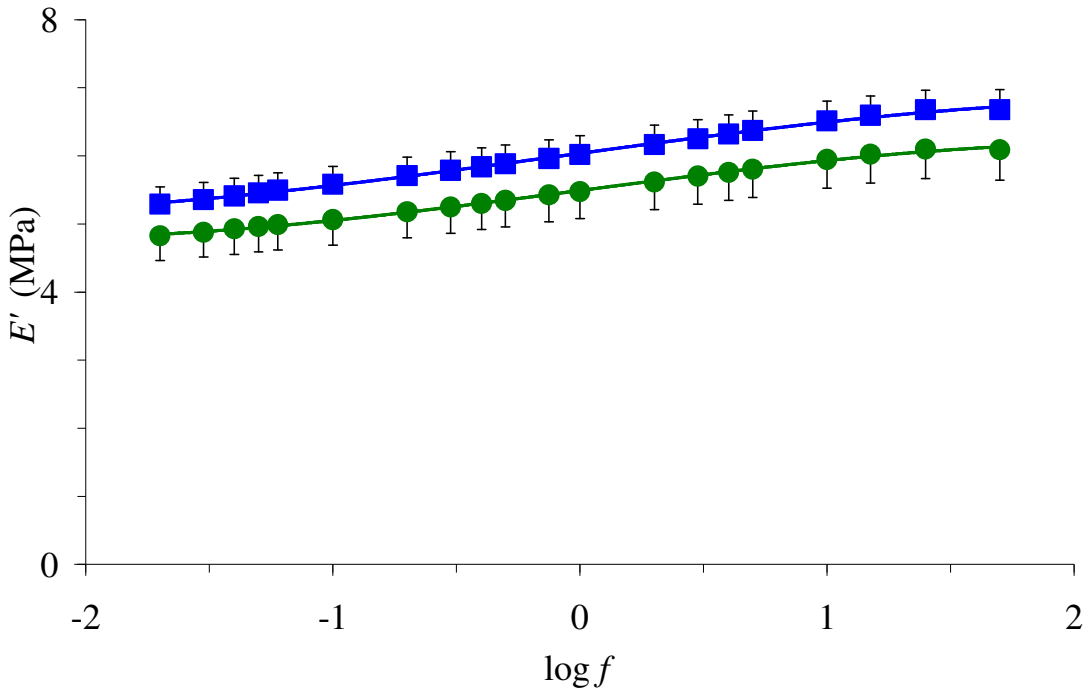

Figure 4.5: Mean values of E' plotted against the $\log_{10} f$ for Silastic® Q7-4720 (●) and Silastic® Q7-4735 (■). Error bars represent the standard deviations and the lines shown are third-order polynomials.

The coefficients of the polynomials in Figure 4.5 are given in Table 4.3. The coefficients given here enable the *E'* at a given frequency to be determined, as discussed in §3.8.

Table 4.3: Coefficients of the polynomials fitted to E' plotted against $\log_{10} f$ for each Silastic® grade of silicone. R^2 is the square of the correlation coefficient and shows how well the polynomial curve fits the data. When $R^2 = 1$, there is a perfect correlation.

Grade	a'_0	a'_1	a'_2	a'_3	R^2
Q7-4720 *E'*	5.4911	0.4731	0.0000	-0.0331	0.998
Q7-4735 *E'*	6.0373	0.4922	- 0.0067	-0.0268	0.9982

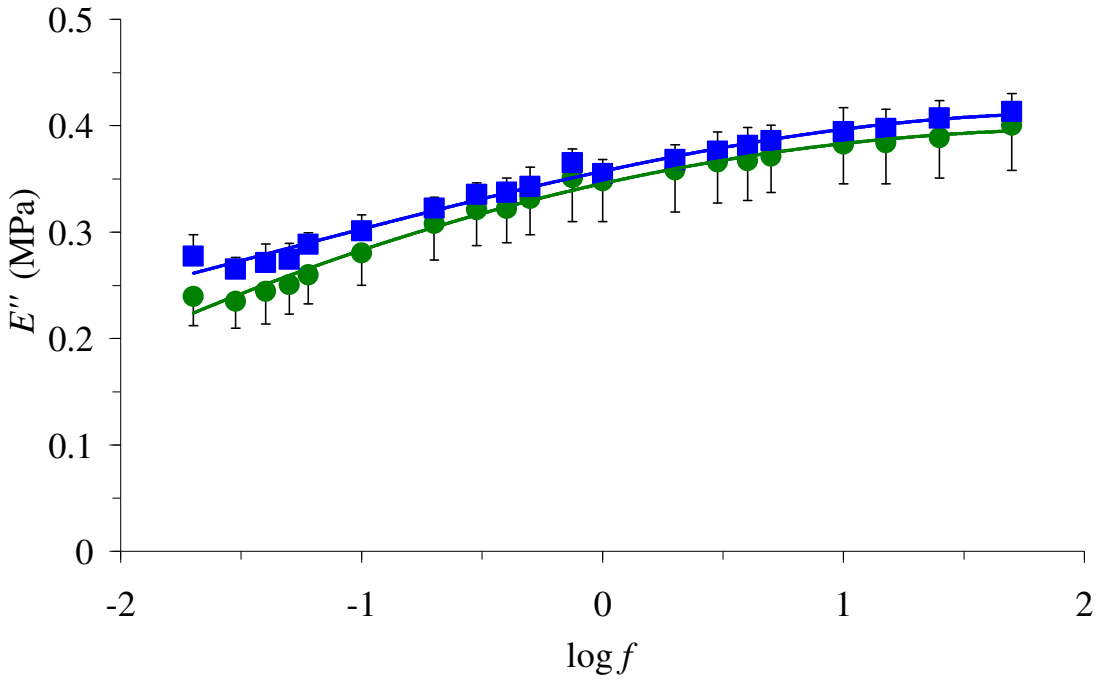

Figure 4.6: Mean values of E'' plotted against the $\log_{10}f$ for Silastic® Q7-4720 (●) and Silastic® Q7-4735 (■). Error bars represent the standard deviations and the lines shown are third-order polynomials.

The coefficients of the polynomials in Figure 4.6 are given in Table 4.4. The coefficients given here enable the *E''* at a given frequency to be determined, as discussed in §3.8.

Table 4.4: Coefficients of the polynomials fitted to E'' plotted against $\log_{10}f$ for each Silastic® grade of silicone. R^2 is the square of the correlation coefficient and shows how well the polynomial curve fits the data. When $R^2 = 1$, there is a perfect correlation.

Grade	a''_0	a''_1	a''_2	a''_3	R^2
Q7-4720 *E''*	0.3457	0.05	-0.0125	0.0001	0.9881
Q7-4735 *E''*	0.3573	0.0486	-0.0074	-0.0017	0.9828

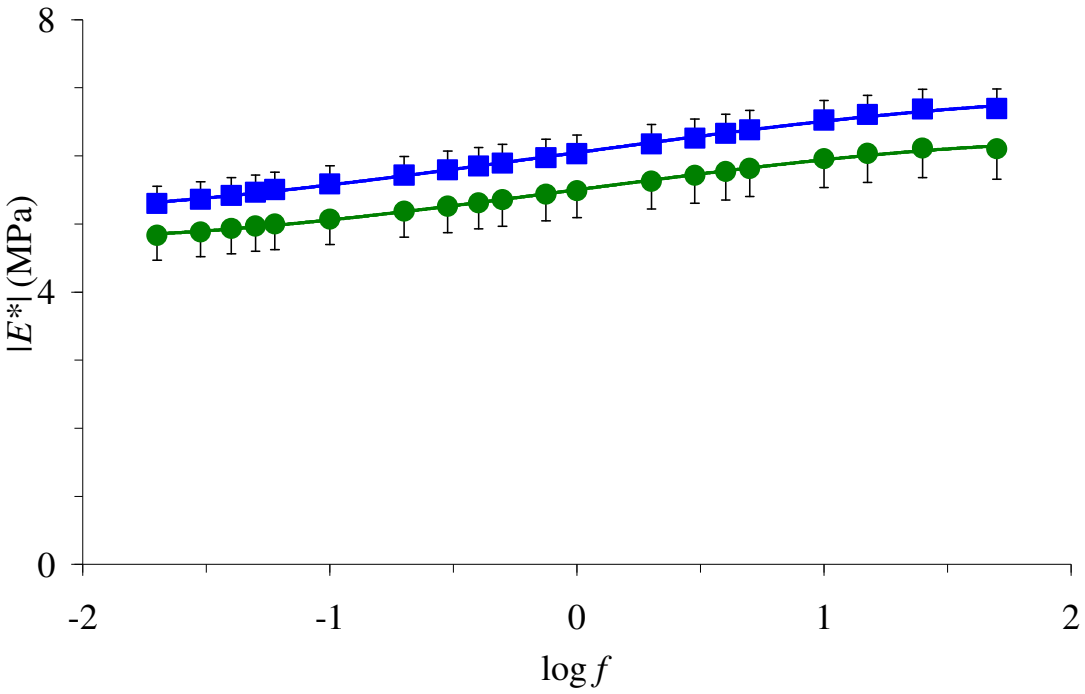

Figure 4.7: Mean values of |E*| plotted against the $\log_{10} f$ for Silastic® Q7-4720 (●) and Silastic® Q7-4735 (■). Error bars represent the standard deviations and the lines shown are third-order polynomials.

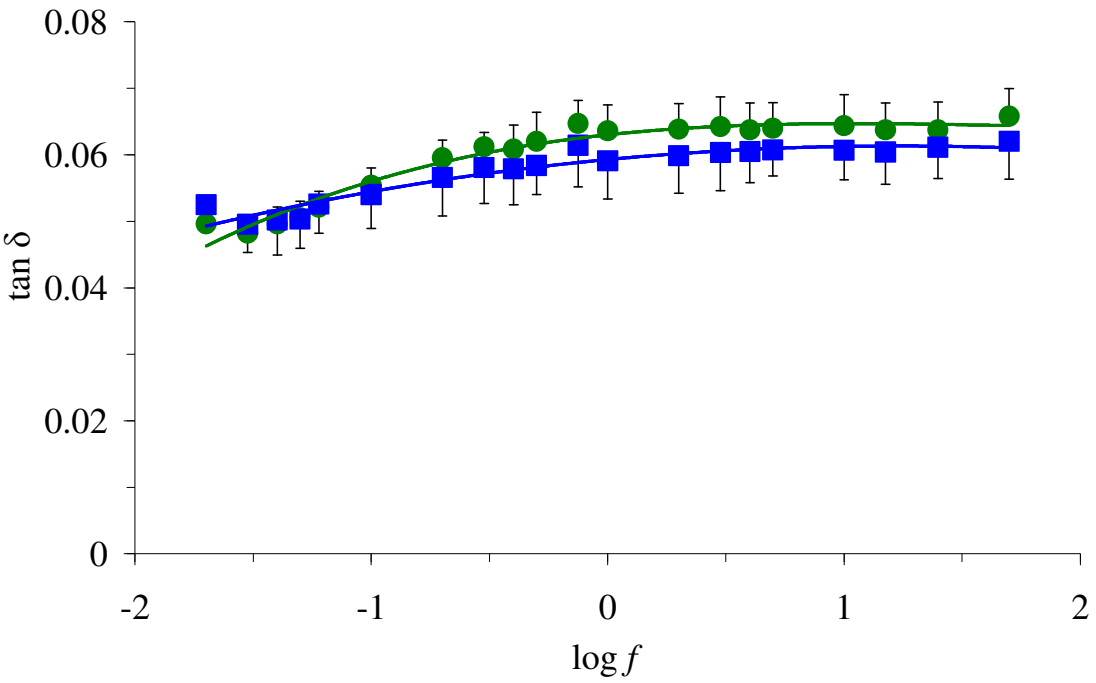

Figure 4.8: Mean values of* tanδ *plotted against the* $\log_{10}f$ *for Silastic® Q7-4720 (●) and Silastic® Q7-4735 (■). Error bars represent the standard deviations and the lines shown are third-order polynomials.

Figure 4.5, Figure 4.6 and Figure 4.7 show the dependence of E', E'' and $|E^*|$ on $\log_{10}f$ for Silastic® Q7-4720 and Silastic® Q7-4735. For both Silastic® Q7-4720 and Silastic® Q7-4735 the E' and E'' values increase slowly until a log$f$ value of –1.22, which is equivalent to a loading frequency of approximately 0.06 Hz. After this point, both moduli increase more steeply until a log$f$ value of 1.18, which is equivalent to a loading frequency of approximately 15 Hz, demonstrating frequency-dependent behaviour. After this point, both moduli are fairly constant for the rest of the frequency range. The tanδ values (shown in Figure 4.8), increase slowly until a log$f$ value of 0 (equivalent to 1 Hz), and are then are fairly constant throughout the rest of the frequency range.

4.5 Does pre-treating the short-term silicones affect the viscoelastic properties?

The results showed that pre-treating the silicones for 29 days (in physiological solution at 37 °C), may affect the properties slightly. Figure 4.9 shows the 95% confidence intervals (discussed in §3.8), for *E'* for cured (○) and pre-treated (△) MED-4080 plotted against the $\log_{10}$ of loading frequency, *f*. The confidence intervals do overlap, except when $\log f \geq 1.5$, or $f \geq 30$ Hz, i.e. the pre-treatment has no significant effect on *E'* values except at these higher frequencies. For *E''*, shown in Figure 4.10, the confidence intervals overlapped throughout the frequency range, i.e. the pre-treatment had no significant effect on *E''* values. The pre-treatment had no significant effect on the moduli values of grades C6-165 and C6-180 and the results have been included in Appendix G (§G.2).

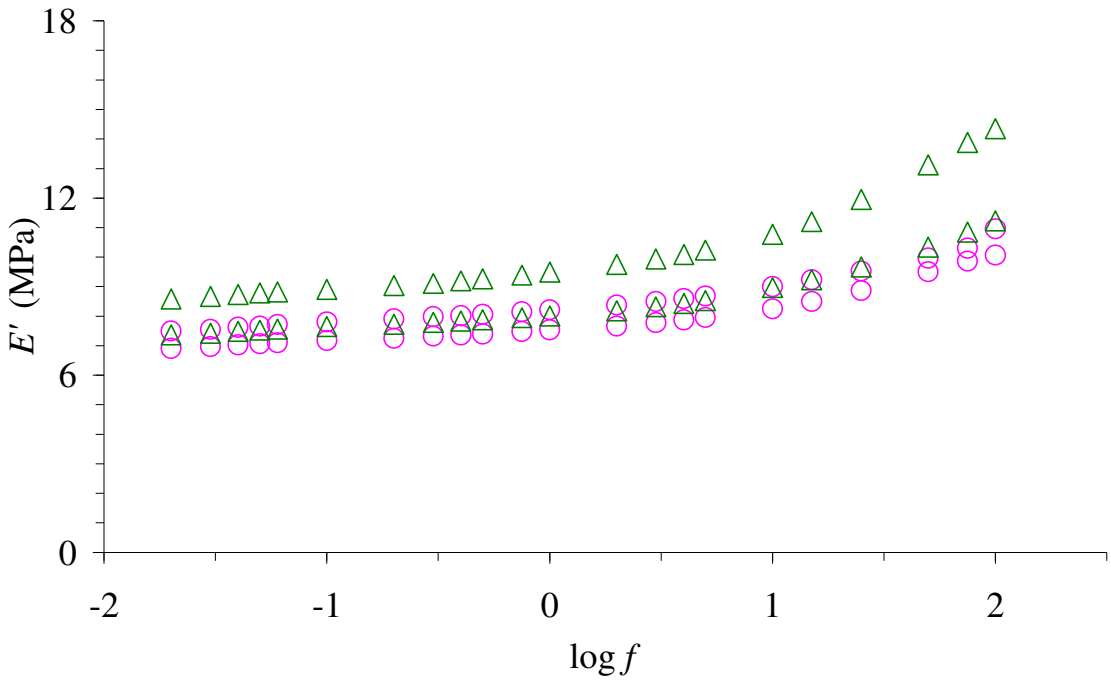

Figure 4.9: Upper and lower 95% confidence intervals of E', for cured (○) and pre-treated (△) MED-4080.

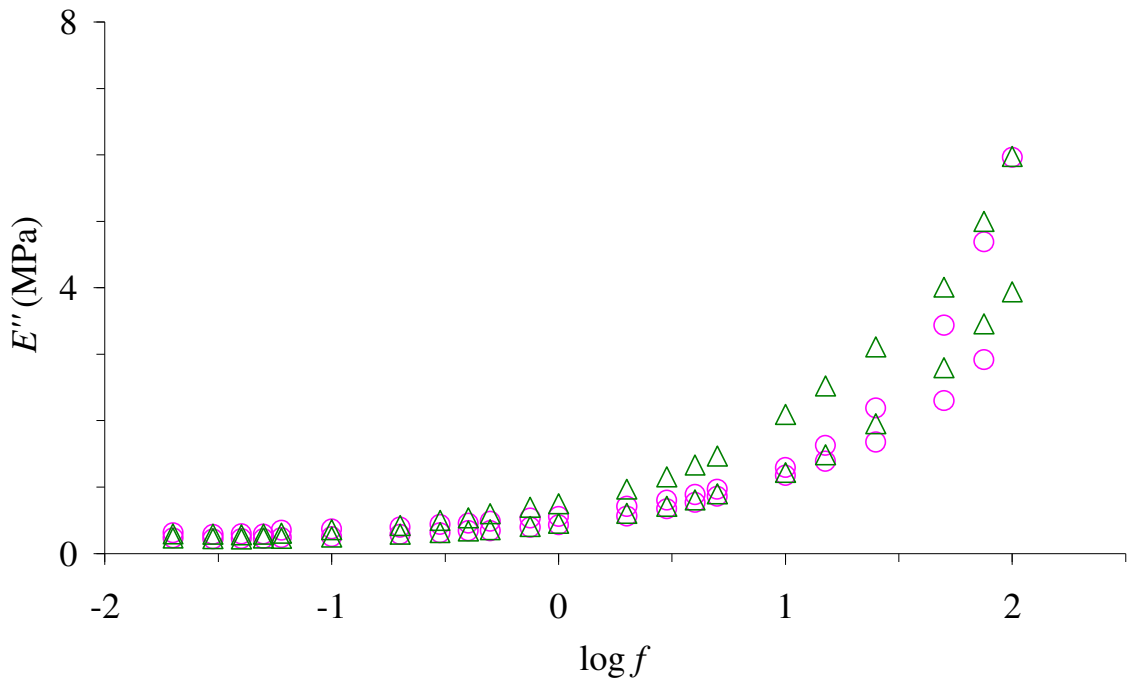

Figure 4.10: Upper and lower 95% confidence intervals of E'', for cured (○) and pre-treated (△) MED-4080.

4.6 Does pre-treating the medium-term silicones affect the viscoelastic properties?

The results showed that pre-treating the silicones for 90 days (in physiological solution at 37 °C), may affect the properties of the softer medium-term silicones. Figure 4.11 and Figure 4.12 show the 95% confidence intervals (discussed in §3.8), of *E'* and *E''* for cured (○) and pre-treated (△) Silastic® Q7-4720 specimens plotted against the $\log_{10}$ of loading frequency, *f*. For *E'* the confidence intervals did not overlap throughout the frequency range, i.e. the pre-treatment had a significant effect on *E'*. For *E''* the confidence intervals did overlap at some frequencies but not at others, i.e. the pre-treatment had a significant effect on *E''* at some frequencies. Similar results were obtained for Silastic® Q7-4735 and have been included in Appendix G (§G.3).

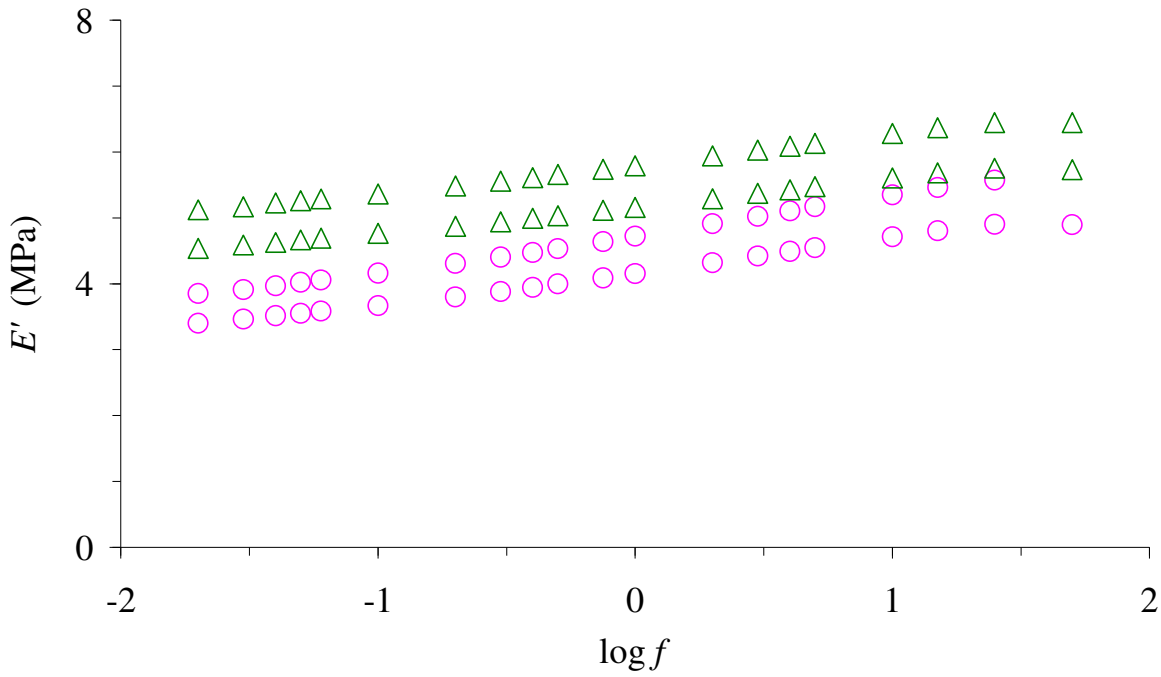

Figure 4.11: Upper and lower 95% confidence intervals of E', for cured (○) and pre-treated (△) Silastic® Q7-4720.

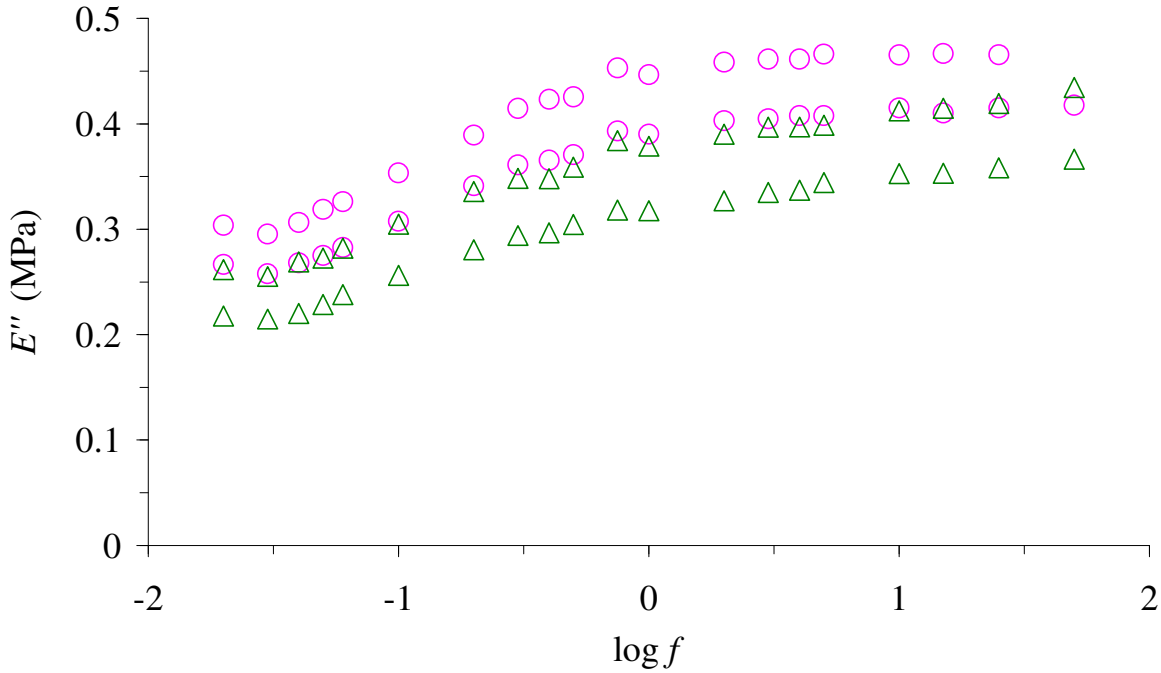

Figure 4.12: Upper and lower 95% confidence intervals of E'', for cured (○) and pre-treated (△) Silastic® Q7-4720.

The 95% confidence intervals for *E'* and *E''* for cured and pre-treated Silastic® Q7-4780 overlapped throughout the frequency range, i.e. the pre-treatment did not have a significant effect on the moduli. The results have been included in Appendix G (§G.3).

4.7 Are the viscoelastic properties of silicones with different implantation times different?

The results demonstrated that the properties were not significantly different. Figure 4.13 and Figure 4.14 show the 95% confidence intervals (discussed in §3.8), for *E'* and *E''*, for pre-treated MED-4080 (△) and Silastic® Q7-4780 (○). The 95% confidence intervals of *E'* and *E''* for Silastic® Q7-4780, overlapped throughout the frequency range with those of both grade C6-180 and MED-4080, i.e. implantation time had no significant effect on *E'* and *E''* values, as shown in the figures. The graphs obtained when C6-180 and Silastic® Q7-4780 were compared have been included in Appendix G (§G.4).

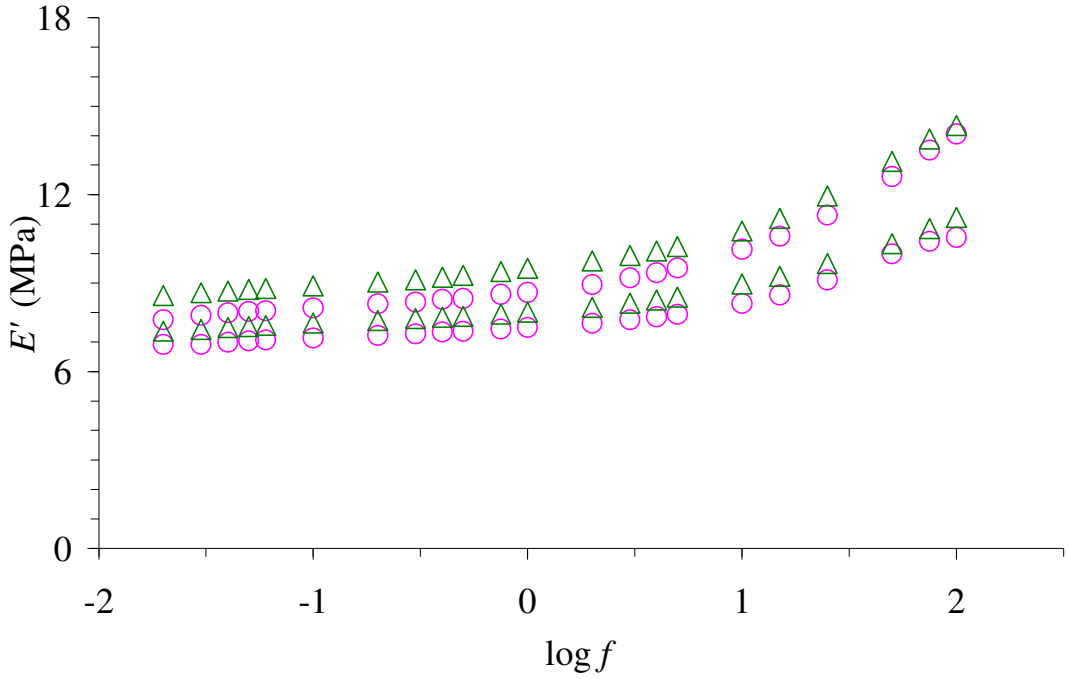

Figure 4.13: Upper and lower 95% confidence intervals of E', for pre-treated MED-4080 (△) and Silastic® Q7-4780 (○).

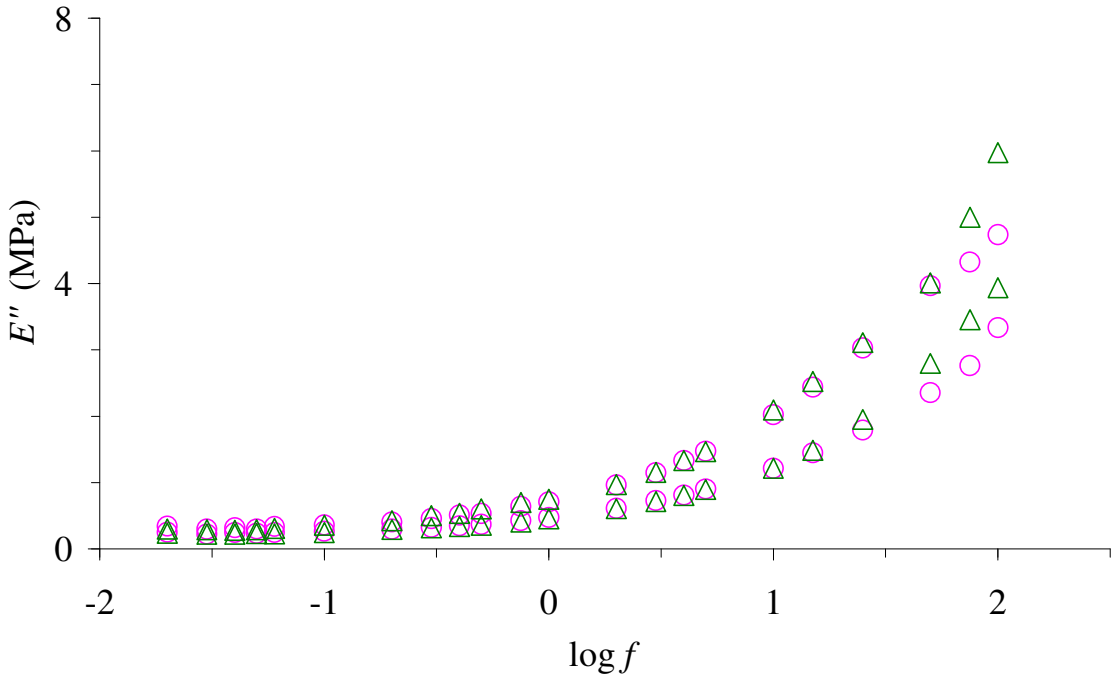

Figure 4.14: Upper and lower 95% confidence intervals of E'', for pre-treated MED-4080 (△) and Silastic® Q7-4780 (○).

4.8 Does pre-soaking the specimen for 24 hours in physiological saline affect the viscoelastic properties?

There results showed that pre-soaking the specimen in physiological saline solution for 24 hours before testing, may affect the properties slightly. Figure 4.15 shows the 95% confidence intervals (discussed in §3.8), for *E'* for unsoaked (△) and pre-soaked (○) MED-4080. The confidence intervals do not overlap below log*f* = 1.0, or *f* = 10 Hz; above this frequency there is an overlap. Therefore, physiological saline appears to have a small but significant effect on *E'* values below, but not above *f* = 10 Hz. For *E''*, shown in Figure 4.16, the confidence intervals overlapped throughout the frequency range, i.e. pre-soaking had no significant effect on *E''* values. The graphs obtained when the viscoelastic properties of unsoaked and pre-soaked grade C6-165 specimens were compared have been included in Appendix G (§G.5). These graphs showed that pre-soaking had a small but significant effect on the *E''* values below *f* = 1 Hz and above *f* = 30 Hz.

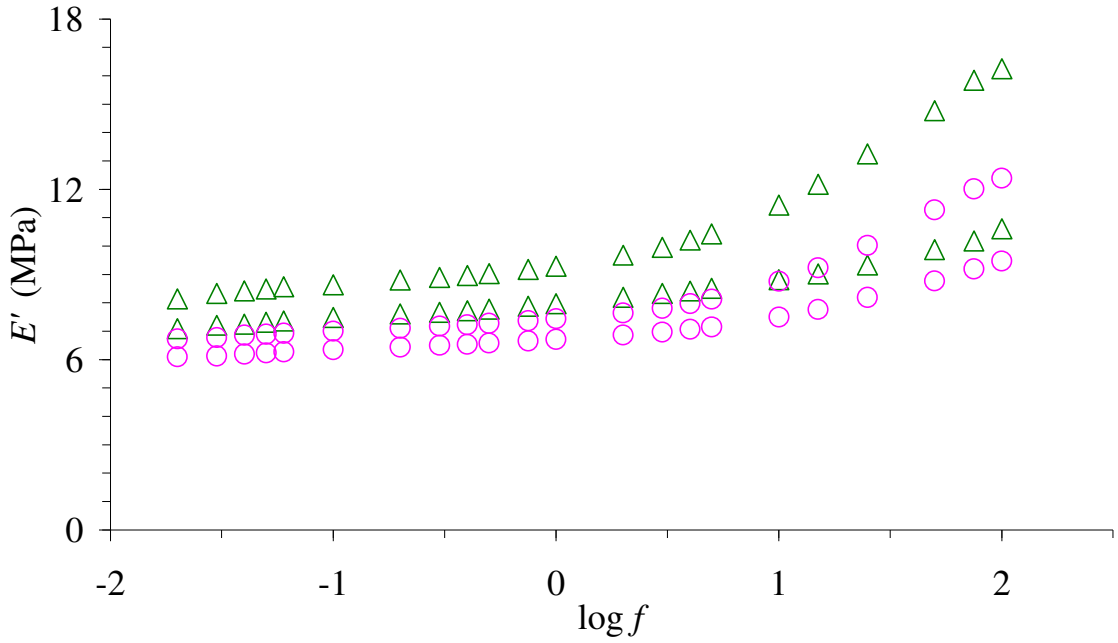

Figure 4.15: Upper and lower 95% confidence intervals of E', for unsoaked (△) and pre-soaked (○) MED-4080 specimens.

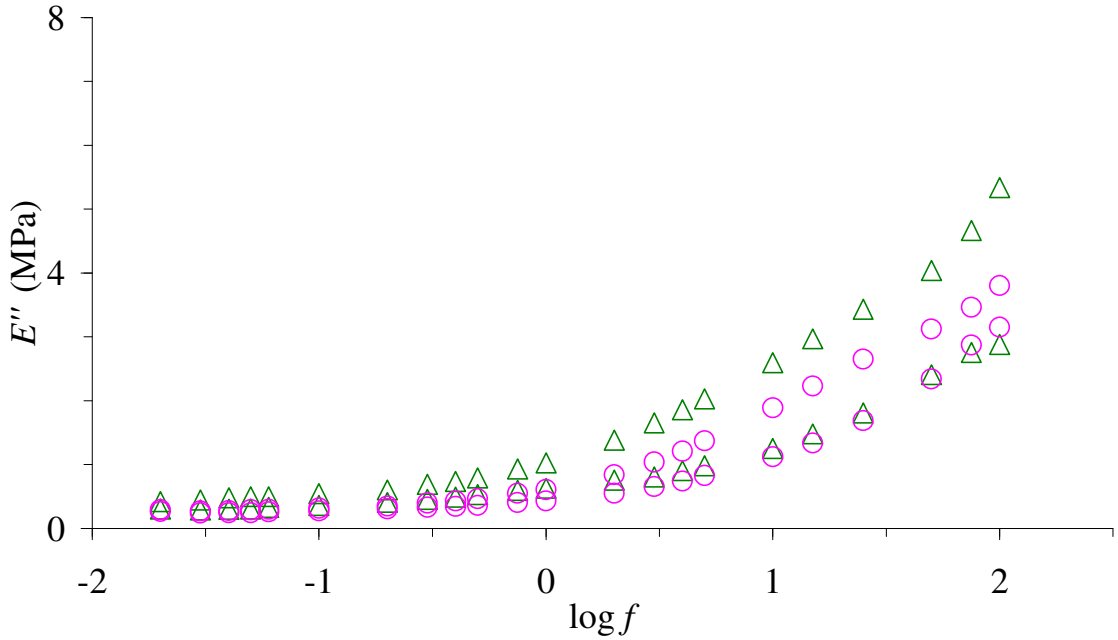

Figure 4.16: Upper and lower 95% confidence intervals of E'', for unsoaked (△) and pre-soaked (○) MED-4080 specimens.

4.9 Are the viscoelastic properties different when measured at 23°C or 37°C?

The results showed that the temperature did not significantly affect the properties. Figure 4.17 and Figure 4.18 show the 95% confidence intervals (discussed in §3.8), for *E'* and *E''*, for MED-4080 measured in physiological saline solution at either 23°C (△) or 37°C (○). There was no significant effect of temperature on *E'* and *E''* values for MED-4080 as their 95% confidence intervals overlapped throughout the frequency range.

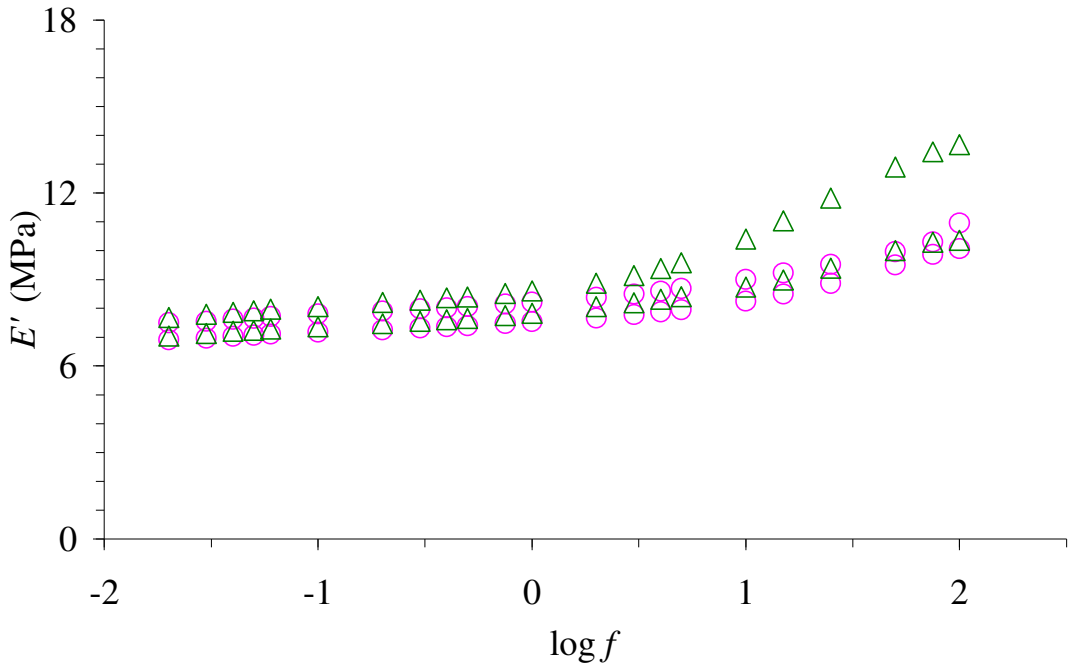

Figure 4.17: Upper and lower 95% confidence intervals of E', for MED-4080 specimens in physiological saline solution at 23°C (△) or 37°C (○).

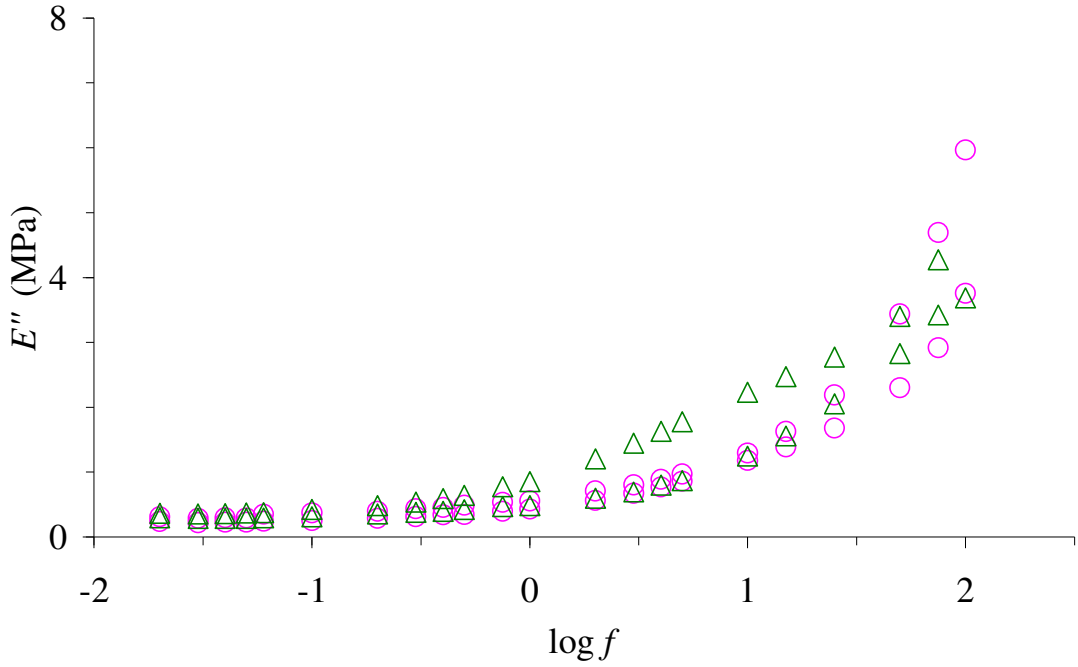

Figure 4.18: Upper and lower 95% confidence intervals of E'', for MED-4080 specimens in physiological saline solution at 23°C (△) or 37°C (○).

4.10 Discussion

4.10.1 The frequency-dependent behaviour of the storage and loss moduli

The results show that both the short and medium-term medical grade silicones investigated here, all had E' and E'' values and, hence, $|E^*|$ and $\tan\delta$ values, which depended on frequency. Furthermore, the results from the three short-term grades and Q7-4780 were closely similar. These results are consistent with a study (Murata *et al.*, 2003) carried out on silicones used for maxillofacial applications.

However, they contradict the results of earlier work on silicones used in dental liners, which concluded that the silicones were either insensitive to frequency changes or at best only slightly affected (Murata *et al.*, 2002; Murata *et al.*, 2000; Wagner *et al.*, 1995a). However, silicones do not all necessarily behave in the same way, as different types of silicones are used for different applications (Murata *et al.*, 2003; Murata *et al.*, 2002; Polyzois, 2000).

4.10.2 The transition from the rubbery to the glassy state

The results demonstrated that the silicones appear to undergo a transition from the rubbery to the glassy state. For both the short and medium-term silicones, above a certain frequency there is initially a slow increase in E' and $|E^*|$. This is then followed by a rapid increase in the moduli. This behaviour is characteristic of a material undergoing a transition from the rubbery to the glassy state (Meakin *et al.*, 2003; Ward, 1990b). For the short-term silicones and for Q7-4780 (medium-term), E' increases slowly between 0.3–1 Hz and then increases rapidly above about 1 Hz. However, for Silastic® Q7-4720 and Silastic® Q7-4735 (the softer medium-term silicones) the E' increases slowly until 0.06 Hz and then increases rapidly until 15 Hz. Above this, the increase appears to be levelling off, as between 15-50 Hz the moduli are fairly constant. This suggests that between 15-50 Hz, these silicones (Silastic® Q7-4720 and Silastic® Q7-4735) could be behaving more like a glass than a rubber (Meakin *et al.*, 2003; Ward, 1990b). The results on previous studies on silicones for medical applications (Huba and Molnár, 2001; Huba et al., 2005; Murata et al., 2003) also showed trends whose E' increased rapidly above a frequency of 10 Hz.

4.10.3 The effect of intended implantation time on the viscoelastic properties of comparable silicones

The results demonstrated that intended implantation time does not affect the viscoelastic properties of comparable silicone. The values of *E'* and *E''* are the same for comparable silicones irrespective of whether they are intended for short-term or medium-term implantation. Table 3.2 and Table 3.3 show that Silastic® Q7-4780 appears to be very similar to MED-4080 and C6-180, silicones intended for short-term implantation. This result is consistent with the assumption made in previous studies (Hutchinson *et al.*, 1997; Leslie *et al.*, 2008b; Pylios and Shepherd, 2008b; Savory *et al.*, 1994) that, silicones intended for shorter term implantation can be used as models for silicones with similar properties, that are intended for longer term implantation, in laboratory studies of mechanical properties.

4.10.4 The effect of pre-soaking on the viscoelastic properties

The results showed that pre-soaking can affect the viscoelastic properties of the silicones. Soaking the specimens in physiological saline solution for 24 hours had no significant effect on *E'* values, except for a small effect at frequencies below about 10 Hz. The *E''* values were not significantly affected throughout the frequency range. After storing their samples in distilled water for up to 3 years, Murata *et al.* (2000) also concluded that the changes in the viscoelastic properties of Molloplast-B and Tokuyama Soft Reclining (silicone for dental liners) were insignificant throughout the frequency range.

4.10.5 The effect of pre-treating the silicones on the viscoelastic properties

The results showed that pre-treating the silicones can affect the viscoelastic properties of some grades of silicone. Pre-treating the short-term implant grades for 29 days only had a small but significant effect on the *E'* values, at frequencies above about 30 Hz for grade MED-4080.

Pre-treating the medium-term implant grades for 90 days had a significant effect on the viscoelastic properties of two grades of the medium-term silicones, Silastic® Q7-4720 and Silastic® Q7-4735. This result suggests that the *E'* and *E''* values of softer silicones such as Silastic® Q7-4720 and Silastic® Q7-4735 are more likely to increase as a result of pre-treating the silicones. This increase in the value of *E'*, is consistent with a study (Ward and Perry, 1981) carried out on Silastic® medical grade silicones. Other studies (Polyzois, 2000; Swanson and Lebeau, 1974) also concluded that pre-treating silicone at 37°C for six months slightly increased the modulus.

4.10.6 The effect of testing at 23°C or 37°C on the viscoelastic properties

The results showed that reducing the temperature from 37°C to 23°C had no significant effect on the viscoelastic properties. This is consistent with previous studies carried out (Murata *et al.*, 2003; Podnos *et al.*, 2006; Saber-Sheikh *et al.*, 1999b; Wagner *et al.*, 1995a; Waters *et al.*, 1996), on the properties of the silicones for dental liners and maxillofacial applications.

4.11 Summary of main conclusions

The main conclusions from this chapter are summarised below.

- Storage, *E'*, and loss, *E''*, moduli for all the different grades of silicone cylinders, depend on loading frequency and appear to be undergoing a glass transition as the frequency increases towards 100 Hz. An equivalent statement is that the magnitude of the complex modulus $|E^*|$ and the loss tangent, $\tan\delta$, depend on frequency.
- The dependence of *E'* and *E''* values on the logarithm (base 10) of frequency, can be represented by third-order polynomials whose coefficients are tabulated.
- Grades C6-165, C6-180, MED-4080 and Q7-4780 appear to undergo a transition from the rubbery to the glassy state above about 0.3 Hz.
- Silastic® grades Q7-4720 and Q7-4735 appear to undergo and complete the transition from the rubbery to the glassy state over the frequency range 0.06 –15 Hz. While, the other harder silicones mentioned above, appear to still be undergoing this transition at 100 Hz.
- The constant moduli value between 15 -50 Hz for Q7-4720 and Q7-4735, suggest that these softer silicones have reached the glassy state and will behave more like a glass much earlier than the harder silicones: C6-165; C6-180; MED-4080; Q7-4780.
- For grade MED-4080, values of *E'* and *E''* are not affected by the pre-treatment (29 days in physiological saline solution at 37^{o}C), except for *E'* values at a loading frequency greater than about 30 Hz.
- For grade Q7-4720 and Q7-4735 (medium-term silicones), the 90 day pre-treatment had a significant effect on the *E'* and *E''* (at some frequencies).

- For grade MED-4080, values of *E'* and *E''* are not affected by soaking in physiological saline before testing, except for *E'* values at a loading frequency of less than about 10 Hz.
- There was no significant effect on the values of *E'* and *E''* for MED-4080, when the temperature was reduced from 37°C to 23°C.
- The frequency dependence of *E'* and *E''* values for Silastic® grade Q7-4780, intended for medium-term (90 day) implantation, is not significantly different (at the 5% level,) to those of grade MED-4080 and C6-180, which are intended for short-term (29 day) implantation.

Chapter 5. DYNAMIC MECHANICAL ANALYSIS OF MEDICAL GRADE SILICONES IN TENSION

5.1 Chapter overview

In Chapter 4 it was reported that the storage, E^*, E', E'' and $\tan\delta$ were measured as a function of frequency, f, in the range 0.02-100 Hz for medical grade silicones in compression. This chapter describes comparable measurements for the same silicones made in tension, in order to compare the results with those made in compression. The silicone dumb-bells used in the experiments, were made using the method described in §3.3 and were tested in tension, in simulated *in vivo* conditions, as discussed in §3.4 and §3.6, using the experimental method described in §3.7.

§5.2 is a review on previous studies that have been carried out. §5.3-5.4 summarises the experimental results. These results have been presented in such a way that they answer the specific questions that are being investigated. The headings of §5.3-5.4 are these specific questions. §5.5 discusses these results. The main conclusions of the study are summarised in §5.6.

5.2 Previous studies on the viscoelastic properties of silicones

It is not clear whether the properties of a silicone will be the same in tension as in compression (Mahomed *et al.*, 2009). Although, a previous study (Scherbakov and Gurvich, 2005) has compared the properties of rubber, an elastomer whose chemical composition is very different to that of silicone, in tension and in compression.

In this study the viscoelastic properties of an elastomer (50% natural rubber with a carbon black filler), in pure tension and in pure and bonded compression were measured. The testing was done at a frequency of 1 Hz and at room temperature. It was concluded that the *E'* and *E''* values were higher in compression than in tension, although the trends and observations made in both modes were similar. It was suggested that the properties of a material tested in tension and compression may be different because of the different size and shape of the specimens and the differences in loading conditions.

In another study (Rios *et al.*, 2001), the Young's modulus of natural rubber reinforced with either carbon fibre or glass fibre or sand was measured. It concluded that the initial value of the Young's modulus was greater in compression than in tension. However, as the concentration volume of the reinforcement increased, the increase in Young's modulus was greater in tension than in compression when fibres were present, but the reverse was true when sand was used.

The frequency dependence of the viscoelastic properties of silicones used for facial and dental applications was discussed in §4.2. In these studies, the dependence appears to be greater when they are measured in compression (Murata *et al.*, 2003) than, when they were measured in tension (Murata et al., 2000; Wagner et al., 1995a) or shear (Murata *et al.*, 2002). However, only the tension and shear studies used the same silicone grades.

This aim of this chapter is to investigate whether the viscoelastic properties of the short-term implantable silicones are the same in tension and compression.

5.3 Are the viscoelastic properties affected by loading frequency and pre-treatment?

The results demonstrated that, the properties are slightly frequency-dependent and can be affected by pre-treating the silicones for 29 days (in physiological solution at 37 °C). Figure 5.1 and Figure 5.2 show the dependence of *E'* and *E''* on frequency, *f*, for grade C6-165. Results are given for cured (▲ or △) and pre-treated (● or ○) dumb-bells. Similar graphs are shown in Figure 5.3 and Figure 5.4 for grade MED-82-5010-80. Error bars represent the 95% confidence intervals and the lines shown are the second-order polynomials that gave the best fit to the data, as discussed in §3.8. The results obtained for grades MED-4080 and C6-180 have been included in Appendix H (§H.1).

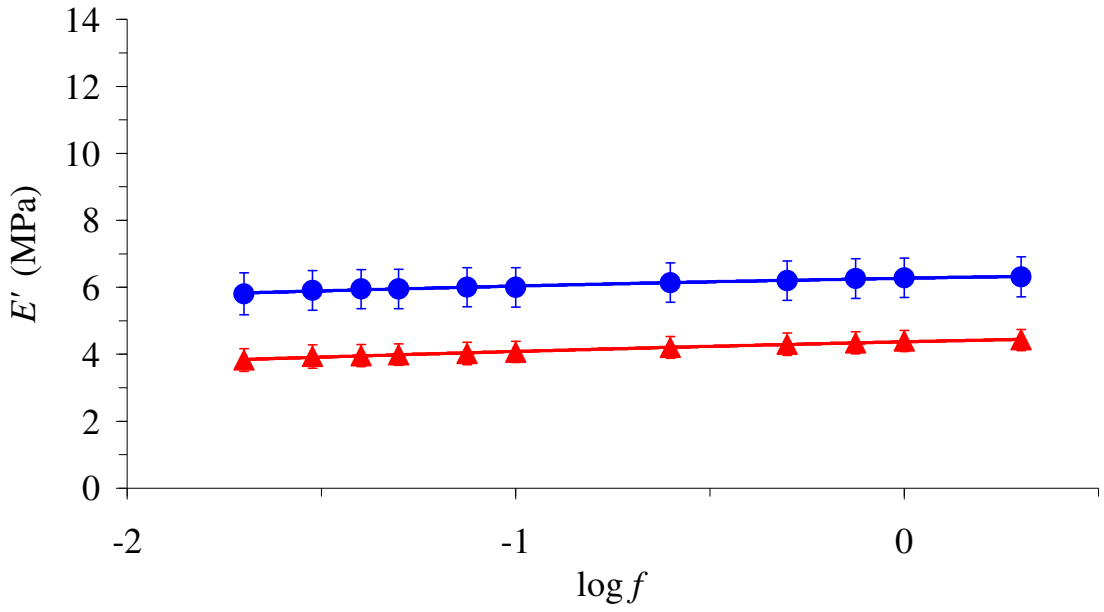

Figure 5.1: Mean values of E' plotted against the $\log_{10} f$, for cured (▲) and pre-treated (●) C6-165 dumb-bells. Error bars represent the 95 % confidence intervals and the lines shown are second-order polynomials.

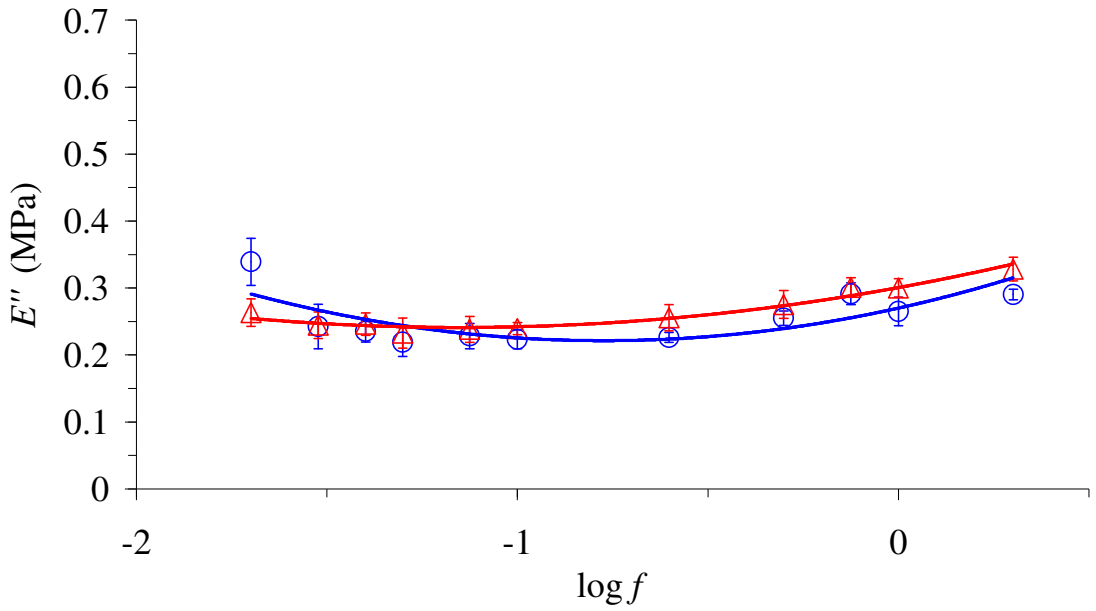

Figure 5.2: Mean values of E'' plotted against the $log_{10}f$, for cured (△) and pre-treated (○) C6-165 dumb-bells. Error bars represent the 95 % confidence intervals and the lines shown are second-order polynomials.

Figure 5.1 shows that *E*' increases slowly with frequency from a value of 3.8 MPa to 4.43 MPa (cured (▲)) and from 5.8 MPa to 6.31 MPa (pre-treated (●)). The confidence intervals did not overlap, throughout the frequency range, i.e. pre-treating the silicones had a significant effect on the *E'* values.

In Figure 5.2, for the cured data points (△), below a log*f* value of -1 (equivalent to $f = 0.1$) *E''* is fairly constant, with a value of approximately 0.25 MPa. Above this, *E''* increases slowly with frequency and eventually attains a value of 0.33 MPa at a log*f* value of 0.3, which is equivalent to a frequency of 2 Hz.

For the pre-treated data points (○), graphs of *E''* against $\log_{10}f$ are shallow curves that pass through a minimum when $\log_{10}f$ was in the range -0.65 to -0.89, corresponding to a frequency range of 0.13 to 0.22 Hz. The confidence intervals did not overlap at frequencies of 0.02, 0.25 and 2 Hz, i.e. pre-treating the silicones can have an effect.

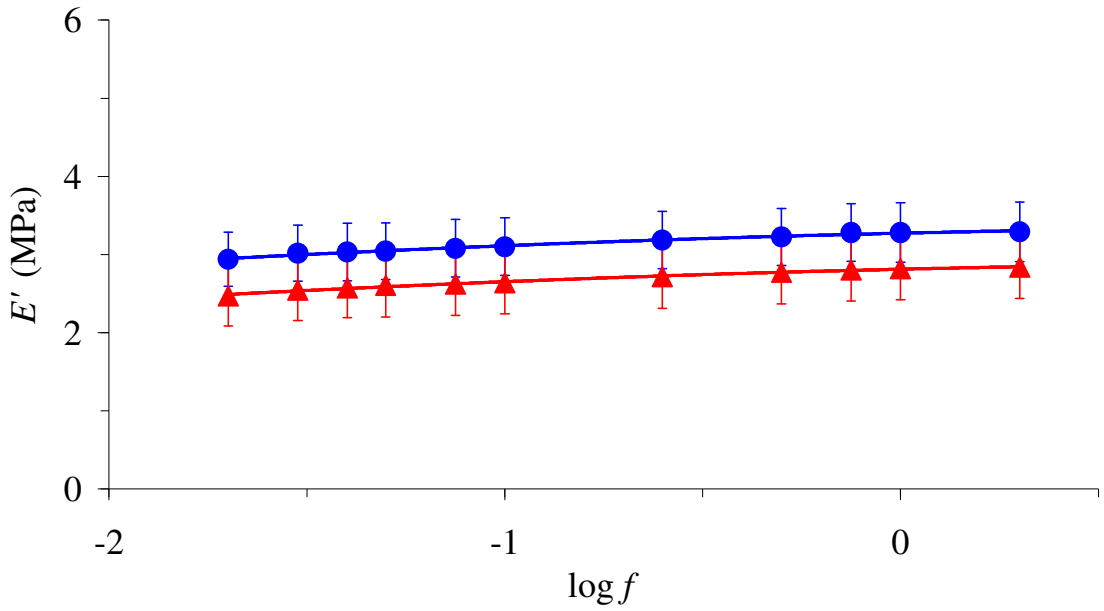

Figure 5.3: Mean values of E' plotted against the $\log_{10}f$, for cured (▲) and pre-treated (●) MED-82-5010-80 dumb-bells. Error bars represent the 95 % confidence intervals and the lines shown are second-order polynomials.

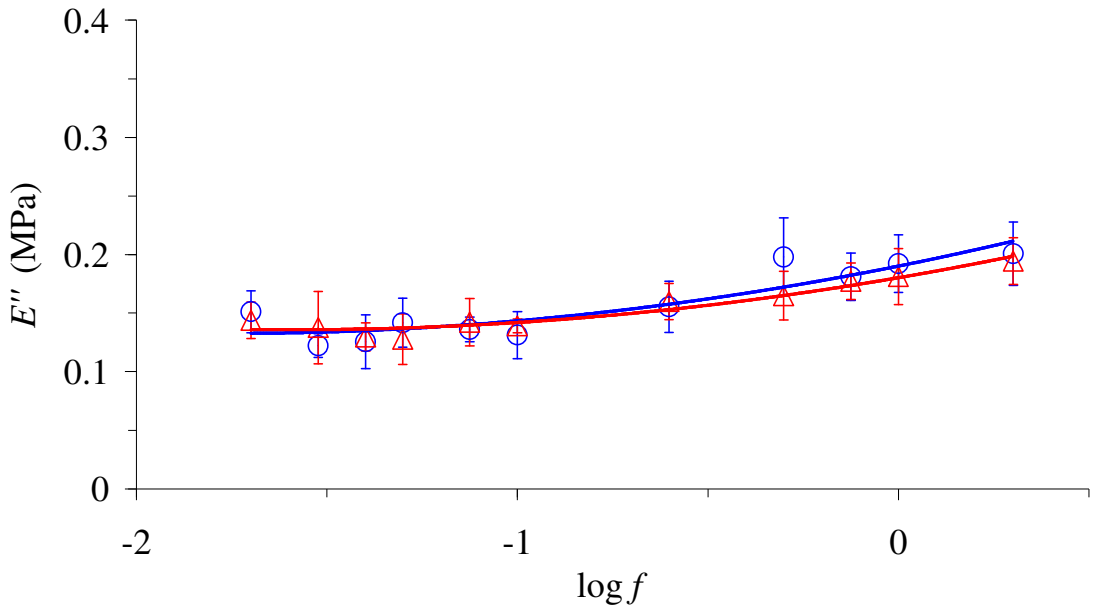

Figure 5.4: Mean values of E'' plotted against the $\log_{10}f$, for cured (△) and pre-treated (○) MED-82-5010-80 dumb-bells. Error bars represent the 95 % confidence intervals and the lines shown are second-order polynomials.

Figure 5.3 shows that *E*' increases slowly with frequency from a value of 2.5 MPa to 2.8 MPa (cured (▲)) and from 2.9 MPa to 3.3 MPa (pre-treated (●)). The confidence intervals overlapped, throughout the frequency range, i.e. the pre-treatment had a significant effect on the *E'* values. Figure 5.4 shows that below a log*f* value of -0.6 (equivalent to $f = 0.25$) *E''* is fairly constant, with a value between 0.13-0.15 MPa. Above this, *E''* increases slowly with frequency and eventually attains a value of approximately 0.20 MPa at a log*f* value of 0.3, which is equivalent to a frequency of 2 Hz. The 95% confidence intervals overlapped throughout the frequency range, suggesting that the pre-treatment had no effect on the *E''* values.

The coefficients of the polynomials in Figure 5.1 and Figure 5.3 are given in Table 5.1. The coefficients given here enable the *E'* at a given frequency to be determined, as discussed in §3.8.

Table 5.1: Coefficients of the polynomials fitted to E' (cured and pre-treated dumb-bells) for each grade of silicone. R^2 is the square of the correlation coefficient and shows how well the polynomial curve fits the data. When R^2 = 1, there is a perfect correlation.

Grade	a_0'	a_1'	a_2'	R^2
C6-165	4.3705	0.2549	-0.0329	0.9942
MED-82-5010-80	2.8111	0.117	-0.043	0.9908
C6-165	6.2691	0.1948	-0.0381	0.986
MED-82-5010-80	3.2721	0.117	-0.0431	0.9884

The coefficients of the polynomials in Figure 5.2 and Figure 5.4 are given in Table 5.2. The coefficients given here enable the *E''* at a given frequency to be determined, as discussed in §3.8.

Table 5.2: Coefficients of the polynomials fitted to E'' (cured and pre-treated dumb-bells) for each grade of silicone. R^2 is the square of the correlation coefficient and shows how well the polynomial curve fits the data. When R^2 = 1, there is a perfect correlation.

Grade	a_0''	a_1''	a_2''	R^2
C6-165	0.3006	0.1035	0.0449	0.9573
MED-82-5010-80	0.1802	0.0557	0.0175	0.942
C6-165	0.27	0.1259	0.0814	0.5715
MED-82-5010-80	0.1902	0.0652	0.0185	0.8275

5.4 Are the viscoelastic properties of silicones different in tension compared to in compression?

The results demonstrated that the properties are significantly different in tension compared to in compression. Figure 5.5 and Figure 5.6, show the dependence of *E'* and *E''* on $\log_{10}f$, for the grade C6-165 of silicone in tension (●). Similar graphs are shown for grade C6-180 in Figure 5.7 and Figure 5.8 and for grade MED-4080 on Figure 5.9 and Figure 5.10. The results for the same three silicones tested in compression (■) reported in Chapter 4 are included in the figures for comparison. Error bars represent the 95% confidence intervals and the lines shown are the second (tension) or third (compression)-order polynomials as discussed in §3.8.

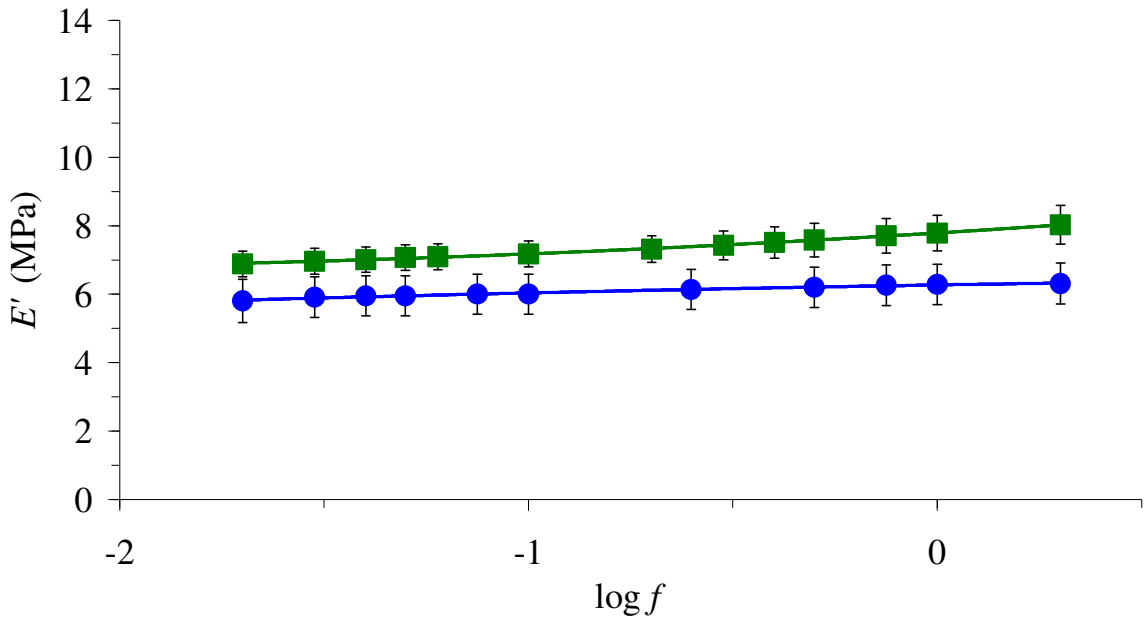

Figure 5.5: Mean values of E' plotted against the $\log_{10}f$, for grade C6-165 in tension (●) and in compression (■). Error bars represent the 95 % confidence intervals.

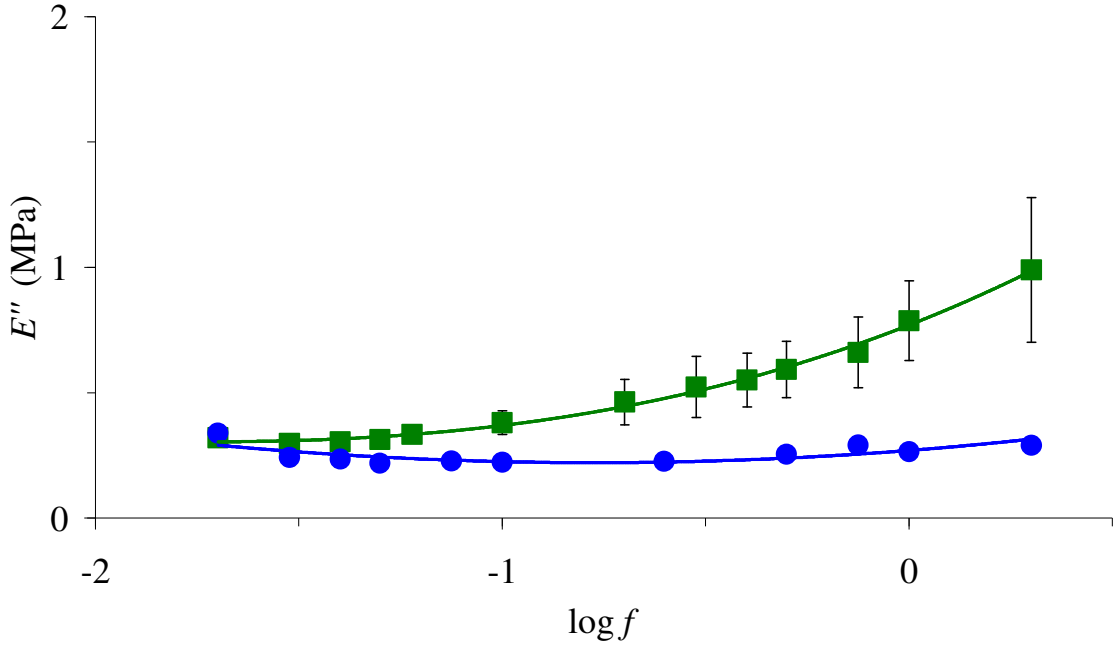

Figure 5.6: Mean values of E'' plotted against the $log_{10}f$, for grade C6-165 in tension (●) and in compression (■). Error bars represent the 95 % confidence intervals.

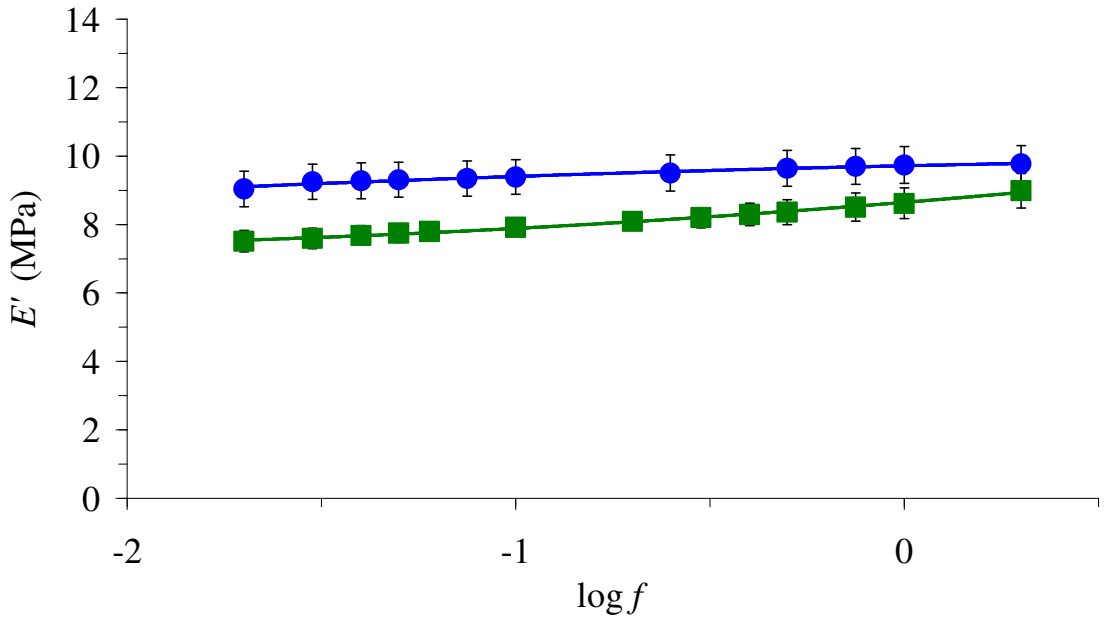

Figure 5.7: Mean values of E' plotted against the $log_{10}f$, for grade C6-180 in tension (●) and in compression (■). Error bars represent the 95 % confidence intervals.

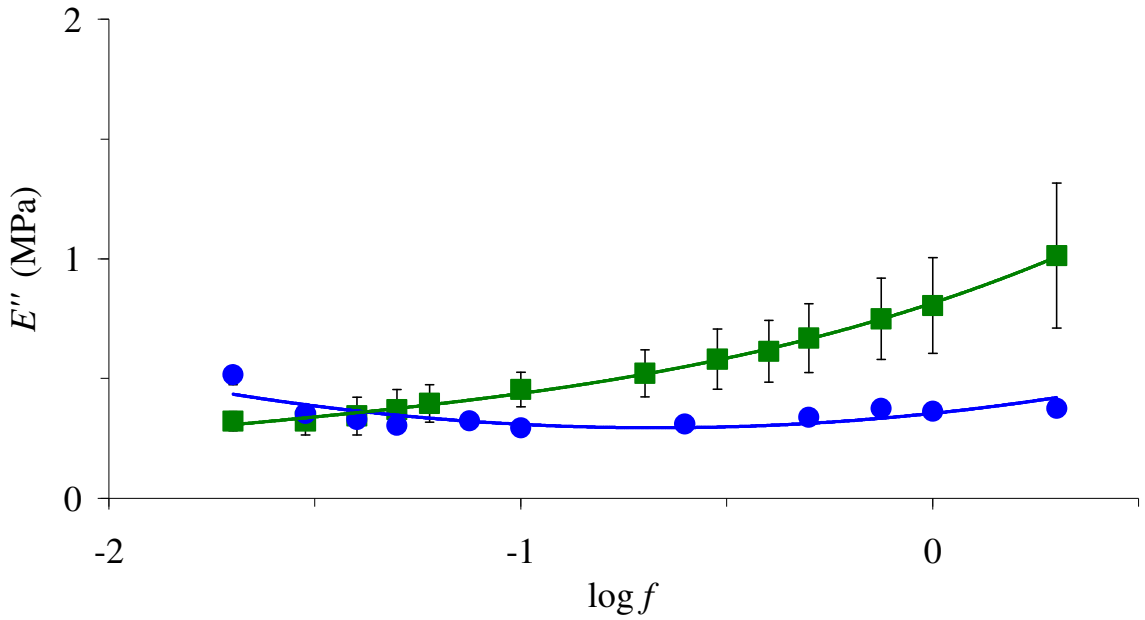

***Figure 5.8**: Mean values of E'' plotted against the $log_{10}f$, for grade C6-180 in tension (●) and in compression (■). Error bars represent the 95 % confidence intervals.*

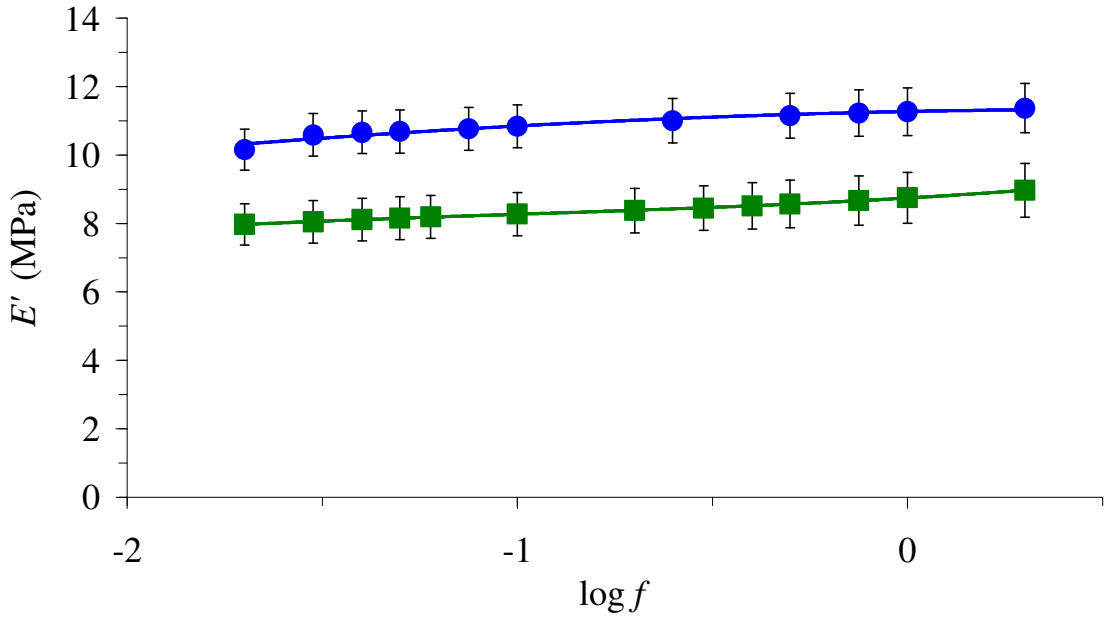

Figure 5.9: Mean values of E' plotted against the $log_{10}f$, for grade MED-4080 in tension (●) and in compression (■). Error bars represent the 95 % confidence intervals.

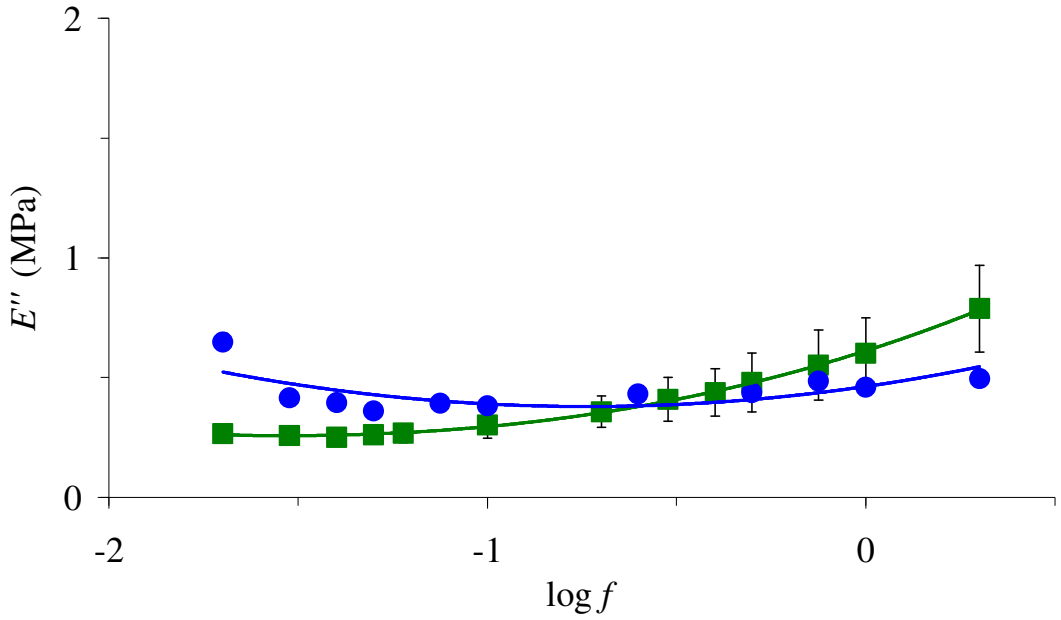

Figure 5.10: Mean values of E'' plotted against the $\log_{10}f$, for grade MED-4080 in tension (●) and in compression (■). Error bars represent the 95 % confidence intervals.

The figures show that the 95% confidence intervals did not overlap at most frequencies, suggesting that there is a statistical difference between the tensile and compressive *E'* and the tensile and compressive *E''* values.

5.5 Discussion

5.5.1 The frequency-dependent behaviour of the storage and loss moduli

The results showed that the moduli may depend slightly on frequency. In general, for both grades of silicone tested and reported here, the values for the storage modulus, *E'*, measured in tension increased slowly with frequency.

Values for the loss modulus, *E''*, of the silicones depended slightly on frequency, in the range 0.02-2 Hz, passing through a shallow minimum, when measured in tension. This result is consistent with results obtained for silicones used for dental liners (Murata et al., 2002; Murata et al., 2000). It was concluded that, in the range 0.01-100 Hz, the moduli of the silicones were almost independent of frequency when measured in tension and shear.

5.5.2 The effect of pre-treating the silicones on the moduli in tension

It was not clear from the results whether the pre-treatment affects the moduli. Pre-treating the silicones for 29 days, had a significant effect on *E'* for grade C6-165 but not for MED-82-4010-50. As the results contradict each other, it is unclear whether the pre-treatment has an appreciable effect on *E'*. However, the increase of the C6-165 *E'* values after the pre-treatment, is consistent with a previous study carried out (Ward and Perry, 1981), on Silastic® medical grade silicones, discussed in §4.2.

The results showed that the pre-treatment may slightly affect the *E''* values of C6-165 as the confidence intervals did not overlap at some frequencies, (no overlap at 0.02, 0.25 and 2 Hz). However, the effect of the pre-treatment on *E''* is not as distinctive, as discussed previously for the *E'* (C6-165 values).

5.5.3 Comparing the moduli in tension and compression using 95% confidence intervals

For all three silicones there appeared to be a very small, but a statistically significant difference between the values of *E'* measured in tension and the values obtained in compression (Chapter 4); however, because the values were systematically greater for only two of the three (C6-180 and MED-4080; see Figure 5.7 and Figure 5.9) silicones investigated and lower for the remaining one (C6-165; see Figure 5.5), no general conclusions can be drawn from this result. The two silicones for which *E'* is higher when measured in tension have a comparable Durometer hardness, Shore A (80) which is higher than the Durometer hardness, Shore A (65) of the material that shows the opposite effect; values from Table 3.2. The evidence for there being a statistically significant difference between tension and compression curves, for each of the three silicones, is that their 95% confidence intervals (as indicated by the error bars) did not overlap. The increase in *E'* values, with increasing $\log_{10}f$, when measured in tension, was somewhat less steep than when measured in compression.

For all three silicones, the dependence of *E''* on $\log_{10}f$ was very different in tension than in compression. In tension, the graph was a curve that passed through a shallow minimum but in compression *E''* increased steeply but non-linearly. Except for narrow regions, around their intersections, the tension and compression curves were significantly different, in other words their 95% confidence intervals (as indicated by the error bars) did not overlap.

The results are consistent with results obtained for silicones used for maxillofacial implants and dental liners (Murata *et al.*, 2003; Murata *et al.*, 2002; Murata *et al.*, 2000). It was concluded that, in the range 0.01-100 Hz, the moduli of these silicones showed a marked frequency dependence when tested in compression (Murata *et al.*, 2003) but that the results were almost independent of frequency when measured in tension and shear (Murata *et al.*, 2003; Murata *et al.*, 2002; Murata *et al.*, 2000). It has also been suggested that the Young's modulus for reinforced natural rubber, an elastomer whose chemical composition is very different to that of silicone, can be higher in compression than in tension (Rios *et al.*, 2001).

5.6 Summary of main conclusions

The main conclusions of this chapter are summarised below.

- Values for the storage and loss modulus, *E'* and *E''*, of cured silicone, with or without the pre-treatment, depended slightly on frequency, in the range 0.02-2 Hz, for silicones measured in tension.
- Pre-treating the medical grade silicones can significantly increase the values of storage modulus, *E'*, when measured in tension.
- Values for the loss modulus, *E''*, for some grades (C6-165, C6-180, MED-4080) of the pre-treated silicones passed through a shallow minimum.
- Values for the storage modulus, *E'*, of silicones measured in tension may be slightly, but significantly, different from the values measured in compression.
- Values for the storage modulus, *E'*, of silicones measured in tension increased less rapidly, with increasing frequency, than when measured in compression.

- Values for the loss modulus, *E''*, of silicones depended slightly with frequency, in the range 0.02-2 Hz, passing through a shallow minimum, when measured in tension, but showed a non-linear increase, in this frequency range, when measured in compression.
- Graphs of *E'* and *E''* plotted against $\log_{10} f$ can be represented by second order polynomials; the tabulated coefficients of these polynomials can be used to calculate the values of *E'* and *E''*, for the four silicones investigated here, in tension.

Chapter 6. ACCELERATED AGING OF ELAST-EON™ 3 AND NAGOR® MEDICAL GRADE SILICONE

6.1 Chapter overview

It has been suggested that it is possible to accelerate the aging process of polymers used in medical devices, by subjecting the material to elevated temperatures for a period of time (Hemmerich, 1998; Hukins *et al.*, 2008), as discussed in Chapter 2 (§2.8). This chapter investigates the effect of accelerated aging on the properties of Elast-Eon™ 3 and Nagor® silicone cylinders. As discussed in §3.2.3, Nagor® silicone has a similar hardness to Elast-Eon™ 3, and therefore likely to have similar mechanical properties, hence it is used as a comparison material. The materials used and the sizes of the specimens were described in §3.2 and §3.3. The aging conditions of the specimens, the equipment used for the testing and the experimental method were described in §3.4, §3.5 and §3.7.

§6.2 is a review of previous studies on aging of silicone, polyurethanes, natural rubber and Elast-Eon™. §6.3-§6.5 summarises the experimental results. These results have been presented in such a way that they answer the specific questions that are being investigated. The headings of §6.3-6.5 are these specific questions. §6.6 discusses these results. The main conclusions of the study are summarised in §6.7.

6.2 Previous studies on the properties of polyurethanes, silicones and Elast-Eon™

6.2.1 Effect of accelerated aging on the properties of silicones, polyurethanes and natural rubber

A study (Yu *et al.*, 1980) investigated the physical properties of two silicones and a polyurethane used for maxillofacial applications before and after accelerated aging for up to 900 hours at 43°C or 63°C. It was reported that the properties of the silicones were not affected by aging, but the polyurethane aging had to be stopped after 600 hours because of physical degradation. After 600 hours of aging the polyurethane became soft, the tensile strength, Shore A hardness and the shear strength had decreased. It was suggested that, it was possible that acclerated aging did not affect the silicone because of the inert backbone of repeating silicon and oxygen bonds (see §2.5.2) in the chemical structure of the material.

In another study (Saber-Sheikh *et al.*, 1999a), the viscoelastic properties of two silicones (Molloplast-B and Flexibase) for use in denture liners were measured after being stored in distilled water at 37 °C for a year. The experiments were carried out at a frequency of 1 Hz. After aging for a year, the *E'* and $\tan\delta$ of Molloplast-B remained relatively unchanged but the *E'* of Flexibase decreased by 93%. A study (Wilson and Tomlin, 1969) investigated the change in appearance of Molloplast-B and Flexibase and of another silicone, Silastic 390, used for dental liners, after being stored in water at 37°C for six months. The appearance of Molloplast-B and Silastic 390 did not change but Flexibase was covered in a white deposit.

Another study (Wagner *et al.*, 1995b) investigated the effect that accelerated aging (for 900 hours at 43 °C) has on the *E' , E''* and tanδ of two silicones (Molloplast-B and Prolastic) used as denture liners. Accelerated aging only slightly increased the *E'*, *E''* and tanδ of the silicones. The properties remained relatively stable over time.

In an earlier study (Dootz *et al.*, 1993) of the same materials, the physical properties of the two silicones were measured before and after accelerated aging for 900 hours at 43°C. The tensile strength, elongation to failure and tear resistance of Molloplast-B increased after aging, while that of Prolastic decreased. The hardness of Molloplast-B decreased after aging, while that of Prolastic increased. In a further similar study (Dootz *et al.*, 1994), the physical properties of three other silicones (A-2186; MDX 4-4210 and Cosmesil) used for denture liners were studied under the same aging conditions. Only the properties of the MDX 4-4210 did not change after accelerated aging. The tear resistance and hardness of the other two silicones increased after accelerated aging while the elongation to failure decreased. Another study (Kennan *et al.*, 1997) investigated the effect of accelerated aging on the properties of medical grade silicones. The materials were immersed in saline solution at 37°C or 100°C for 45 hours. The tensile strength, elongation at break and stress (at 100 % and 200 % elongation) did not change significantly after accelerated aging.

More recently, the mechanical strength of two types of silicones (MED82-5010-80 and C6-180) were measured after aging in air, distilled water and ringer's solution for 37°C and 80°C (Leslie *et al.*, 2008b). The results showed that the mechanical strength of these silicones may reduce as a result of exposing them to elevated temperatures.

The dynamic mechanical properties of natural rubber (an elastomer whose chemical composition is very different to that of silicone and polyurethane), that had been aged in an oven at 30°C, 50°C and 70°C for 24-240 hours, has also been investigated (Wei et al., 2004; Xie et al., 2004). In these studies, the *E'* and *E''* increased with aging time at all the aging temperatures.

6.2.2 Effect of implantation in sheep and accelerated aging on the properties of Elast-Eon™

After implantation in sheep, it was found that there were no undesirable changes in the properties of Elast-Eon™ (Martin *et al.*, 2000; Simmons *et al.*, 2004; Simmons *et al.*, 2006; Simmons *et al.*, 2008). Simmons *et al.* (2004; 2008) implanted Elast-Eon™ in sheep for either six or twelve months and reported that the Young's Modulus increased and the extension at failure decreased significantly (two sample t-test; significance level $p < 0.05$), after implantation. In their first study (Simmons *et al.*, 2004) the ultimate tensile strength increased after implantation, but the opposite occurred in their second study (Simmons *et al.*, 2008). A simple polyurethane showed signs of degradation and surface cracking after sterilisation (autoclaving or ethylene oxide or γ-irradiation) and accelerated aging (70°C for 2 weeks, equivalent to 20 weeks at 37°C); Elast-Eon™ only showed such adverse changes after being autoclaved and aged (Simmons *et al.*, 2006). Elast-Eon™ has also been reported as being more resistant to oxidation than an aliphatic polycarbonate (Hernandez *et al.*, 2008).

Apart from the studies by Simmons *et al*. (2006; 2008), statistical analysis of the mechanical properties before and after implantation in the sheep, was not carried out. However, even for the studies by Simmons *et al*. (2006; 2008), no statistical analysis was reported for the accelerated aged samples.

There have been several studies that have suggested that accelerated aging can affect the properties of polyurethanes but it may not necessarily affect the properties of silicones. As discussed in §2.6, Elast-Eon™ is a combination of both these materials, but no previous study has measured its Young's modulus before and after accelerated aging or discussed the mechanisms of behaviour of the properties of Elast-Eon™ after accelerated aging. The aim of this chapter is to measure the viscoelastic properties of Elast-Eon™ 3 and Nagor® silicone before and after accelerated aging (at 70°C for 38 days).

6.3 Are the viscoelastic properties of Elast-Eon™ 3 frequency-dependent?

The results demonstrated that the properties are frequency-dependent. Figure 6.1 and Figure 6.2 show the frequency dependence of *E'* and *E''* for Elast-Eon™ 3 cylinders before (△) and after (□) accelerated aging (in physiological solution at 70°C for 38 days). Error bars represent the 95% confidence intervals and the lines shown are the second-order polynomials that gave the best fit to the data, as discussed in §3.8. Figure 6.1 shows that, before and after accelerated aging, *E'* gradually increases as *f* increases. *E''* values are much less than *E'* values and show a less pronounced dependence on *f*, especially below $\log_{10} f$ values of approximately 0 (corresponding to $f \approx 1$ Hz).

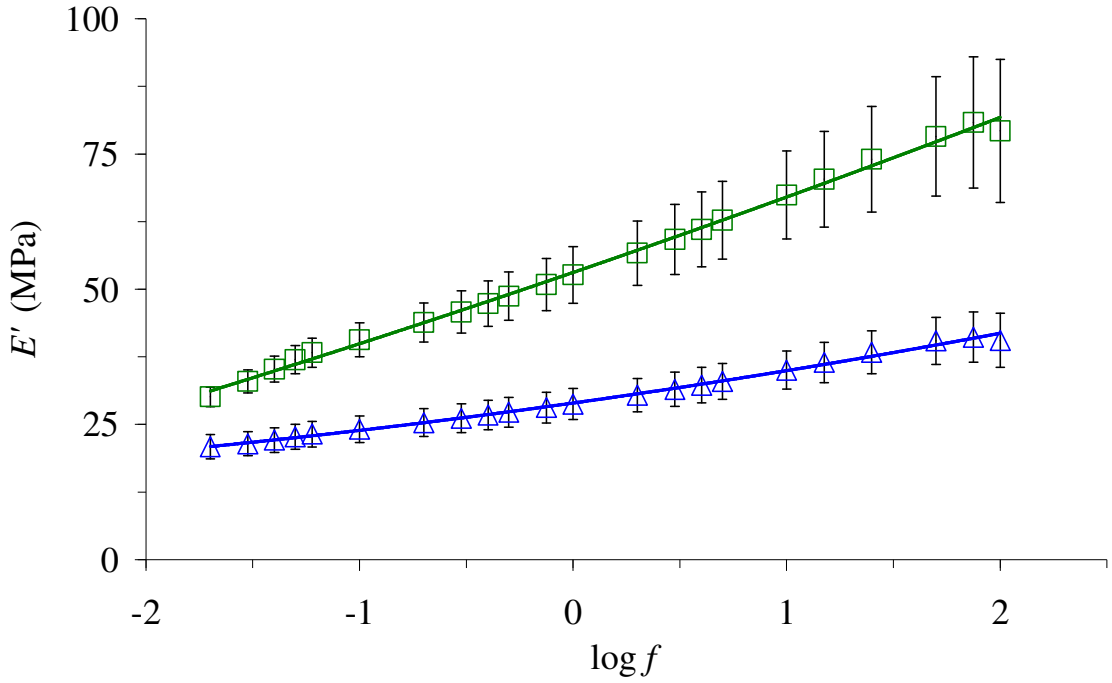

Figure 6.1: Mean values of E' plotted against the $log_{10}f$, for Elast-Eon™ 3 specimens before (△) and after (□) accelerated aging (in physiological solution at 70°C for 38 days). The error bars represent the 95% confidence intervals. The lines shown are second-order polynomials.

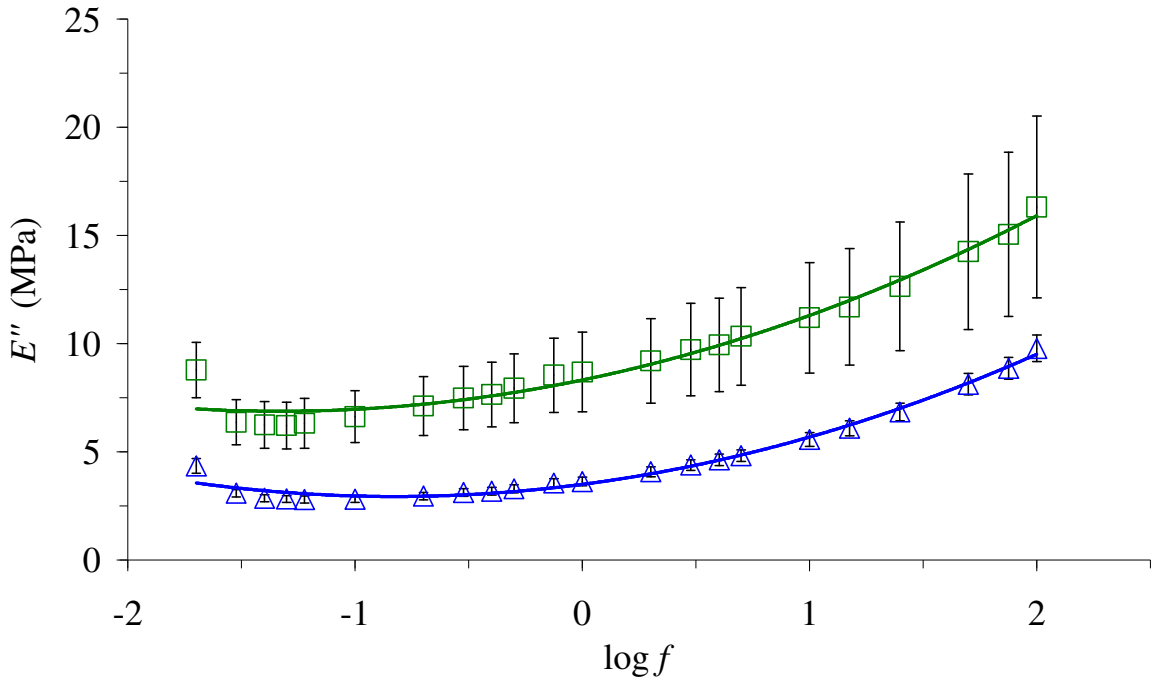

Figure 6.2: Mean values of E'' plotted against the $\log_{10}f$, for Elast-Eon™ 3 specimens before (△) and after (□) accelerated aging (in physiological solution at 70°C for 38 days). The error bars represent the 95% confidence intervals. The lines shown are second-order polynomials.

The coefficients of the polynomials in Figure 6.1 are given in Table 6.1. The coefficients given here enable the *E'* at a given frequency to be determined, as discussed in §3.8.

Table 6.1: Coefficients of the polynomials fitted to the E' for Elast-Eon™ 3. R^2 is the square of the correlation coefficient and shows how well the polynomial curve fits the data. When $R^2 = 1$, there is a perfect correlation.

	a_0'	a_1'	a_2'	R^2
Before aging *E'*	28.948	5.5251	0.4642	0.996
After aging *E'*	53.089	13.563	0.3887	0.997

The coefficients of the polynomials in Figure 6.2 are given in Table 6.2. The coefficients given here enable the *E''* at a given frequency to be determined, as discussed in §3.8.

Table 6.2: Coefficients of the polynomials fitted to the E'' for Elast-Eon™3. R^2 is the square of the correlation coefficient and shows how well the polynomial curve fits the data. When R^2 = 1, there is a perfect correlation.

	a_0''	a_1''	a_2''	R^2
Before aging *E''*	3.4936	1.3615	0.8234	0.986
After aging *E''*	8.3172	2.1701	0.8143	0.969

6.4 What effect does accelerated aging have on the properties of Elast-Eon™ 3?

Accelerated aging (in physiological solution at 70°C) changed the appearance of the Elast-Eon™ 3 specimens. Before aging, they were transparent with a slight yellow colouration. After aging, they became darker and more opaque, as shown in Figure 6.3.

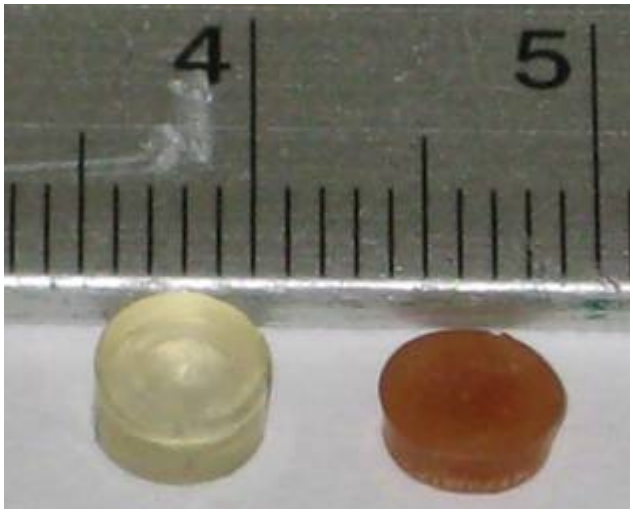

Figure 6.3: Elast-Eon™ 3 specimens before (left hand side) and after (right hand side) accelerated aging (in physiological saline solution at 70°C).

The results reported in §6.3 demonstrated that the viscoelastic properties of Elast-Eon™ 3 were affected by accelerated aging. Figure 6.1 shows that accelerated aging had an effect on *E'* values. Values of *E'* increased significantly as a result of aging. Also, it appears that the slope of *E'* plotted against $\log_{10} f$ increased. Figure 6.2 shows that there was also a slight, but significant, increase in *E''* values, following accelerated aging, across the frequency range. Further results are included in Appendix G (§G.6).

6.5 What effect does accelerated aging have on the properties of Nagor® silicone?

The results demonstrated that the properties were not significantly affected by accelerated aging (in physiological solution at 70°C for 38 days). Figure 6.4 shows the 95% confidence intervals (as discussed in §3.8), for *E'* before (○) and after (△) accelerated aging for Nagor® silicone cylinders plotted against the $\log_{10}$ of loading frequency, *f*. Similar graphs are shown for *E''* in Figure 6.5. The confidence intervals overlapped throughout the frequency range, i.e. accelerated aging had no significant effect on *E'* and *E''* values. Accelerated aging did not change the appearance of the specimens. Further results are included in Appendix G (§G.7).

In Figure 6.4, *E*' also increases slowly up to a log*f* value of -0.125, (corresponding to $f \approx 0.75$ Hz). After this point, *E*' increases more steeply. Similarly, the *E''* is fairly constant until a log*f* value of -1.22 (corresponding to $f \approx 0.06$ Hz) and then increases rapidly. Both *E'* and *E''* clearly demonstrated frequency-dependent behaviour.

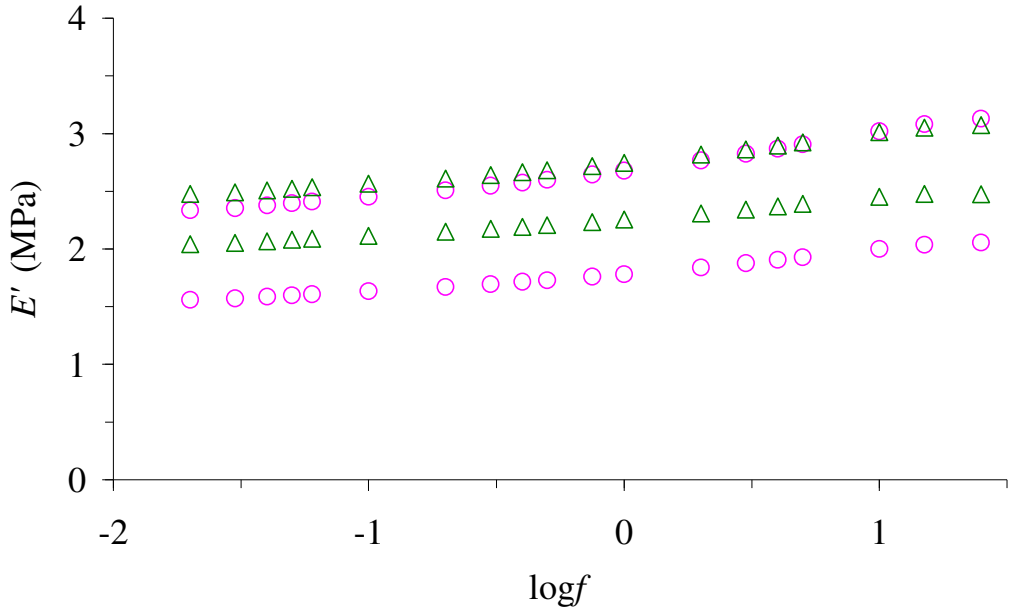

Figure 6.4: Upper and lower 95% confidence intervals of E' before (○) and after (△) accelerated aging (in physiological solution at 70°C for 38 days) of Nagor® silicone cylinders.

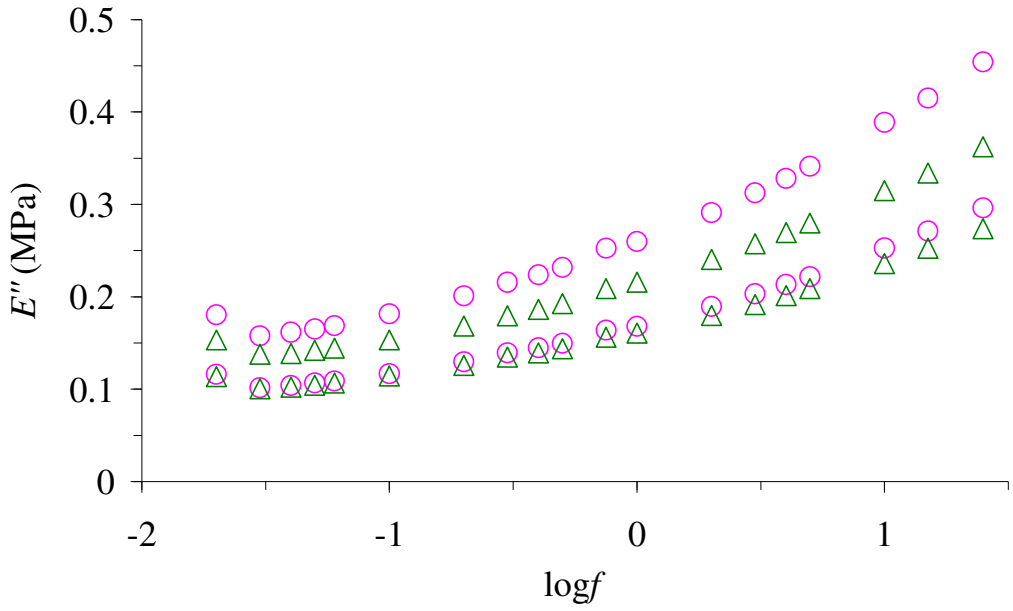

Figure 6.5: Upper and lower 95% confidence intervals of E'' before (○) and after (△) accelerated aging (in physiological solution at 70°C for 38 days) of Nagor® silicone cylinders.

6.6 What effect does aging at 37°C have on the properties of Elast-Eon™3?

The results demonstrated that aging the Elast-Eon™ 3 at 37°C for six months significantly affected the properties. Figure 6.6 and Figure 6.7 shows that aging at 37°C for six months slightly increased the values of *E'* and *E''*. The 95% confidence intervals (shown as error bars as discussed in §3.8.), of both the *E'* and *E''* before (△) and after (□) aging did not overlap i.e. aging had a significant effect throughout the frequency range on both the moduli. Aging at 37°C for 6 months did not change the appearance of the specimens.

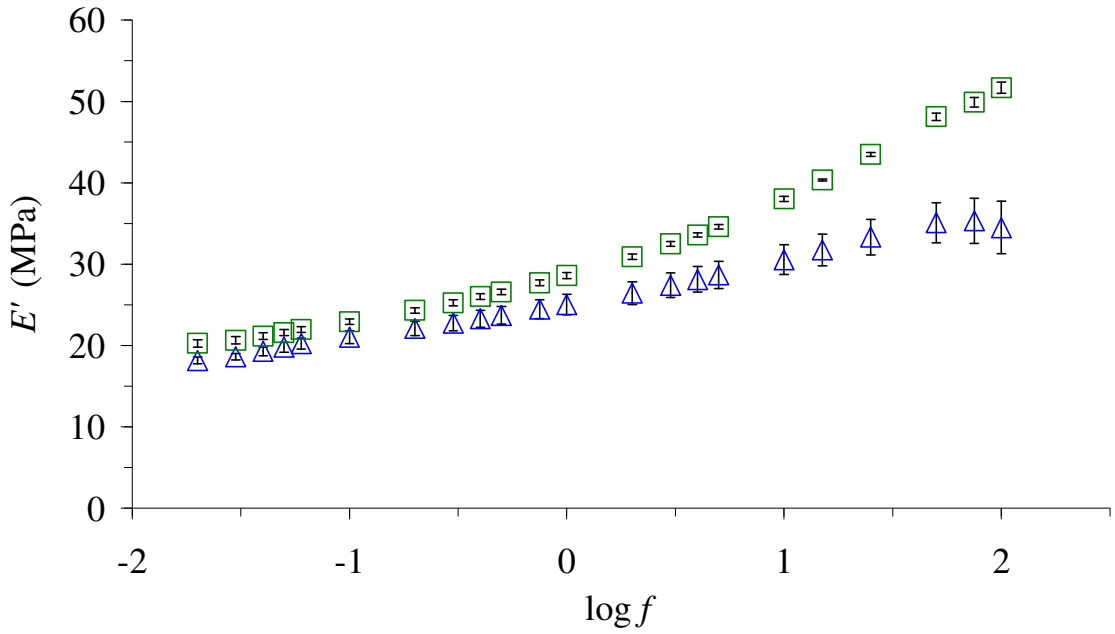

Figure 6.6: Mean values of E' plotted against the $\log_{10} f$, for Elast-Eon™ 3 before (△) and after (□) aging in a bath at 37°C for six months. The error bars represent the 95% confidence intervals.

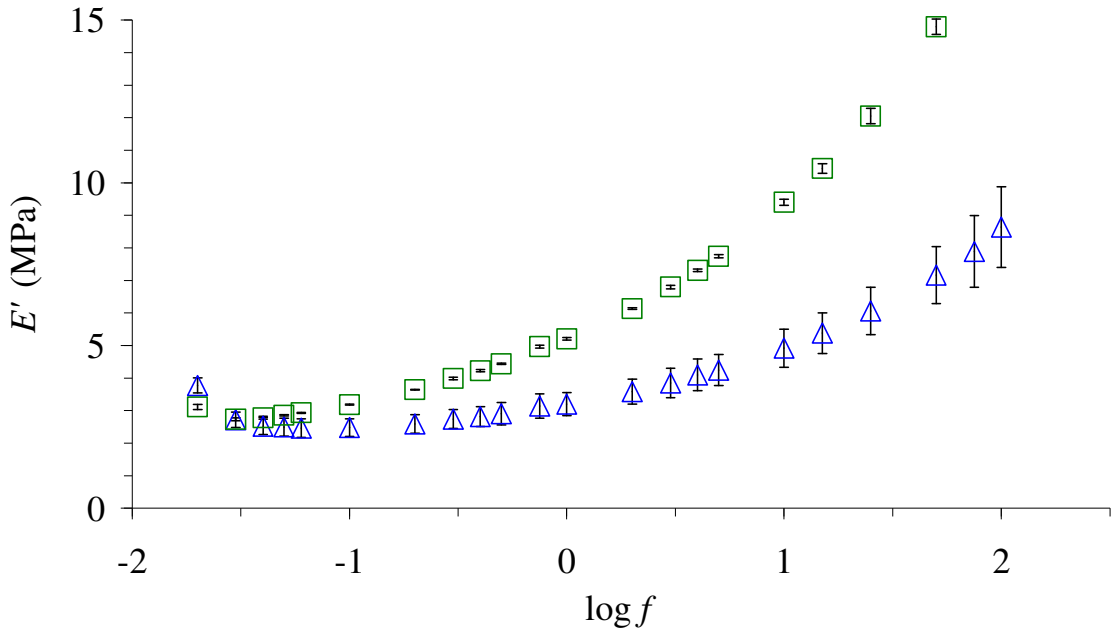

Figure 6.7: Mean values of E'' plotted against the $\log_{10} f$, for Elast-Eon™ 3 before (△) and after (□) aging in a bath at 37°C for six months. The error bars represent the 95% confidence intervals.

6.7 Discussion

6.7.1 The frequency-dependent behaviour of the storage and loss moduli

The results demonstrated that both storage, *E'*, and loss, *E''*, moduli of Elast-Eon™ 3 depended on the frequency, *f*, at which it was loaded. The coefficients in Table 6.1 and Table 6.2 enable the values to be calculated, for any frequency in the range 0.02–100 Hz, for the linear region of the Elast-Eon™ stress-strain curve. The frequency dependence was more marked for *E'* than for *E''*, especially when *f* was less than about 1 Hz.

Furthermore, *E''* values were consistently much less than *E'* values, showing that most of the energy supplied to Elast-Eon™ 3 in compression was stored and used in recoil, i.e. little of this energy is dissipated.

For the Nagor® silicone cylinders, the *E'* and *E''* demonstrated frequency-dependent behaviour, as expected and discussed in Chapter 4, for other medical grade silicones cylinders.

6.7.2 The effect of accelerated aging on the viscoelastic properties of Elast-Eon™ 3

Accelerated aging, at 70°C, affected the viscoelastic properties and the appearance of Elast-Eon™ 3. Values of both *E'* and *E''* increased significantly, as a result of accelerated aging, although the effect was greater for *E'* values. In addition, the slope of the graph of *E'* plotted against $\log_{10} f$ (Figure 6.1) appeared to increase as a result of accelerated aging. Although accelerated aging affected the properties of simple polyurethanes, used for maxillofacial implants and dental liners, the effect led to degradation of mechanical properties rather then the stiffening shown here (Craig *et al.*, 1980; Goldberg *et al.*, 1978; Yu *et al.*, 1980). However, the stiffness of Elast-Eon™ was found to increase after implantation in sheep (Simmons *et al.*, 2004; Simmons *et al.*, 2008). Discolouration was observed in Elast-Eon™, after accelerated aging; discolouration has also been observed in simple polyurethanes after immersion in cow blood at 37°C for 28 days (Yu *et al.*, 1980). The rate of increase of the *E'* with frequency was greater after accelerated aging, resulting in a steeper *E'* versus $\log f$ curve.

Our results are consistent with the observation that, the Young's modulus of Elast-Eon™ increased after implantation in sheep for either six (Simmons *et al.*, 2008) or twelve (Simmons *et al.*, 2004) months. In order to relate this result to those presented here, note that the Young's modulus of a viscoelastic material, for a given loading rate, is given by $|E^*|$, defined in equation 2.22. No previous studies have measured Young's modulus before and after accelerated aging. Previous studies showed no signs of degradation or surface cracking of Elast-Eon™ after ethylene oxide or γ-irradiation sterilisation and accelerated aging at 70°C for 2 weeks (Simmons *et al.*, 2006). However, signs of degradation or surface cracking of Elast-Eon™ were observed (Simmons *et al.*, 2006) after autoclaving and accelerated aging at 70°C for 2 weeks.

6.7.3 The effect of accelerated aging on the viscoelastic properties of Nagor® silicone cylinders

Nagor® silicone cylinders, that were treated in exactly the same way as Elast-Eon™ 3 showed no changes in viscoelastic properties or appearance as a result of aging. This seems to be in general agreement with previous studies (Craig *et al.*, 1980; Dootz *et al.*, 1994; Goldberg *et al.*, 1978; Jepson *et al.*, 1993; Saber-Sheikh *et al.*, 1999a; Wagner *et al.*, 1995b; Yu *et al.*, 1980) that, accelerated aging of silicone is not likely to cause the silicone to degrade or greatly affect its viscoelastic properties or change its appearance. A study (Wilson and Tomlin, 1969) also concluded that the appearance of two silicones for dental liners, Molloplast-B and Silastic 390, did not change after being immersed in water at 37°C for six months.

6.7.4 The effect of aging at 37°C on the viscoelastic properties of Elast-Eon™ 3

Aging at 37°C in a bath for 6 months, affected the *E'* and *E''* but not the appearance of Elast-Eon™ 3. Values of *E'* and *E''* increased significantly, as a result of aging. Although, rubber and Elast-Eon™ 3 have different chemical properties, a study on rubber (Wei *et al.*, 2004; Xie *et al.*, 2004) also concluded that the *E'* and *E''* increased with aging time (24-240 hours) at all the aging temperatures (30°C, 50°C and 70°C).

6.8 Summary of main conclusions

The main conclusions from this study are summarised below. They are based on results from Elast-Eon™ 3 that had been stored for 5 years (see §3.2.2).

- Storage, *E',* and loss, *E''*, moduli of Elast-Eon™ 3 depended on loading frequency, *f,* regardless of whether or not accelerated aging had occurred.
- Accelerated aging (at 70°C) darkened the colour and increased the opacity of Elast-Eon™ 3. Accelerated aging led to a statistically significant ($p < 0.05$) increase in *E'* and *E''* values.
- The slope of a graph of *E'* plotted against $\log_{10} f$ for Elast-Eon™ 3 appeared to increase after accelerated aging.
- Aging (at 37°C) did not change the appearance of Elast-Eon™ 3. It led to a statistically significant ($p < 0.05$) increase in *E'* and *E''* values.
- Accelerated aging (at 70°C) did not change the appearance of Nagor® silicone and did not significantly increase the *E'* and *E''* values.

Chapter 7. CROSS-LINK DENSITY OF MEDICAL GRADE SILICONES

7.1 Chapter overview

This chapter describes the measurement of the cross-link density, υ_c, of short-term implant medical grade silicones. The theoretical background information for this chapter has been discussed in Chapter 2 (§2.5.3 and §2.5.4). The materials and the sample preparation methods used, the experimental methods and the necessary calculations made have been described in Chapter 3 (§3.2, §3.3, §3.8 and §3.9).

§7.2 summarises the previous studies that have used solvents to swell silicones. §7.3-§7.9 summarises the experimental results. These results have been presented in such a way that they answer the specific questions that are being investigated. The headings of §7.3-§7.10 are the specific questions. In the results section, there are areas where the results are discussed in more detail than usual, because they needed to be considered very carefully. An extended discussion of the results is given in §7.11. The main conclusions of the study are summarised in §7.12. The swelling measurements of the pre-treated samples (discussed in §3.9.2) are only preliminary results and therefore have been relegated to Appendix I (§I.5).

The aim of this chapter is to swell short–term implant medical grade silicones (described in Chapter 3; §3.2 and §3.9). The swelling measurements will be used to calculate the values of three parameters: the volume fraction of polymer in the swollen silicone, i.e. ϕ_P (using equation 2.8); the Flory polymer-solvent interaction parameter, i.e. χ (using equation 2.9 and 2.12) and the cross-link density, i.e. υ_c (using equation 2.7). These parameters have been discussed previously in Chapter 2 (§2.5.4).

7.2 Previous studies on the use of solvents to swell silicones

The cross-link density of silicone gel breast implants have been measured by swelling the implant shells in toluene (Brandon *et al.*, 2003; Brandon *et al.*, 2001). In the first of these studies (Brandon *et al.*, 2001), rectangular pieces of Silastic I and Silastic II control silicone shells were swollen until constant mass. The ϕ_P and the cross-link density were calculated from these measurements, using the Flory-Rehner equation (equation 2.7). The interaction parameter, χ, was taken from previous published data. The Silastic I and Silastic II pieces swelled to a maximum of 217% and 216% of their original mass, respectively. This corresponded to a cross-link density of 4.02 x 10^{-4} mol/cm^3 and 3.52 x 10^{-4} mol/cm^3 respectively. In their second study, two rectangular pieces were cut from control and explanted Cronin implants, Silastic 0, Silastic I and Silastic II shells. Using the same procedure as above, cross-link density was measured and it was noted that for the Cronin, and Silastic I implants, the control pieces had a lower cross-link density than the explanted pieces.

In another study (Andreopoulos *et al.*, 1993), the swelling properties of cross-linked silicones for maxillofacial applications were measured. Silicone discs were swollen in toluene, ethyl acetate, n-butanol and ethyl metyl ketone at 25°C, until constant mass and the measurements used to calculate χ. The discs swelled the most in toluene (130-184% of their original mass) and the least in n-butanol (10.7-13.3% of their original mass). χ values for toluene, ethyl acetate, ethyl methyl ketone and n-butanol were calculated as 0.610, 0.667, 0.695 and 1.252 respectively. Discs with a higher cross-linker percentage swelled the least. It was concluded that χ ranges between 0.6-0.7 in good solvents. The explanation of what is meant by a good solvent and the criteria used to identify a good solvent have been discussed in Chapter 2 (§2.5.4.1 and 2.5.4.8).

Another study (Bueche, 1955b) swelled rectangular pieces of cross linked PDMS in various solvents (including toluene) at 25 ± 1°C, until constant mass. It was noted that the PDMS swelled quickly at first and then slowed with time. ϕ_P and χ were calculated from the swelling measurements. A χ value of 0.465 was calculated for toluene. The use of Hildebrand's solubility parameter theory to calculate χ (discussed previously in Chapter 2 (§2.5.4.6)) was also investigated. It was concluded that the estimation of the solubility parameters, δ_P, by swelling is useful for comparison purposes only.

In another study (Favre, 1996), a filler-free cross linked PDMS was swollen in 22 solvents (including toluene, ethyl acetate, ethyl methyl ketone and n-butanol) at 30-80°C. In this study, the swollen samples were weighed every second day until constant mass. ϕ_P and χ were calculated from the swelling measurements.

χ values of 0.792, 0.820, 0.869 and 1.277 were obtained for toluene, ethyl acetate, ethyl methyl ketone and n-butanol. The χ values were also found to increase moderately with temperature.

A study (Yerrick and Beck, 1964) used the swelling equilibrium method to determine the δ_P of silicones, discussed previously in Chapter 2 (§2.5.4.6). Rectangular samples of 11 types of silicones were swollen in 33 solvents at 22°C. Solvents with different solvent-polymer interaction properties were used and were classified according to their electrical properties. Solvents were categorised as having weak electrical properties (i.e. a neutral molecule with even distribution of charge), moderate electrical properties (i.e. some uneven distribution of charge; net dipole) or strong electrical properties (i.e. more marked uneven distribution of charge; more obvious dipole). During the swelling period, the mass of the samples were recorded every 24 hours until it remained constant. The swelling was then calculated as a percentage of the original volume.

To analyse the results only solvents with weak or strong electrical properties were considered, in order to minimise the scatter in the data. The swelling (as a percentage of the original volume) was plotted against the solubility parameter of the solvent, δ_S, (discussed in §2.5.4.6). These plots showed that the silicones swelled the most in n-heptane (225% of their original volume). The solubility parameter of the silicone, δ_P (discussed in §2.5.4.6), was equated to the δ_S of n-heptane i.e. where maximum swelling occurred (as discussed in §2.5.4.6).

The cross-link density of explanted silicone rubber tubing used in pacemakers has been measured (Doležel *et al.*, 1989b). The silicone rubber was implanted *in vivo* for a period between 3 – 4500 days. The samples were swollen in toluene at 25°C and weighed until constant mass. The value of ϕ_P was calculated from the swelling measurements and substituted into the Flory-Rehner equation (equation 2.7) to calculate the cross-link density. A value of $\chi = 0.465$ from previous published data (Bueche, 1955a) was used for the cross-link density calculation. The results showed that the cross-link density and ϕ_P rose for the initial 1000 days after implantation but then decreased sharply.

Another study (Muramoto, 1982) used the swelling method to calculate the ϕ_P and χ values of PDMS with different molecular weights. The samples were swollen in ethyl methyl ketone at 30°C. χ values in the range $0.470 \leq \chi \leq 0.736$ were obtained and it was concluded that the value of χ was not dependent on the molecular weight. The swelling characteristics of two silicones, Silastic® 595 and 599 in three solvents, ethyl methyl ketone, cyclohexane and benzene, at room temperature, was investigated (Knaub *et al.*, 1988). The samples were weighed periodically until constant mass. Constant mass was achieved within one day for some samples and within a few days for other samples. χ values of 0.688, 0.479, 0.597 and 0.612 were obtained for, Silastic® 595 in ethyl methyl ketone, Silastic® 595 in cyclohexane, Silastic® 595 in benzene and Silastic® 599 in benzene, respectively. It was concluded that ethyl methyl ketone was a bad swelling agent for these samples.

7.3 Do different solvents have different swelling abilities?

The results demonstrated that different solvents have different swelling abilities. Table 7.1 shows the amount of swelling (as a percentage of the original volume) of the four silicone grades, in the five solvents used. A similar table, showing the amount of swelling (as a percentage of the original mass) is shown in Appendix I (§I.1).

The results presented in Table 7.1 can be used to determine whether different solvents have different swelling abilities. For example, by comparing the swelling of grade C6-165 in the five solvents, the table shows that the silicone samples swelled the most in cyclohexane, followed by toluene, ethyl acetate, ethyl methyl ketone and then n-butanol. Similar conclusions can be made for the other three silicone grades shown. Figure 7.1 shows the amount of swelling (as a percentage of the original volume) of the same silicone grades in different solvents. In this figure, the 95 % confidence intervals (discussed in §3.8) did not overlap (i.e. the amount of swelling of the same silicone grade in different solvents, were significantly different).

Table 7.1: Mean and standard deviation values of swelling (as a percentage of the original volume) of the medical grade silicones after swelling in cyclohexane, toluene, ethyl acetate, ethyl methyl ketone and n-butanol. The values for ρ_p, which are required in the calculations, are given in Table 3.2 (§3.2.1).

Solvent	**Grades**	**Mean swelling (as a percentage of the original volume)**	**Standard deviation**
cyclohexane			
	C6-165	197	6
	C6-180	145	5
	MED82-5010-80	208	8
	MED-4080	134	6
toluene			
	C6-165	151	7
	C6-180	113	2
	MED82-5010-80	162	3
	MED-4080	102	2
ethyl acetate			
	C6-165	96	2
	C6-180	71	2
	MED82-5010-80	103	2
	MED-4080	68	2
ethyl methyl ketone			
	C6-165	78	7
	C6-180	60	5
	MED82-5010-80	86	7
	MED-4080	56	5
n-butanol			
	C6-165	21	4
	C6-180	13	3
	MED82-5010-80	26	2
	MED-4080	22	3

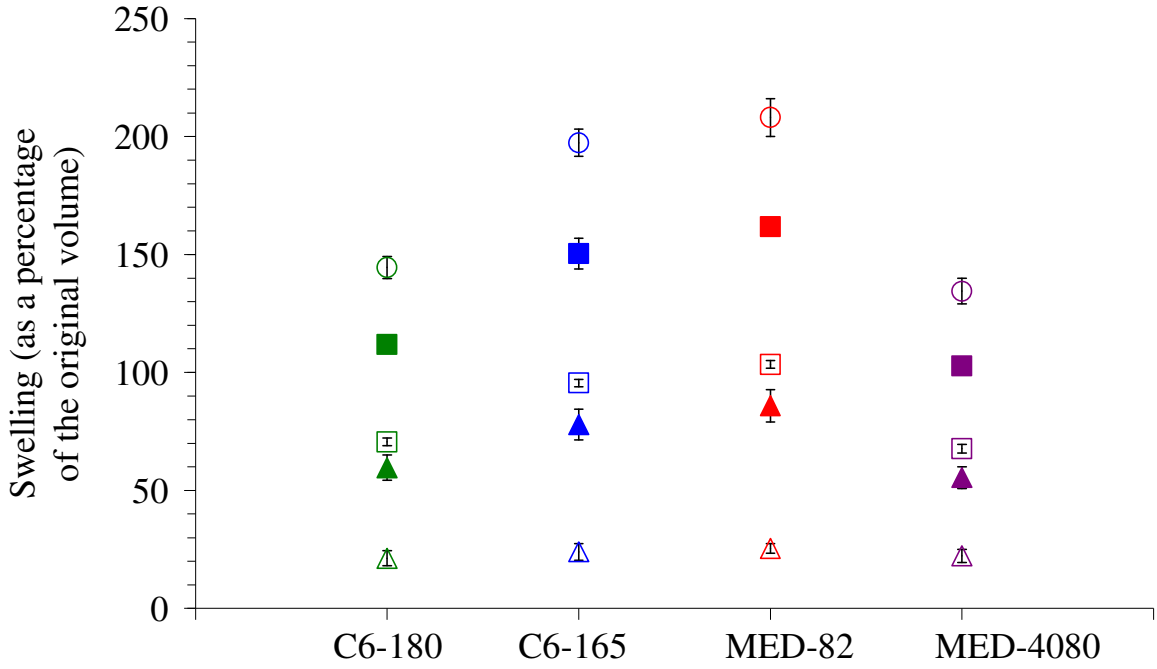

Figure 7.1: Mean values of swelling (as a percentage of the original volume) in different solvents plotted against the different silicone grades (C6-180, C6-165, MED-82-5010-80 (which has been abbreviated to MED-82 on the figure) and MED-4080). The solvents used are shown as: cyclohexane (unfilled circles); toluene (filled squares); ethyl acetate (unfilled squares); ethyl methyl ketone (filled triangles) and n-butanol (unfilled triangles). The values were obtained from Table 7.1. The error bars shown represent the 95% confidence intervals. Error bars that are not visible have been obscured by the data point.

7.4 Will the amount of swelling vary between the different silicone grades?

The results showed that different silicone grades swell by different amounts. Table 7.1 shows that grade MED-82-5010-80 swelled the most, followed by grade C6-165, then grade C6-180 and then grade MED-4080, in four out of the five solvents (cyclohexane, toluene, ethyl acetate and ethyl methyl ketone).

Figure 7.2 shows the amount of swelling (as a percentage of the original volume) for the four silicone grades in the same solvents. In this figure, the 95 % confidence intervals (discussed in §3.8) of grades MED-82-5010-80 and C6-165 did not overlap with those of grades MED-4080 and C6-180, (i.e. the amount of swelling between these different grades were significantly different). The confidence intervals (discussed in §3.8) of grade MED-4080 and C6-180 (which have similar properties, as shown in Table 3.2) did overlap in some solvents (e.g. ethyl acetate and ethyl methyl ketone). Hence, the amount of swelling between these similar grades, was not significantly different.

The trend of the data points in Figure 7.2, clearly demonstrate that it is possible to classify the solvents into good, fair or bad solvents, in terms of their swelling ability (discussed in Chapter 2; §2.5.4.1 and 2.5.4.8). As expected, these results show that cyclohexane and toluene were good solvents, ethyl acetate and ethyl methyl ketone were fair solvents and n-butanol was a bad solvent, for the silicones. Therefore, only the swelling measurements of the good solvents (i.e. cyclohexane and toluene) are analysed further in the next section.

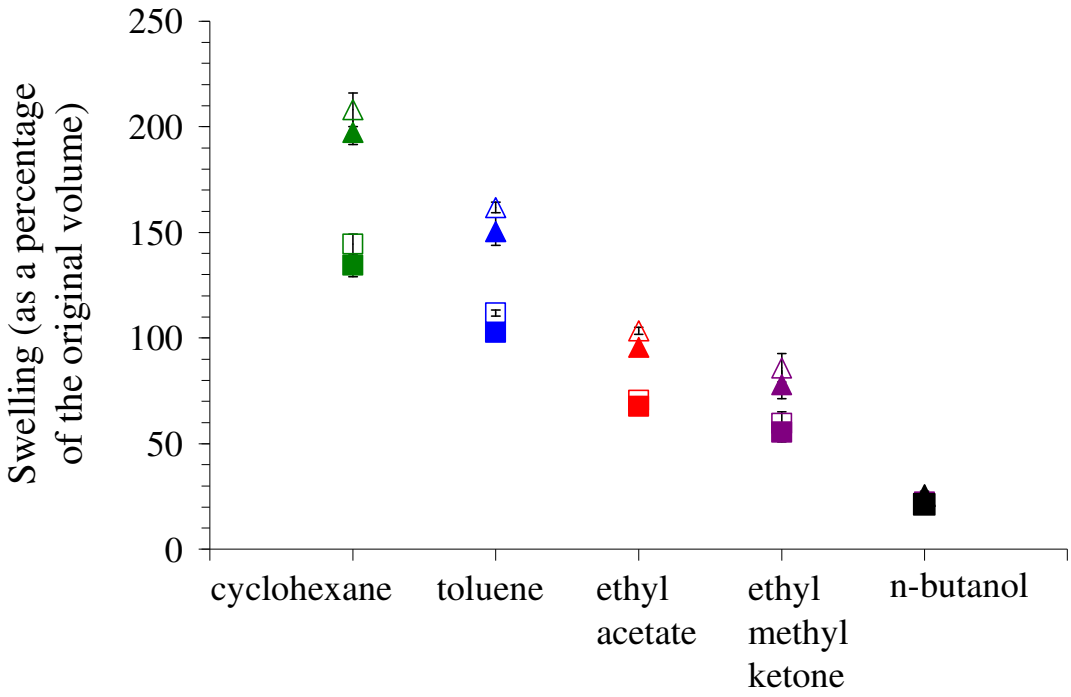

Figure 7.2: Mean values of swelling (as a percentage of the original volume) for the different silicone grades plotted against the solvent used: cyclohexane (■□△▲); toluene (■□△▲); ethyl acetate (■□△▲); ethyl methyl ketone (■□△▲); n-butanol (■□△▲). The silicone grades are shown as: C6-180 (unfilled squares); C6-165 (filled triangles); MED-82-5010-80 (unfilled triangles) and MED-4080 (filled squares). The values were obtained from Table 7.1. The error bars shown represent the 95% confidence intervals. Error bars that are not visible have been obscured by the data point.

7.5 Is it possible to calculate ϕ_P and the corresponding χ and υ_c from the swelling measurements using the swelling equilibrium method (equations 2.7, 2.8 and 2.9)?

Table 7.2 lists the mean and standard deviation values obtained for ϕ_P and χ. The results demonstrated that precise (i.e. with low standard deviations) ϕ_P and χ values, can be calculated from the swelling measurements using the swelling equilibrium method (see §2.5.4.5 and §2.5.4.6), as shown in Table 7.2. The χ values from toluene appeared to be reasonable (i.e. consistent with previous studies, as discussed further in §7.11.2). In Table 7.2, the ϕ_P values calculated from the swelling measurements in cyclohexane and toluene were in the range $0.325 \leq \phi_P \leq 0.426$ and $0.382 \leq \phi_P \leq 0.493$, respectively. The corresponding χ values were in the range $0.644 \leq \chi \leq 0.712$ and $0.680 \leq \chi \leq 0.766$, respectively. However, as discussed previously in §2.5.4.6, substitution of these ϕ_P and χ values into the cross-link density equation (equation 2.9), gives a value of $\upsilon_c = 0$, which is not physically possible. Note that the values in Table 7.2 have been rounded off, hence if any non-zero υ_c values are obtained with these ϕ_P and χ values, this is because of a rounding off error.

Table 7.2: Mean and standard deviation values of ϕ_P and χ obtained for the medical grade silicones using the swelling equilibrium method (see §2.5.4.5 and §2.5.4.6). The swelling measurements were substituted into equation 2.8 (to calculate ϕ_P) and equation 2.9 (to calculate χ). The values for ρ_p and ρ_s, which are required in the calculations, are given in Table 3.2 (§3.2.1) and Table 3.5 (§3.9.1) respectively.

Solvent	**Grades**	**Mean ϕ_P**	**Standard deviation ϕ_P**	**Mean χ**	**Standard deviation χ**
cyclohexane	C6-165	0.337	0.007	0.651	0.004
	C6-180	0.410	0.008	0.699	0.006
	MED82-5010-80	0.325	0.009	0.644	0.005
	MED-4080	0.426	0.01	0.712	0.007
toluene	C6-165	0.398	0.011	0.691	0.008
	C6-180	0.475	0.003	0.750	0.003
	MED82-5010-80	0.382	0.004	0.680	0.002
	MED-4080	0.493	0.005	0.766	0.004

7.6 Is it possible to swell silicone in various solvents to estimate its solubility parameter (δ_P)?

The results showed that it is possible to use the swelling equilibrium method to estimate δ_P, by plotting the mean values of swelling (as a percentage of the original volume) against the solubility parameter of the solvent, δ_S, as discussed in §2.5.4.6 and §3.9.4.

Figure 7.3 and Figure 7.5 shows the swelling (as a percentage of the original volume) for grade C6-180 and MED82-5010-80, plotted against the δ_S of eight solvents (listed in §3.9.4). These figures show that the maximum swelling of the silicones occurred in n-heptane (i.e. the figures show that in terms of swelling (as a percentage of the original volume), there was more swelling in n-heptane than in the other solvents). The δ_S for n-heptane is 15.3 $MPa^{½}$ (see Table 3.5; §3.9.1), suggesting that a δ_P value of 15.3 $MPa^{½}$ can be used for these silicones. However, because all the data points were plotted on the curve (i.e. points on the lower end of the curve were not excluded from the figure; discussed in §3.9.4), it was not possible to fit and differentiate a n^{th} ($n \geq 2$) order polynomial through the data points (see §3.9.4) and check whether the maximum point of the curve occurred at δ_S = 15.3 $MPa^{½}$. The next paragraph shows the results obtained, when less data points were used and the maximum point of the curve was obtained by fitting and differentiating a second-order polynomial through the data points (discussed in §3.9.4).

As discussed in §3.9.4, the swelling measurements of the fair or bad solvents do not necessarily need to be considered, to locate the point of maximum swelling, particularly if the data points are extremely low on the swelling curve (as shown in Figure 7.3 and Figure 7.5, for bad solvents such as n-butanol and ethanol). Therefore, Figure 7.4 and Figure 7.6 show the same data as in Figure 7.3 and Figure 7.5, but only for the four solvents with the greatest swelling ability. Two of these solvents (cyclohexane and toluene) were also previously suggested as good solvents for silicone in §7.4. The lines shown are the second-order polynomials that gave the best fit to the data.

When these polynomials were differentiated and the derivative set equal to zero (i.e. finding the δ_S value at the maximum point of swelling as discussed in §3.9.4), the maximum swelling points occurred at δ_S = 15.9 $MPa^{½}$ (for grade C6-180), at δ_S = 15.8 $MPa^{½}$ (for grade C6-165), at δ_S = 15.7 $MPa^{½}$ (for grade MED-4080) and at δ_S = 15.6 $MPa^{½}$ (for grade MED-82-5010-80). The δ_P values for these silicones were then equated to these δ_S values. The equations of the second-order polynomials are given in Figure 7.4 and Figure 7.6. These enable the swelling (as a percentage of the original volume) at a given δ_S to be determined. Similar plots obtained for grades C6-165 and MED-4080 are in Appendix I (§I.3).

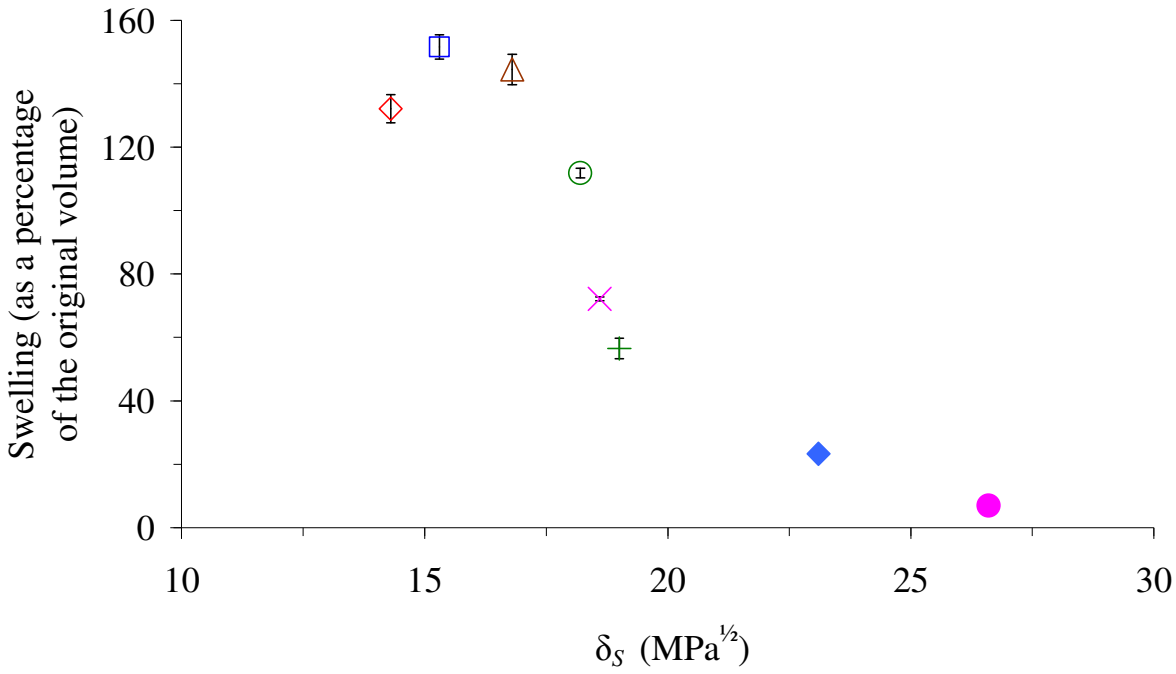

Figure 7.3: Mean values of swelling (as a percentage of the original volume) plotted against δ_S for grade C6-180. Error bars represent the standard deviations. The solvents shown are: 2,2,4-trimethylpentane (◇); n-heptane (□); cyclohexane (△); toluene (○); ethyl acetate (×); ethyl methyl ketone (+); n-butanol (◆) and ethanol (●). Further information on these solvents, including values for ρ_s, which are required in the calculations, are available in Table 3.5 (§3.9.1). Error bars that are not visible have been obscured by the data point.

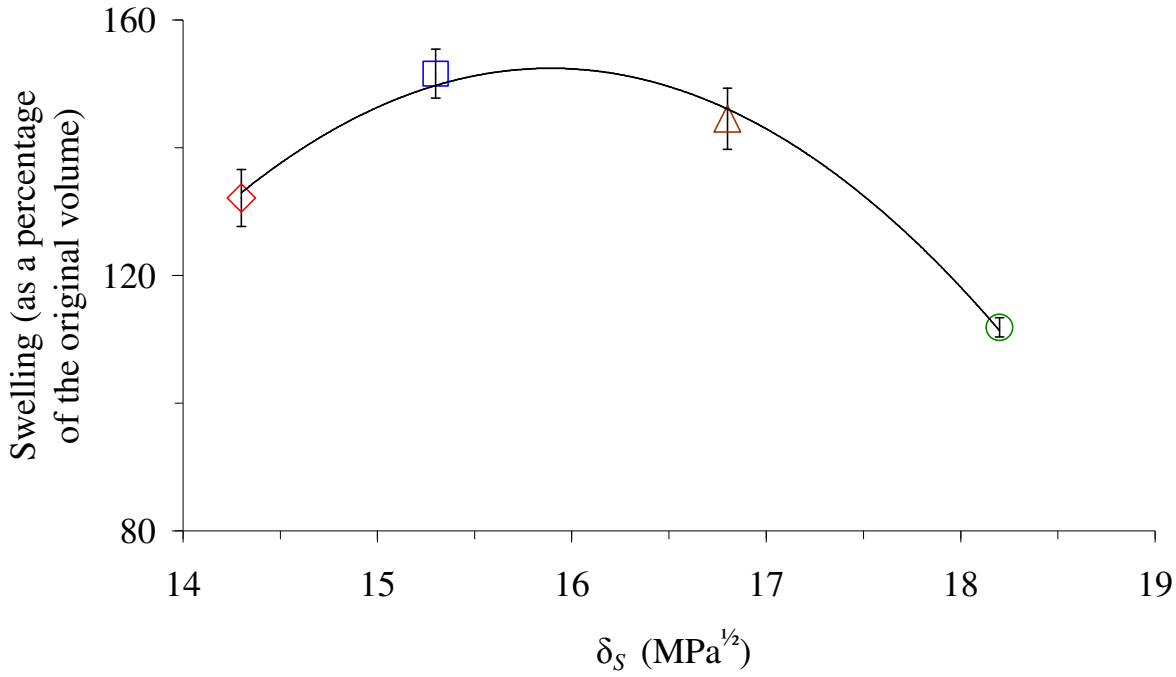

Figure 7.4: Mean values of swelling (as a percentage of the original volume) plotted against δ_S of the solvents with the greatest swelling ability, for grade C6-180. Error bars represent the standard deviations. The lines shown are the second-order polynomials that gave the best fit to the data. (The equation of the line is $y = -7.6982x^2 + 244.65x - 1791.4$ and $R^2 = 0.99$). The solvents shown are: 2,2,4-trimethylpentane (◇); n-heptane (□); cyclohexane (△) and toluene (○). Further information on these solvents, including the values for ρ_s, which are required in the calculations, are available in Table 3.5 (§3.9.1).

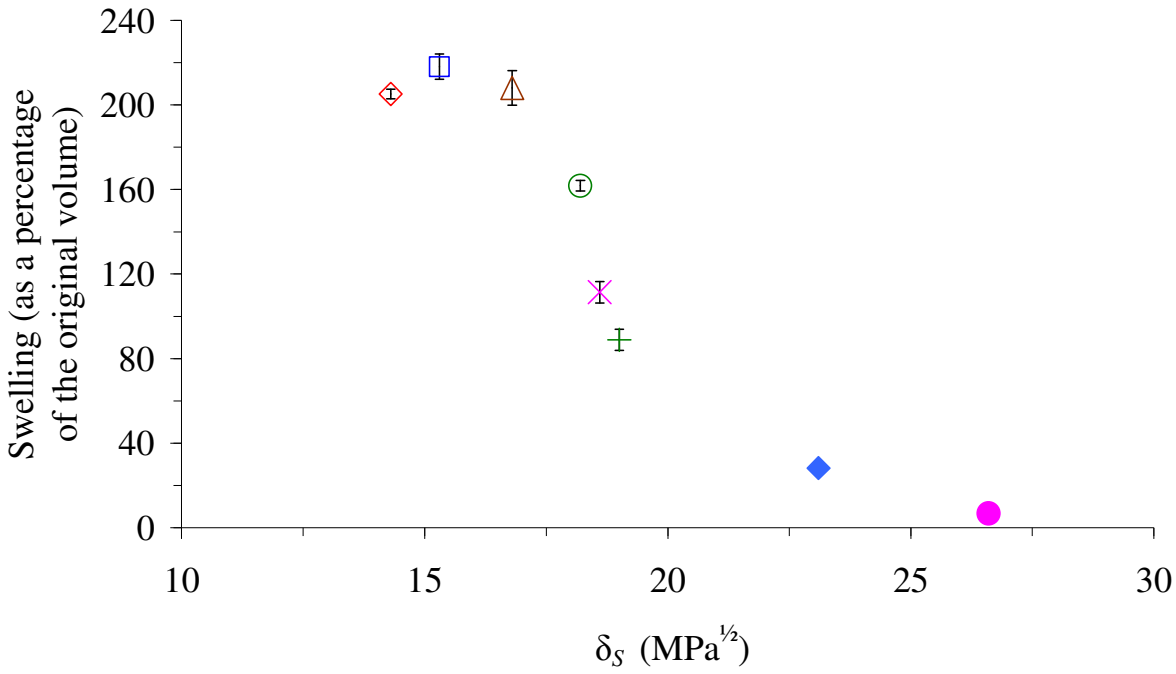

Figure 7.5: Mean values of swelling (as a percentage of the original volume) plotted against δ_S for grade MED 82-5010-80. Error bars represent the standard deviations. The solvents shown are: 2,2,4-trimethylpentane (◇); n-heptane (□); cyclohexane (△); toluene (○); ethyl acetate (×); ethyl methyl ketone (+); n-butanol (◆) and ethanol (●). Further information on these solvents, including values for ρ_s, which are required in the calculations, are available in Table 3.5 (§3.9.1). Error bars that are not visible have been obscured by the data point.

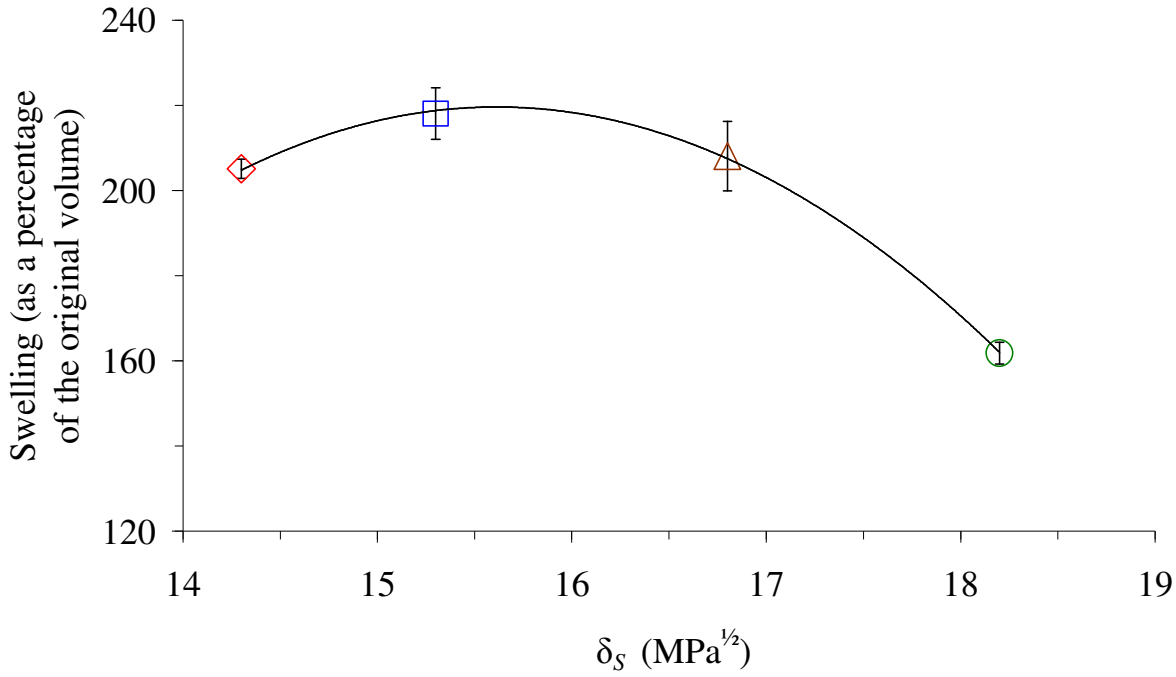

Figure 7.6: Mean values of swelling (as a percentage of the original volume) against δ_S of the solvents with the greatest swelling ability, for grade MED 82-5010-80. Error bars represent the standard deviations. The lines shown are the second-order polynomials that gave the best fit to the data. (The equation of the line is $y = -8.6056x^2 + 268.71x - 1878.1$ and $R^2 = 1.0$). Further information on these solvents is available in Table 3.5 (§3.9.1). The solvents shown are: 2,2,4-trimethylpentane (◇); n-heptane (□); cyclohexane (△) and toluene (○). Further information on these solvents, including the values for ρ_s, which are required in the calculations, are available in Table 3.5 (§3.9.1).

Although, the medical grade silicones were swollen in eleven solvents as mentioned in §3.9.1 and §3.9.4, Figure 7.3 and Figure 7.5 only show the swelling results in a selection of solvents (eight solvents) , as suggested (Yerrick and Beck, 1964) and discussed in §7.2. The swelling results of the different silicone grades in all the eleven solvents are in Appendix I (§I.3).

7.7 Using the δ_P value obtained in § 7.6, is it possible to calculate χ using Hildebrand's solubility parameter theory (equation 2.12) and then calculate the corresponding υ_c (equation 2.7)?

The results demonstrated that reasonable χ values were obtained, as shown in the next paragraphs and discussed further in §7.11.2. The υ_c values obtained were not absolute, as shown in the next paragraphs and discussed further in §7.11.3.

Table 7.3 lists the mean χ and υ_c values calculated, using δ_P = 15.3 $MPa^{½}$, obtained in §7.6 (Figure 7.3 and Figure 7.5). The values shown here are for the good solvents (i.e. cyclohexane and toluene; reported in §7.4). Similar tables for the swelling measurements in ethyl acetate, ethyl methyl ketone and n-butanol are in Appendix I (§I.4).

Table 7.3 shows that a χ value of 0.438 and 0.701 was calculated for cyclohexane and toluene, respectively. The corresponding υ_c values were in the range $38.5 \leq \upsilon_c \leq 86.0 \times 10^{-5}$ mol/cm^3 and $-5.3 \leq \upsilon_c \leq 27.6 \times 10^{-5}$ mol/cm^3. Imprecise (i.e. with high standard deviations) and negative υ_c, which is not physically possible (discussed in §7.11.3 and §8.5), were obtained for some grades, when the samples were swollen in toluene, a good solvent. The υ_c values for the samples swollen in cyclohexane were precise and non-negative.

Table 7.4 lists the same parameters, but using the δ_P values obtained from Figure 7.4 and Figure 7.6 (i.e. ranging between 15.6-15.9 $MPa^{½}$). Table 7.4 shows that slightly lower χ values in the range $0.392 \leq \chi \leq 0.402$ and $0.567 \leq \chi \leq 0.630$ was calculated for cyclohexane and toluene, respectively. The corresponding υ_c values were in the range $4.5 \leq \upsilon_c \leq 11.6 \times 10^{-4}$ mol/cm^3 and $1.3 \leq \upsilon_c \leq 6.7 \times 10^{-4}$ mol/cm^3. For both solvents, these χ values were reasonable and υ_c values were precise (i.e. low standard deviations).

By comparing the values obtained in the two tables, the results in Table 7.4 indicated that when δ_P values ranging between 15.6-15.9 $MPa^{½}$ were used, χ appeared to be reasonable and precise (i.e. with low standard deviations), while non-negative and precise (i.e. low standard deviations) υ_c values were obtained with good solvents (i.e. cyclohexane and toluene, as discussed in §7.4). However, Table 7.3 shows that, when a δ_P value of 15.3 $MPa^{½}$ was used, non-negative and precise υ_c values were only obtained with cyclohexane, although reasonable χ values were obtained with both solvents. For example, for grade C6-165 (from Table 7.3, in toluene), when δ_P = 15.3 $MPa^{½}$, then χ = 0.701 and $\upsilon_c = -2.3 \times 10^{-5}$ mol/cm^3. However, Table 7.4 shows that, for the same grade and solvent (i.e. C6-165 in toluene), when δ_P = 15.8 $MPa^{½}$, then χ = 0.597 and $\upsilon_c = 2.7 \times 10^{-4}$ mol/cm^3.

Figure 7.7 compares the υ_c values obtained from the two tables, for the same grades, after swelling in cyclohexane. The figure shows that the values of υ_c obtained in Table 7.3 (with a lower δ_P value of 15.3 $MPa^{½}$) were slightly but significantly lower than the υ_c values obtained in Table 7.4 (with a higher δ_P value in the range 15.6-15.9 $MPa^{½}$), i.e. the 95 % confidence intervals, shown as error bars (discussed in §3.8), did not overlap.

Similarly, comparing the υ_c values obtained from the two tables, for the same four grades, after swelling in toluene, also showed that the values obtained in Table 7.3 were significantly lower than those obtained in Table 7.4. The figure is shown in Figure I. 9; Appendix I (§I.4).

Figure 7.8 compares the υ_c values obtained in Table 7.4, for the same silicone grade but in the two different solvents. The figure shows that the values of υ_c obtained in cyclohexane and toluene, were significantly different (i.e. the 95 % confidence intervals shown as error bars, as discussed in §3.8, did not overlap). Similarly, when the υ_c values obtained in Table 7.3 were compared, the values were significantly different, as shown in Figure I. 10; Appendix I (§I.4). Consequently, there is no clear indication from the results reported in the previous paragraphs, that absolute υ_c values can be obtained; discussed further in §7.11.3.

Table 7.3: Mean values of χ and υ_c obtained for the medical grade silicones using Hildebrand's solubility parameter theory, when a constant δ_P value of 15.3 $MPa^{1/2}$ is used (assuming K=1, χ_s =0.34, R=8.31 J/Kmol and T=298K). As the value of χ does not alter for each grade, standard deviation values are only shown for υ_c. Standard deviation values for ϕ_P have previously been shown in Table 7.2. The values for V_S, δ_S, ρ_p and ρ_s, which are required in the calculations, are given in Table 3.2 (§3.2.1) and Table 3.5 (§3.9.1).

Solvent	**Grades**	ϕ_P	χ	υ_c (x 10^{-5} mol/cm^3)	**Standard deviation υ_c (x 10^{-5})**
cyclohexane	C6-165	0.337	0.438	42.6	2.4
	C6-180	0.410	0.438	75.4	4.4
	MED82-5010-80	0.325	0.438	38.5	3
	MED-4080	0.426	0.438	86.0	6
toluene	C6-165	0.398	0.701	-2.3	2.1
	C6-180	0.475	0.701	19.4	1.4
	MED82-5010-80	0.382	0.701	-5.3	5.7
	MED-4080	0.493	0.701	27.6	2.4

Table 7.4: Mean values of χ and υ_c obtained for the medical grade silicones using Hildebrand's solubility parameter theory, when δ_P varies between 15.6-15.9 MPa^{½} (assuming K=1, χ_s =0.34, R=8.31 J/Kmol and T=298K). As the value of χ does not alter for each grade, standard deviation values are only shown for υ_c. Standard deviation values for ϕ_P have previously been shown in Table 7.2. The values for V_S, δ_S, ρ_p and ρ_s, which are required in the calculations, are given in Table 3.2 (§3.2.1) and Table 3.5 (§3.9.1).

Solvent	**Grades**	**δ_P MPa^{½}**	ϕ_P	χ	**υ_c (x 10^{-4} mol/cm^3)**	**Standard deviation υ_c (x 10^{-4})**
cyclohexane	C6-165	15.8	0.337	0.393	5.2	0.3
	C6-180	15.9	0.410	0.375	9.4	0.5
	MED82-5010-80	15.6	0.325	0.402	4.5	0.3
	MED-4080	15.7	0.426	0.392	10.7	0.7
toluene	C6-165	15.8	0.398	0.597	2.7	0.4
	C6-180	15.9	0.475	0.567	7.0	0.2
	MED82-5010-80	15.6	0.382	0.630	1.3	0.1
	MED-4080	15.7	0.493	0.608	6.7	0.3

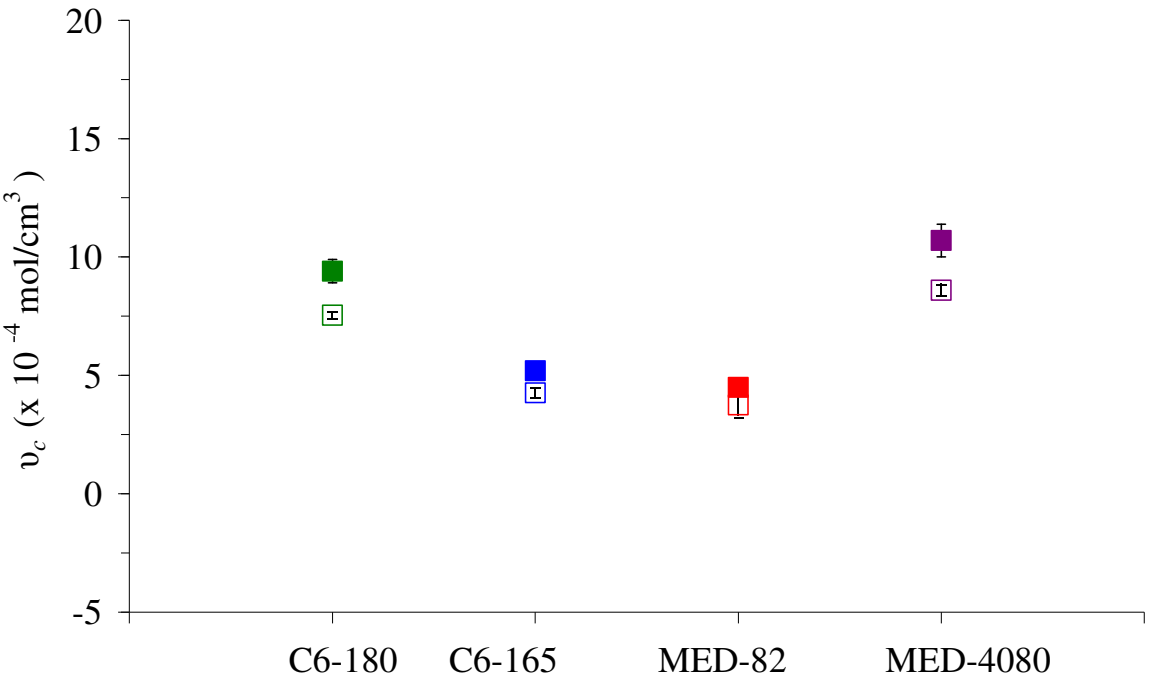

Figure 7.7: Mean values of υ_c plotted against the silicone grades: C6-180 (□■); C6-165 (□■); MED-82-5010-80 ((□■) abbreviated to MED-82 on the figure) and MED-4080 (□■). The values were obtained from Table 7.3 (unfilled squares) and Table 7.4 (filled squares) and are shown for samples swollen in cyclohexane. The error bars shown represent the 95% confidence intervals. Error bars not shown have been obscured by the data point.

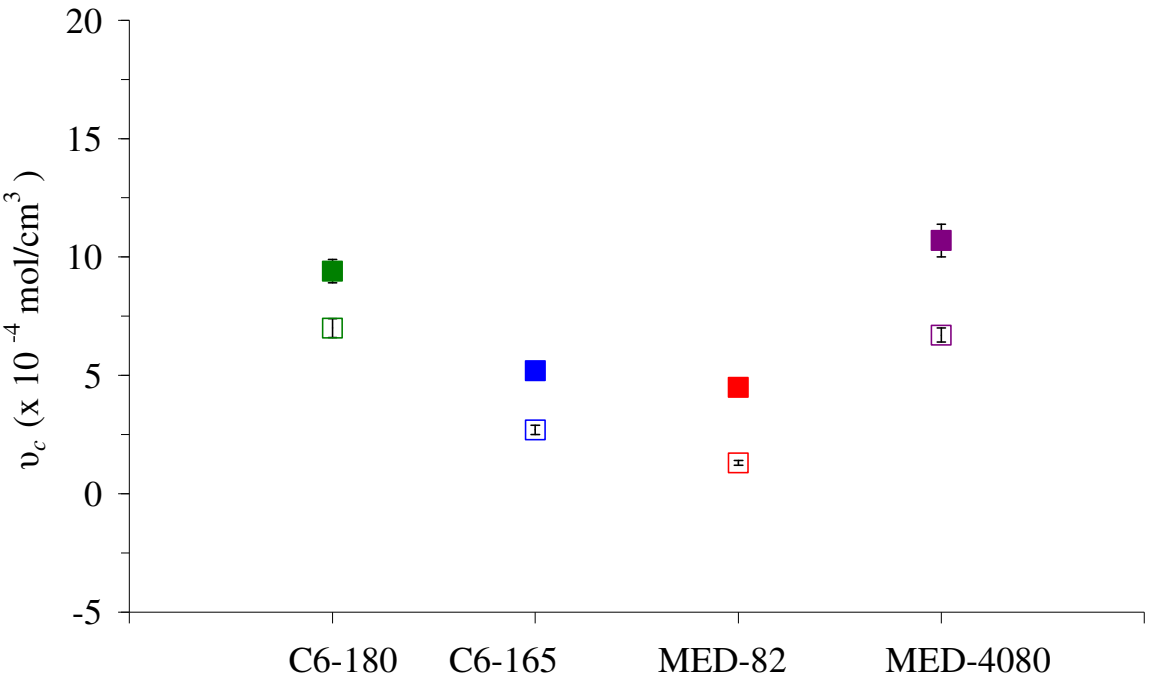

Figure 7.8: Mean values of υ_c plotted against the silicone grades: C6-180 (□■); C6-165 (□■); MED-82-5010-80 ((□■) abbreviated to MED-82 on the figure) and MED-4080 (□■). The values were obtained from Table 7.4 and are shown for samples swollen in cyclohexane (filled squares) and toluene (unfilled squares). The error bars shown represent the 95% confidence intervals. Error bars not shown have been obscured by the data point.

7.8 What effect will varying K, χ_s and δ_P (used in equation 2.12 to calculate χ) have on computed values of υ_c (equation 2.7)?

7.8.1 Effect of varying χ_s on computed values of υ_c

Previously, in Chapter 2 (§2.5.4.6) and in Chapter 3 (§3.9.4) it was discussed that in equation 2.12 (equation used to calculate χ according to Hildebrand's solubility parameter theory) the value for χ_s can vary. This section shows the effect of varying χ_s (which will consequently affect χ, because of the form of equation 2.12) on computed υ_c values (computed using equation 2.7). In Figure 7.9 computed values of υ_c are plotted against χ_s. It shows that an increase in χ_s decreased the computed values of υ_c.

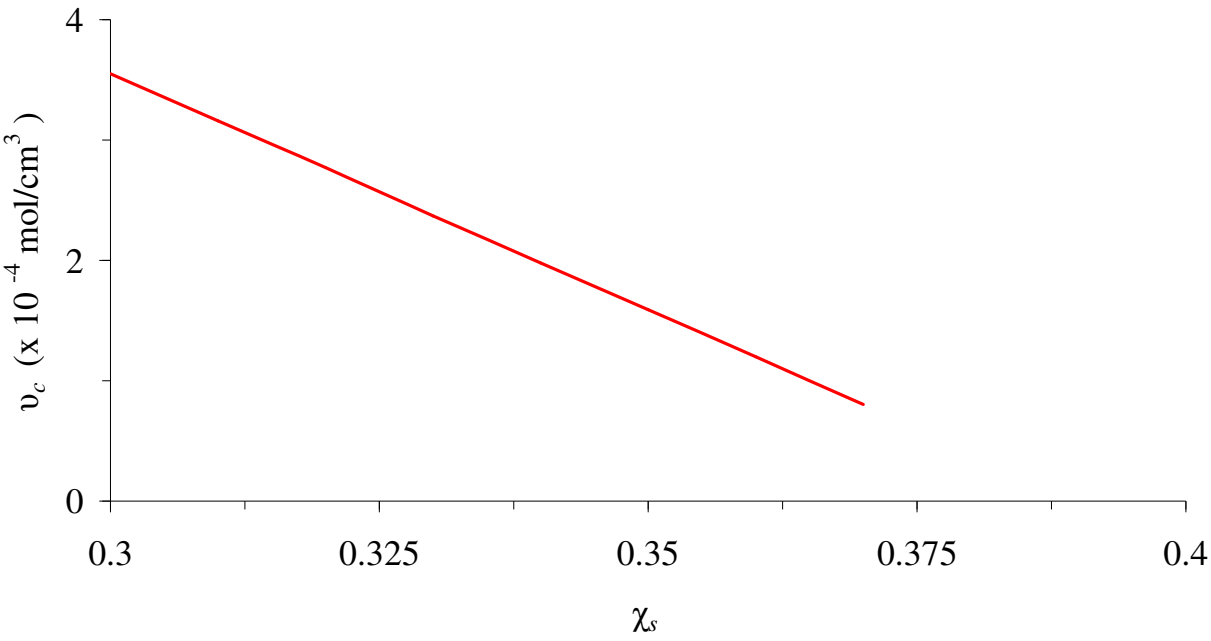

Figure 7.9: Computed values of υ_c plotted against χ_s (for grade C6-180 in toluene: K = 1; δ_P = 15.3 $MPa^{½}$; δ_S = 18.2 $MPa^{½}$; ϕ_P = 0.475; V_S = 106.8 cm^3/mol; R=8.31 J/Kmol; T=298K). The line shown is y = -39.237x + 15.322; R^2 = 1. The υ_c values have been computed using equation 2.7 (where the χ values used for this computation have been computed using equation 2.12) to show the form of the equations.

7.8.2 Effect of varying *K* on computed values of υ_c

Previously, in Chapter 2 (§2.5.4.6) and in Chapter 3 (§3.9.4) it was discussed that in equation 2.12 (equation used to calculates χ according to Hildebrand's solubility parameter theory) the value for *K* can vary. This section shows the effect of varying *K* (which will consequently affect χ, because of the form of equation 2.12) on computed υ_c values (computed using equation 2.7).

In Figure 7.10, computed values of υ_c are plotted against K. It shows that an increase in K decreased the computed values of υ_c.

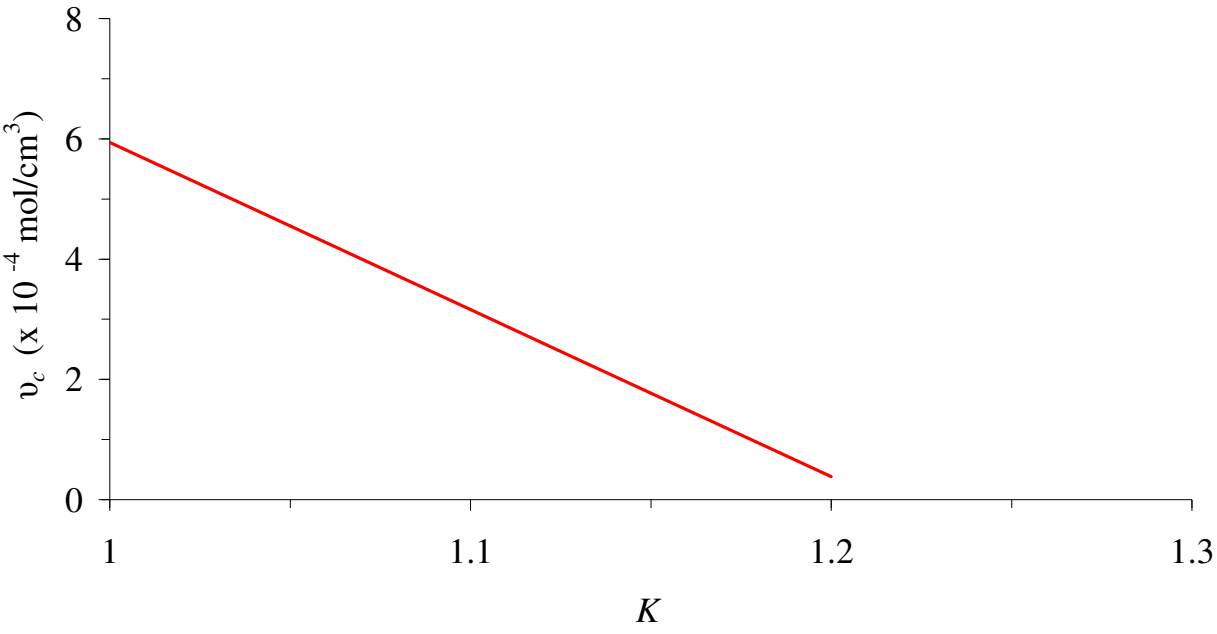

Figure 7.10: Computed values of υ_c plotted against K (for MED-4080 in ethyl acetate: χ_s =0.34; δ_P = 15.3 MPa^{½}; δ_S = 18.6 MPa^{½}; ϕ_P = 0.597; V_S = 97.8 cm^3/mol; R=8.31 J/Kmol; T=298K). The line shown is y = -39.237x + 15.322; R^2 = 1. The υ_c values have been computed using equation 2.7 (where the χ values used for this computation have been computed using equation 2.12) to show the form of the equations.

7.8.3 Effect of varying δ_P on computed values of υ_c

Previously, in Chapter 2 (§2.5.4.6) and in Chapter 3 (§3.9.4) it was discussed that in equation 2.12 (equation used to calculates χ according to Hildebrand's solubility parameter theory) the value for δ_P can vary.

The results in §7.7 suggested that varying δ_P can affect υ_c and this is investigated further here, using computed υ_c values (i.e. this section shows the effect of varying δ_P on computed υ_c values (computed using equation 2.7); varying δ_P will consequently affect χ (see equation 2.12)). In Figure 7.11 computed values of υ_c are plotted against δ_P. It shows that, provided $\delta_P < \delta_S$, an increase in δ_P also increased υ_c. When $\delta_P > \delta_S$, an increase in δ_P, decreased υ_c.

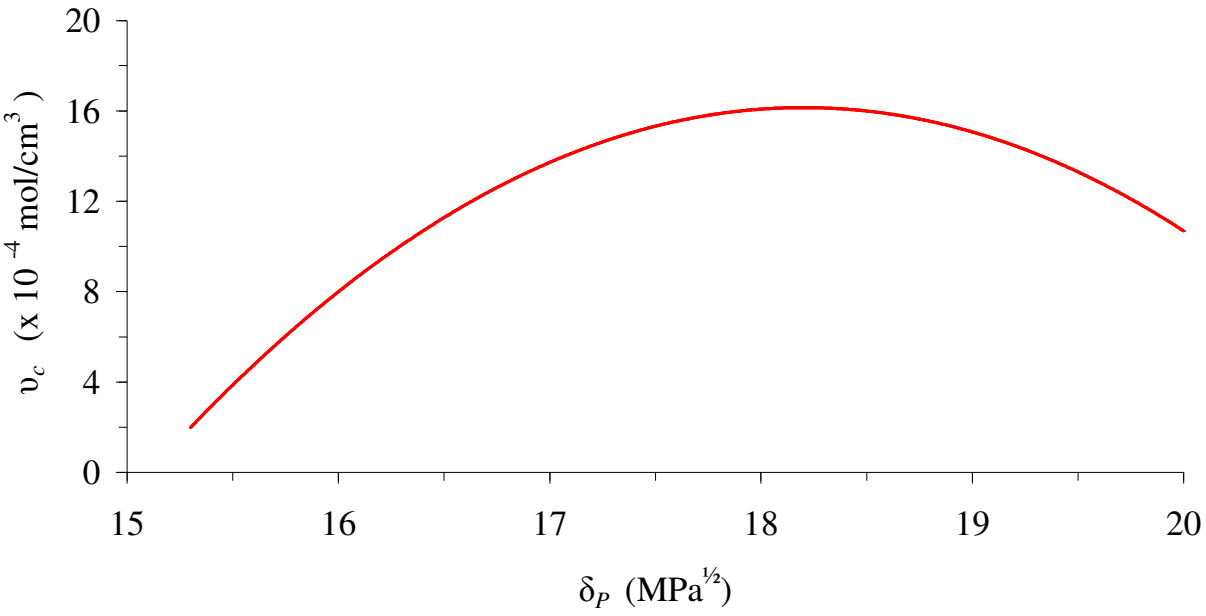

Figure 7.11: Computed values of υ_c versus δ_P (for grade C6-180 in toluene: K=1; χ_s =0.34; δ_S=18.2 $MPa^{½}$; ϕ_P = 0.475; V_S = 106.8 cm^3/mol; R=8.31 J/Kmol; T=298K). The line shown is the second-order polynomial that gave the best fit to the data. The equation of the line is $y = -1.6848x^2 + 61.326x - 541.91$, with ($R^2$ = 1). The υ_c values have been computed using equation 2.7 (where the χ values used for this computation have been computed using equation 2.12) to show the form of the equations.

7.8.4 Effect of varying χ_s and K (in equation 2.12) on computed values of υ_c

In this section, both K and χ_s are varied (which will consequently affect χ). Table 7.5 shows that an increase in K and χ_s, decreased the computed value of υ_c for grade MED-4080.

Table 7.5 : Effect of increasing K and χ_s on computed values of υ_c, (for MED-4080 in ethyl acetate: δ_P = 15.3 MPa$^{1/2}$; δ_S = 18.6 MPa$^{1/2}$; ϕ_P = 0.597; V_S = 97.8 cm^3/mol; R=8.31 J/Kmol; T=298K)

χ_s	K	υ_c (x 10^{-4} mol/cm^3)
0.3	1	8.5
0.31	1.05	6.5
0.32	1.1	4.5
0.33	1.15	2.4

Table 7.6 and Table 7.7 show that an increase in χ_s and a decrease in K decreased the computed values of υ_c for grade MED-4080. If the inverse occurs, the computed values of υ_c increased.

Table 7.6: Effect of decreasing K and increasing χ_s on υ_c. (for MED-4080 in ethyl acetate: δ_P = 15.3 MPa$^{1/2}$; δ_S = 18.6 MPa$^{1/2}$; ϕ_P = 0.597; V_S = 97.8 cm^3/mol; R=8.31 J/Kmol; T=298K).

χ_s	K	υ_c (x 10^{-4} mol/cm^3)
0.3	1.1	5.8
0.35	1.05	3.9
0.4	1	2.1

Table 7.7: Effect of increasing K and decreasing χ_s on υ_c. (for MED-4080 in ethyl acetate: δ_P=15.3 MPa$^{1/2}$; δ_S = 18.6 MPa$^{1/2}$; ϕ_P = 0.597; V_S = 97.8 cm^3/mol; R=8.31 J/Kmol; T=298K).

χ_s	K	υ_c (x 10^{-4} mol/cm^3)
0.4	1	2.1
0.35	1.05	3.9
0.3	1.1	5.8

7.9 Do the two equations for χ (equation 2.9 and 2.12) calculate similar values?

The results demonstrated that the two equations did not calculate the same value for χ and did not give the same relative χ values (i.e. the values were not related by a common factor). Although, similar χ values were obtained when the silicone samples were swollen in toluene. Figure 7.12 compares the χ values obtained in cyclohexane for each silicone grade, which are listed in: Table 7.2 (swelling equilibrium method; equation 2.9); Table 7.3 (Hildebrand's solubility parameter theory with δ_P =15.3 $MPa^{½}$; equation 2.12); Table 7.4 (Hildebrand's solubility parameter theory with δ_P values ranging between 15.6-15.9 $MPa^{½}$; equation 2.12). It was only possible to calculate 95% confidence intervals for the data points obtained using the swelling equilibrium method and these are shown as error bars in the figure. Figure 7.12 shows that the χ values obtained using equation 2.12, did not lie within the 95 % confidence intervals of the values obtained using equation 2.9. The χ values obtained using equation 2.9 were greater than those obtained using equation 2.12.

The χ values obtained using equation 2.9 and equation 2.12, for the silicone grades that were swollen in toluene, are compared in Figure 7.13. The figure shows that the χ values obtained using equation 2.9 and equation 2.12 (for δ_P =15.3 $MPa^{½}$) were similar; for one of the grades (C6-165), the χ value obtained using equation 2.12 (for δ_P =15.3 $MPa^{½}$) appeared to lie just within the 95 % confidence intervals of the value obtained using equation 2.9. For two of the four silicone grades (C6-165 and MED-82-5010-80), the χ values obtained using equation 2.9 were slightly lower than those obtained using equation 2.12 (for δ_P =15.3 $MPa^{½}$). The χ values obtained using equation 2.12 (for δ_P values ranging between 15.6-15.9 $MPa^{½}$) were the lowest for all the grades.

Both figures also show that the two methods used to calculate χ did not give the same relative values for each silicone grade (i.e. the values were not related by a common factor). For example, Figure 7.13 shows that for grade C6-180, the values obtained using the swelling equilibrium method (shown as unfilled squares) and Hildebrand's solubility parameter theory (shown as filled circles) differ by a factor of 1.3. However, those of grade MED-82-5010-80 differ by a factor of 1.1.

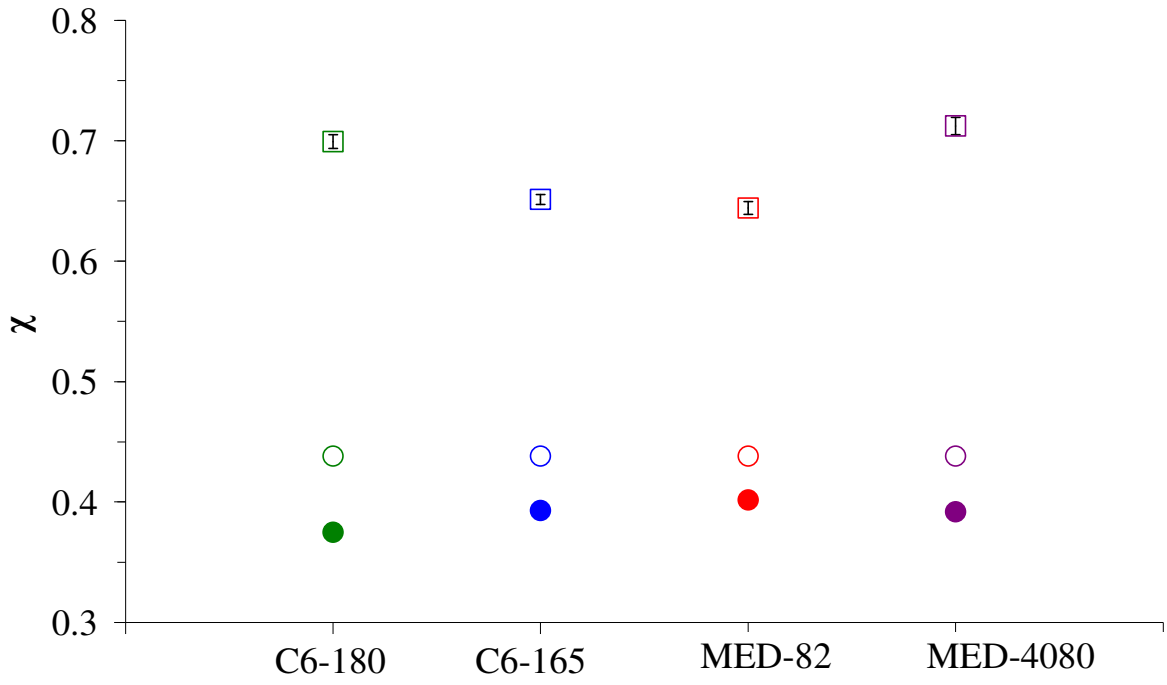

Figure 7.12: Mean values of χ plotted against the silicone grades: C6-180 (□○●); C6-165 (□○●); MED-82-5010-80 ((□○●) abbreviated to MED-82 on the figure) and MED-4080 (□○●).The values were obtained from: Table 7.2 (in cyclohexane), which used the swelling equilibrium method and is shown as (unfilled squares); from Table 7.3 (in cyclohexane), which used Hildebrand's solubility parameter theory and is shown as (unfilled circles); from Table 7.4 (in cyclohexane), which used Hildebrand's solubility parameter theory and is shown as (filled circles). The error bars shown on the data points obtained with the swelling equilibrium method (□□□□) represent the 95% confidence intervals. It was not possible to calculate error bars for the values calculated using Hildebrand's solubility parameter theory.

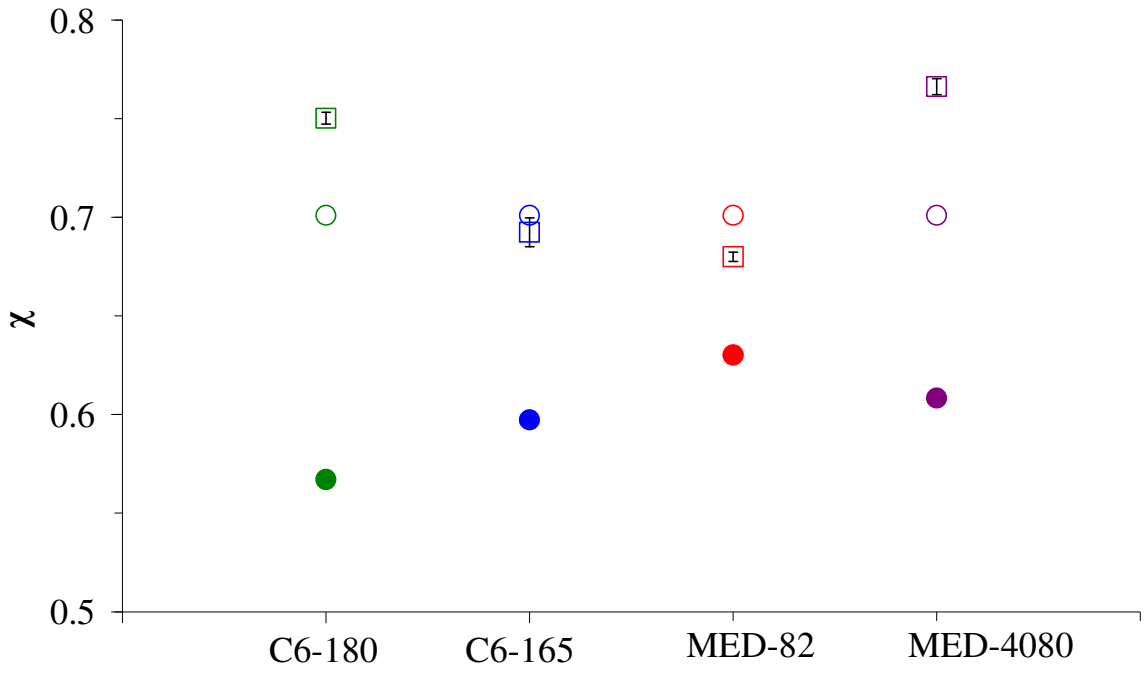

Figure 7.13: Mean values of χ plotted against the silicone grades: C6-180 (□○●); C6-165 (□○●); MED-82-5010-80 ((□○●) abbreviated to MED-82 on the figure) and MED-4080 (□○●).The values were obtained from: Table 7.2 (in toluene), which used the swelling equilibrium method and is shown as (unfilled squares); from Table 7.3 (in toluene), which used Hildebrand's solubility parameter theory and is shown as (unfilled circles); from Table 7.4 (in toluene), which used Hildebrand's solubility parameter theory and is shown as (filled circles). The error bars shown on the data points obtained with the swelling equilibrium method (□□□□) represent the 95% confidence intervals. It was not possible to calculate error bars for the values calculated using Hildebrand's solubility parameter theory.

7.10 Does the method used to calculate χ affect υ_c?

Since the swelling equilibrium method gives a value of $\upsilon_c = 0$ (which is not physically possible), non-zero υ_c values were only obtained using Hildebrand's solubility parameter theory.

7.11 Discussion

7.11.1 Swelling silicones in different solvents

The results in §7.3 demonstrated that different solvents have different swelling abilities. The swelling measurements of the silicones showed that the solvent with the greatest swelling ability was cyclohexane, followed by toluene, then ethyl acetate and then ethyl methyl ketone. Only a very limited amount of swelling occurred in n-butanol. Hence, cyclohexane and toluene were considered to be good solvents, ethyl acetate and ethyl methyl ketone were considered to be fair solvents, while n-butanol was considered to be a bad solvent, for silicones. The results reported are consistent with the results from previous studies (Andreopoulos *et al.*, 1993; Favre, 1996; Yerrick and Beck, 1964) on silicones and have been discussed in §7.2 and §2.5.4.1. Other studies (Brandon *et al.*, 2003; Brandon *et al.*, 2001; Doležel *et al.*, 1989b) on silicone gel breast implants and on silicone rubber tubing respectively, also used toluene to swell their samples and measure the cross-link density.

7.11.2 Calculating χ using two different methods

The results showed that both the swelling equilibrium method and Hildebrand's solubility parameter theory could be used to calculate χ. However, the two methods did not calculate the same value for χ, but did calculate some similar χ values when the samples were swollen in toluene. The two methods used did not give the same relative χ values for each silicone grade. When the Hildebrand's solubility parameter theory was used, the choice of K, χ_s and δ_P affected χ, and consequently υ_c, as reported in §7.7 and §7.8

When the swelling equilibrium method was used to calculate χ (described in §2.5.4.6), precise values in the range $0.644 \leq \chi \leq 0.712$ and $0.68 \leq \chi \leq 0.766$ were obtained when the silicone samples were swollen in toluene and cyclohexane, respectively. These range of values obtained for χ in toluene, appeared to be reasonable and are consistent with a previous study (Favre, 1996), which obtained a χ value of 0.792. Another study (Summers *et al.*, 1972) obtained χ values of approximately 0.8 for PDMS-hydrocarbon systems in toluene. A study (Andreopoulos *et al.*, 1993) on silicones for maxillofacial applications obtained a χ value of 0.61 in toluene. A previous study (Knaub *et al.*, 1988) obtained a χ value of 0.479 after swelling silicone in cyclohexane; suggesting that the range of χ values obtained in §7.5, for the samples swollen in cyclohexane, were possibly high.

The Hildebrand's solubility parameter theory (equation 2.12; §2.5.4.6) was also used to calculate χ. The results in §7.7 and §7.8 showed that χ is dependent on the choice of K, χ_s and δ_P; parameters in equation 2.12. In particular, comparing the results in Table 7.3 and Table 7.4 (§7.7), showed that χ is sensitive to the value of δ_P, because when δ_P increased, χ decreased. Furthermore, the results in §7.6 showed that the data points which were extremely low on the swelling curve (see n-butanol and ethanol data points in Figure 7.3 and Figure 7.5), did not necessarily need to be considered to determine a δ_P value for the silicones.

For instance, when these low data points were excluded from the plots, it was possible to fit and differentiate a suitable order polynomial through the data points. δ_P values in the range 15.6 - 15.9 $MPa^{½}$ were obtained, which produced reasonable χ values in the range $0.392 \leq \chi \leq 0.402$ and $0.567 \leq \chi \leq 0.630$, when the silicone samples were swollen in cyclohexane and toluene, respectively. These χ values are consistent with those obtained in previous studies (Andreopoulos *et al.*, 1993; Knaub *et al.*, 1988); discussed in §7.2.

While, when all the data points were considered (i.e. the low data points were not excluded), it was not possible to plot a n^{th} ($n \geq 2$) order polynomial that fitted through the data points reasonably well. Therefore, the δ_P was equated to the δ_S of n-heptane, the solvent in which the silicone swelled the most (i.e. for n-heptane, δ_S = 15.3 $MPa^{½}$ = δ_P for all the silicone grades), as suggested by Yerrick and Beck (1964). This lower value of δ_P produced slightly higher χ values of 0.438 and 0.701, after swelling the silicone samples in cyclohexane and toluene, respectively. These χ values obtained are consistent with those obtained in previous studies (Favre, 1996; Knaub et al., 1988); discussed in §7.2.

However, estimating δ_P by equating it to δ_S of the solvent in which the silicone swelled the most, can produce slightly higher χ values that can result in negative cross-link densities, which are not physically possible (reported in §7.7 and discussed in §7.11.3), in good solvents. These negative cross-link densities were not obtained when δ_P was estimated by plotting a suitable order polynomial through the swelling measurements and the maximum point of swelling determined by setting the derivative of the polynomial to zero (discussed in §3.9.4); suggesting that this is a better method for estimating δ_P.

7.11.3 Effect of using different methods to calculate χ on υ_c

The results showed that the calculation of υ_c was sensitive to the method used to calculate χ. Since the swelling equilibrium method gives a value of $\upsilon_c = 0$ (which is not physically possible), non-zero υ_c values can only be obtained using Hildebrand's solubility parameter theory.

As reported in §7.7, in some instances negative υ_c, which are not physically possible (discussed in further §8.5), were obtained with Hildebrand's solubility parameter theory. This suggests that equation 2.7 (used to calculate υ_c and stated in §2.5.4.4) is sensitive to the combination of ϕ_P and χ used, as some combinations give negative υ_c; discussed further in §8.5. The form of an equation that can give a negative υ_c is not reliable. Furthermore, Figure 7.7 (§7.7; χ is calculated using Hildebrand's solubility parameter theory) showed that, when two different methods were used to estimate δ_P, the υ_c values obtained with $\delta_P = 15.3$ MPa^{½}, were slightly but significantly lower, than those obtained using δ_P values in the range 15.6 - 15.9 MPa^{½}.

Figure 7.8 showed that when the υ_c values of a silicone grade swollen in toluene (a good solvent) were compared to the υ_c values of the same silicone grade, but swollen in cyclohexane (a good solvent), the values obtained in toluene were significantly lower than those obtained in cyclohexane. Therefore, there is no clear indication from the results reported and the comparisons made, that it is possible to calculate absolute values for the υ_c. The values obtained for υ_c were dependent on the solvent used and on the method used to calculate χ.

7.11.4 The relationship between the silicone grades, the swelling measurements and the cross-link densities

The results showed that the amount of swelling varied between the different grades. As suggested (Brandon *et al.*, 2001), the cross-link density and the swelling measurements were inversely related. For instance, the results demonstrated that the harder grades (C6-180 and MED-4080; hardness properties shown in Table 3.2) swelled the least and had the highest υ_c while the softer grades (C6-165 and MED-82-5010-80) swelled the most and had the lowest υ_c. This was expected as it has been discussed in §2.5.4.1 that the amount of swelling is directly related to the number of vacant sites (i.e. areas with no cross-links) within the molecular structure of the polymer. It has been discussed that softer grades have a greater number of vacant sites (i.e. fewer cross-links and consequently a lower cross-link density), hence the more the polymer swells (Starch, 2002). Further evidence of this comes from another study (Andreopoulos *et al.*, 1993) who concluded from their swelling measurements that silicones with a higher percentage of cross-linker swelled the least.

7.12 Summary of main conclusions

The main conclusions from this chapter are summarised below.

- Out of the five solvents used, as expected, the silicones swelled the most in cyclohexane, followed by toluene, then ethyl acetate and then ethyl methyl ketone. Only a very limited amount of swelling occurred in n-butanol.
- Using the swelling equilibrium method, precise χ values in the range $0.644 \leq \chi \leq 0.712$ and $0.68 \leq \chi \leq 0.766$, were obtained when the silicone samples were swollen in cyclohexane and toluene, respectively. However, this method of calculating χ, gave a value of $\upsilon_c = 0$, which is not physically possible.
- Using the Hildebrand solubility parameter theory to calculate χ (with $\delta_P = 15.3$ MPa^{½}), reasonable χ values of 0.438 and 0.701, were obtained after swelling the silicone samples in cyclohexane and toluene, respectively. Negative υ_c, which are not physically possible, were obtained for some grades, in toluene, a good solvent.
- Using the Hildebrand solubility parameter theory to calculate χ (with δ_P in the range 15.6-15.9 MPa^{½}), reasonable values in the range $0.392 \leq \chi \leq 0.402$ and $0.567 \leq \chi \leq 0.630$ were obtained, when the silicone samples were swollen in cyclohexane and toluene, respectively. Precise but not absolute υ_c values were also obtained for these χ values. χ and consequently υ_c were dependent on the choice of K, χ_s and δ_P.

Chapter 8 . CONCLUSIONS

8.1 Chapter Overview

This chapter summarises the conclusions from each of the experimental chapters and relates them to the aims discussed previously in Chapter 1. It also discusses the implications of the results. To do this, the results reported in Chapter 4-7 are related to how the silicone or Elast-Eon™ might perform in implants. Where possible, it also attempts to link the results from each of the chapters together and explain how a combination of the factors investigated here may contribute to the performance of silicone or Elast-Eon™ in an implant. Future research has been suggested where it is believed to be required.

§8.2 discusses the first aim of this thesis. It summarises the viscoelastic properties of the medical grade silicones reported in Chapter 4 and 5 and relates them to how a silicone implant might perform *in vivo*. §8.3 is related to the second aim of this thesis. It discusses the effect that pre-treating has on the properties of the silicone, which was reported in Chapter 4 and 5. §8.4 is related to the third aim of this thesis and summarises the effect that accelerated aging has on the properties of Elast-Eon™ 3 and on Nagor® medical grade silicones, which was reported in Chapter 6. §8.5 is related to the fourth aim of this thesis and discusses the use of the swelling method to measure the cross-link density of silicones, which was reported in Chapter 7. §8.6 links the cross-link density measurements (Chapter 7) to the moduli measurements (Chapter 4) of the silicones tested. §8.7 is the final section of the main body of this thesis and has the concluding remarks.

8.2 Summary of the viscoelastic properties of the silicones tested and their relation to how a silicone implant might perform *in vivo*

The first aim mentioned in Chapter 1, was to examine whether changing the loading frequency, *f*, will affect the storage, *E',* and loss moduli, *E''*, of medical grade silicones in compression and in tension. This aim was investigated in Chapter 4 and 5.

Chapter 4 concluded that both the short and medium-term medical grade silicones investigated in compression, have frequency-dependent viscoelastic behaviour. These results are consistent with a previous study (Murata *et al.*, 2003) on silicones for facial applications, as discussed in §4.10.1. The silicones tested in Chapter 4 appear to have the required viscoelastic properties needed for materials used to manufacture finger implants (i.e. allow implant to retain its shape, *E'*, and dissipate energy, *E''*). These properties were discussed in Chapter 2. Of particular interest here is that, for the short-term implant silicones (C6-165, C6-180 and MED 4080) and Silastic® Q7-4780 (medium-term implant silicone), above about 0.3 Hz, *E'* increases slowly. Then above about 1 Hz, *E'* increases more rapidly, which was described as characteristic of a material undergoing a transition from the rubber to the glassy state, as described in §4.10.2.

As a result, it is possible that the silicones will start experiencing a slight reduction in their lifetime as the *E'* increases slowly (between 0.3 -1 Hz), from the onset of the transition. Above about 1 Hz, it is possible that the loading frequency will have a greater impact on the reduced lifetime of the silicones, since the *E'* begins to increase more rapidly than *E''*. This is of some concern, because §3.7.2.2 discussed that a finger joint can normally operate at frequencies of up to 3 Hz (Joyce and Unsworth, 2002b; Serina *et al.*, 1997).

When *E*' increases, the stress associated with a given deformation, and hence, the deformation energy, increases. This may have an adverse effect on the life of the material, at high values of *E*' (Swanson *et al.*, 1973), since there is a danger that if *E*' is very much higher than *E*'', the silicone will store a high deformation energy. This high energy may lead to fracture because formation of fracture surfaces then provides a mechanism for dissipating excess deformation energy (Benham *et al.*, 1996). Figure 4.1 and Figure 4.2 (Chapter 4; §4.3) show that at frequencies above 1 Hz, *E'* increases more rapidly, compared to *E''*. Hence, it is possible that the silicones dissipate a lower proportion of its energy by means other than fracture, above 1 Hz. However, a high value of *E*', compared with *E*'', after the onset of the transition from the rubbery to the glassy state, means that the silicones investigated here will rapidly return towards their original shape and dimensions when they are unloaded (Ward and Perry, 1981). Therefore, silicone selection for an artificial finger or wrist joint is a compromise between *E*' and *E*''.

The results in Chapter 4 also show that, when compared to the harder silicones (C6-165, C6-180, MED-4080 and Silastic® Q7-4780), the two softest Silastic® grades Q7-4720 and Q7-4735 (durometer hardness values shown in Table 3.2 and Table 3.3) behave more like a glass above about 15 Hz. This suggests that these softer silicones will experience a reduced lifetime at lower loading frequencies. This may explain why the longer-term implant materials, Silastic HP-100 and FLEXSPAN, used to manufacture the silicone finger implants, have similar properties (shown in Table 3.2) to the harder grades. It is more beneficial to manufacture a silicone finger implant from a material that will exhibit a reduced lifetime (i.e. glassy behaviour) only at higher loading frequencies.

The results in Chapter 4 show that, softer silicones will have a lower *E'*, when compared to harder silicones. This lower *E'* may be ideal for silicones used for dental applications as it will provide more cushioning (Murata *et al.*, 2003; Wagner *et al.*, 1995a; Wagner *et al.*, 1995b), but may not necessarily be ideal for silicones used in finger implants. As discussed in §4.2, it has also been recognised that the viscoelastic properties of different silicones may be different because of differences in the amount of silica, the degree of cross-linking and the composition (Murata *et al.*, 2003; Murata *et al.*, 2002; Polyzois, 2000). Therefore, the behaviour of maxillofacial silicones may not necessarily be applicable to silicones used in other applications (Polyzois, 2000).

Chapter 5 concluded that the viscoelastic properties of the short-term medical grade silicones in tension, may depend slightly on frequency, in the range 0.02-2 Hz. This result is consistent with results obtained for silicones used for dental liners (Murata *et al.*, 2002; Murata *et al.*, 2000), as discussed in §5.5.1. Pre-treating of the silicones increases the *E'* of grade C6-165 and C6-180 significantly, which is consistent with a previous study (Ward and Perry, 1981). The results also showed that *E'* for silicones measured in tension may be slightly, but significantly, different from the values measured in compression (Chapter 4). However, because the values are systematically greater for only two of the three (C6-180 and MED-4080; see Figure 5.7 and Figure 5.9) silicones investigated and lower for the remaining one (C6-165; see Figure 5.5), no general conclusions can be drawn from this result.

E'' for silicones measured in tension increase less rapidly with increasing frequency, than when measured in compression. *E''* for silicones depends slightly with frequency, in the range 0.02-2 Hz, passing through a shallow minimum, but show a non-linear increase, in this frequency range, when measured in compression. The results are consistent with results obtained for silicones used for maxillofacial implants and dental liners (Murata *et al.*, 2003; Murata *et al.*, 2002; Murata *et al.*, 2000), as discussed in §5.5.3.

The results in Chapter 5 also show that, the behaviour of silicone in tension may not necessarily be the same as in compression and therefore the properties of the material should be investigated in both modes of deformation, as this may affect the performance of silicone in an implant. A previous study (Scherbakov and Gurvich, 2005) on natural rubber, an elastomer whose chemical composition is very different to that of silicone, suggested that the properties of a material tested in tension and compression may be different because of the different size and shape of the specimens and the differences in loading conditions, as discussed in §5.2. Hence, it is possible that, the difference in the specimen sizes and shapes used for the compression and tension tests (see §3.3.2 and §3.3.3), could explain this difference in the material properties; since the machine software calculates the moduli using the stiffness, specimen shape and specimen geometry.

However, the results show that for the silicones in tension, $E' > E''$, just as it was in compression (Chapter 4). As discussed previously, there is the danger that if $E' >> E''$, the energy may be dissipated by formation of fracture surfaces, which is undesirable.

Furthermore, the results indicate that, particularly at higher frequencies, *E''* increases steeply in compression, but not in tension, i.e. viscous response of the material appears to be less dominant in tension or when a tensile stress is applied. This suggests that, particularly at higher frequencies, less energy can be dissipated in tension and formation of fracture surfaces are more likely to occur.

8.3 The effect that pre-treating has on the viscoelastic properties of silicones

The second aim of this thesis, mentioned in Chapter 1, was to examine whether different pre-treating conditions affects the moduli of silicones. The results are shown for one short-term implant grade (MED-4080) and two medium–term implant grades (Silastic ® Q7-4720 and Q7-4735) in Chapter 4 and for another three grades (C6-165 ,C6-180 and Silastic ® Q7-4780) in Appendix G. The results show that pre-treating the short and medium-term implant silicones for 29 and 90 days respectively (in physiological saline solution at 37^{o}C) significantly affects the *E'* (increases) of the softer Silastic ® medium-term implant grades (Q7-4720 and Q7-4735) and slightly but significantly increases the *E'* of grade MED-4080 (short-term implant) at high frequencies. Previous studies on silicones (Polyzois, 2000; Swanson and Lebeau, 1974; Ward and Perry, 1981), discussed in §4.10.5, have also suggested that pre-treating may affect the viscoelastic properties of some grades of silicone.

The results in §4.8 show that pre-soaking the specimens in physiological saline solution before testing, slightly but significantly affects the *E'* and *E''* of grades MED-4080 and C6-165 respectively. For MED-4080, the physiological saline does not affect the viscoelastic properties, except for *E'* values at a low loading frequency. While for C6-165, the physiological saline appears to have an effect on *E''* values at a low and high loading frequency.

For the short-term implant grade MED-4080, the small but apparently significant effects of soaking and pre-treatment on *E'* are contradictory; soaking (24 hours) appears to have an effect at a low frequency; pre-treatment (29 days) appears to have an effect at a high frequency. For another short term grade (C6-165) only soaking (24 hours) appears to have an effect on *E''*. Since these apparent effects are small and contradictory, there appears to be no good evidence for their having an appreciable effect.

The results in §4.9 show that reducing the temperature from 37^{o}C to 23^{o}C had no significant effect on the results for the short-term implant silicone grade MED-4080. This is consistent with results from previous studies, as discussed in §4.2. It has been suggested (Murata *et al.*, 2003) that the cross-linked structure of the material may explain the temperature-independence of the material.

Since the properties (shown in Table 3.2 and Table 3.3) of the three short-term implant grades (C6-165, C6-180 and MED-4080) and of Silastic ® Q7-4780 (medium-term) are very similar, this conclusion is likely to hold for the others. Despite the small but significant difference in behaviour of the silicones in some pre-treated conditions, the results suggest that generally the properties of the silicones are not greatly affected by pre-treating. However, on balance, it is probably sensible to determine the properties of materials in a similar environment to that of their intended use.

8.4 The effect of accelerated aging on the viscoelastic properties of Elast-Eon™ and on Nagor® medical grade silicone

The third aim of this thesis mentioned in Chapter 1, was to compare the effect of accelerated aging on the viscoelastic properties of Elast-Eon™ 3 and on Nagor® medical grade silicone. The results in Chapter 6 show that accelerated aging (in saline solution at 70°C for 38 days, which is equivalent to aging for a year at 37°C), significantly increases the *E'* and *E''* of the Elast-Eon™ 3 cylinders but not of the Nagor® medium hardness silicone cylinders. These results are consistent with previous studies on aging of polyurethanes and silicones (Craig *et al.*, 1980; Dootz *et al.*, 1994; Goldberg *et al.*, 1978; Jepson *et al.*, 1993; Saber-Sheikh *et al.*, 1999a; Wagner *et al.*, 1995b; Yu *et al.*, 1980); see §6.7.2 and §6.7.3. Aging an Elast-Eon™ 3 cylinder in a water bath at 37°C for 6 months, also significantly increases *E'* and *E''*.

Yu *et al.* (1980) suggested that it is possible that the properties of the silicones they tested, were not affected by aging because of the inert backbone of repeating silicon and oxygen bonds; see §2.5.2 and §6.2.1. No previous studies have discussed the mechanisms of behaviour of the properties of Elast-Eon™ after accelerated aging. It has been suggested (Polyzois, 2000) that the cross-link density and consequently the modulus of silicones increases after storage in water. Increased cross-linking may occur in the PDMS segments of Elast-Eon ™ 3, which will increase its modulus. Unfortunately, it has been found (see Appendix I (§I.6)) that, Elast-Eon ™ 3 dissolves or does not swell appreciably in several solvents used previously to swell silicones (Andreopoulos *et al.*, 1993; Favre, 1996) and polyurethanes (Zhang *et al.*, 2008), to measure the cross-link density, so there is no simple way to test this hypothesis. Changes in the surface characteristics after storage in an aqueous environment may also affect the property of the material (Polyzois, 2000).

The result obtained for the accelerated aged of the Nagor® medium hardness silicone cylinders is also consistent with the results obtained in Chapter 4, since in these investigations, the moduli of grades C6-165, C6-180, MED-4080 (apart for E' at $f < 30$ Hz) and Silastic® Q7-4780 are not significantly affected as a result of pre-treating (in saline solution at 37°C for 29 or 90 days), as shown by the results in §4.5, §4.6 and Appendix G (§G.2 -§G.3). It is recommended that, before Elast-Eon™ 3 is used as a substitute for silicone in finger and wrist implants, further studies are required to determine its effectiveness as an implant material, particularly as the results in Chapter 6 show that aging can affect its properties.

8.5 The use of the swelling method to measure the cross-link density (υ_c) of the silicones

The fourth aim of this thesis mentioned in Chapter 1, was to use the solvent swelling method to measure the cross-link density, υ_c, of the short-term implant medical grade silicones. Chapter 7 shows that, as expected, the silicones swell the most in cyclohexane (a good solvent), followed by toluene (a good solvent), then ethyl acetate (a fair solvent), then ethyl methyl ketone (a fair solvent) and then n-butanol (a bad solvent). The criteria for a good, fair and bad solvent has been discussed in Chapter 2 (§2.5.4.1 and §2.5.4.8). χ was calculated using the swelling equilibrium method and using Hildebrand's solubility parameter theory (Hildebrand and Scott, 1950), as discussed in §2.5.4.6. The results demonstrated that the two methods do not calculate the same value for χ, but similar χ values can be obtained for some solvents. For example, similar χ values were obtained with the two methods when the samples were swollen in toluene; see §7.9. The two methods did not give the same relative χ values for each silicone grade.

Using the swelling equilibrium method, χ values in the range $0.644 \leq \chi \leq 0.712$ and $0.68 \leq \chi \leq 0.766$, are obtained for silicone samples swollen in cyclohexane and toluene, respectively. The χ values of toluene appear to be reasonable (i.e. consistent with previous studies, as discussed in §7.11.2) and precise, while those of cyclohexane appear to be precise, but were higher than those obtained in a previous study (Knaub *et al.*, 1988); discussed in §7.11.2. However, this method of calculating χ, gives a value of $\upsilon_c = 0$, which is not physically possible; discussed in §2.5.4.6 and §7.11.3.

As discussed in §2.5.4.6, in order to be able to use the Hildebrand solubility parameter theory to calculate χ, it is necessary to know the solubility parameter of the silicones, δ_P. The latter can be determined using the swelling equilibrium method, by plotting the mean values of swelling (as a percentage of the original volume) against the solubility parameter of the solvent, δ_S, as discussed in §2.5.4.6 and §3.9.4. The results in §7.6 suggest that if this method is used to estimate δ_P and the latter used to calculate χ (discussed in §2.5.4.6 and §3.9.4), simply equating the δ_P to the δ_S of the particular solvent in which the silicones swell the most, as suggested (Barton, 1975; Grulke, 1989; Takahashi, 1983; Yerrick and Beck, 1964; Zellers, 1993), may not be appropriate. For example, the results in §7.6 show that if δ_P is equated to δ_S of n-heptane (i.e. the solvent in which the silicone swells the most), then δ_P = 15.3 $MPa^{½}$ for all the silicones. Consequently, χ values of 0.438 and 0.701 are obtained for silicone samples swollen in cyclohexane and toluene, respectively, as shown in §7.7. For some grades (in toluene, a good solvent) these χ values have the adverse effect of producing imprecise and negative υ_c, which are not physically possible.

On the other hand, the results in §7.6 also show that by using a suitable method to determine the maximum point of swelling, such as fitting and differentiating a second-order polynomial through the data points of the swelling plots, reasonable δ_P values in the range 15.6 - 15.9 $MPa^{½}$ are obtained. Using these δ_P values, reasonable χ values in the range $0.392 \leq \chi \leq 0.402$ and $0.567 \leq \chi \leq 0.630$ are obtained, for silicone samples swollen in cyclohexane and toluene, respectively, as shown in §7.7. Consequently, non- negative and precise υ_c values can be obtained with these χ values, as shown in §7.7.

However, although the results indicate that when this method is used to determine δ_P, it is possible to obtain reasonable δ_P values (i.e. similar to values suggested in previous studies as discussed in §2.5.4.6), it has been recognised (see §2.5.4.6), that using the swelling method to determine the solubility parameter of silicones, δ_P, is error prone.

This is because, in order to predict reasonable values for χ, the precision of the δ_P value should be in the range of 0.1 $MPa^{½}$, which may not be possible to achieve. Hence, this method can only estimate a value for δ_P, but not provide absolute values. Any errors or inaccuracy in calculating δ_P will propagate through to the value of χ (Blanks and Prausnitz, 1964) and consequently, υ_c. For example, as shown in §7.7 if the δ_P obtained for the silicones used in this study are increased from 15.3 $MPa^{½}$ to 15.6 $MPa^{½}$, then χ reduces from 0.701 to 0.597 (see Table 7.3 and Table 7.4; for grade C6-165 in toluene). Therefore, as discussed in §2.5.4.6 and §7.2, it has been suggested (Bueche, 1955b; Favre, 1996) that, using the swelling method to calculate the solubility parameter, δ_P, should be used for comparisons purposes only.

Hildebrand's theory also makes use of two other parameters, K and χ_s. There is a general agreement from previous studies, as discussed in §2.5.4.6, that these parameters can vary and they are difficult to predict or measure accurately. It has also been shown in §7.8 that χ and υ_c are also dependent on the choice of K and χ_s. An equation used to calculate χ that is extremely sensitive to the choice of parameters used, such as equation 2.12, needs to be used with caution and all the assumptions made should be stated clearly. This also implies that the υ_c values obtained with these χ values are not absolute values.

Chapter 7 also shows that the calculation of υ_c is sensitive to the solvent used and the method used to calculate χ. Non-zero υ_c values can only be obtained when Hildebrand's solubility parameter theory is used to calculate χ. Furthermore, the υ_c values obtained for the same silicone grades, after swelling in different good solvents (i.e. toluene and cyclohexane), were slightly but significantly different. These significant differences in υ_c and the negative υ_c obtained, indicate that the form of the υ_c equation (equation 2.7) is sensitive to the combination of ϕ_P and χ used and the equation is not always reliable. All these factors imply that there is no clear indication from the results, that it is possible to calculate absolute values for υ_c.

As discussed in §2.5.4.7, it has been suggested that once $\chi > 0.5$, not all combinations of ϕ_P and χ will yield a value of ΔG_M is < 0, when substituted into Flory-Huggins equation (equation 2.2; Chapter 2). This is because these conditions are physically impossible as they would violate the second law of thermodynamics and yield the physically impossible result of a negative υ_c. For example, this happens if the values obtained for grade C6-165 (in toluene) from Table 7.3 are substituted into equation 2.2.

Figure 8.1 provides further evidence that for all ϕ_P values, there is a critical value for χ, above which, υ_c is negative. For instance, in this figure, for samples that are swollen in toluene, when $\phi_P = 0.35$, the critical value for χ is ≈ 0.65 and as ϕ_P increases, the critical value for χ also increases. Hence, the figure indicates that the critical value for χ (above which, υ_c is negative) is dependent on the value of ϕ_P and it is not necessarily 0.5 for all ϕ_P values.

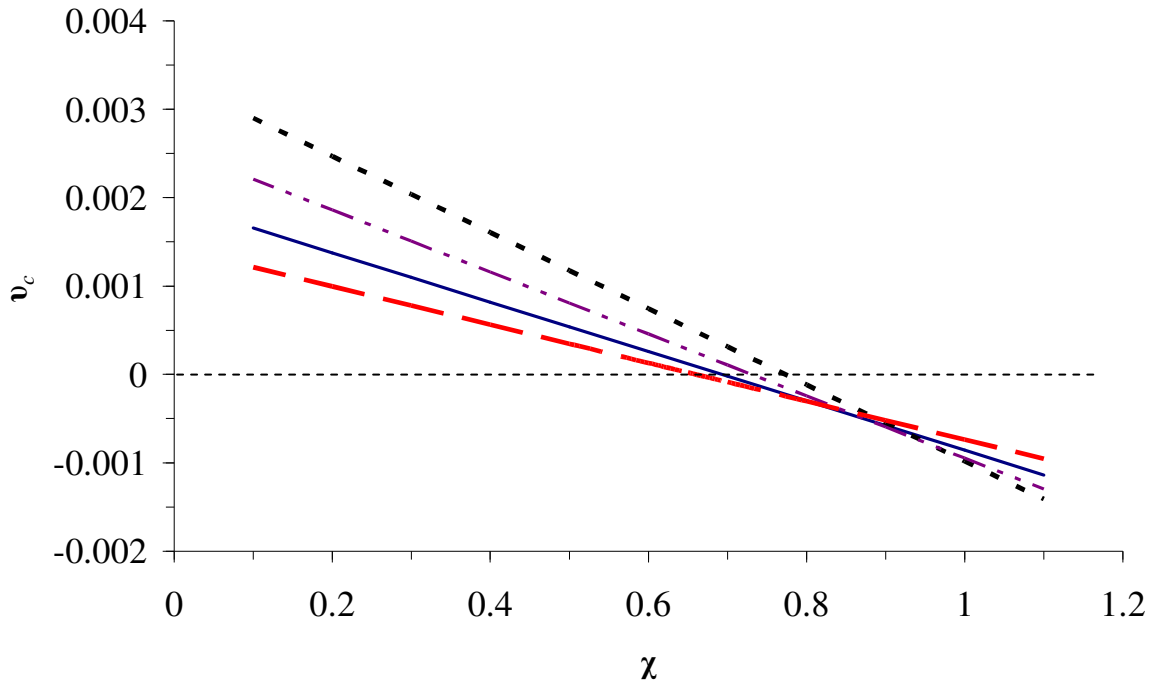

Figure 8.1: Computed υ_c values plotted against χ, when ϕ_P=0.35 (— —); ϕ_P=0.4 (——); ϕ_P=0.45 (— · · —); ϕ_P=0. 5 (·····). The υ_c values have been computed using equation 2.7, to show the form of the equation, assuming that the samples are swollen in toluene. The critical value of χ (above which, υ_c is negative) at various ϕ_P values is also shown.

It has been recognised that the Flory-Huggins theory provides useful simple equations that can be applied to experimental data to estimate the cross-link density (Carpenter, 1990; Jacques and Wyzgoski, 1979; Takahashi, 1983). However, the theory does make several assumptions and has limitations as discussed in §2.5.4.9. It is generally agreed that the Flory-Rehner equation is only applicable as an approximate model of the solvent-polymer interaction, particularly as it violates the assumption that there is zero excess volume change upon mixing (Flory, 1970; Zellers, 1993). However, it is accepted that it provides a useful framework for solvent-polymer interactions studies (Jacques and Wyzgoski, 1979; Takahashi, 1983; Zellers, 1993).

8.6 Relating the cross-link density and the modulus of a material

Previous studies on silicones for breast implants (Brandon *et al.*, 2003) and on silicones for rubber pacemakers (Doležel *et al.*, 1989b; Vondráček and Doležel, 1984) have discussed that the cross-link density and modulus of a material are directly related. A study (José *et al.*, 2004) on organic-inorganic films with PDMS concluded that the *E'* (storage modulus) of the films increased with cross-link density, υ_c. To investigate this relationship, the *E'* and υ_c of the silicones measured in Chapter 4 and 7 respectively, have been plotted against each other, as shown in Figure 8.2. Figure 8.2 shows that *E'* appears to be dependent on υ_c and, as υ_c increases, *E'* increases. This apparent dependency can be calculated using the line of best fit plotted through the data points. Hence, the grade with the highest υ_c (i.e. C6-180) had the highest *E'* and the inverse is true for the grade with the lowest υ_c (i.e. C6-165). Therefore, the greater the number of cross-links, the higher the modulus of the silicone used to manufacture a finger implant, i.e. the greater the mechanical strength of the material in an implant.

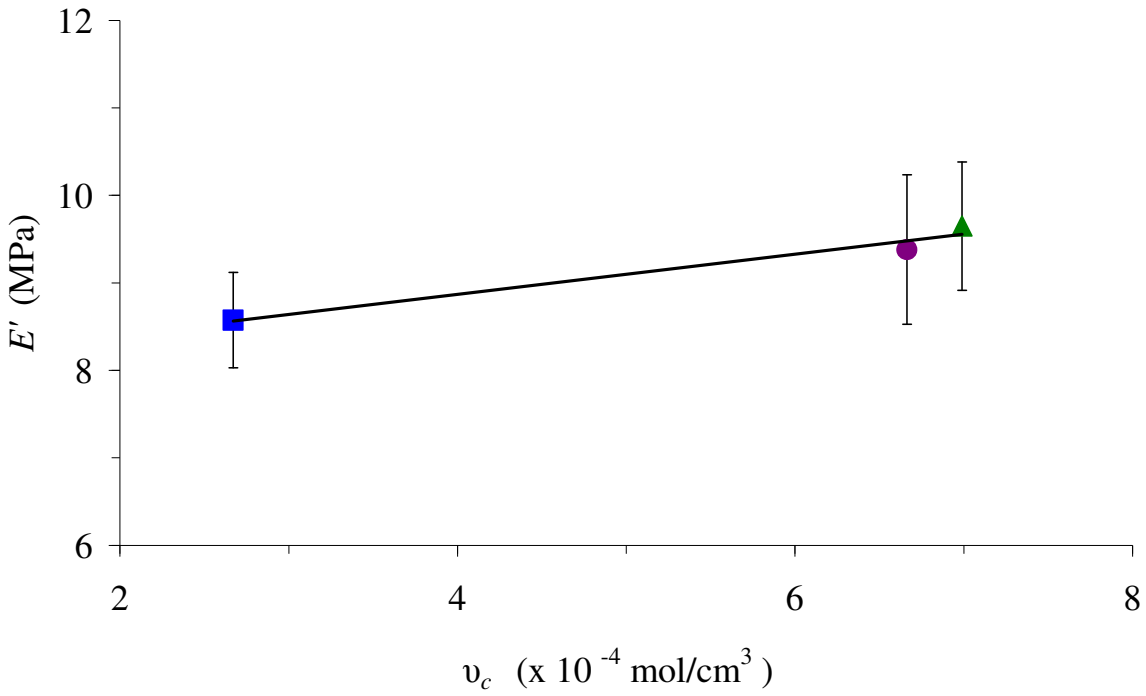

Figure 8.2: υ_c plotted against E' for grades C6-165 (■), MED-4080 (●) and C6-180 (▲). υ_c values taken after toluene swelling (Table 7. 5) and E' values taken at 5 Hz (after pre-treatment for 29 days in physiological saline solution). Error bars represent the standard deviation. The equation of the line is y = 0.2293x + 7.9521 and R^2 = 0.97 (associated with a p value=0.11), which can be used to calculate values of E' in the range (2.7 ≤ υ_c ≤7.0) x 10^{-4} mol/cm^3

However, the extent to which the results shown in Figure 8.2 can be interpreted is limited, primarily because only three data points have been used. For instance, in the caption of Figure 8.2, it has been stated that R^2 is close to 1, which suggests that the linear equation plotted through the data points is a good fit (as discussed in §3.8). Therefore, it is possible that the results in Figure 8.2 might also be interpreted as having a good linear correlation (i.e. a good linear relationship between the two variables) (Bland, 2000), but this may not be the case, as only three data points have been used in the analysis.

To test for linear correlation, the p value associated with R^2 has to be determined (Bland, 2000). As stated in the caption of Figure 8.2, the R^2 value calculated for the linear equation in Figure 8.2 is associated with a $p = 0.11$. Since $p > 0.05$ (i.e. p level = 0.05 or 5% level of significance), the linear correlation associated with the data points is not significant (i.e. the p value does not suggest that the data points are linearly correlated). This is not unexpected since only three data points have been used. More points are needed to examine the possibility of linear correlation more thoroughly.

8.7 Concluding remarks

It is important to clarify that the results and conclusions reported in Chapter 4, 5 and 7 are applicable to the grades of silicone, cured under the conditions recommended by the supplier. At this stage, the extent to which these results can be applied to the *in vivo* performance of silicone finger implants, such as the Swanson implant (Wright Medical Technology, Arlington, TN 38002, USA), is limited. This is because precise mechanical, formulation, composition and curing data for the silicone used to manufacture implants are not generally available. This issue has previously been discussed by Joyce (2004), who concluded that the lack of the availability of precise information on the silicones used to manufacture the implants makes it difficult to assess the advantages and disadvantages of the different silicone implant designs.

In particular, it was discussed in Chapter 2 (§2.5.5) that the silica filler used in medical grade silicones enhances the mechanical properties of the material and therefore plays an important role in the overall properties of the silicone. The properties of the filler are given by the suppliers for the short and medium-term implant silicones, as shown in Table 3.1, Table 3.2 and Table 3.3, but no values have been disclosed for FLEXSPAN, (the silicone used to manufacture the Swanson finger implant), as this level of detail is confidential and proprietary information. It is difficult to measure the filler content experimentally; this is further discussed in Appendix A (§A.2). The confidentiality issue also applies to the cross-link density of FLEXSPAN.

However, the results reported here provide an indication of the performance of these silicones and suggest how they might perform in an implant. Further evidence of this comes from the results discussed in §4.10.3, that suggest that the values of *E'* and *E''* are the same for comparable silicones, irrespective of whether they are intended for short-term or medium-term implantation. This conclusion suggests that silicones intended for shorter term implantation can be used as models for silicones with similar properties, which are intended for longer term implantation. Laboratory investigations on the mechanical properties of silicones (Hutchinson *et al.*, 1997; Leslie *et al.*, 2008a; Leslie *et al.*, 2008b; Pylios and Shepherd, 2008b; Savory *et al.*, 1994) have also used silicones intended for short-term (29 day) and medium-term (90 day) implantation, as at present, it is not possible to obtain FLEXSPAN or other longer-term implant silicones. Whilst it is possible to obtain silicone finger implants, it is not feasible to carry out routine laboratory experiments on them, because they are too expensive.

APPENDIX A: FILLER PROPERTIES AND FILLER CONTENT IN SILICONES

A.1 Equations used to calculate filler properties

As mentioned in §2.5.5, this appendix contains the equations that can be used to calculate the properties of the filler used in medical grade silicones. If the surface area, *S*, of the silica filler is known, it is possible to calculate the diameter of the silica particles. The equations used are shown below.

Surface area, *S*, is defined as:

$$S = \frac{A}{m} \tag{A.1}$$

where *A* is the area; *m* is the mass.

m can be defined as $m = \rho V$ and for a sphere, $A = 4\pi r^2$ and $V = \frac{4}{3}\pi r^3$, where *r* is the radius.

Hence, equation A.1 can be written as:

$$S = \frac{4\pi r^2}{\rho V} = \frac{4\pi r^2}{\rho \frac{4}{3}\pi r^3} = \frac{3}{\rho r} = \frac{6}{\rho d} \tag{A.2}$$

Hence, rearranging equation A.2 gives:

$$d = \frac{6}{\rho S} \tag{A.3}$$

where *d* is the average particle diameter in μm; *S* is the specific surface area or BET specific surface area in m^2 /g; ρ is the true density of the particle in g/cm^3.

A.2 Difficulties in measuring the properties of the filler and the filler content in silicone

As mentioned in §8.7, this section discusses the experimental difficulties in characterising the silica filler in the medical grade silicones.

It would be beneficial to be able to calculate or quantify more precisely the silica filler properties, as the filler contributes to the overall strength and properties of the material (Brandon *et al.*, 2003). However, it is virtually impossible to determine this information through analytical means. One of the reasons for this is that the silica filler consists of small spheroid particles, which fuse irreversibly while in the semi-molten state and create aggregates (Colas and Curtis, 2004b). Once this fusion occurs, it is difficult to measure the diameter of the spheroid. The experimental analysis described and reported in the next paragraphs, also show the difficulty in measuring the filler content in silicone experimentally.

Firstly, it was proposed that, if a silicone sample was heated to a sufficiently high temperature, then it was possible that after heating the silicone sample, the residue would consist mainly or entirely of the silica filler particles, because the other particles would not be able to withstand the heat and would be burnt off. Therefore, thermogravimetric analysis (TGA) was carried out on a MED-4080 silicone sample over the temperature range 60-1000°C, on a NETZSCH thermal analysis (NETZSCH Instruments, Aldridge, Walsall**,** West Midlands WS9 8UG). The experiment was carried out at a constant heating rate of 10°C/min under an Argon environment.

The TGA recorded that loss in mass of the sample with temperature. Although it was possible to perform the TGA on the sample, it was not clear whether the residue left after the TGA only consisted of the silica filler.

Therefore, the sample that had undergone TGA was coated with platinum and looked at under a scanning electron microscope (SEM) on a JEOL JSM 7000F (JEOL Ltd., Tokyo, Japan). A chemical element analysis was also performed on the SEM to investigate whether it was possible to identify whether the residue only consisted of silica. The analysis showed that the residue consisted of C, O, Si and Pt (i.e. it did not suggest that the residue only consisted of the silica (SiO_2) filler). Another issue that needs to be considered is that, the chemical structure of the silica filler and PDMS both consist of Si and O particles (see §2.5.2 and §2.5.5); once the two are mixed together, it is difficult to distinguish between the Si and O of the PDMS and the silica.

APPENDIX B: USE OF DMTA, WLF EQUATION AND DSC ON MEDICAL GRADE SILICONES AND ELAST-EON™

B.1 Introduction

Chapter 4 and 5 measured the frequency-dependent behaviour of the viscoelastic properties of medical grade silicones directly, using Dynamic Mechanical Analysis (DMA). As discussed in §2.7.10, an alternative method would be to measure the frequency dependence indirectly by first measuring the temperature dependence of the properties, and then use the Williams-Landel-Ferry equation (WLF; see §2.7.9) (Ferry, 1961b; Meakin *et al.*, 2003; Ward, 1990b) to calculate the dependence of the viscoelastic behaviour on frequency. Dynamic Mechanical Thermal Analysis (DMTA) can be used to measure the temperature dependence of the viscoelastic properties (Cheremisinoff et al., 1993; Menard, 1999).

DMTA measures the *E'*, *E''* and $\tan\delta$ of a material over a large temperature range and at a fixed frequency, using an oscillatory mechanical deformation experiment (Cheremisinoff *et al.*, 1993), which applies a small sinusoidal stress to the material (Cowie, 1994). Thermograms of *E'*, *E''* and $\tan\delta$ against temperature can be plotted and often the corresponding temperature at which the peak of $\tan\delta$ occurs (centre of relaxation), is taken as the glass transition temperature (T_g); discussed in §2.7.2.4. (Cheremisinoff *et al.*, 1993).

Differential Scanning Calorimetry (DSC) is another technique that is frequently used to measure the $T_{g,}$. It can also measure the T_m (highest temperature at which crystalline can still be detected or peak of an endothermic process) and T_c (peak of an exothermic process) of a material (Cheremisinoff *et al.*, 1993; Clarson *et al.*, 1985; Ghanbari-Siahkali *et al.*, 2005; Murayama, 1978). It is a technique which measures the difference in energy inputs between a small weighed polymer sample (usually 10 mg) in a sealed aluminium pan and an empty pan (known as the reference material) (Cheremisinoff *et al.*, 1993). In other words, it measures the power differential (heat energy per unit time) between the weighed sample in a pan and an empty pan (Cheremisinoff *et al.*, 1993).

Firstly, the viscoelastic properties and T_g of the same short-term implant silicones used in Chapter 4 and 5 were measured using DMTA. The experiments were run on a NETZSCH DMA 242 C (NETZSCH Instruments, Aldridge, Walsall**,** West Midlands WS9 8UG). However, the experimental method used did not produce reliable results, but the applicability of the WLF equation to these medical grade silicones can still be discussed using the results obtained.

Secondly, the T_g of the silicones and Elast-Eon^{TM}3 were measured using DSC. Due to lack of availability of the necessary required equipment in the School of Mechanical Engineering and School of Metallurgy and Materials (University of Birmingham), the experiments were carried out by Mr Brian Patterson at the College of Physical Sciences (University of Aberdeen) and the results are shown here. A Mettler Toledo DSC 821e (Mettler-Toledo Ltd, Leicester, LE4 1AW) was used to run the experiments. DSC was conducted over a temperature range of -150 to 60°C at a constant heating rate of 10°C/min.

B.2 DMTA Results and Discussion

Figure B. 1, Figure B. 2 and Figure B. 3 show the show the dependence of *E', E''* and tanδ on temperature, T, at 10 Hz, for the four grades of silicones. The values of the T_g taken at the maxima *E''* and tanδ values at 1, 10 and 33.3 Hz are tabulated in Table B. 1.

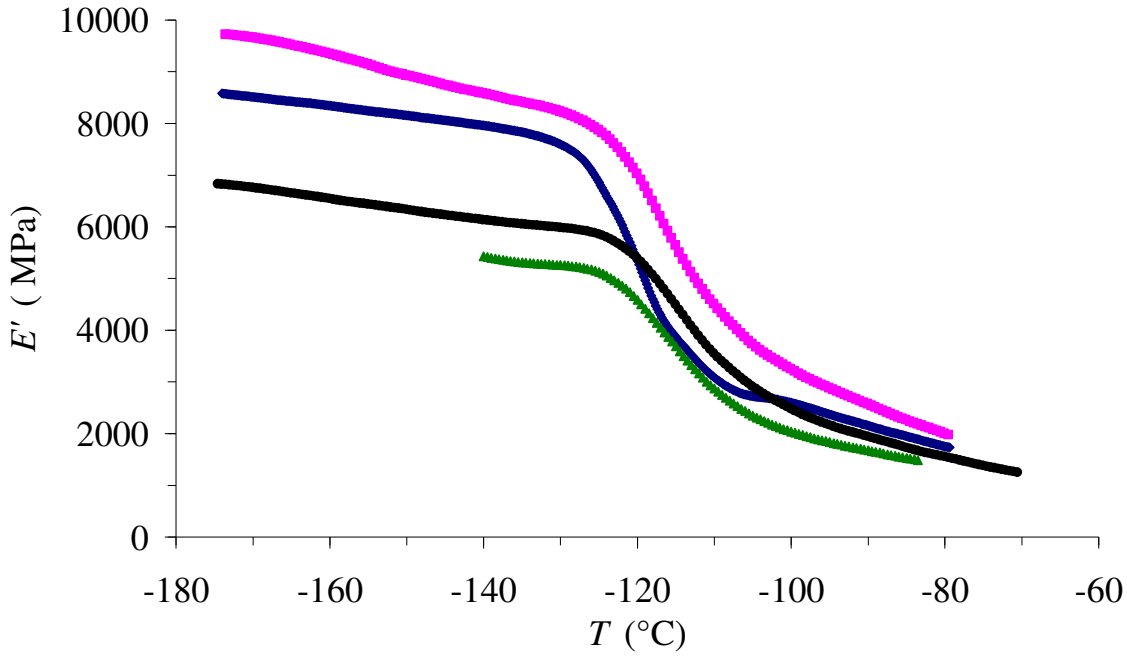

Figure B. 1: Value of E' against T at 10 Hz Results are given for C6-165 (■), MED-82-5010-80 (◆), MED-4080 (◆) and C6-180 (▲).

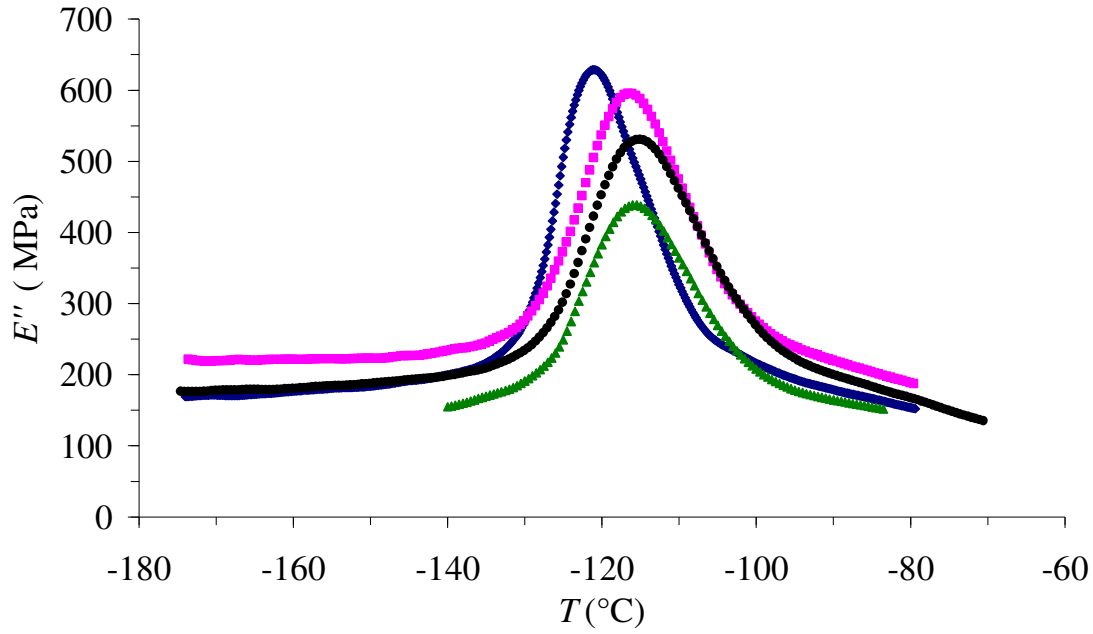

Figure B. 2: Value of E'' against T at 10 Hz. Results are given for C6-165 (■), MED-82-5010-80 (◆), MED-4080 (◆) and C6-180 (▲).

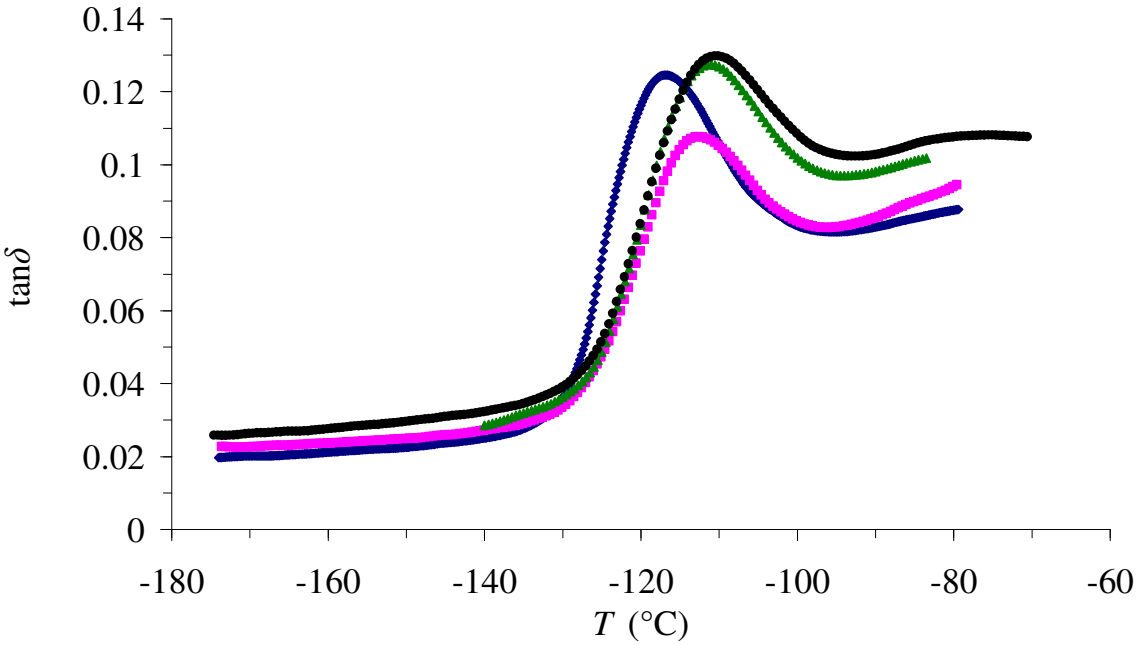

Figure B. 3: Value of tan δ against T at 10 Hz. Results are given for C6-165 (■), MED-82-5010-80 (◆), MED-4080 (◆) and C6-180 (▲).

Table B. 1:T_g measurements using DMTA.

Grades	**T_g (°C) at tanδ peak**		
	1 Hz	**10 Hz**	**33.3 Hz**
C6-165	-115.1	-112.6	-111.1
C6-180	-113.5	-111	-110
MED-4080	-120	-116.8	-114.6
MED-82-5010-80	-113.1	-110.6	-108.6

In general the figures and Table B. 1 show that, the T_g values for these 4 medical grades of silicones are very close to the quoted value of -123°C (Birkefeld *et al.*, 2004; Brydson, 1999; Clarson *et al.*, 1985; Dvornic and Lenz, 1990; Helmer and Polmanteer, 1969; Murayama, 1978; Nielsen, 1974; Weir *et al.*, 1950).

B.3 Results and Discussion of converting the DMTA data using the WLF equation into the frequency domain

Figure B. 4 and Figure B. 5 show the plots of *E'* and *E''* against log f_o, obtained when the DMTA results were converted into the frequency domain using the WLF equation.

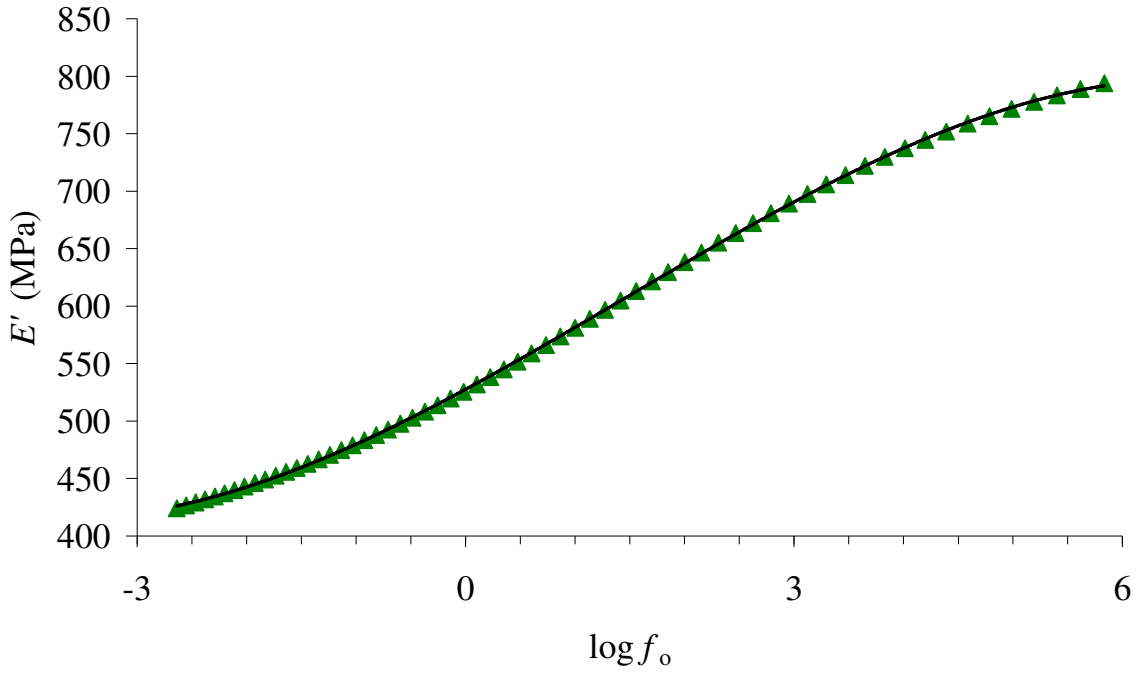

Figure B. 4: E' plotted against f_o for Grade MED-82-5010-80. The data obtained in the temperature domain was converted into the frequency domain using the WLF equation. Values taken at 10 Hz using T_o=T_g= -114.5 °C. The line shown is the third-order polynomial, 82 $y = -0.7111x^3 + 3.0793x^2 + 51.504x + 527.68$. $R^2 = 0.9999$, that gave the best fit to the data.

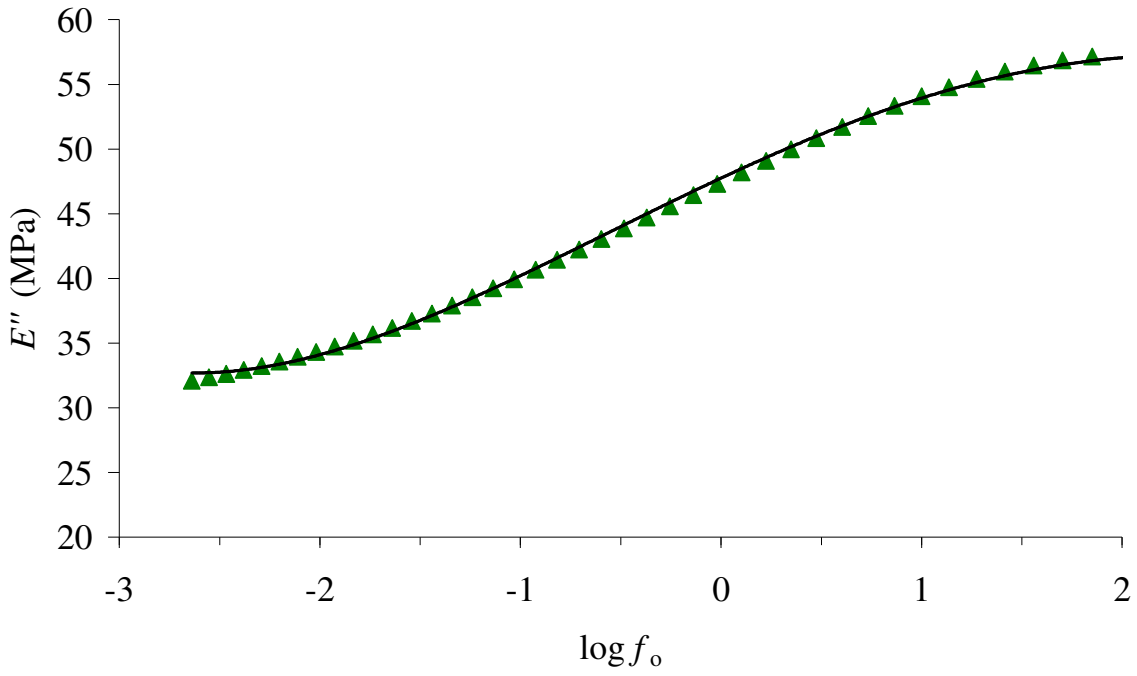

Figure B. 5: E'' plotted against f_o for Grade MED-82-5010-80. The data obtained in the temperature domain was converted into the frequency domain using the WLF equation. Values taken at 10 Hz using T_o=T_g= -114.5 °C. The line shown is the fourth-order polynomial, $y = 0.0456x^4 - 0.3743x^3 - 0.7248x^2 + 7.2394x + 47.75$ and $R^2 = 0.9993$, that gave the best fit to the data.

The results show that when T_o=T_g, the trend of the data points obtained, are similar to those obtained in Chapter 4 (§4.3). Hence, these preliminary results suggest that it is possible to convert between the temperature and frequency domain using the WLF equation when T_o=T_g. The reproducibility of values of the *E'* and *E''* obtained here cannot be evaluated because of the unreliable experimental method.

B.4 Results and Discussion of DSC on medical grade silicones

The T_g and T_m values from the DSC measurements for silicone grades C6-165, C6-180, MED-4080 and MED-82-5010-80 are shown in Figure B. 6, Figure B. 7, Figure B. 8 and Figure B. 9. The values of T_g and T_m are also tabulated in Table B. 2. "Endothermic" has been abbreviated to "endo" in the figures.

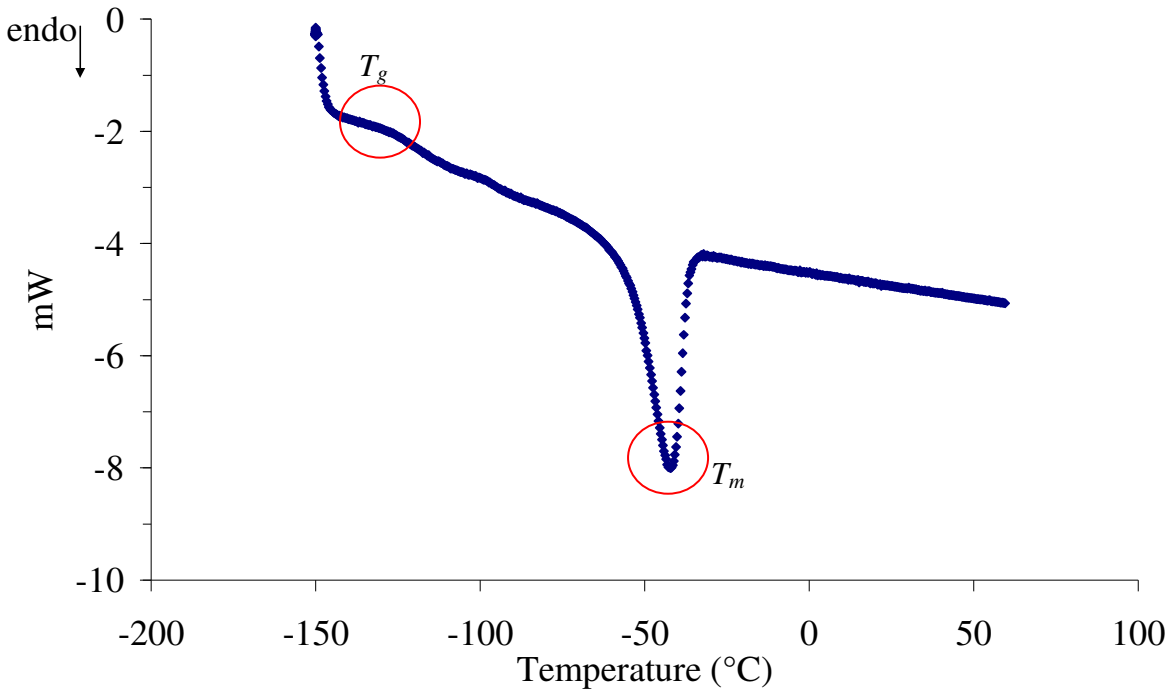

Figure B. 6: T_g and T_m values for C6-165.

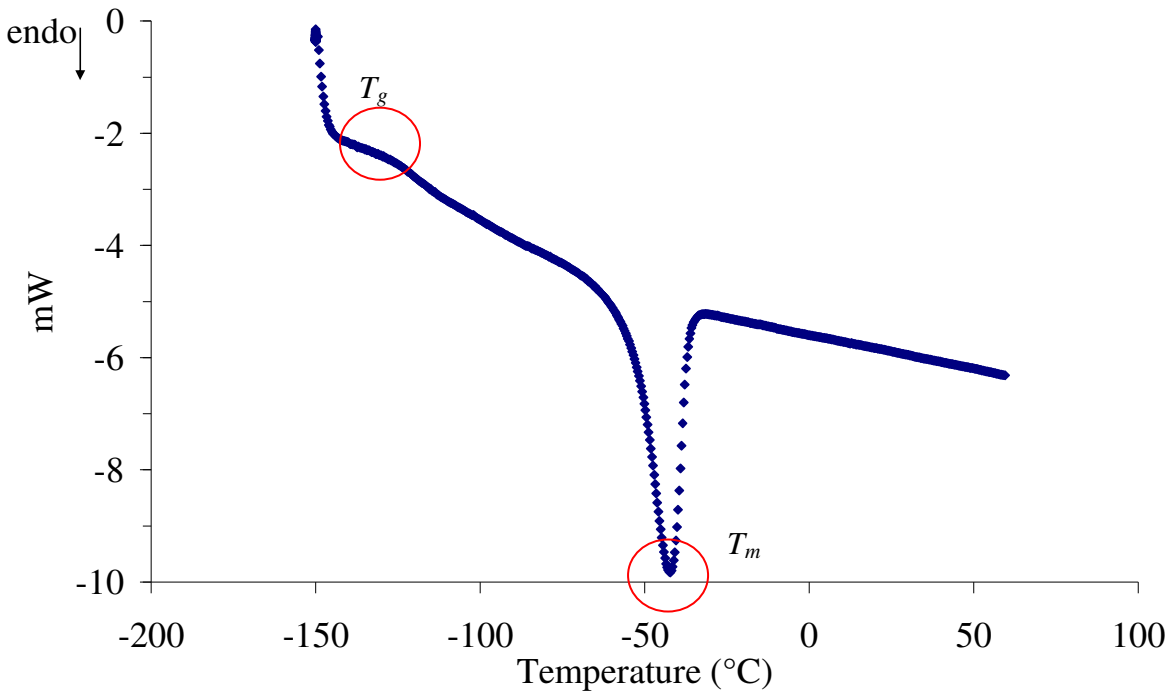

Figure B. 7: T_g and T_m values for C6-180.

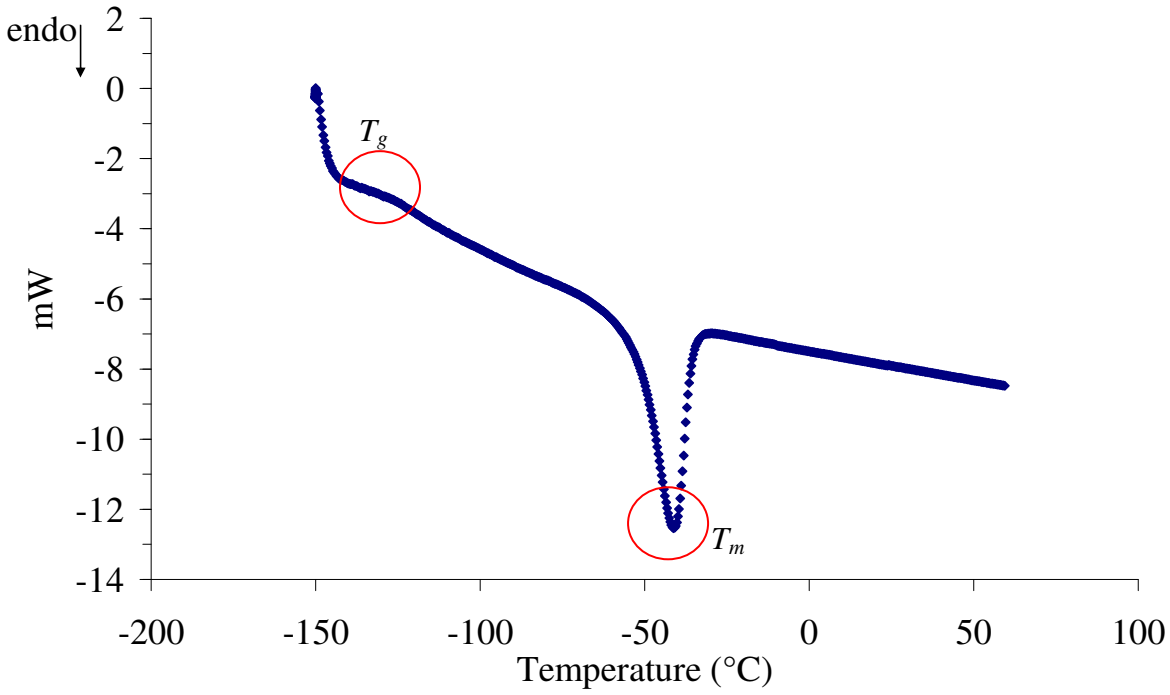

Figure B. 8: T_g and T_m values for MED-4080.

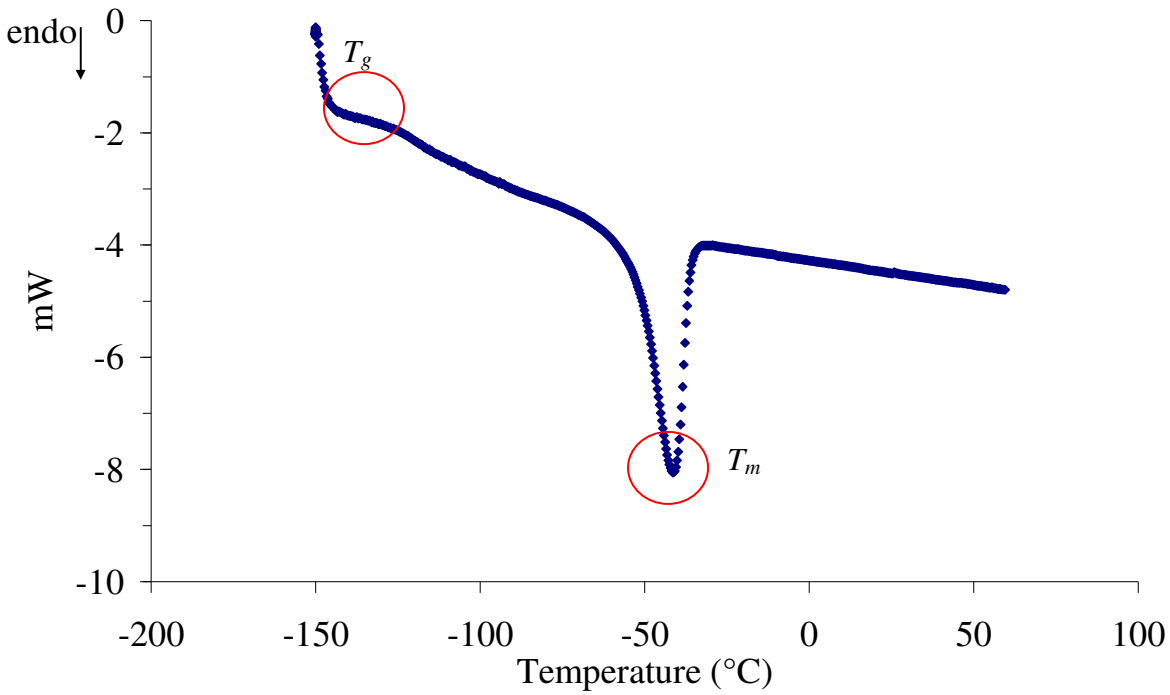

Figure B. 9: T_g and T_m values for MED-82-5010-80.

Table B. 2: T_g and T_m measurements obtained using DSC for silicones.

Grade	**T_g (°C)**		**T_m (°C)**	
	Onset	**Midpoint**	**Onset**	**Midpoint**
C6-165	-123.14	-116.62	-55.13	-41.97
C6-180	-125.18	-118.23	-53.81	-42.17
MED-4080	-124.37	-119.90	-52.63	-41.22
MED82-5010-80	-123.93	-116.60	-52.87	-41.47

In general the figures and table show that the T_g and T_m (endothermic peak) values for these 4 medical grades of silicones are very close to the quoted value of -123°C (Birkefeld *et al.*, 2004; Brydson, 1999; Clarson *et al.*, 1985; Dvornic and Lenz, 1990; Helmer and Polmanteer, 1969; Murayama, 1978; Nielsen, 1974; Weir *et al.*, 1950) and -40 °C (Birkefeld *et al.*, 2004; Clarson *et al.*, 1985; Ghanbari-Siahkali *et al.*, 2005; Helmer and Polmanteer, 1969; Murayama, 1978) respectively.

B.5 Results and Discussion of DSC on Elast-Eon™ 3

The T_g values from the DSC measurements for Elast-Eon™ 3 are shown in Figure B. 10

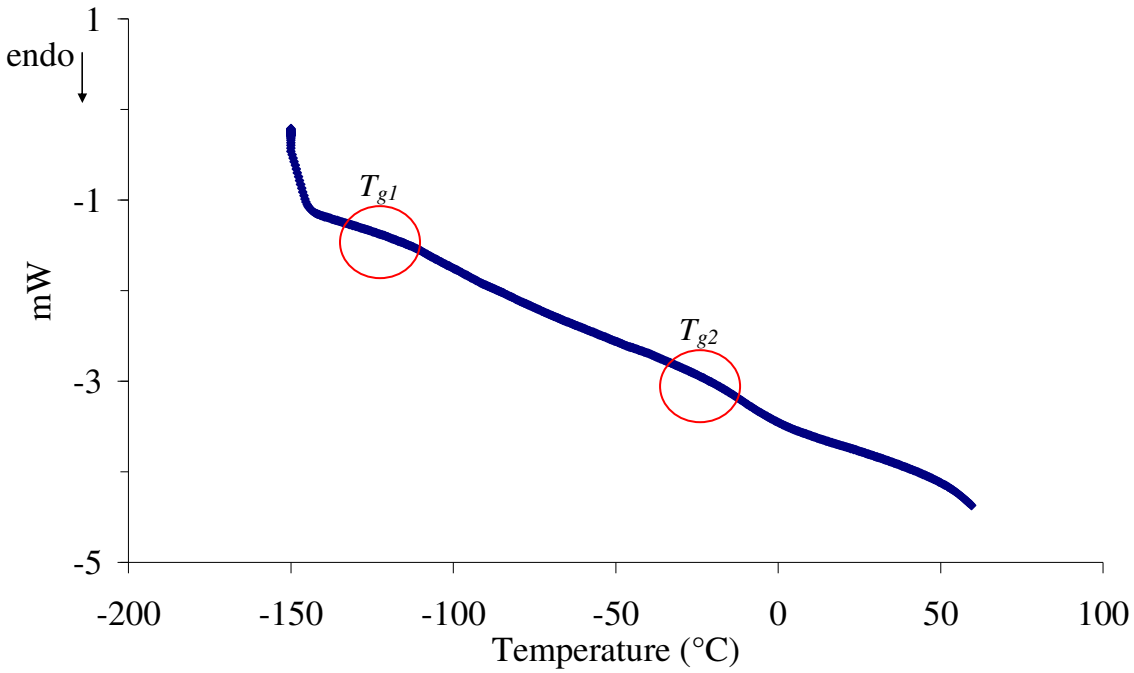

Figure B. 10: T_g values for Elast-Eon™ 3.

Table B. 3: T_{g1} and T_{g2} measurements obtained using DSC for Elast-Eon™ 3.

T_{g1} (°C)		**T_{g2} (°C)**	
Onset	**Midpoint**	**Onset**	**Midpoint**
-111.87	-98.40	-17.60	-5.84

T_{g1} and T_{g2} correspond to the T_g values of the soft (PDMS) and hard (polyurethane) segments respectively (Hernandez *et al.*, 2008; Xue-Hai *et al.*, 1985; Yang *et al.*, 1991).

APPENDIX C: ADDITIONAL CAD DRAWINGS

As mentioned in §3.3 and §3.5-3.6, additional CAD drawings have been included in this section.

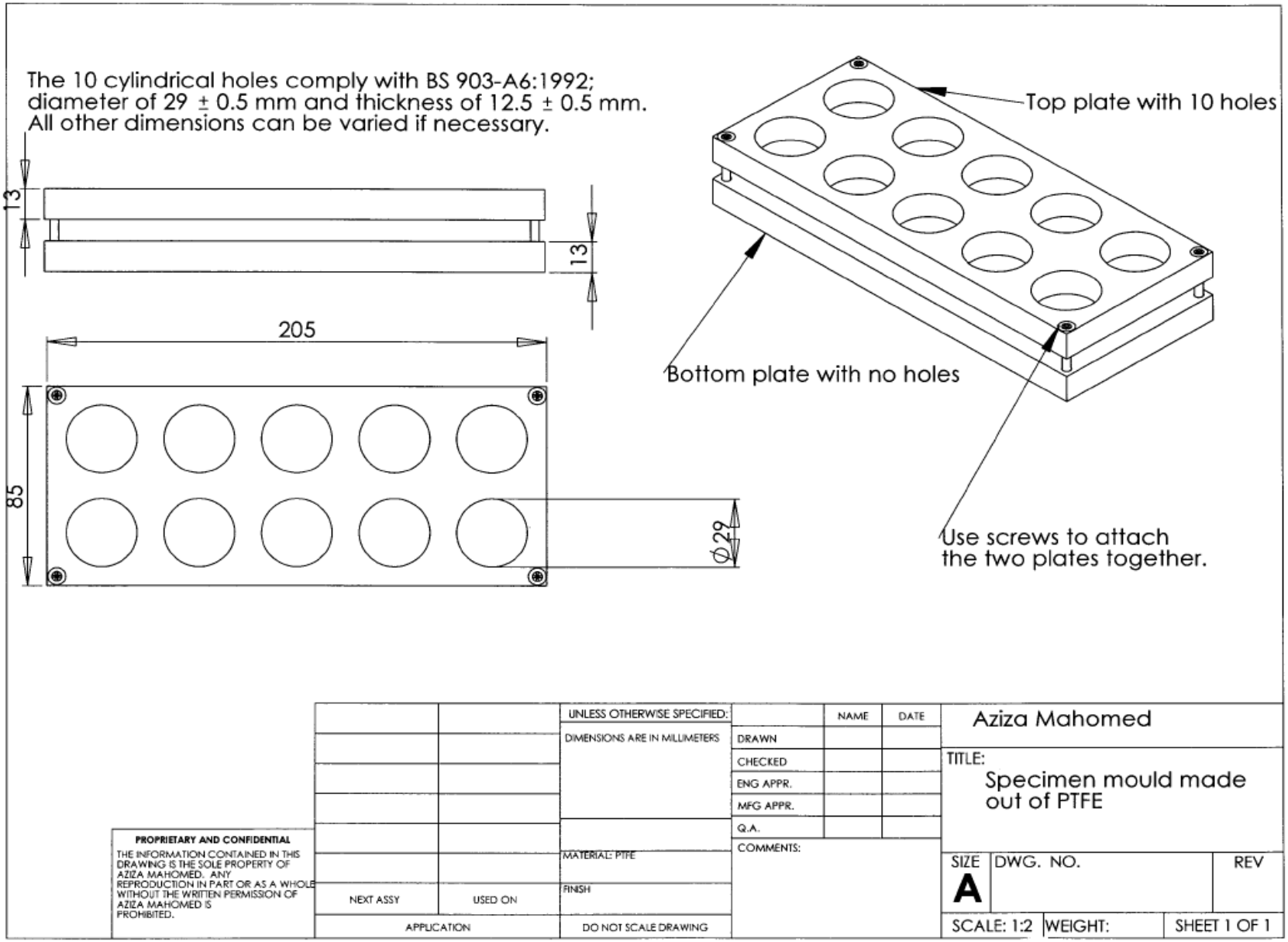
The 10 cylindrical holes comply with BS 903-A6:1992;
diameter of 29 ± 0.5 mm and thickness of 12.5 ± 0.5 mm.
All other dimensions can be varied if necessary.
13
13
205
85
Ø29
Top plate with 10 holes
Bottom plate with no holes
Use screws to attach
the two plates together.
UNLESS OTHERWISE SPECIFIED:
DIMENSIONS ARE IN MILLIMETERS
MATERIAL: PTFE
FINISH
DO NOT SCALE DRAWING
NEXT ASSY
USED ON
APPLICATION
DRAWN
CHECKED
ENG APPR.
MFG APPR.
Q.A.
COMMENTS:
NAME
DATE
Aziza Mahomed
TITLE:
Specimen mould made
out of PTFE
SIZE
A
DWG. NO.
REV
SCALE: 1:2
WEIGHT:
SHEET 1 OF 1
PROPRIETARY AND CONFIDENTIAL
THE INFORMATION CONTAINED IN THIS DRAWING IS THE SOLE PROPERTY OF AZIZA MAHOMED. ANY REPRODUCTION IN PART OR AS A WHOLE WITHOUT THE WRITTEN PERMISSION OF AZIZA MAHOMED IS PROHIBITED.

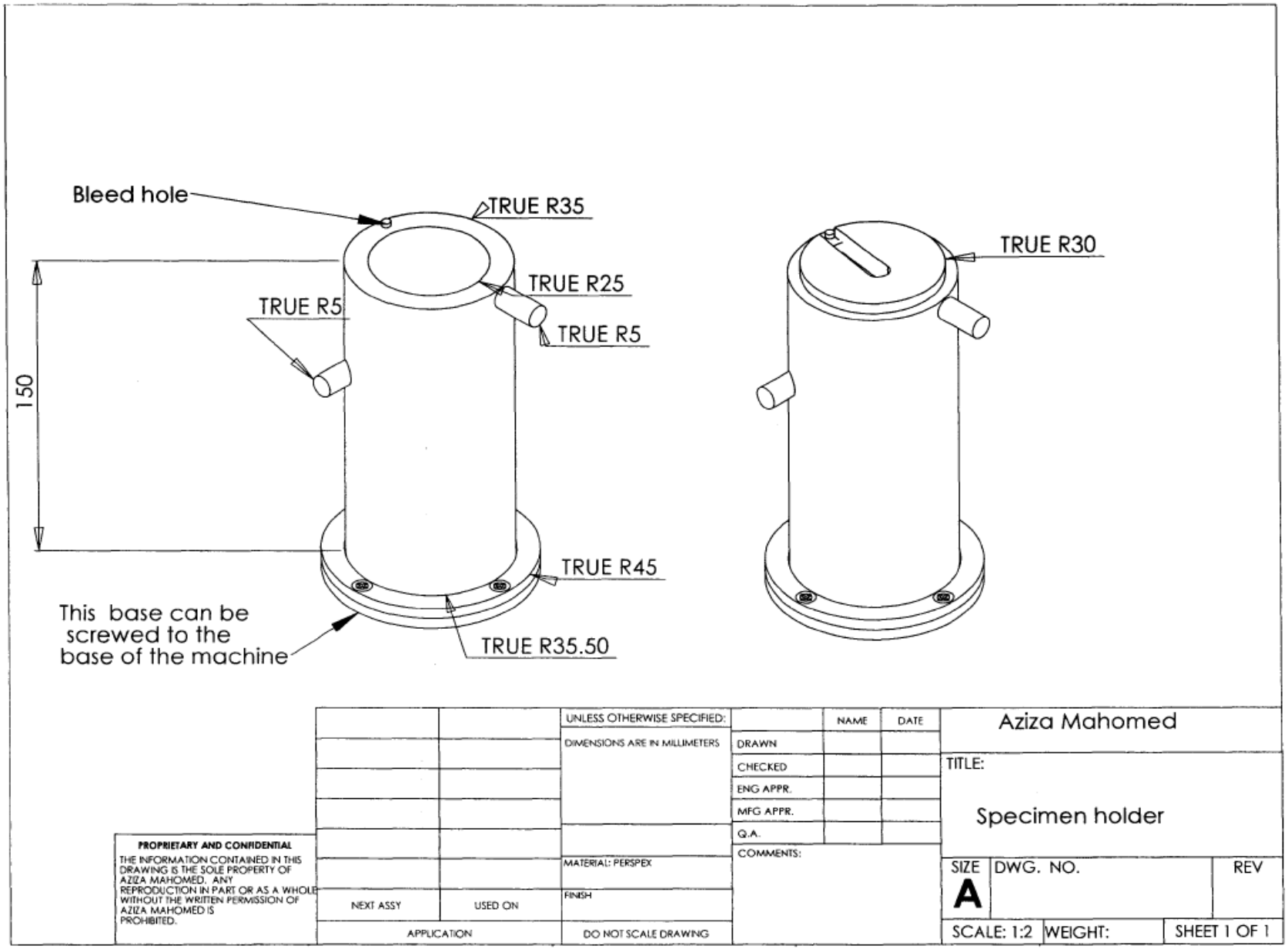
Bleed hole
TRUE R35
TRUE R25
TRUE R5
TRUE R5
150
TRUE R30
TRUE R45
This base can be screwed to the base of the machine
TRUE R35.50
UNLESS OTHERWISE SPECIFIED:
DIMENSIONS ARE IN MILLIMETERS
MATERIAL: PERSPEX
FINISH
DO NOT SCALE DRAWING
NEXT ASSY
USED ON
APPLICATION
NAME
DATE
DRAWN
CHECKED
ENG APPR.
MFG APPR.
Q.A.
COMMENTS:
Aziza Mahomed
TITLE:
Specimen holder
SIZE
A
DWG. NO.
REV
SCALE: 1:2
WEIGHT:
SHEET 1 OF 1
PROPRIETARY AND CONFIDENTIAL
THE INFORMATION CONTAINED IN THIS DRAWING IS THE SOLE PROPERTY OF AZIZA MAHOMED. ANY REPRODUCTION IN PART OR AS A WHOLE WITHOUT THE WRITTEN PERMISSION OF AZIZA MAHOMED IS PROHIBITED.

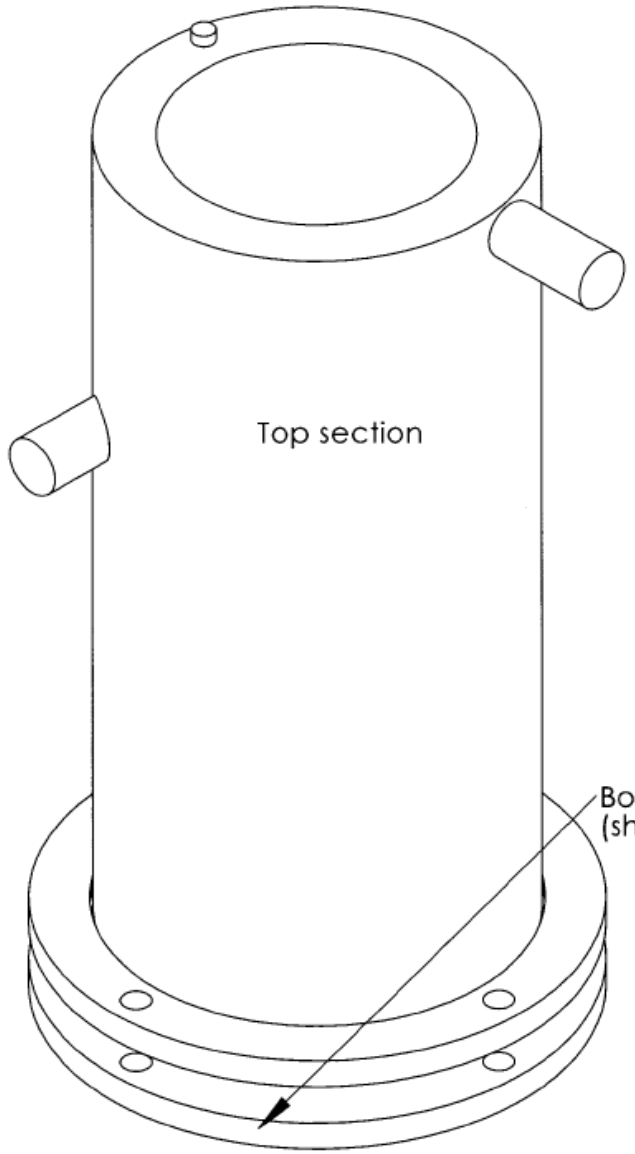

A more detailed view of the bottom section

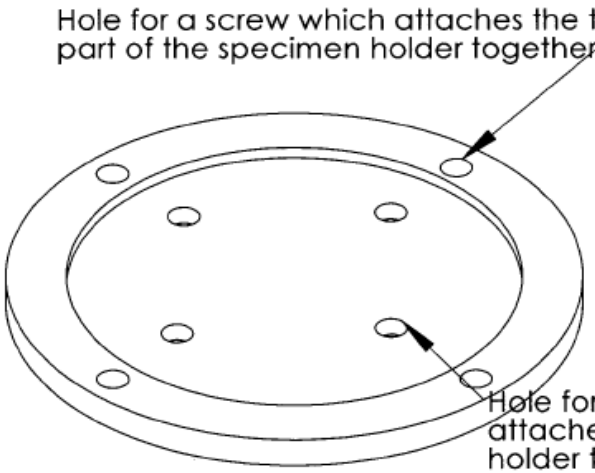

DIMENSIONS ARE IN MILLIMETERS MATERIAL : PERSPEX	Aziza Mahomed TITLE: Specimen holder: A more detailed view of the bottomsection
PROPRIETARY AND CONFIDENTIAL THE INFORMATION CONTAINED IN THIS DRAWING IS THE SOLE PROPERTY OF <INSERT COMPANY NAME HERE>. ANY REPRODUCTION IN PART OR AS A WHOLE WITHOUT THE WRITTEN PERMISSION OF <INSERT COMPANY NAME HERE> IS PROHIBITED.	SIZE A DWG. NO. REV SCALE: 1:1 WEIGHT: SHEET 1 OF 1

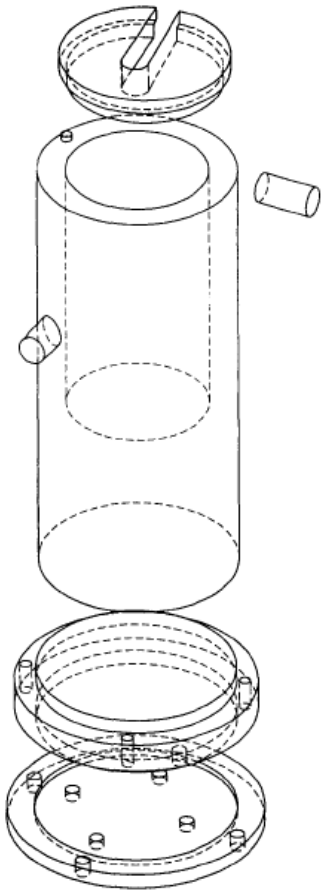

This drawing illustrates how
the sections were attached together
to make the cylindrical specimen holder.
A similar procedure was used to attach the
sections of the dumb-bell holder.

UNLESS OTHERWISE SPECIFIED: DIMENSIONS ARE IN MILLIMETERS	FINISH:				DEBUR AND BREAK SHARP EDGES	DO NOT SCALE DRAWING	REVISION
						Aziza Mahomed	
	NAME	SIGNATURE	DATE			TITLE: Exploded view of the specimen holder	
DRAWN							
CHK'D							
APPV'D							
MFG							
Q.A				MATERIAL:		DWG NO.	A4
				WEIGHT:		SCALE: 1:2	SHEET 1 OF 1

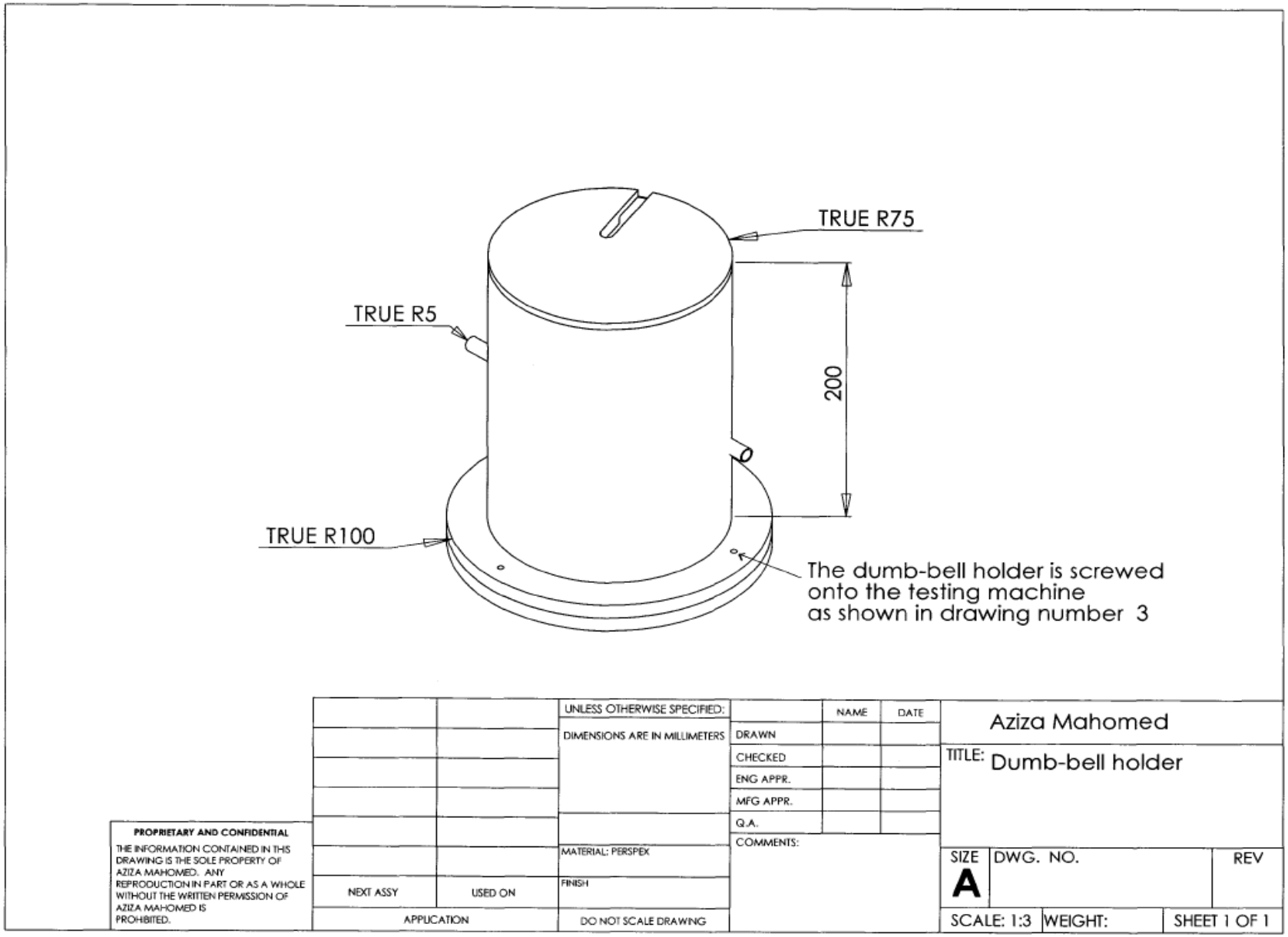
TRUE R75
TRUE R5
200
TRUE R100
The dumb-bell holder is screwed
onto the testing machine
as shown in drawing number 3
UNLESS OTHERWISE SPECIFIED:
DIMENSIONS ARE IN MILLIMETERS
MATERIAL: PERSPEX
FINISH
DO NOT SCALE DRAWING
NEXT ASSY
USED ON
APPLICATION
NAME
DATE
DRAWN
CHECKED
ENG APPR.
MFG APPR.
Q.A.
COMMENTS:
Aziza Mahomed
TITLE: Dumb-bell holder
SIZE A
DWG. NO.
REV
SCALE: 1:3
WEIGHT:
SHEET 1 OF 1
PROPRIETARY AND CONFIDENTIAL
THE INFORMATION CONTAINED IN THIS DRAWING IS THE SOLE PROPERTY OF AZIZA MAHOMED. ANY REPRODUCTION IN PART OR AS A WHOLE WITHOUT THE WRITTEN PERMISSION OF AZIZA MAHOMED IS PROHIBITED.

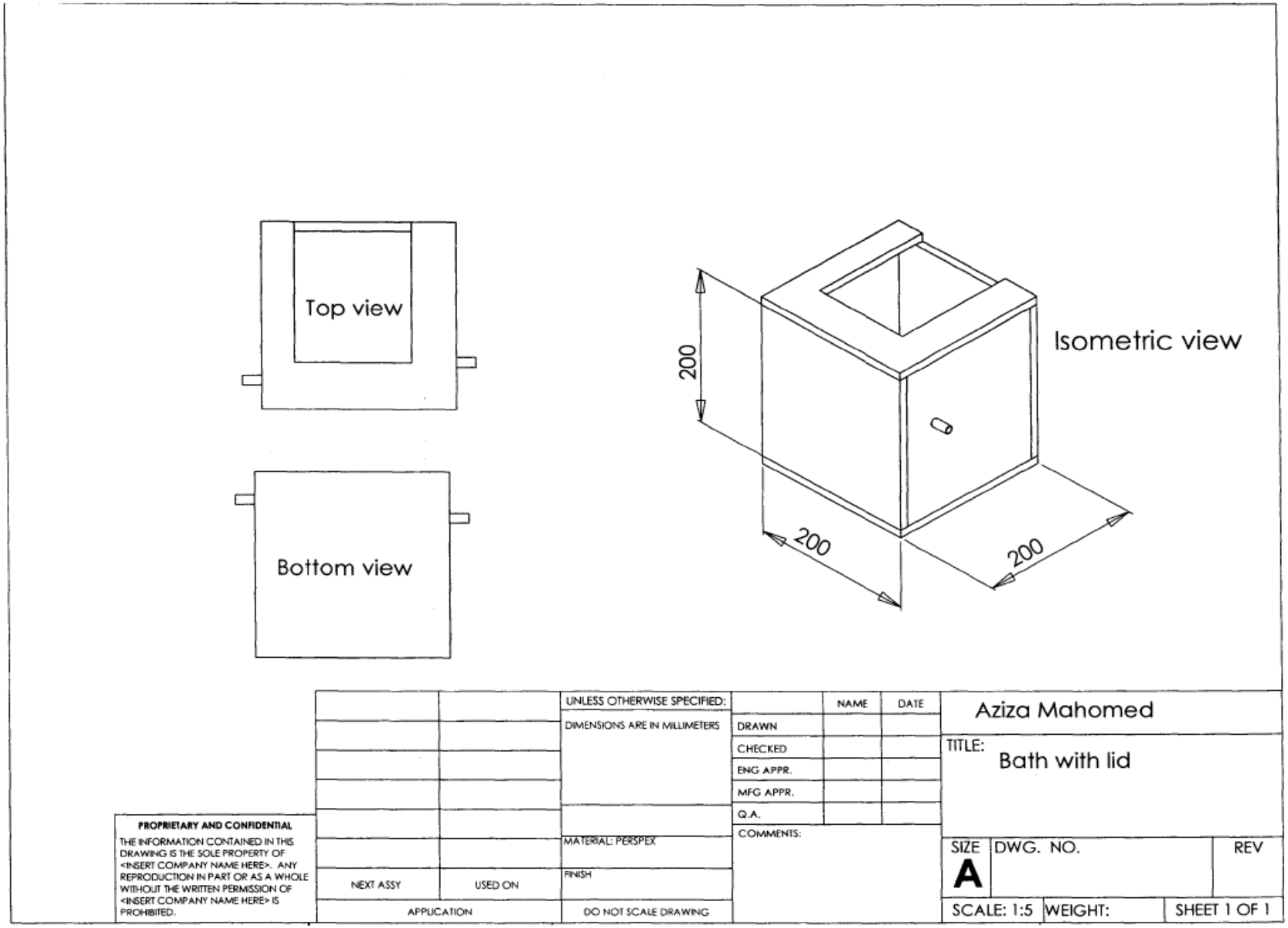

		UNLESS OTHERWISE SPECIFIED:		NAME	DATE
		DIMENSIONS ARE IN MILLIMETERS	DRAWN		
			CHECKED		
			ENG APPR.		
			MFG APPR.		
			Q.A.		
		MATERIAL: PERSPEX	COMMENTS:		
NEXT ASSY	USED ON	FINISH			
APPLICATION		DO NOT SCALE DRAWING			

PROPRIETARY AND CONFIDENTIAL
THE INFORMATION CONTAINED IN THIS DRAWING IS THE SOLE PROPERTY OF <INSERT COMPANY NAME HERE>. ANY REPRODUCTION IN PART OR AS A WHOLE WITHOUT THE WRITTEN PERMISSION OF <INSERT COMPANY NAME HERE> IS PROHIBITED.

Aziza Mahomed

TITLE: Bath with lid

SIZE	DWG. NO.	REV
A		

SCALE: 1:5 | WEIGHT: | SHEET 1 OF 1

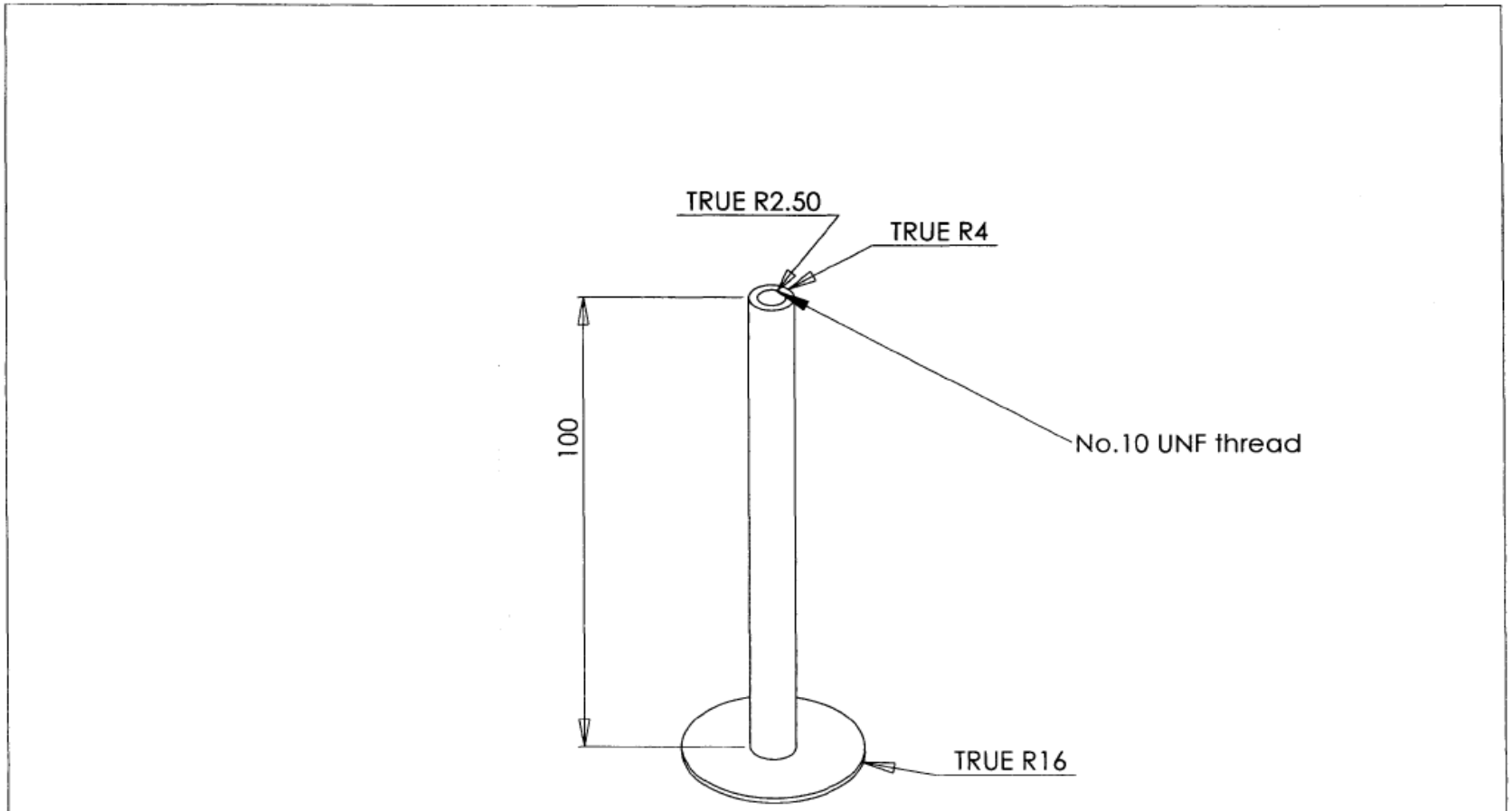

		UNLESS OTHERWISE SPECIFIED:		NAME	DATE
		DIMENSIONS ARE IN MILLIMETERS	DRAWN		25/01/06
			CHECKED		
			ENG APPR.		
			MFG APPR.		
			Q.A.		
		MATERIAL: BRASS	COMMENTS:		
NEXT ASSY	USED ON	FINISH			
APPLICATION		DO NOT SCALE DRAWING			

PROPRIETARY AND CONFIDENTIAL
THE INFORMATION CONTAINED IN THIS DRAWING IS THE SOLE PROPERTY OF AZIZA MAHOMED. ANY REPRODUCTION IN PART OR AS A WHOLE WITHOUT THE WRITTEN PERMISSION OF AZIZA MAHOMED IS PROHIBITED.

Aziza Mahomed

TITLE: Extension

SIZE	DWG. NO.	REV
A		
SCALE: 1:1	WEIGHT:	SHEET 1 OF 1

APPENDIX D: LOAD PLOTTED AGAINST DISPLACEMENT

D.1 Load/displacement plots for medical grade silicones in compression

As discussed in §3.7.2.2, preliminary quasi-static tests showed that the plots of load against displacement had a linear portion centred around a static load of 40 N as shown in Figure D. 1, Figure D. 2, Figure D. 3, Figure D. 4, Figure D. 5 and Figure D. 6 for grades C6-180, MED-4080, Silastic® Q7-4720, Silastic® Q7-4735, Silastic® Q7-4780 and Nagor ® medium hardness medical grade silicone, respectively.

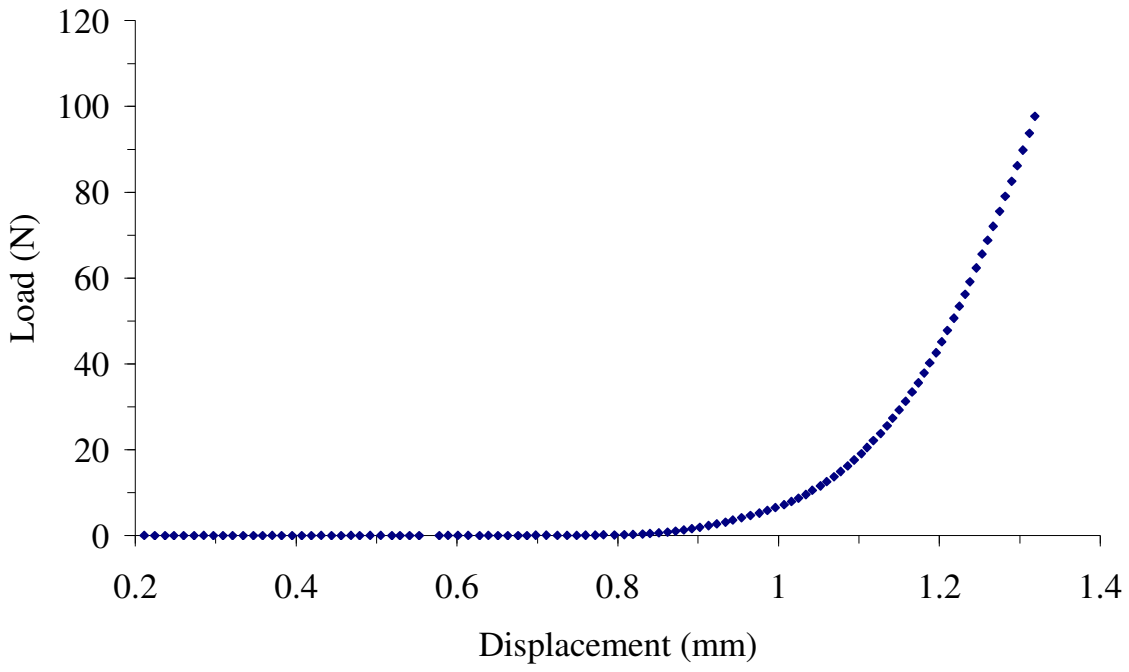

Figure D. 1: Preliminary plot of load against displacement for grade C6-180.

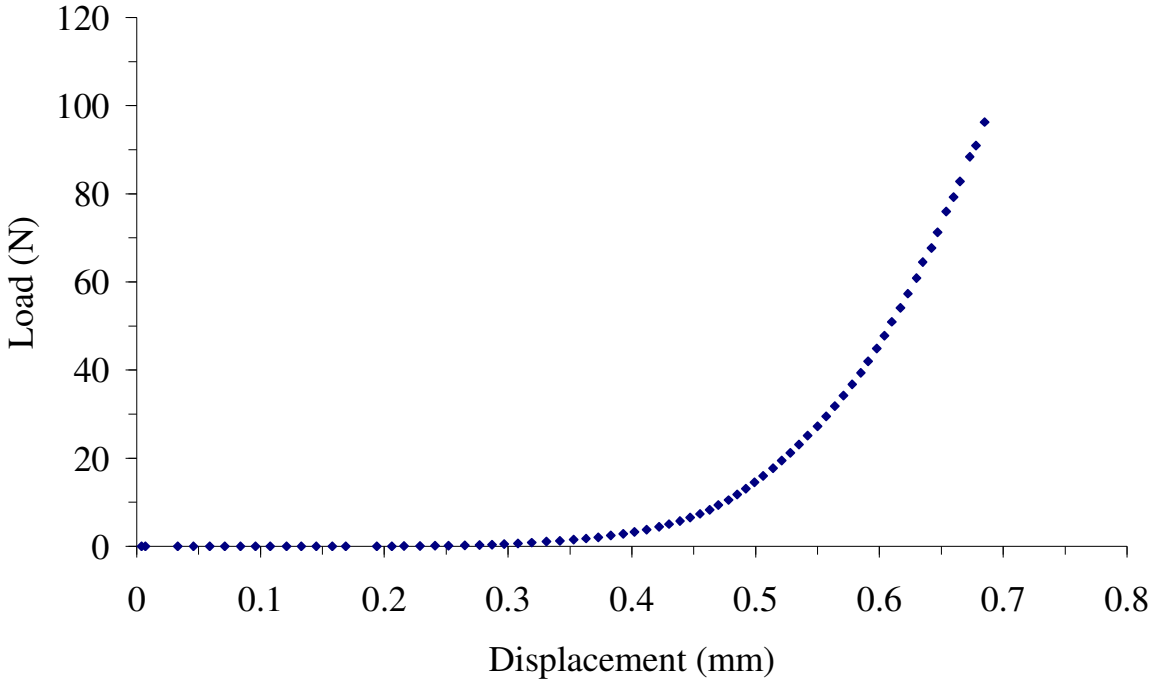

Figure D. 2: Preliminary plot of load against displacement for grade MED- 4080.

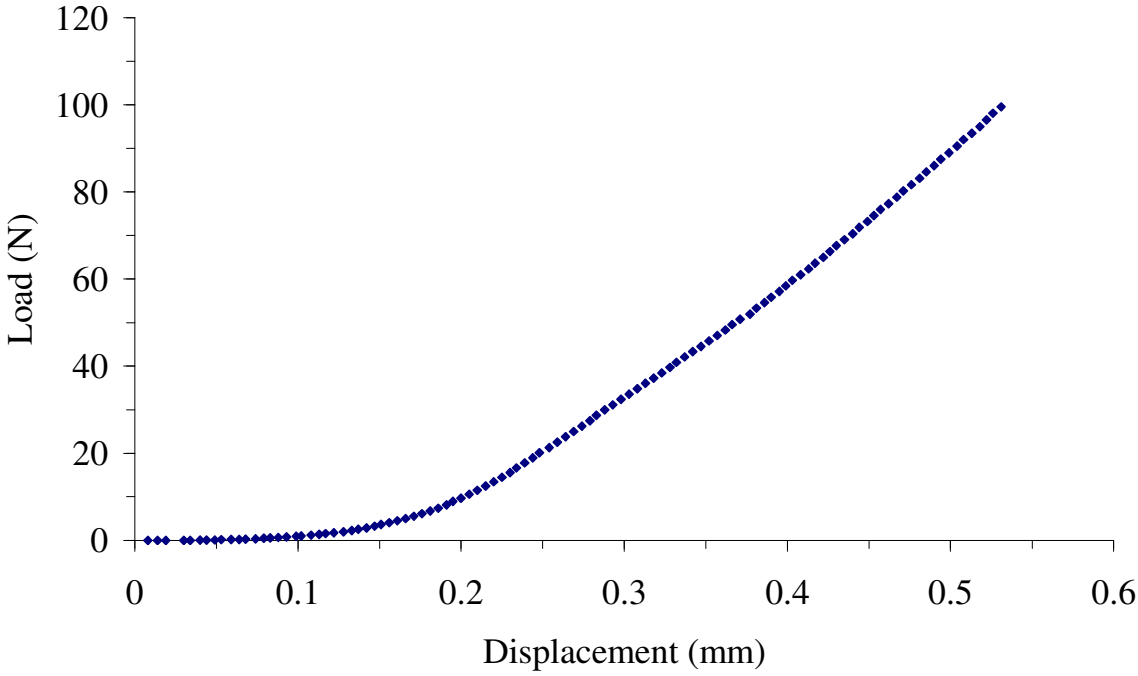

Figure D. 3: Preliminary plot of load against displacement for Silastic® Q7-4720.

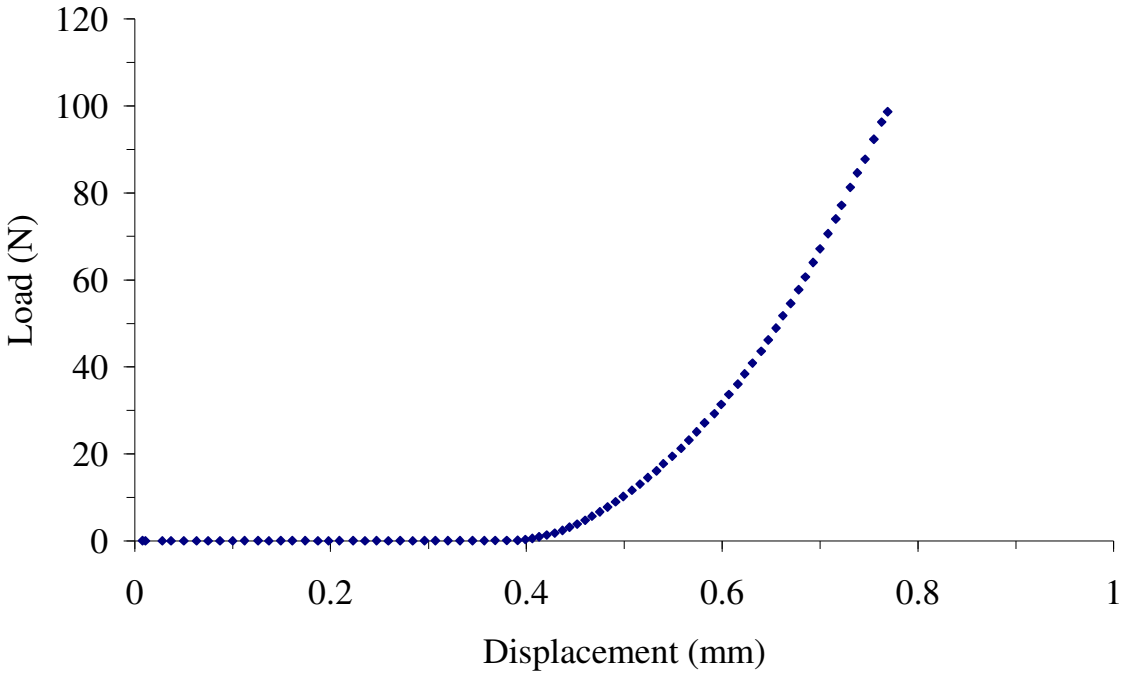

Figure D. 4: Preliminary plot of load against displacement for Silastic® Q7-4735.

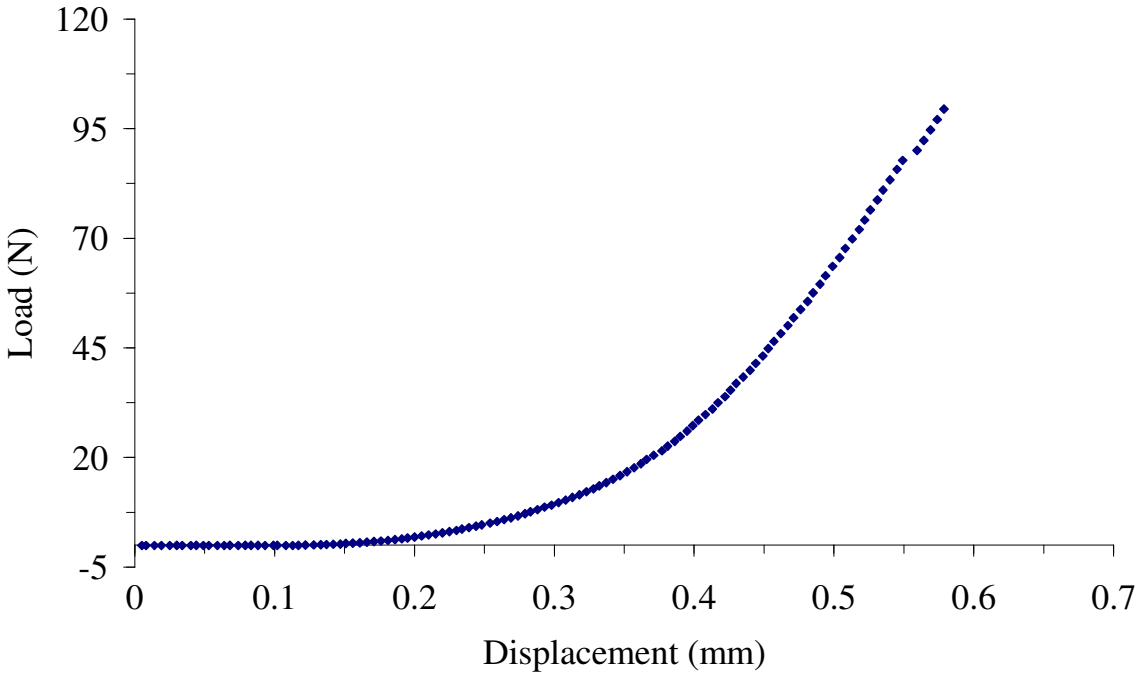

Figure D. 5: Preliminary plot of load against displacement for Silastic® Q7-4780.

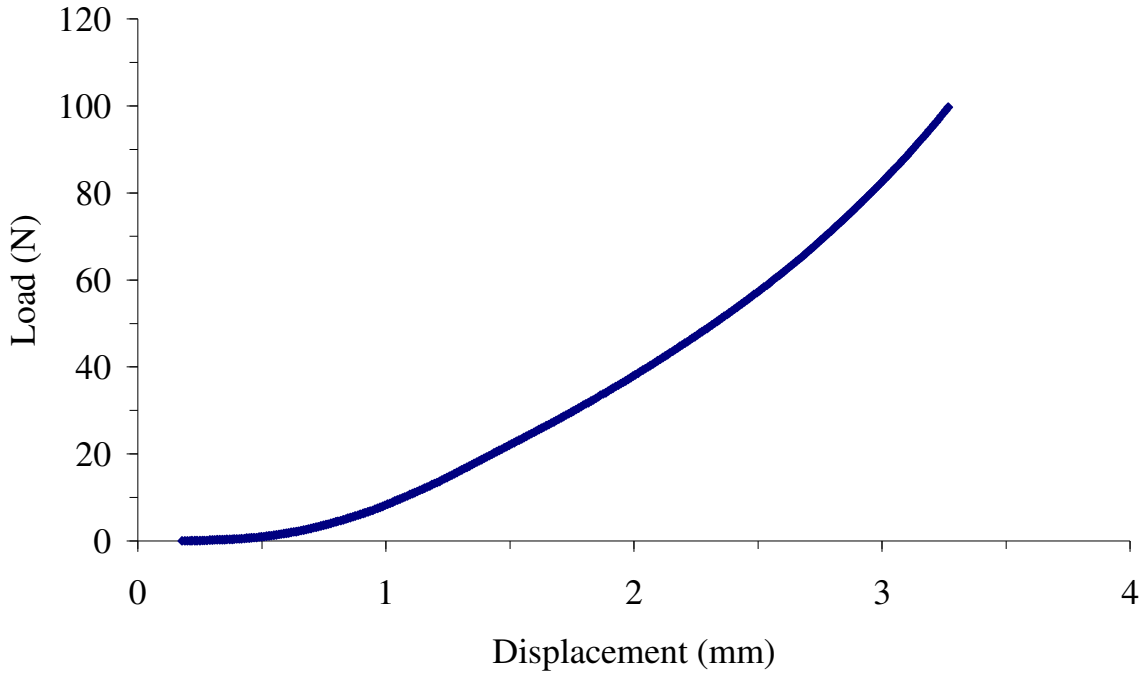

Figure D. 6: Preliminary plot of load against displacement for Nagor ® medium hardness medical grade silicone.

D.2 Load/displacement plots for Elast-Eon™ 3 in compression

As discussed in §3.7.2.2, preliminary quasi-static tests showed that the load/deformation curves had a linear portion centred around a static load of 40 N as shown in Figure D. 7.

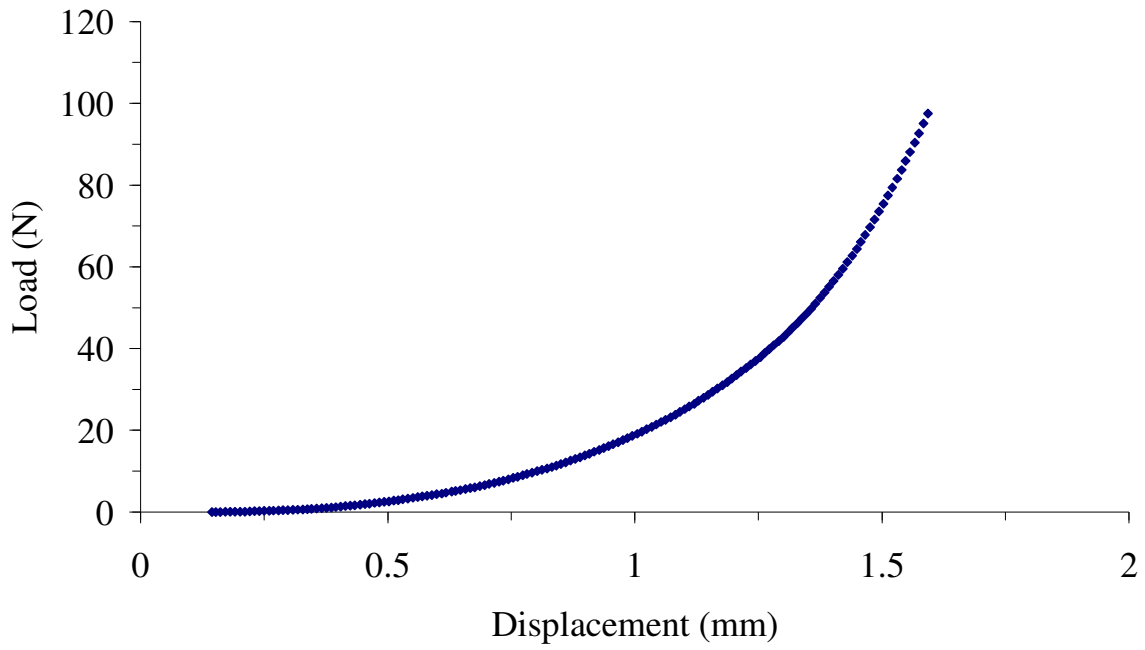

Figure D. 7: Preliminary plot of load against displacement for Elast-Eon™ 3.

D.3 Load/deformation plots for medical grade silicones in tension

As discussed in §3.7.3.2 preliminary quasi-static tests showed that the plot of load against displacement had an almost linear region centred around a displacement of 2.5 mm as shown in Figure D. 8, Figure D. 9 and Figure D. 10 for grades MED-82-5010-80, C6-180 and MED-4080, respectively.

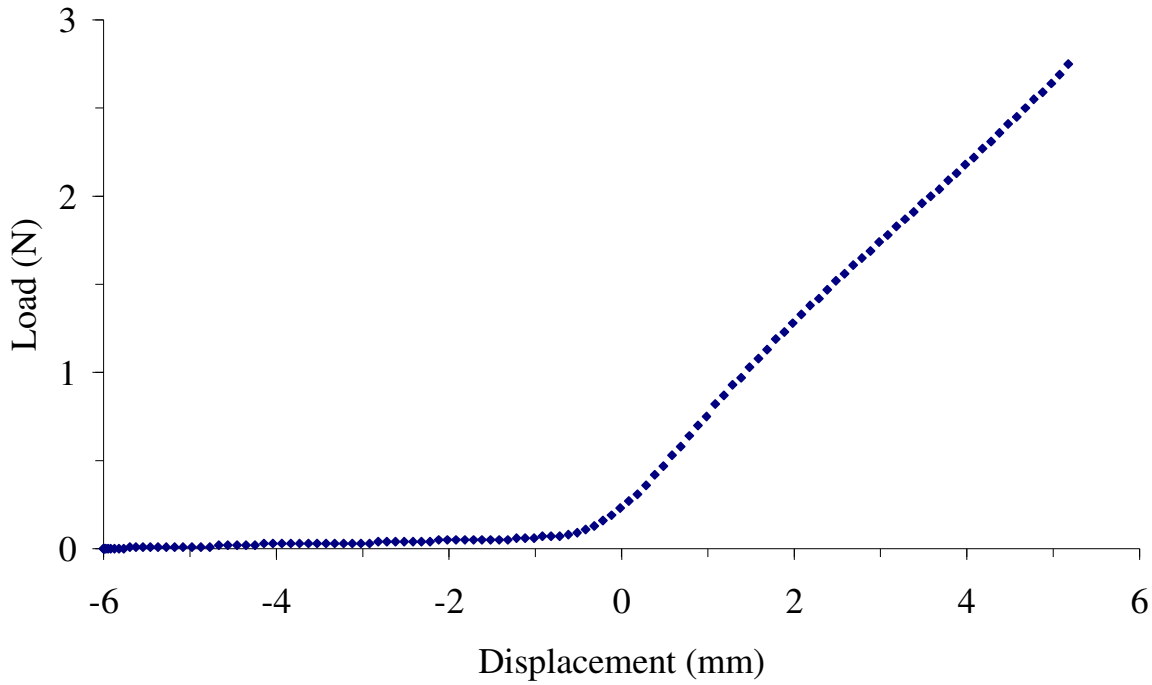

Figure D. 8: Preliminary plot of load against displacement for grade MED-82-5010-80.

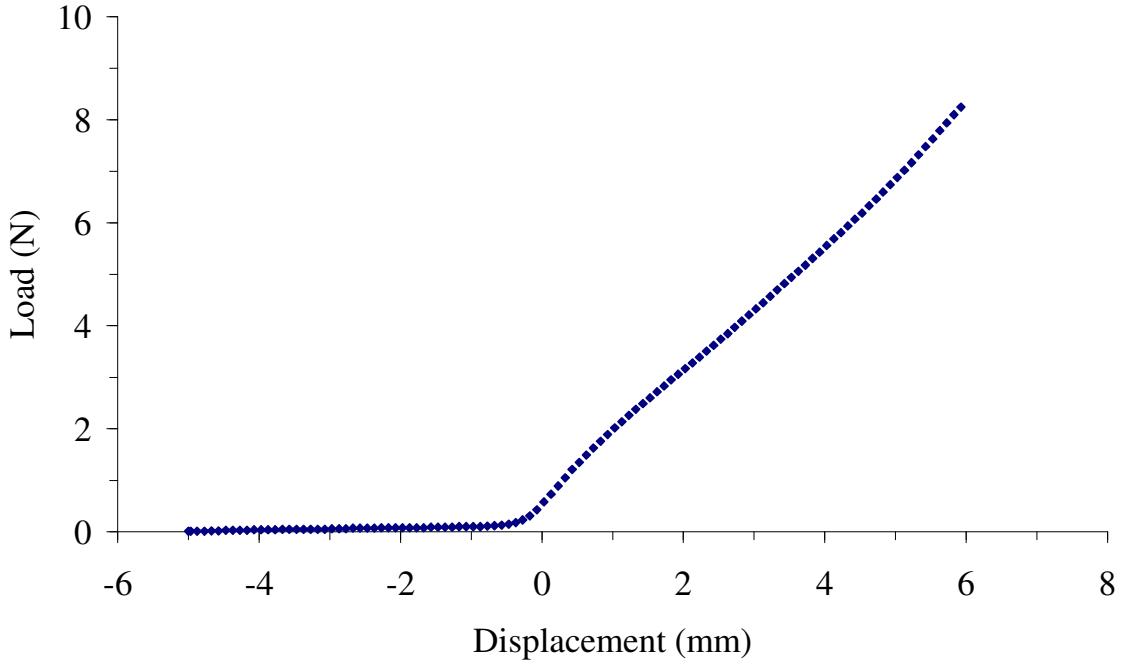

Figure D. 9: Preliminary plot of load against displacement for grade C6-180.

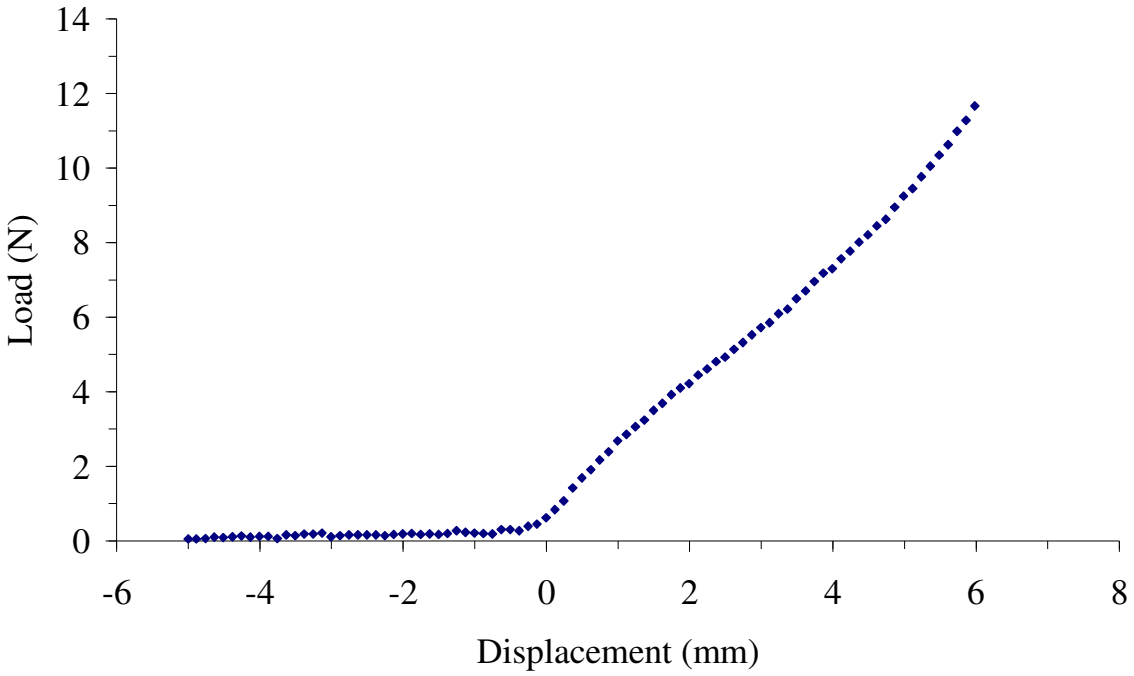

Figure D. 10: Preliminary plot of load against displacement for grade MED- 4080.

APPENDIX E: EFFECT OF TESTING AT HIGH FREQUENCIES

As discussed in §3.7.2.3, to investigate whether the high frequency used in the tests could lead to an increase in temperature within the specimen, a Type T PTFE thermocouple supplied by RS Components Ltd. (Corby, Northants, NN17 9RS, UK), was inserted into one of the specimens (Grade C6-165) during a test, as shown in Figure E. 1, and the internal temperature of the silicone recorded. During the test, the thermocouple readings varied between 37.02°C and 37.15°C, so the internal temperature change was considered to be negligible.

The data logger and software used was a PicoLog TC-08 and PicoLog R5.14.5 respectively (Pico Technology, Eaton Socon, St Neots, Cambridgeshire, PE19 8YP, UK).

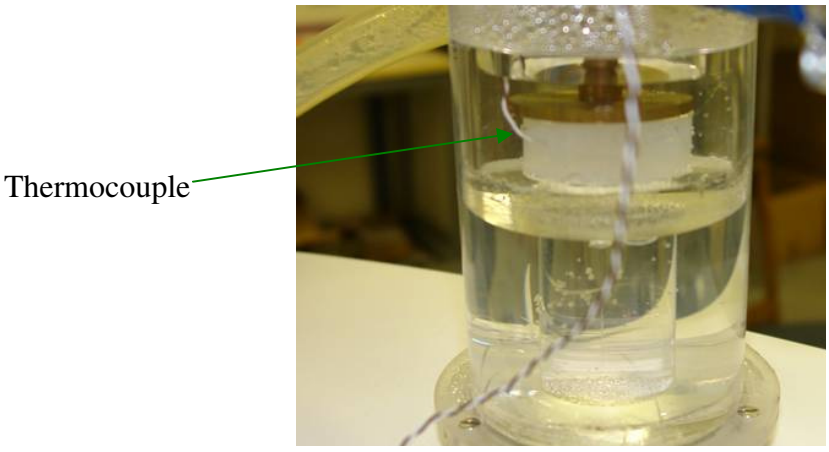

Figure E. 1: A Type T thermocouple inserted into a grade C6-165 specimen.

APPENDIX F: DAMPING ANALYSIS FOR DYNAMIC MECHANICAL ANALYSIS OF MEDICAL GRADE SILICONES AND ELAST-EON^{TM}3 IN COMPRESSION AND IN TENSION

F.1 Damping in the compression tests for the medical grade silicones

As described in Chapter 3 (§3.7.4), variation in the value of damping between different tests, can affect the reliability and reproducibility of the measurements. Hence, it is undesirable. This section and the subsequent sections in this Appendix discusses "damping" in slightly more detail and demonstrates how plots of *E''* against frequency, *f*, from the measurements reported in Chapter 4- 6, can be used to determine the type of damping of the system.

In a system, damping is usually represented by a damper, *C*, as shown in Figure F. 1 (Rao and Gupta, 1984; Thomson, 1964).

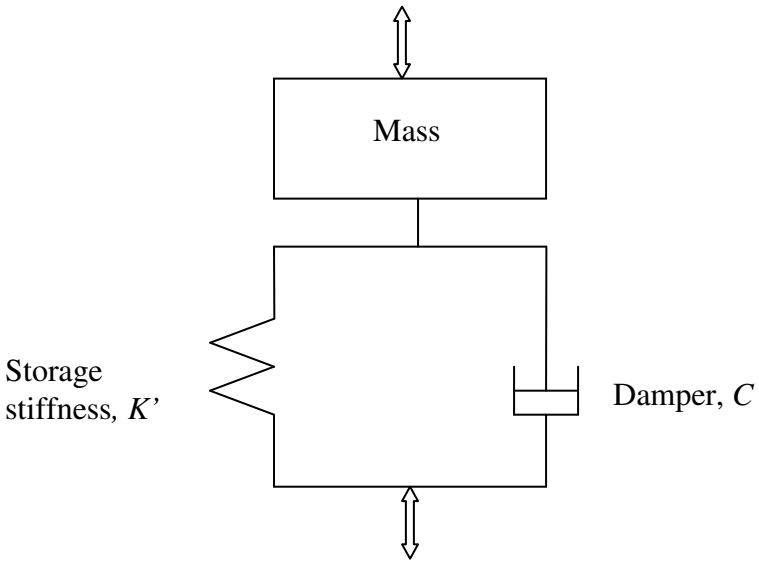

Figure F. 1: A mass-spring-damper system

Mass and stiffness are inherent characteristics of a system but damping may not necessarily be (Rao and Gupta, 1984). In the absence of damping, a system would oscillate indefinitely when a force is applied, which does not occur in real applications (Hukins, 1990; Rao and Gupta, 1984; Thomson, 1964; Tongue, 1996). Damping is an effective way to control large amplitudes of vibrations or oscillations (Rao and Gupta, 1984). Hence, when predicting the dynamic behaviour of a system, it is important to consider damping (Rao and Gupta, 1984). Energy is dissipated in a system that is oscillating in a viscous medium (Thomson, 1965). Hence, such a system can be associated with viscous (energy dissipation) damping (Rao and Gupta, 1984; Thomson, 1964; Tongue, 1996).

Preliminary testing of the silicone cylinders in compression (Chapter 4), showed that E^* and E' measurements with a high value of damping were much higher than those with a lower value of damping. Hence, the values of the two differently damped systems could not be compared. Graphs plotted for measurements with a high damping value did not necessarily show smooth trends, where as graphs with lower damping values were more likely to have better well defined trends, as shown in Figure F. 2, Figure F. 3, Figure F. 4 and Figure F. 5. For the compression specimens, the ideal value of damping was in the range of 120-170 Ns/mm for grades C6-165, C6-180, MED-4080 and Silastic ® Q7-4780.

Figure F. 2, Figure F. 3, Figure F. 4 and Figure F. 5 can also be classified into one of three systems (Hukins, 1990; Rao and Gupta, 1984; Thomson, 1964):

- a critically damped system, where the system oscillates to the desired position without overshooting, which is the required characteristics of an ideal system;
- an overdamped system, where the system may never reach the desired position within the required time;
- an underdamped system, where the system does not move smoothly but exhibits jerky movements.

By comparing the measurements taken, it was concluded that critically damped systems, such as in Figure F. 4, produced the most regular and reproducible values. Therefore only mean values of specimens with critically damped measurements were used or statistically compared in Chapter 4.

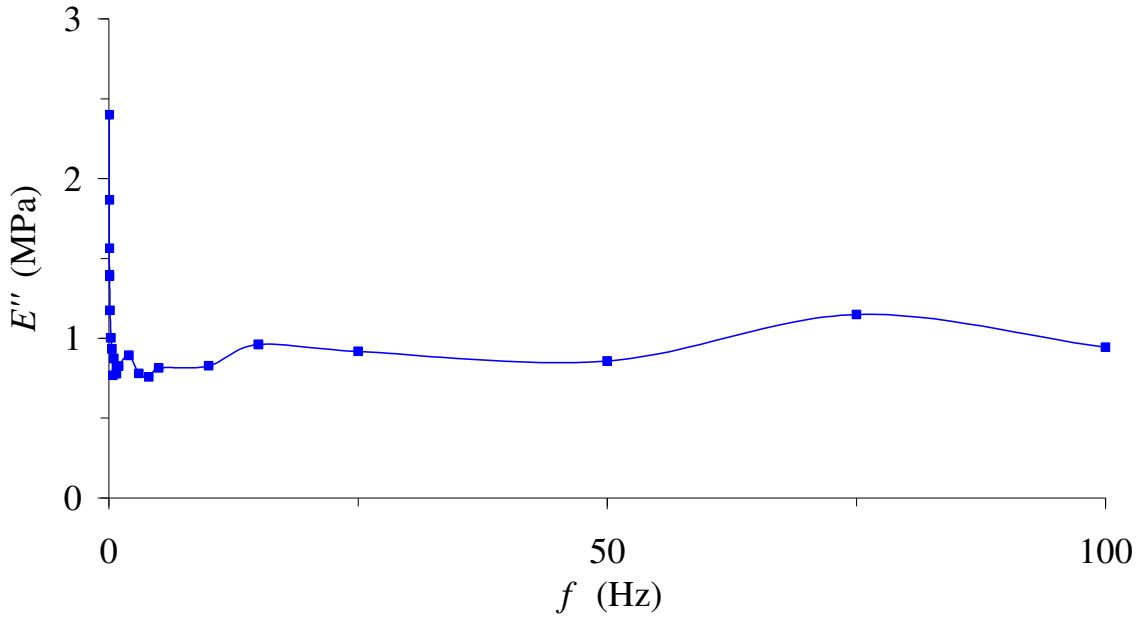

Figure F. 2: Extremely underdamped system (MED-4080, sample 4, damping of 969 Ns/mm, 08/02/07)

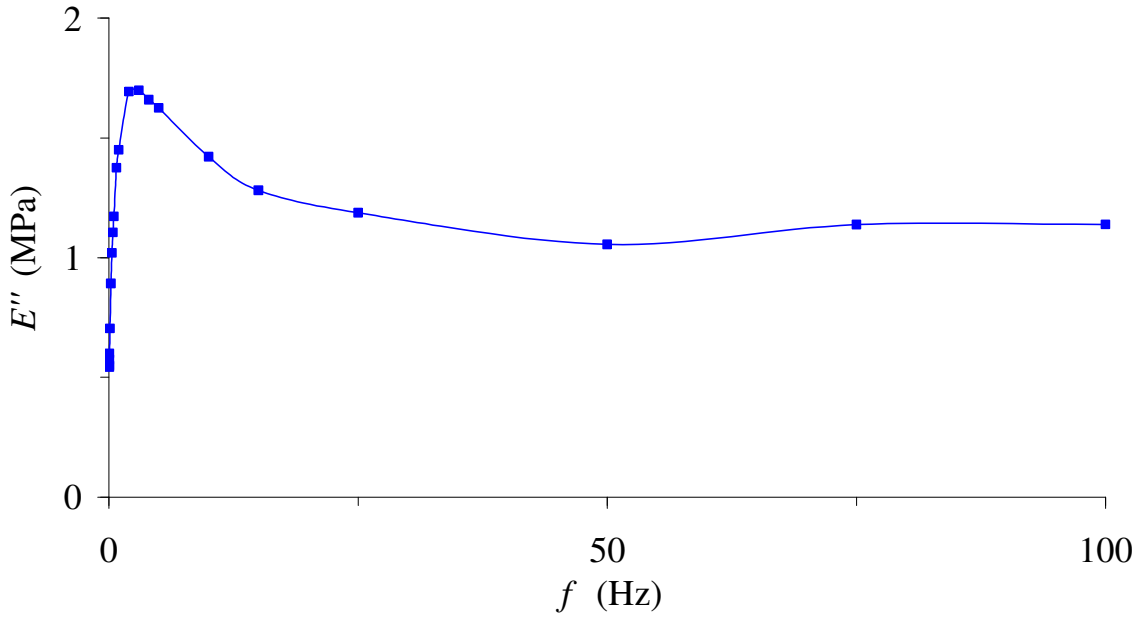

Figure F. 3: Underdamped system (C6-165, sample 1b, damping of 230 Ns/mm, 25/07/06)

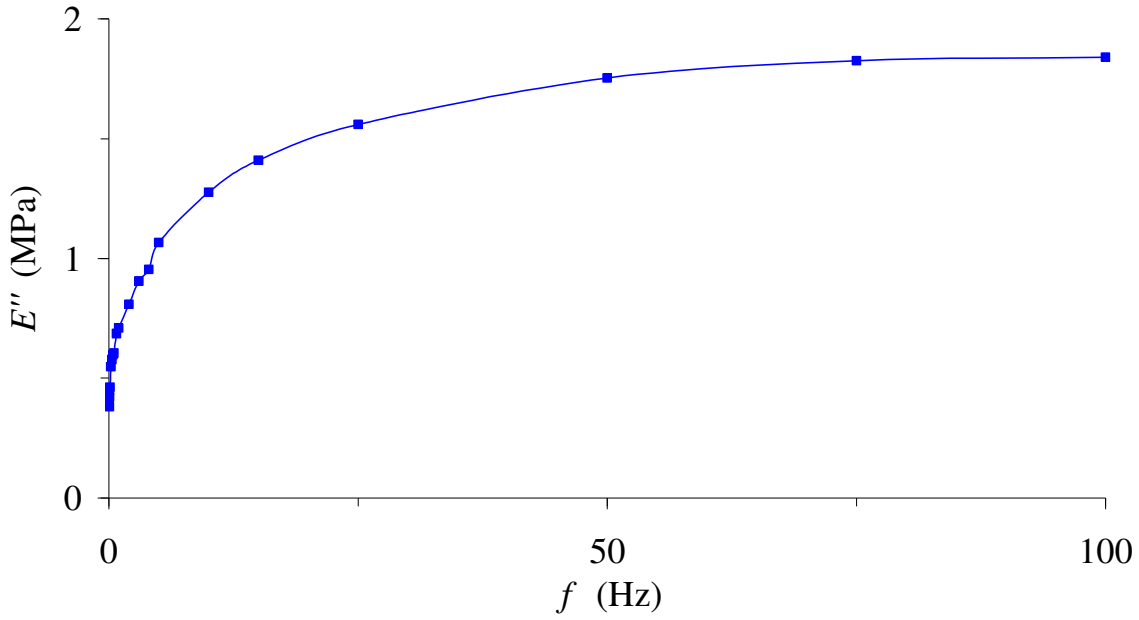

Figure F. 4: Critically damped system (C6-165, sample 1b, damping of 165 Ns/mm, 01/11/06)

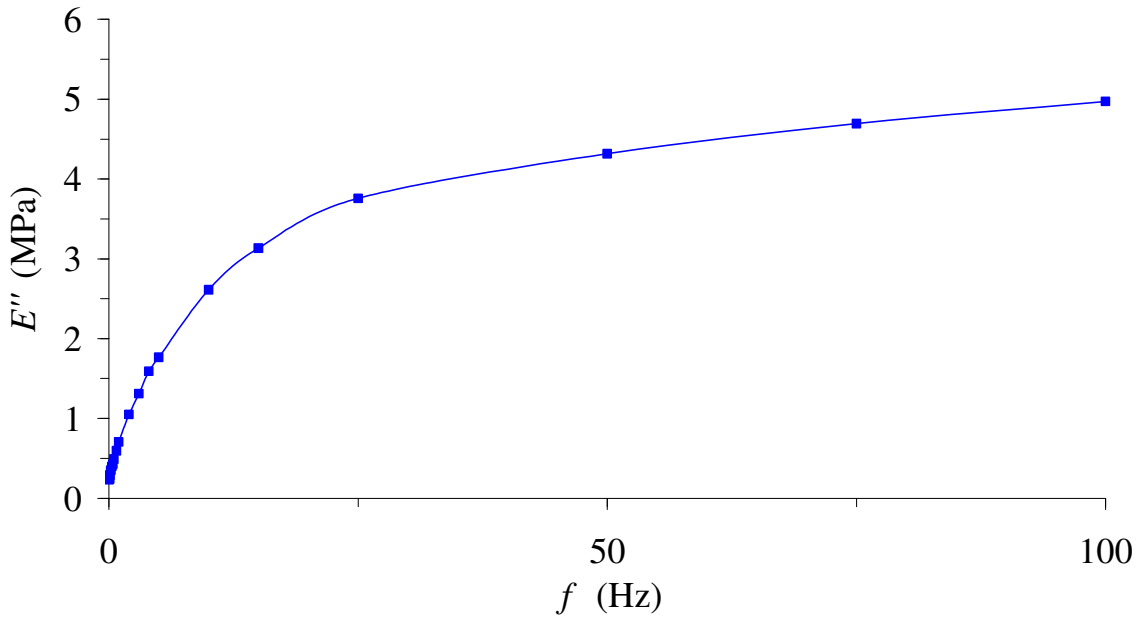

Figure F. 5: Slightly overdamped system (MED-4080, sample 5, damping of 95 Ns/mm, 18/04/07)

F.2 Damping in the tension tests of the medical grade silicones

A typical graph of *E''* against *f* for a silicone dumb-bell in tension, used to determine the type of damping system, is shown in Figure F. 6. It mainly has the characteristic of an overdamped system, although there is an initial instability of the data points at the lower frequencies (0.02 to 0.1 Hz, highlighted by the red circle in Figure F. 6). The damping value obtained in each test, varied with the grade. Typical initial damping values at 0.02 Hz are shown in Table F. 1.

Table F. 1: Damping values for the tension tests at 0.02 Hz.

	Damping value (Ns/mm)	
Grade	**Cured**	**Cured with conditioning**
C6-165	0.6	0.8
C6-180	1.1	1.3
MED-4080	1.3	1.6
MED-82-5080-10	0.35	0.35

It is important to note that none of the damping systems throughout the tension tests could be classified as critically damped systems (the ideal requirements for a system as described in §F.1). This therefore does make the analysis of the results more difficult as ideally one would like to achieve a critically damped system. However, when the results from Chapter 4 of overdamped systems were compared with critically damped systems, it was concluded that the moduli were not greatly affected by overdamping. The results from Chapter 4 showed that, underdamping had a greater effect on the moduli; the moduli (particularly *E'*) increased because of underdamping.

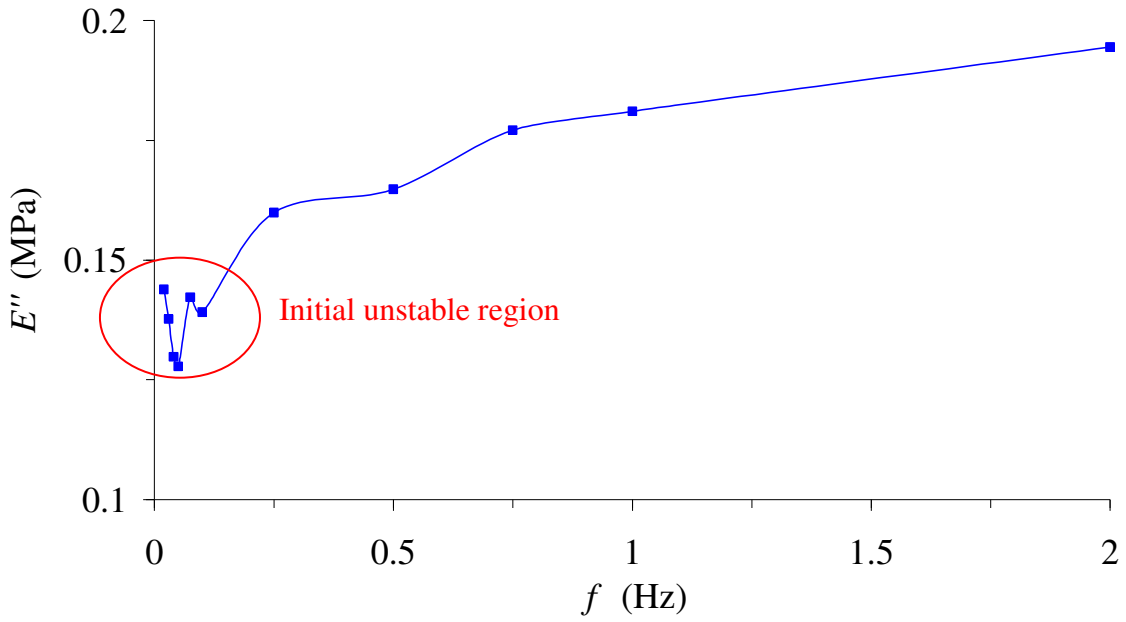

Figure F. 6: Typical damping system for grade MED-82-5080-10 in tension (cured, dumb-bell mean)

F.3 Damping in the compression tests for Elast-Eon™ 3

A typical graph of *E''* against *f* for an Elast-Eon™ 3 is shown in Figure F. 7. This plot shows that at best, this system has characteristics of being overdamped. During the preliminary testing phase, none of the plots obtained showed characteristics of a critically damped system. Typical values of damping for these specimens (before accelerated aging) at 0.02 Hz, were in the range of 200-300 Ns/mm. The values increased after accelerated aging and it was more difficult to control.

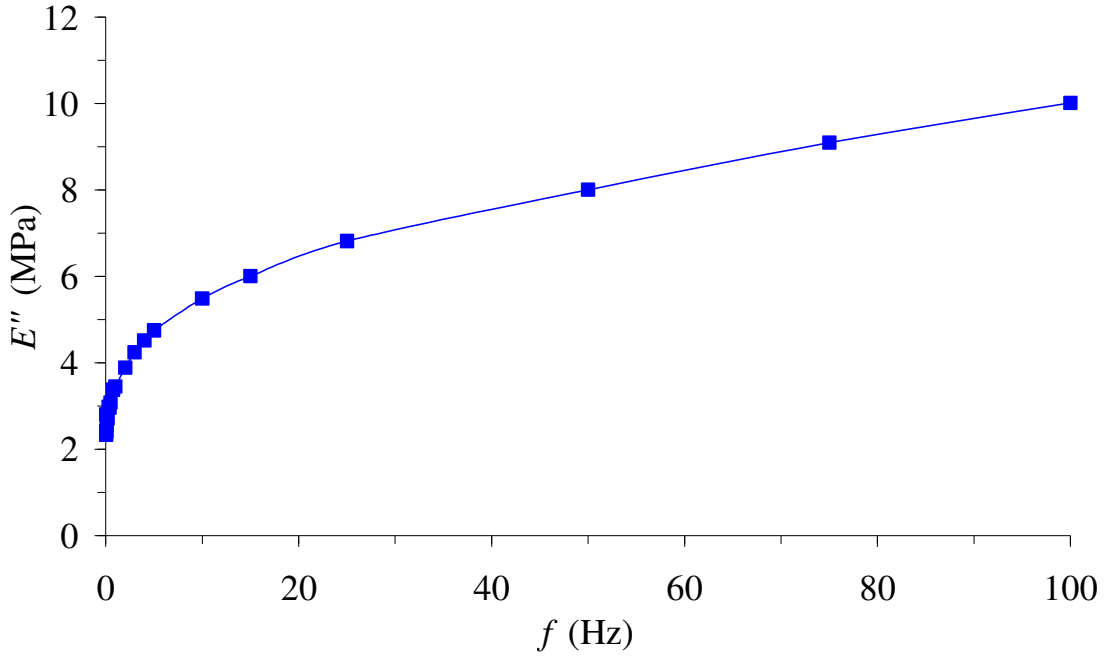

Figure F. 7: Typical damping system for Elast-Eon^{TM}3 (sample 2b, damping of 218 Ns/mm, 26/07/07)

APPENDIX G: ADDITIONAL RESULTS FOR DYNAMIC MECHANICAL ANALYSIS OF MEDICAL GRADE SILICONES AND ELAST-EON™3 IN COMPRESSION

G.1 Are the viscoelastic properties of Silastic® Q7-4780 (medium - term silicone) frequency-dependent?

As discussed in §4.4, the frequency–dependent viscoelastic properties for Silastic® Q7-4780 were plotted and are shown in Figure G. 1, Figure G. 2, Figure G. 3 and Figure G. 4.

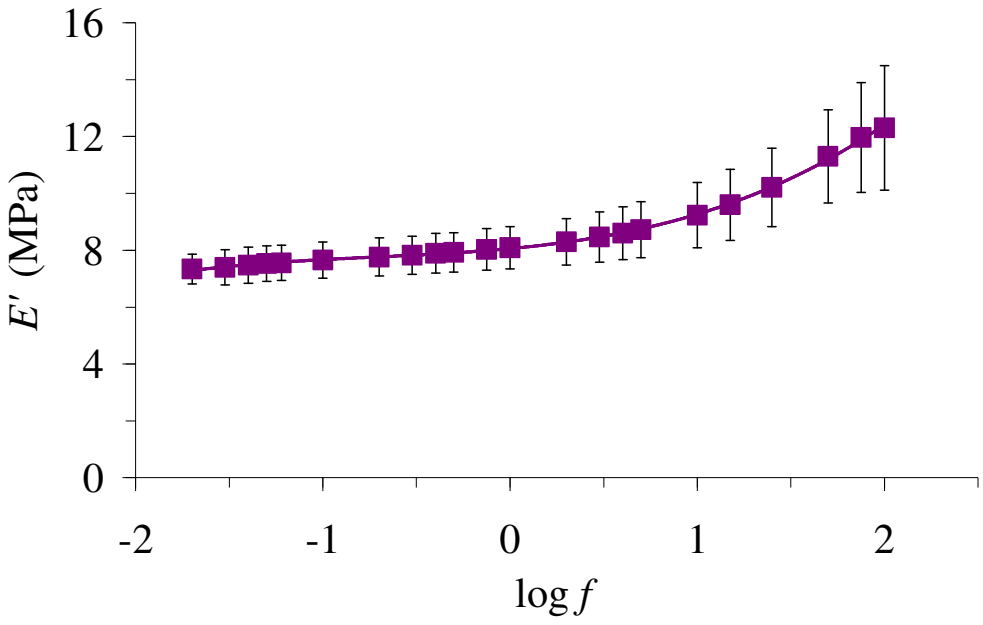

Figure G. 1 Mean values of E' plotted against the $\log_{10}f$ for Silastic® Q7-4780. Error bars represent the standard deviations. The line shown is the third-order polynomial that gave the best fit to the data. (The equation of the line is $y = 0.1868x^3 + 0.4094x^2 + 0.6116x + 8.0591$ and $R^2 = 0.999$).

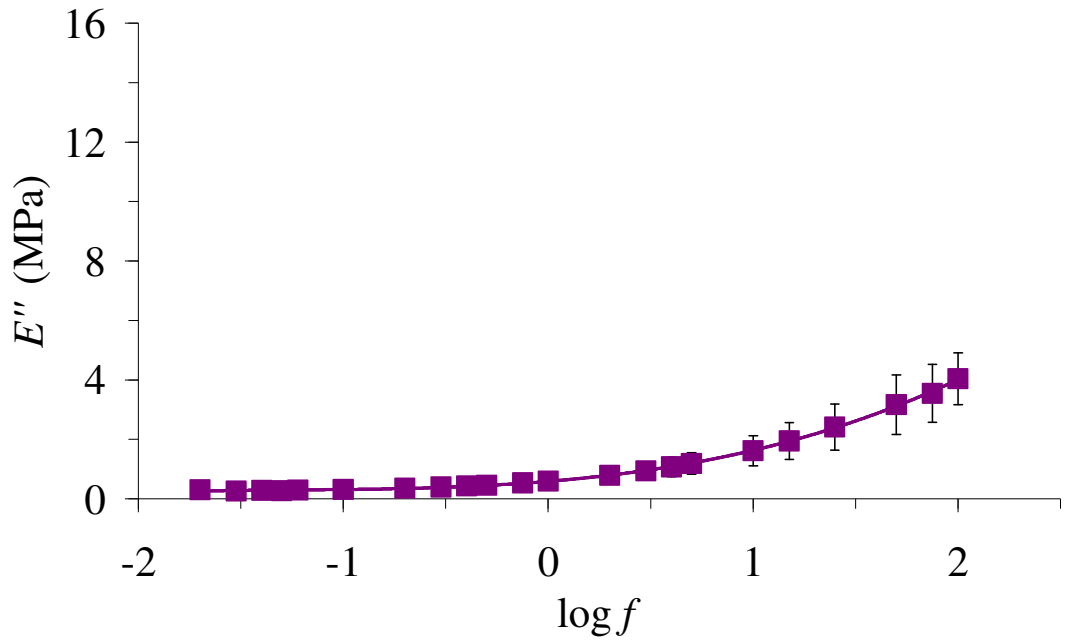

Figure G. 2: Mean values of E'' plotted against the $\log_{10}f$ for Silastic® Q7-4780. Error bars represent the standard deviations. The line shown is the third-order polynomial that gave the best fit to the data. (The equation of the line is $y = 0.0948x^3 + 0.3834x^2 + 0.5652x + 0.5866$ and $R^2 = 0.9996$).

The coefficients of the polynomials in Figure G. 1 and Figure G. 2 are given in Table G. 1 and Table G. 2. The coefficients given here enable the *E'* and *E''* at a given frequency to be determined, as discussed in §3.8.

Table G. 1: Coefficients of the polynomials fitted to E' plotted against logf for Silastic® Q7-4780. R^2 is the square of the correlation coefficient and shows how well the polynomial curve fits the data. When $R^2 = 1$, there is a perfect correlation.

Grade	a'_0	a'_1	a'_2	a'_3	R^2
Q7-4780 *E'*	8.0593	0.6093	0.4111	0.1866	0.9991

Table G. 2: Coefficients of the polynomials fitted to E'' plotted against logf for Silastic® Q7-4780. R^2 is the square of the correlation coefficient and shows how well the polynomial curve fits the data. When R^2 = 1, there is a perfect correlation.

Grade	a_0''	a_1''	a_2''	a_3''	R^2
Q7-4780 *E''*	0.5866	0.565	0.3836	0.0948	0.9996

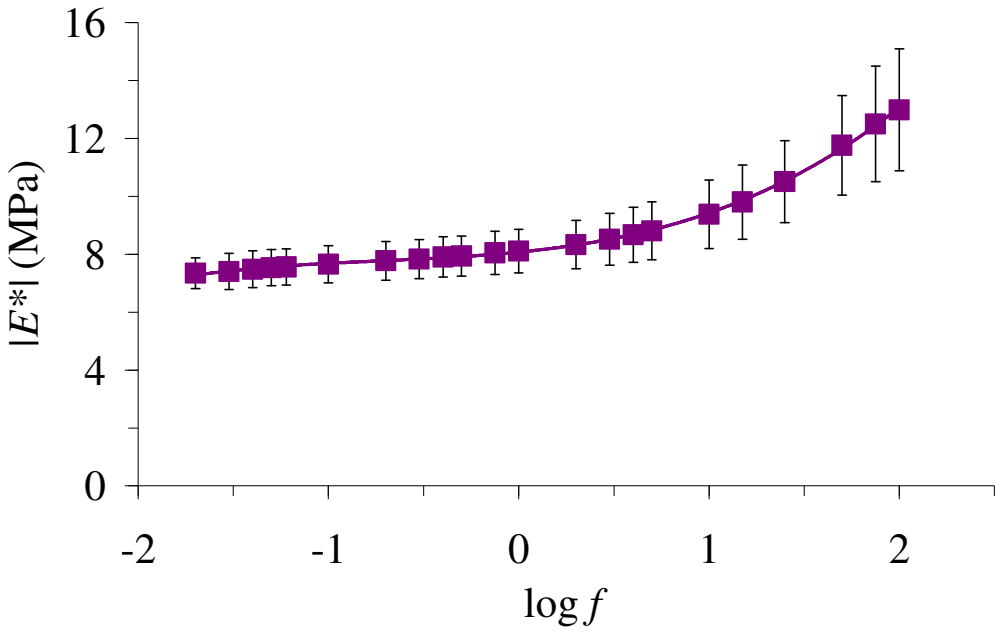

Figure G. 3: Mean values of ¦E*¦ plotted against the $log_{10}f$ for Silastic® Q7-4780. Error bars represent the standard deviations. The line shown is the third-order polynomial that gave the best fit to the data. (The equation of the line is $y = 0.2217x^3 + 0.4819x^2 + 0.6475x + 8.0729$ and $R^2 = 0.9993$).

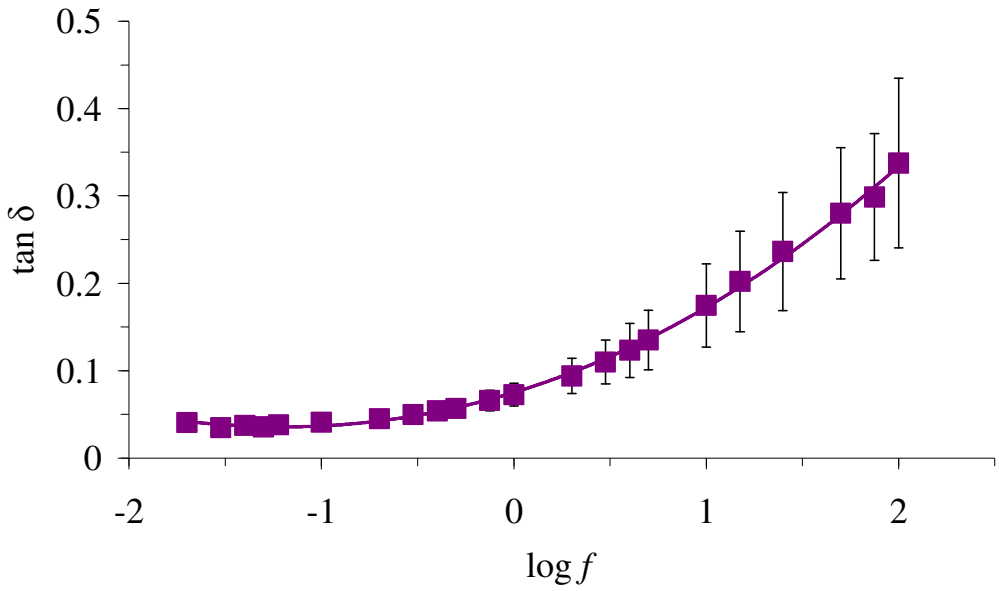

Figure G. 4: Mean values of tanδ plotted against the $log_{10}f$ for Silastic® Q7-4780. Error bars represent the standard deviations. The line shown is the third-order polynomial that gave the best fit to the data. (The equation of the line is $y = 0.0009x^3 + 0.0295x^2 + 0.0669x + 0.0751$ and $R^2 = 0.9982$).

G.2 Does pre-treating the short-term silicones affect the viscoelastic properties?

As discussed in §4.5, pre-treating the silicones had no significant effect on the moduli values of grades C6-165 and C6-180 and the results have been included here.

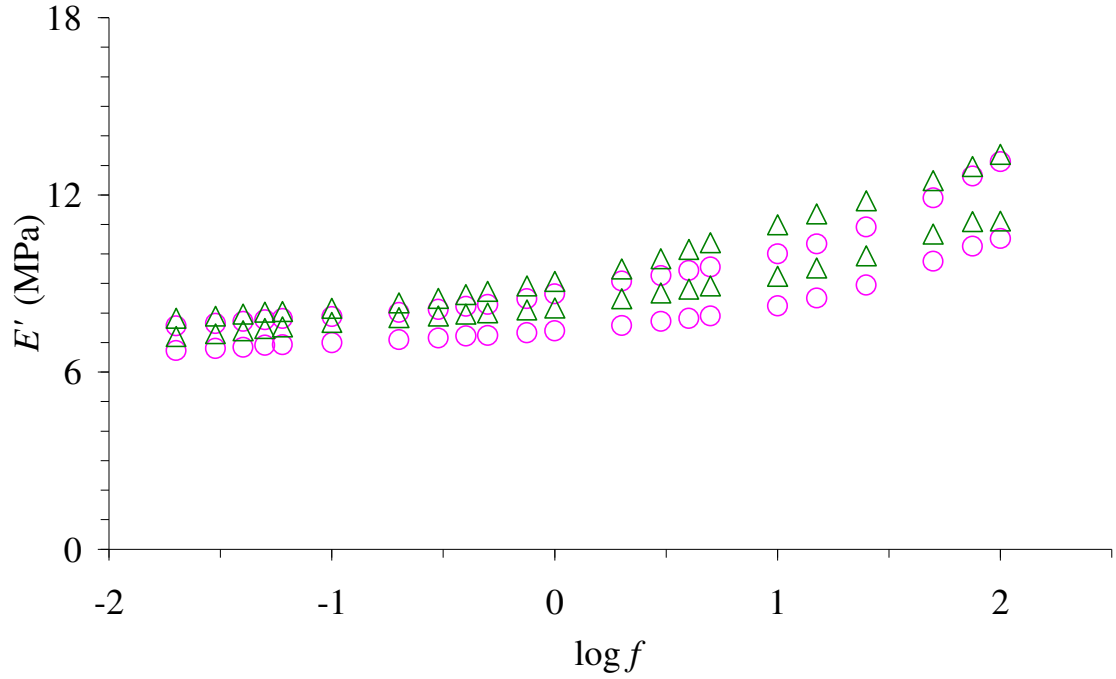

Figure G. 5: Upper and lower 95% confidence intervals of E', for cured (○) and pre-treated (△) C6-180.

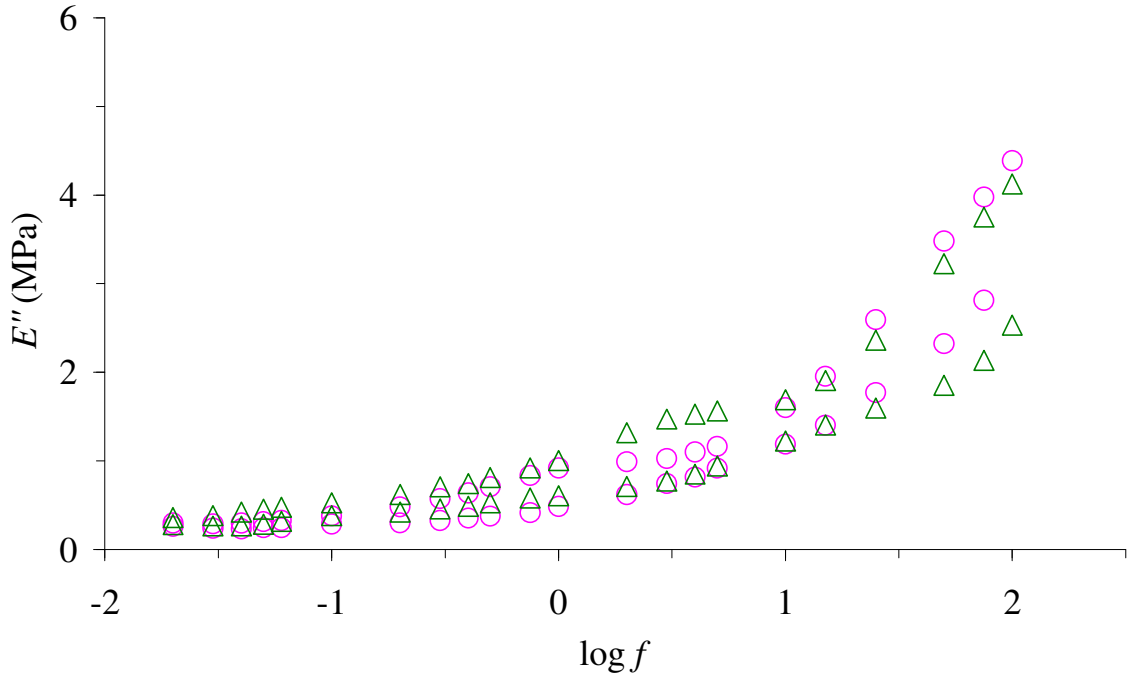

Figure G. 6: Upper and lower 95% confidence intervals of E'', for cured (○) and pre-treated (△) C6-180.

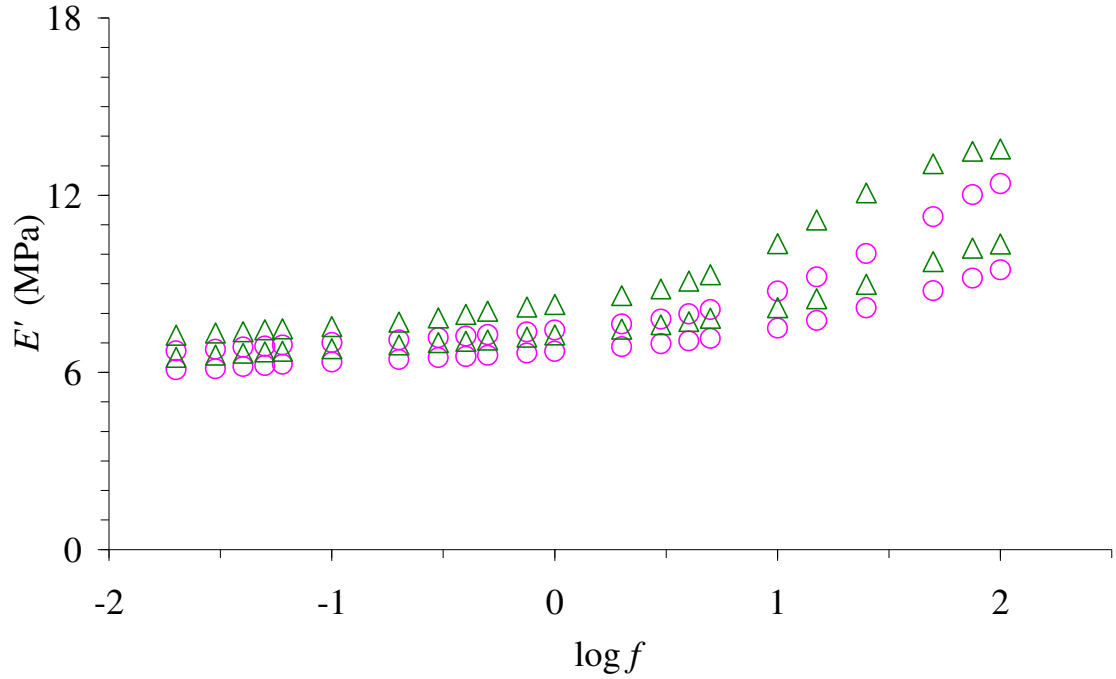

Figure G. 7: Upper and lower 95% confidence intervals of E', for cured (○) and pre-treated (△) C6-165.

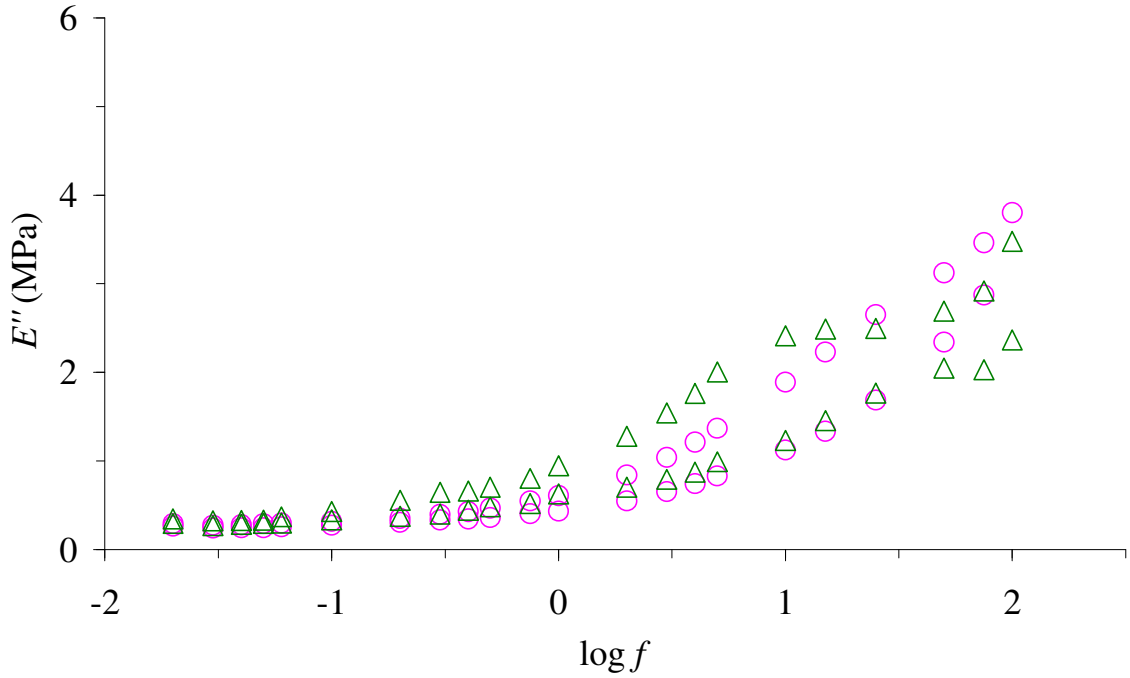

Figure G. 8: Upper and lower 95% confidence intervals of E'', for cured (○) and pre-treated (△) C6-165.

G.3 Does pre-treating the medium-term silicones affect the viscoelastic properties?

As discussed in §4.6 pre-treating the silicones can significantly affect the viscoelastic properties of the softer medium-term silicones, such as for Silastic® Q7-4735, as shown in Figure G. 9 and Figure G. 10. In general, for *E'* and *E''* (at most frequencies) the figures show that the confidence intervals did not overlap, i.e. the pre-treatment had a significant effect on the moduli values.

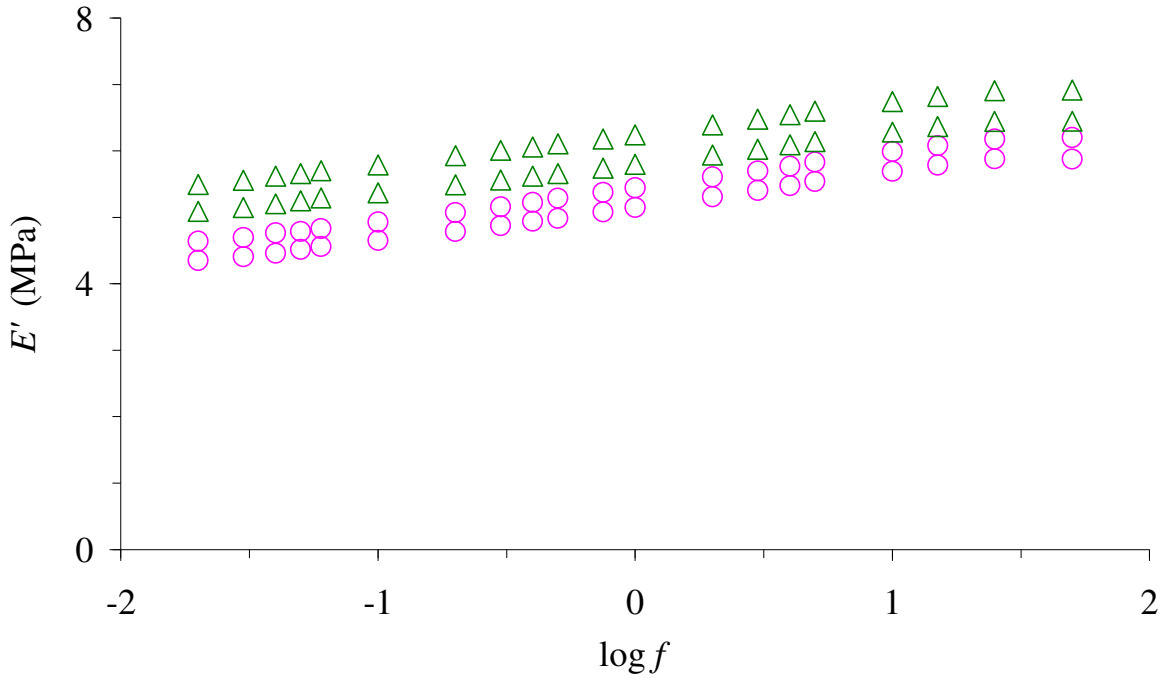

Figure G. 9: Upper and lower 95% confidence intervals of E', for cured (○) and pre-treated (△) Silastic® Q7-4735.

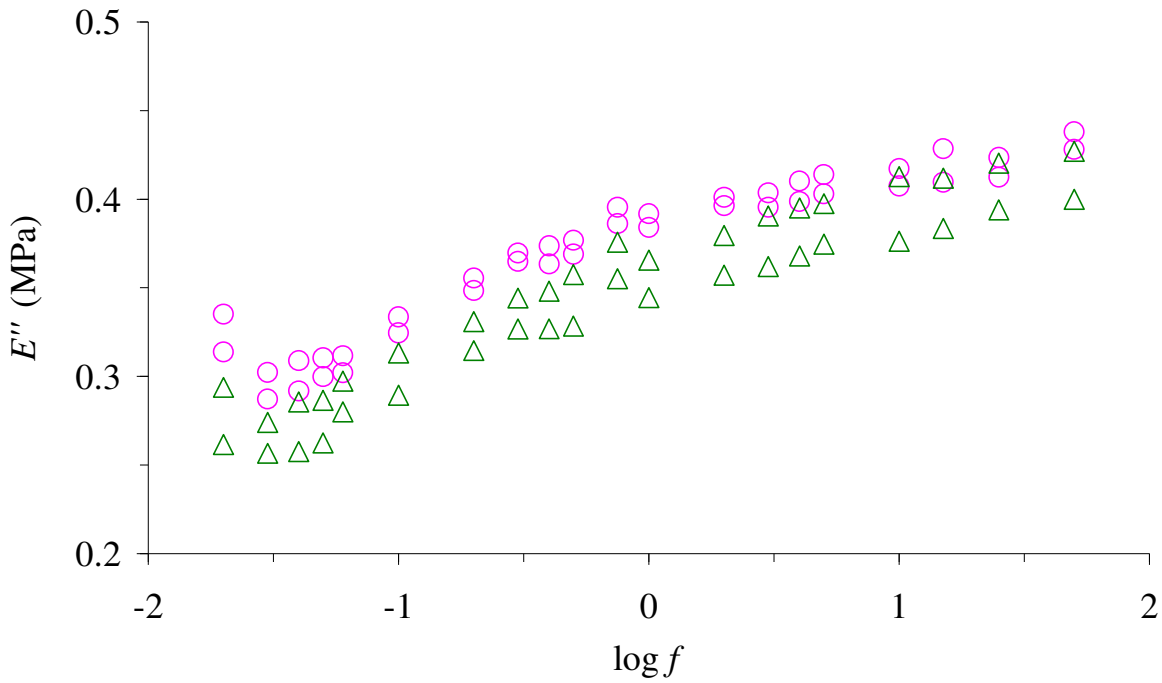

Figure G. 10: Upper and lower 95% confidence intervals of E'', for cured (○) and pre-treated (△) Silastic® Q7-4735.

As discussed in §4.6, the 95% confidence intervals for *E'* and *E''* for cured and for pre-treated (for 90 days or 180 days in physiological solution at 37 °C) Silastic® Q7-4780, were not significantly different at 5 % level and are shown in Figure G. 11, Figure G. 12 Figure G. 13 and Figure G. 14.

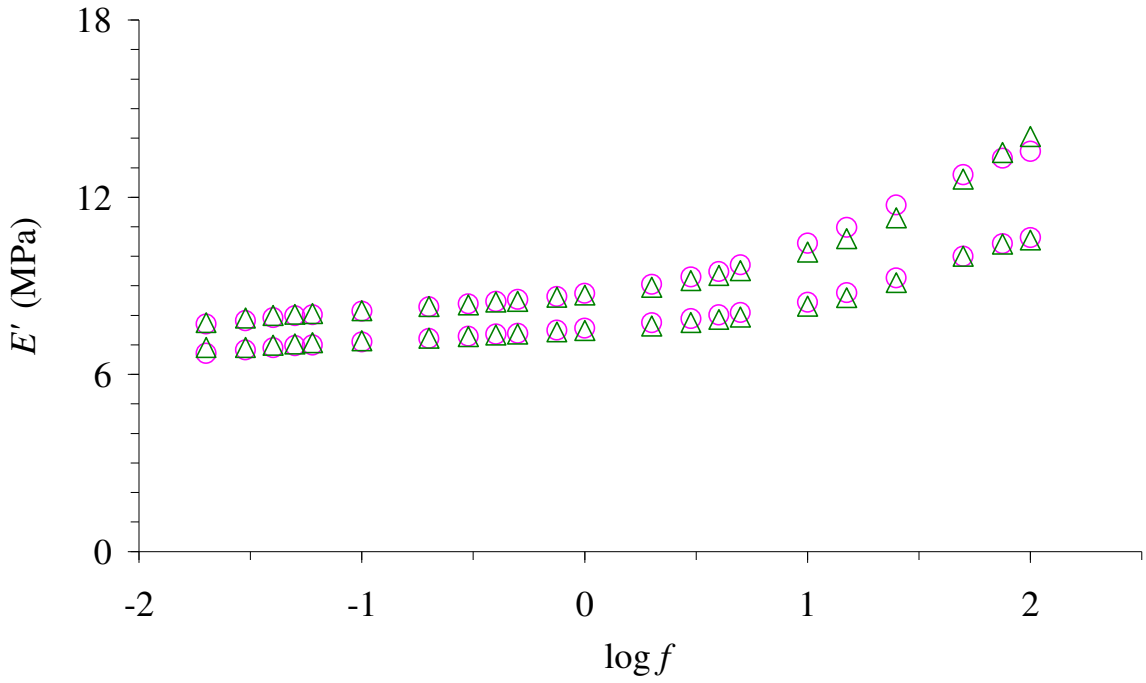

Figure G. 11: Upper and lower 95% confidence intervals of E', for cured (○) and pre-treated (90 days) (△) Silastic® Q7-4780.

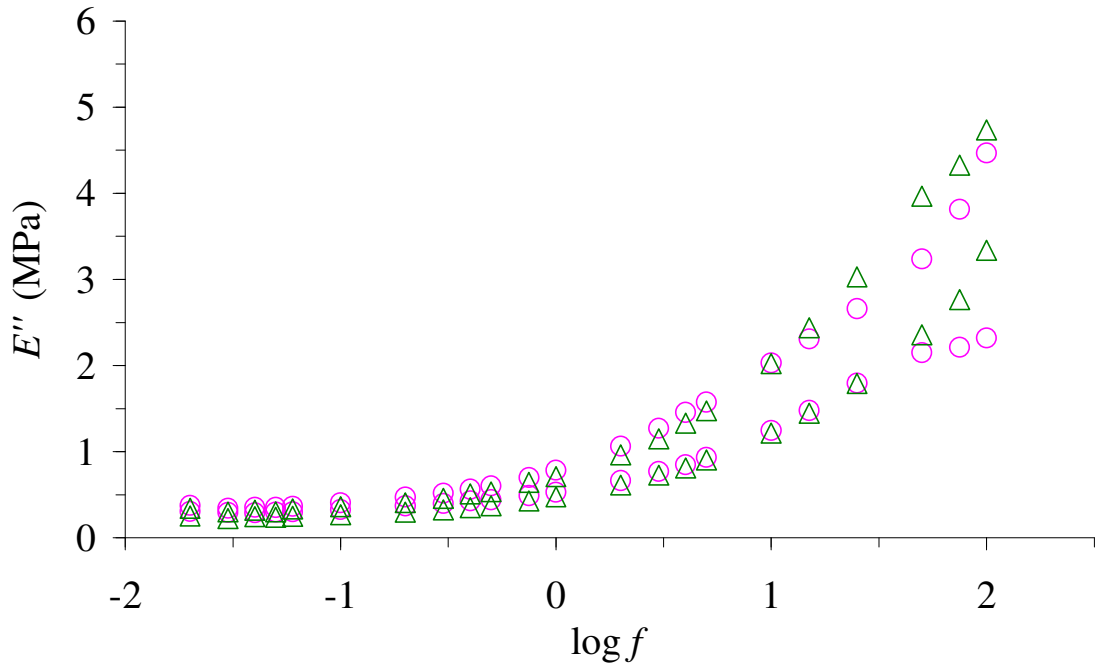

Figure G. 12: Upper and lower 95% confidence intervals of E'', for cured (○) and pre-treated (90 days) (△) Silastic® Q7-4780.

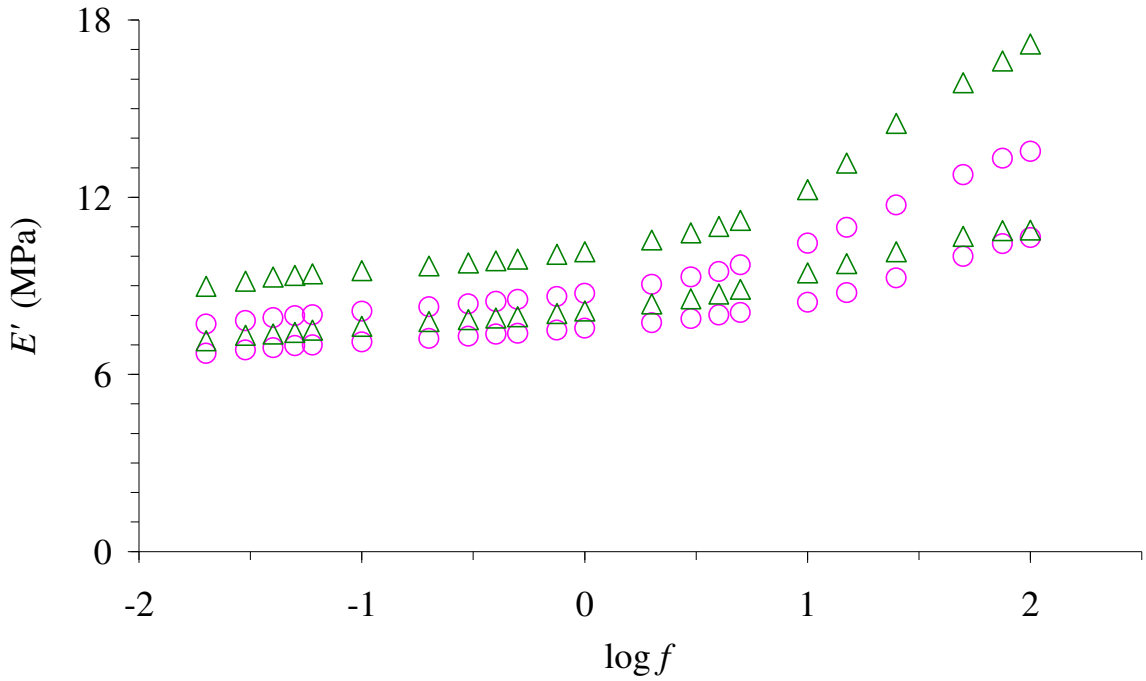

Figure G. 13: Upper and lower 95% confidence intervals of E', for (○) cured and (△) pre-treated (180 days) Silastic® Q7-4780.

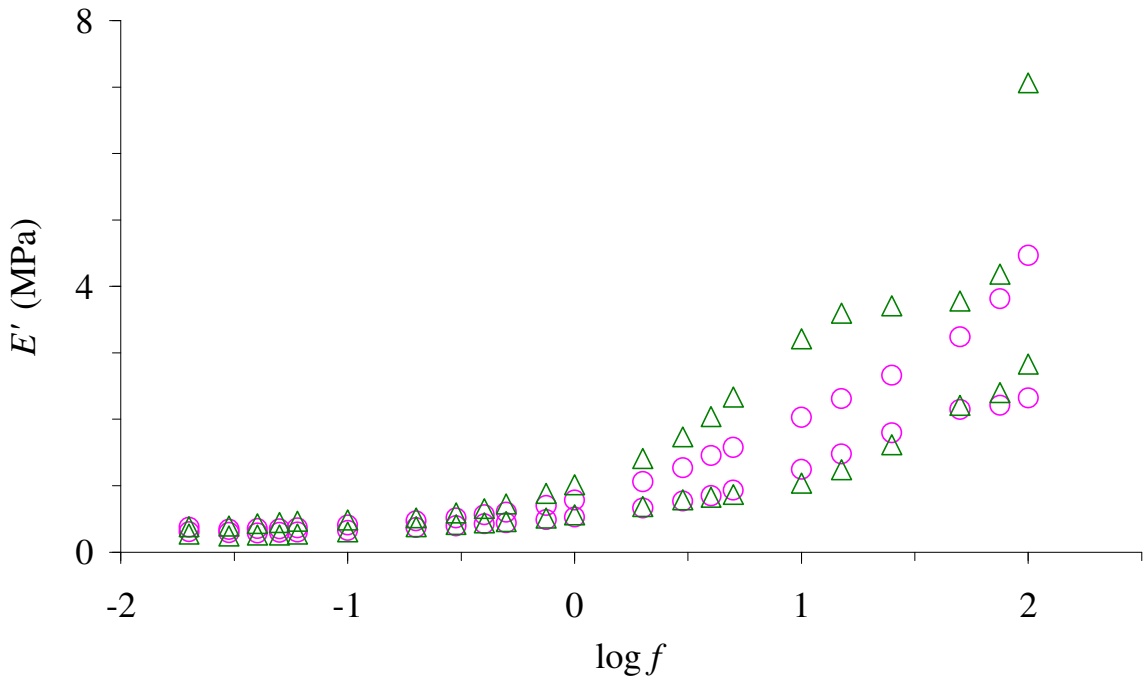

Figure G. 14: Upper and lower 95% confidence intervals of E'', for (○) cured and (△) pre-treated (180 days) Silastic® Q7-4780.

G.4 Are the viscoelastic properties of silicones with different implantation times different?

As discussed in §4.7, the viscoelastic properties of silicones with different implantation times were not significantly different and the graphs obtained when C6-180 and Silastic® Q7-4780 were compared, are shown in Figure G. 15 and Figure G. 16.

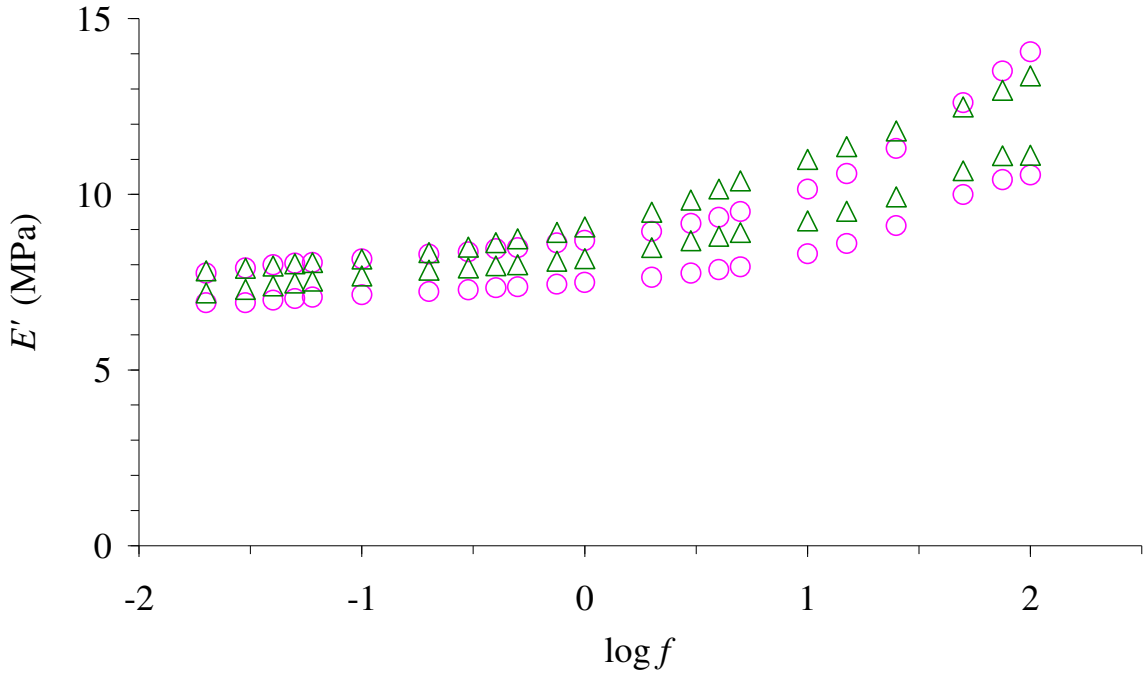

Figure G. 15: Upper and lower 95% confidence intervals of E', for pre-treated C6-180 (△) and Silastic® Q7-4780 (○).

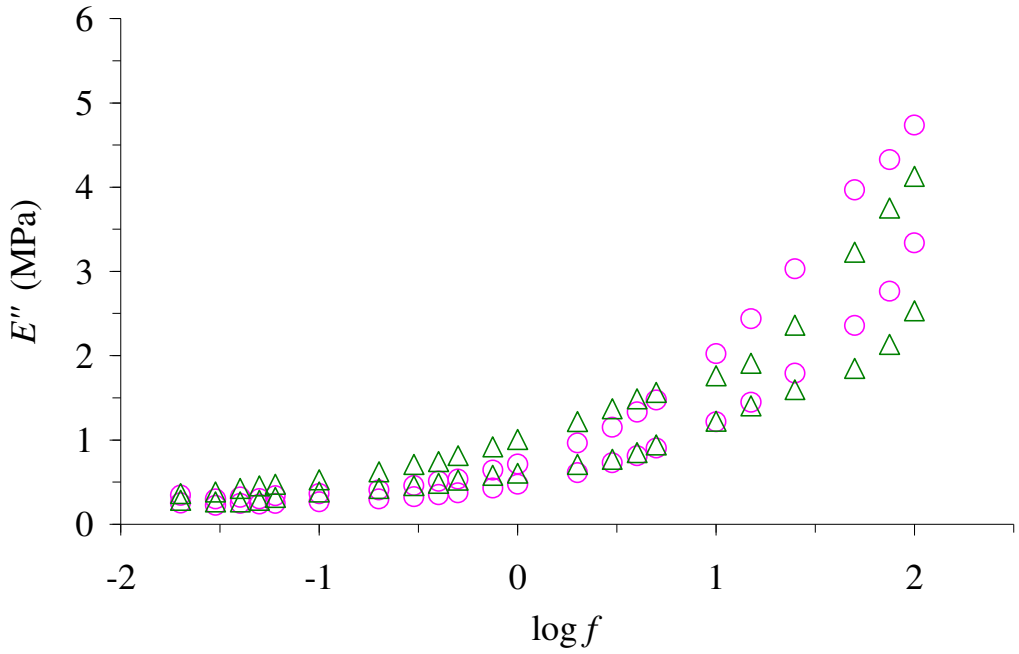

Figure G. 16: Upper and lower 95% confidence intervals of E'', for pre-treated C6-180 (△) and Silastic® Q7-4780 (○).

G.5 Does pre-soaking the specimen for 24 hours in physiological saline affect the viscoelastic properties?

As discussed in §4.8, pre-soaking the grade MED-4080 specimens for 24 hours before testing, in physiological saline may slightly but significantly affect the *E'*. The graphs obtained when the viscoelastic properties of unsoaked and pre-soaked C6-165 specimens were compared, are shown here in Figure G. 17 and Figure G. 18. Figure G. 17 shows that for *E'* the 95% confidence intervals overlapped throughout the frequency range, i.e. the pre-treatment had no significant effect on *E'* values.

For *E''*, Figure G. 18 shows that the confidence intervals did not overlap below log*f* = 0 (i.e *f* = 1 Hz) or above log*f* = 1.5 (i.e. *f* = 30 Hz). Therefore, physiological saline appears to have a small but significant effect on *E''* values below *f* = 1 Hz and above *f* = 30 Hz.

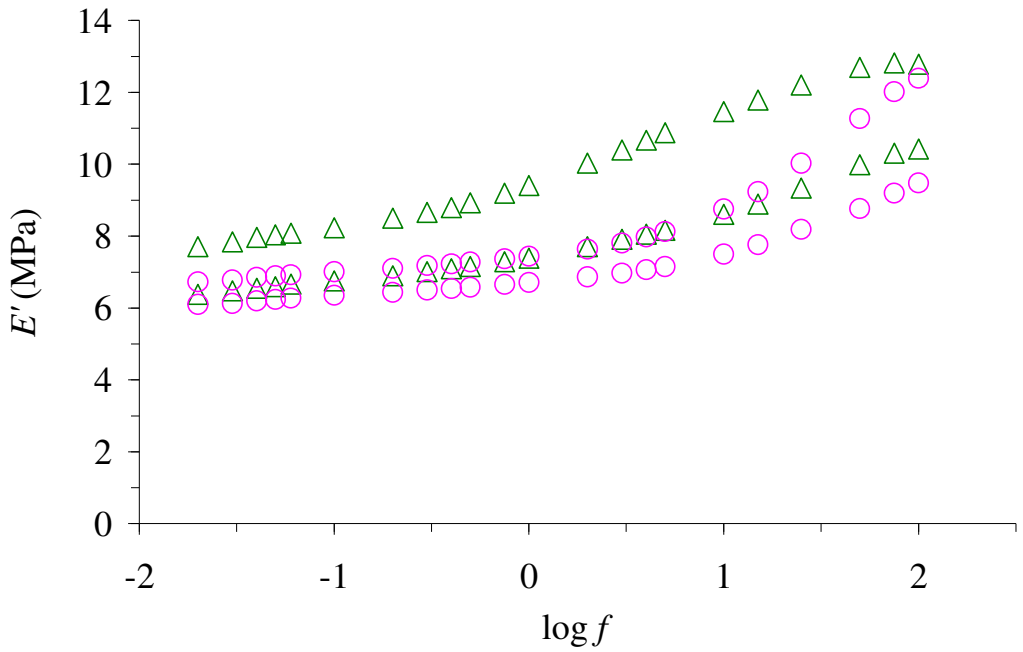

Figure G. 17: Upper and lower 95% confidence intervals of E', for unsoaked (△) and pre-soaked (○) C6-165 specimens.

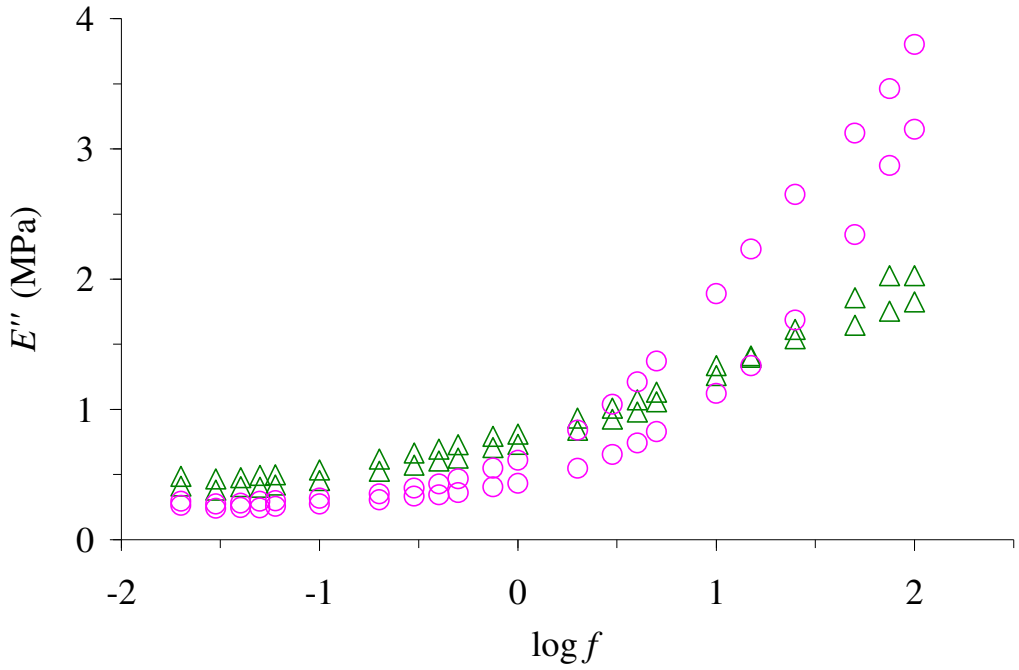

Figure G. 18: Upper and lower 95% confidence intervals of E'', for unsoaked (△) ***and pre-soaked*** (○) ***C6-165 specimens.***

G.6 What effect does accelerated aging have on the properties of Elast-Eon™ 3?

As mentioned in §6.4, further results on the accelerated aging of Elast-Eon™ 3 are included here. The results shown here are for samples that have undergone accelerated aging for 76 days or 114 days (in physiological solution at 70°C). The results demonstrated that the properties were affected by accelerated aging.

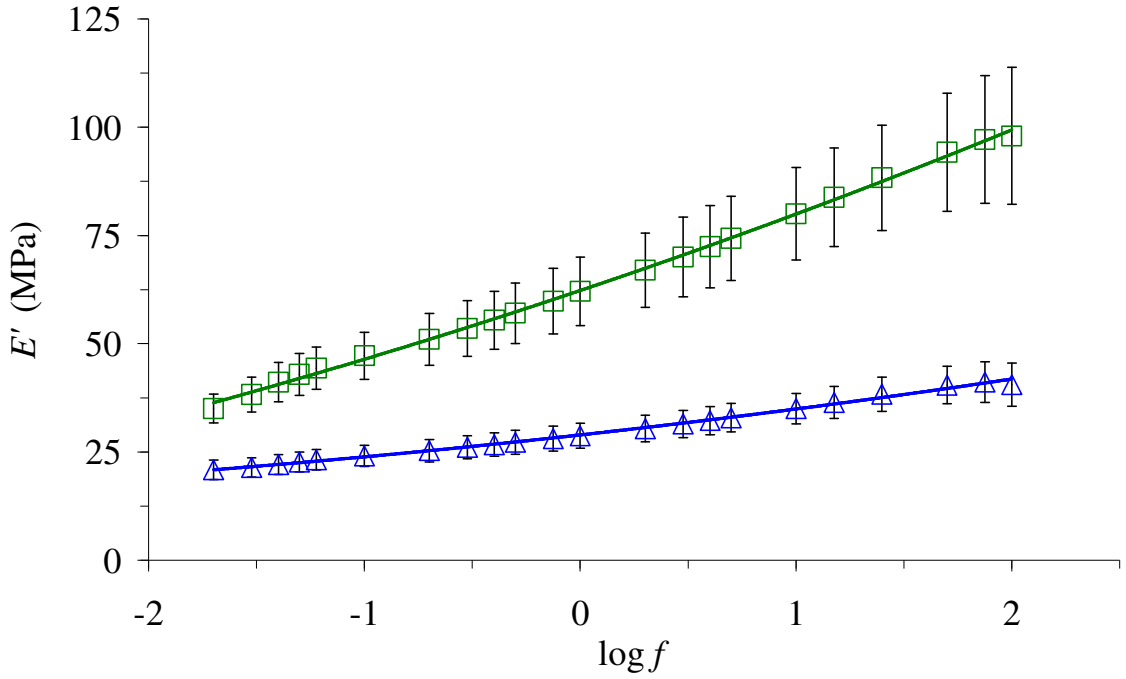

Figure G. 19: Mean values of E' plotted against the $log_{10}f$, for Elast-Eon™ 3 specimens before (△) and after (□) accelerated aging (in physiological solution at 70°C for 76 days). The error bars represent the 95% confidence intervals. The lines shown are second-order polynomials.

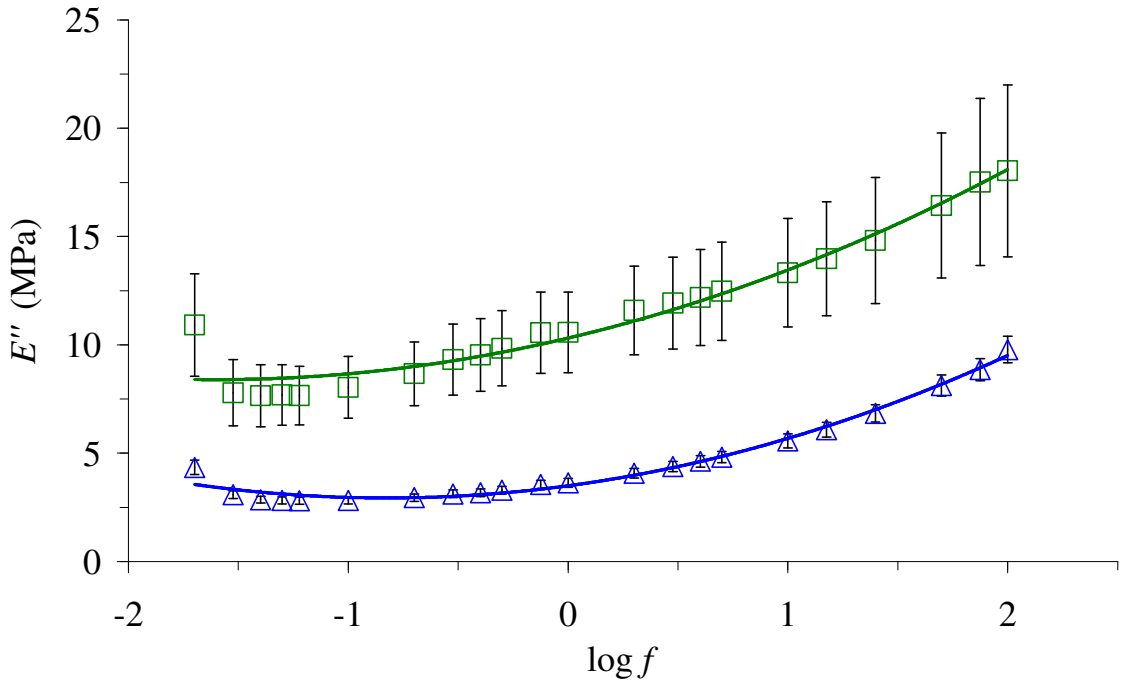

Figure G. 20: Mean values of E'' plotted against the $log_{10}f$, for Elast-Eon™ 3 specimens before (△) and after (□) accelerated aging (in physiological solution at 70°C for 76 days). The error bars represent the 95% confidence intervals. The lines shown are second-order polynomials.

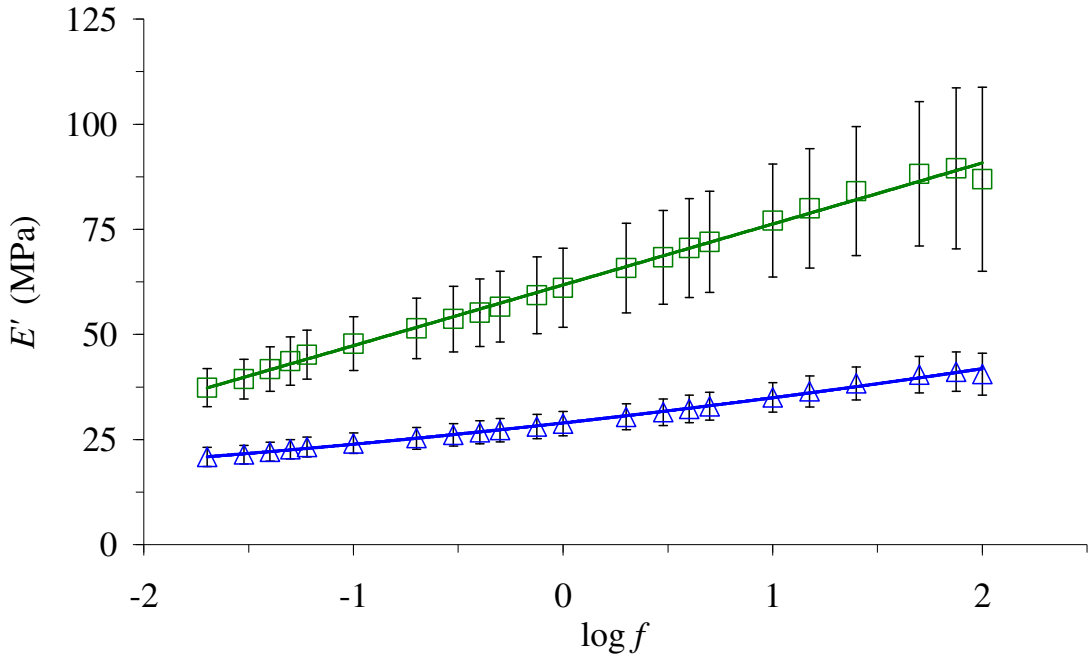

Figure G. 21: Mean values of E' plotted against the $log_{10}f$, for Elast-Eon™ 3 specimens before (△) and after (□) accelerated aging (in physiological solution at 70°C for 114 days). The error bars represent the 95% confidence intervals. The lines shown are second-order polynomials.

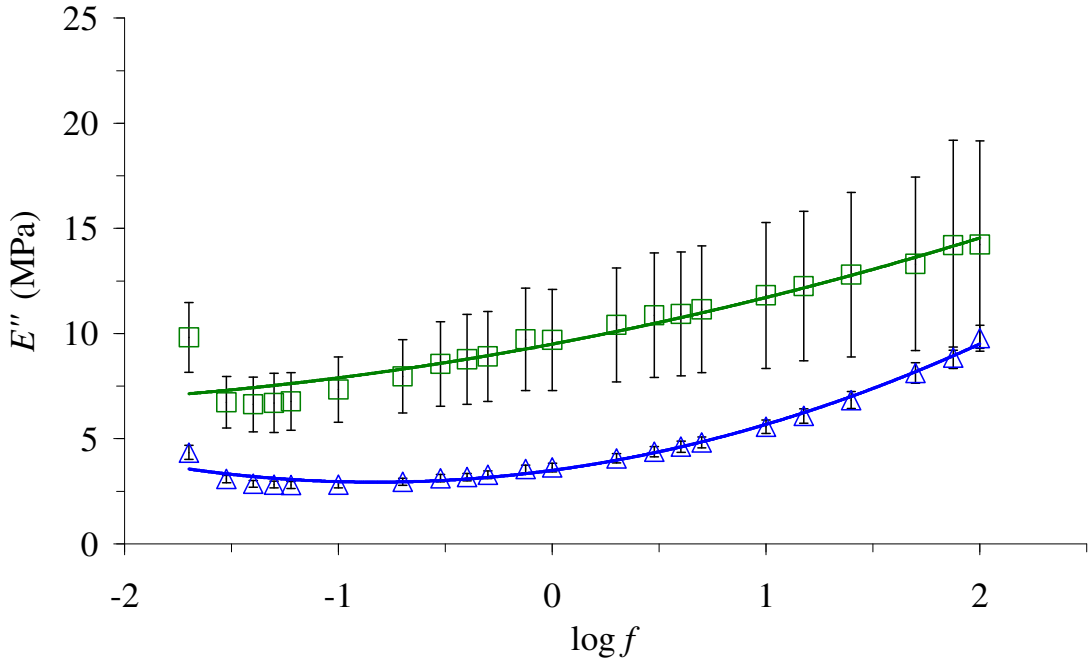

Figure G. 22: Mean values of E'' plotted against the $log_{10}f$, for Elast-Eon™ 3 specimens before (△) and after (□) accelerated aging (in physiological solution at 70°C for 114 days). The error bars represent the 95% confidence intervals. The lines shown are second-order polynomials.

The coefficients of the polynomials in Figure G. 19 and Figure G. 21 are given in Table G. 3. The coefficients given here enable the *E'* at a given frequency to be determined, as discussed in §3.8.

Table G. 3: Coefficients of the polynomials fitted to the E' for Elast-Eon™ 3. R^2 is the square of the correlation coefficient and shows how well the polynomial curve fits the data. When R^2 = 1, there is a perfect correlation.

	a_0'	a_1'	a_2'	R^2
After aging *E'* (78 days)	62.297	16.762	0.8916	0.9988
After aging *E'* (114 days)	61.785	14.467	0.0192	0.995

The coefficients of the polynomials in Figure G. 20 and Figure G. 22 and are given in Table G. 4. The coefficients given here enable the *E''* at a given frequency to be determined, as discussed in §3.8.

Table G. 4: Coefficients of the polynomials fitted to the E'' for Elast-Eon™ 3. R^2 is the square of the correlation coefficient and shows how well the polynomial curve fits the data. When R^2 = 1, there is a perfect correlation.

	a_0''	a_1''	a_2''	R^2
After aging *E''* (76 days)	10.311	2.3962	0.7481	0.9536
After aging *E''* (114 days)	9.4975	1.9104	0.307	0.9143

G.7 What effect does accelerated aging have on the properties of Nagor® silicone?

As mentioned in §6.5, further results on the accelerated aging of Nagor® silicone are included here. The results shown here are for samples that have undergone accelerated aging for 76 days or 114 days (in physiological solution at 70°C). The results demonstrated that the properties were not significantly affected by accelerated aging (in physiological solution at 70°C for 76 days or 114 days).

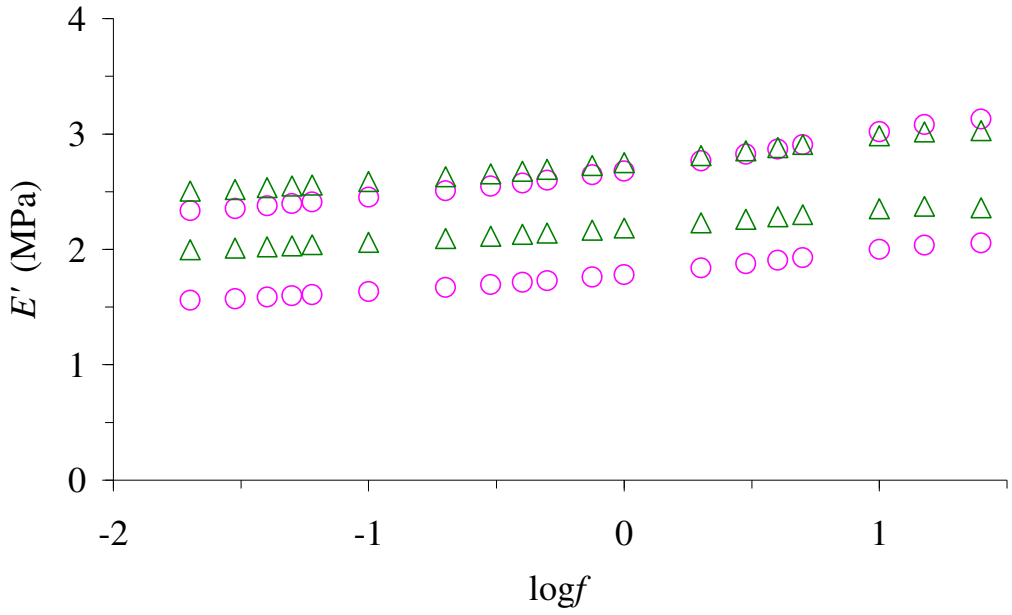

Figure G. 23: Upper and lower 95% confidence intervals of E' before (○) and after (△) accelerated aging (in physiological solution at 70°C for 76 days) of Nagor® silicone cylinders.

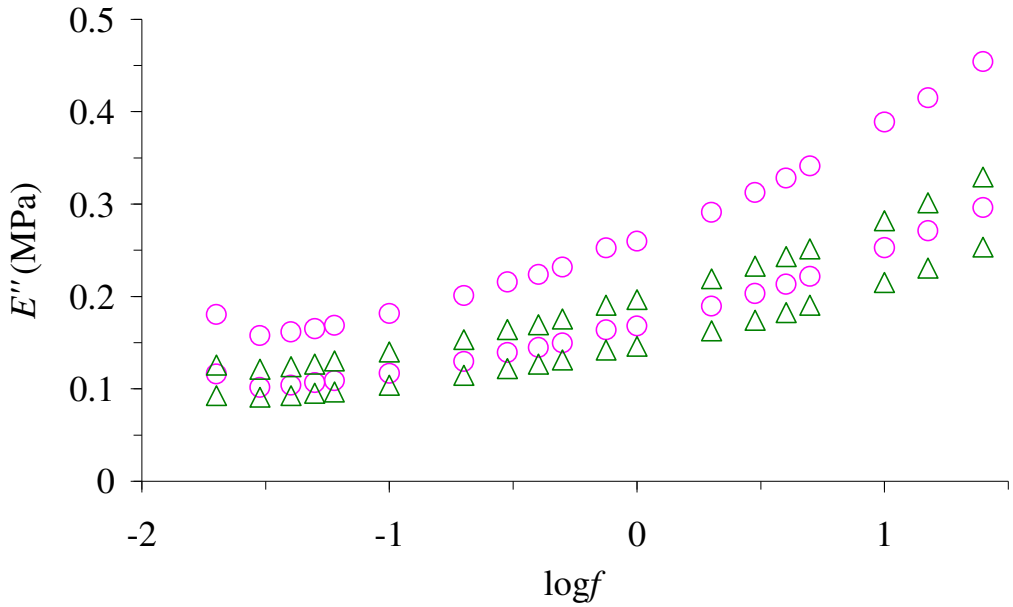

Figure G. 24: Upper and lower 95% confidence intervals of E'' before (○) and after (△) accelerated aging (in physiological solution at 70°C for 76 days) of Nagor® silicone cylinders.

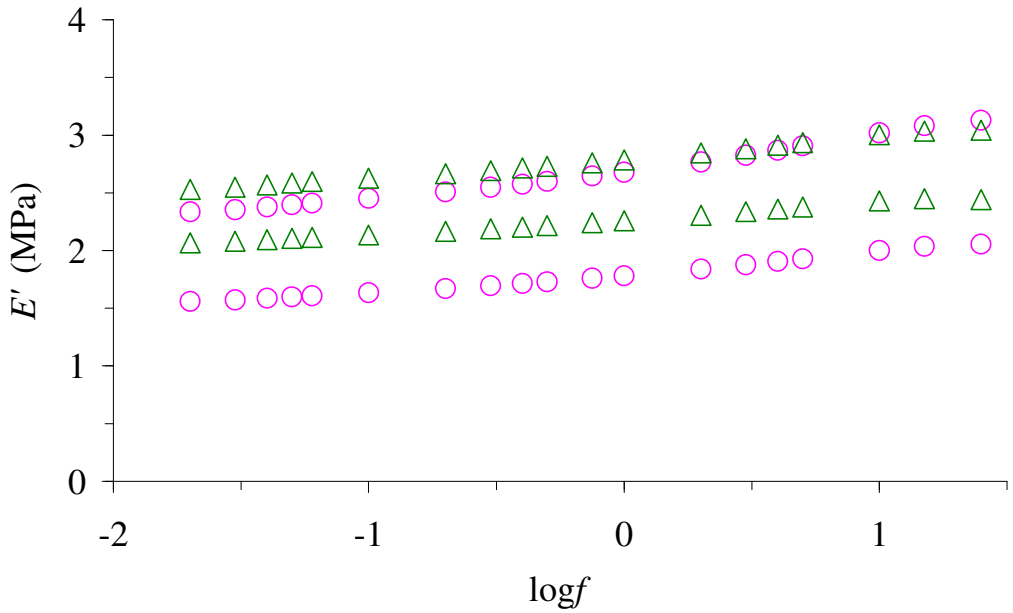

Figure G. 25: Upper and lower 95% confidence intervals of E' before (○) and after (△) accelerated aging (in physiological solution at 70°C for 114 days) of Nagor® silicone cylinders.

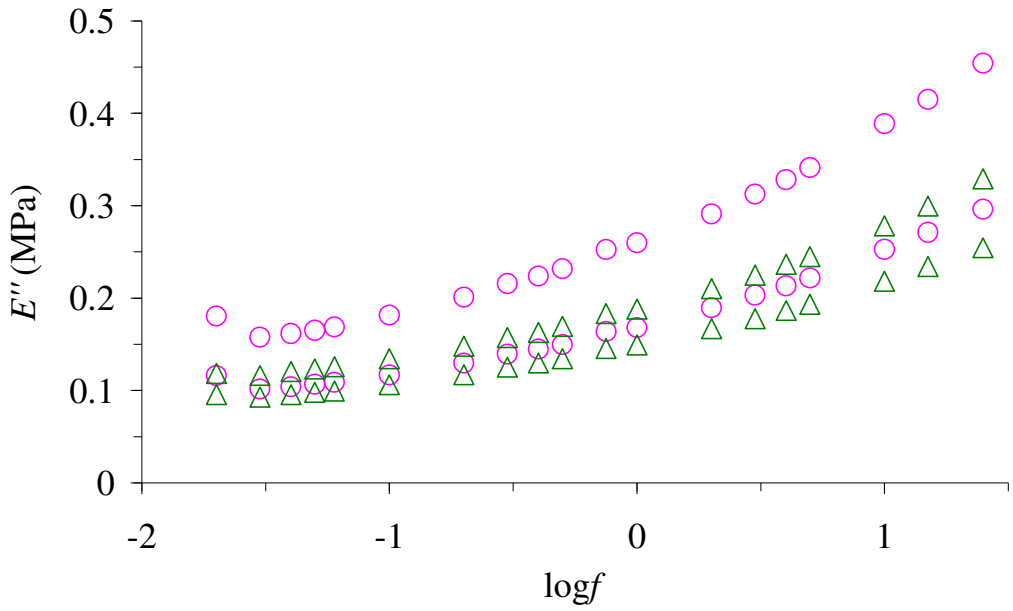

Figure G. 26: Upper and lower 95% confidence intervals of E'' before (○) and after (△) accelerated aging (in physiological solution at 70°C for 114 days) of Nagor® silicone cylinders.

APPENDIX H: ADDITIONAL RESULTS FOR DYNAMIC MECHANICAL ANALYSIS OF MEDICAL GRADE SILICONES IN TENSION

H.1 Are the viscoelastic properties of the silicones affected by loading frequency and pre-treatment?

As mentioned in §5.3, the properties are slightly frequency-dependent and can be affected by pre-treating the silicones for 29 days (in physiological solution at 37 °C). In Figure H. 1 and Figure H. 3, the *E'* increased slowly with frequency. The confidence intervals overlapped, throughout the frequency range for MED-4080 but not for C6-180, i.e. the pre-treatment had a significant effect on the *E'* values of C6-180.

In Figure H. 2, for the cured data points (△), below a log*f* value of -1 (equivalent to $f = 0.1$) *E''* is fairly constant, with a value of approximately 0.39 MPa. Above this, *E''* increases slowly with frequency and eventually attains a value of 0.53 MPa at a log*f* value of 0.3, which is equivalent to a frequency of 2 Hz. For the pre-treated data points (○), graphs of *E''* against $\log_{10} f$ are shallow curves that pass through a minimum when $\log_{10} f$ has a value in the range;-0.65 to -0.85, corresponding to a frequency range of 0.14 to 0.22 Hz. The confidence intervals do not overlap at frequencies of 0.02 and 2 Hz, i.e. the pre-treatment can have an effect.

Figure H. 4 shows that for the cured data points (△), graphs of *E''* against $\log_{10}f$ are shallow curves that pass through a minimum when $\log_{10}f$ has a value in the range;-0.65 to -0.9, corresponding to a frequency range of 0.12 to 0.22 Hz. For the pre-treated data points (○), graphs of *E''* against $\log_{10}f$ are shallow curves that pass through a minimum when $\log_{10}f$ has a value in the range;-0.5 to -0.75, corresponding to a frequency range of 0.17 to 0.32 Hz. In general, the confidence intervals did overlap at frequencies of 0.02 Hz, i.e. the pre-treatment did not have an effect.

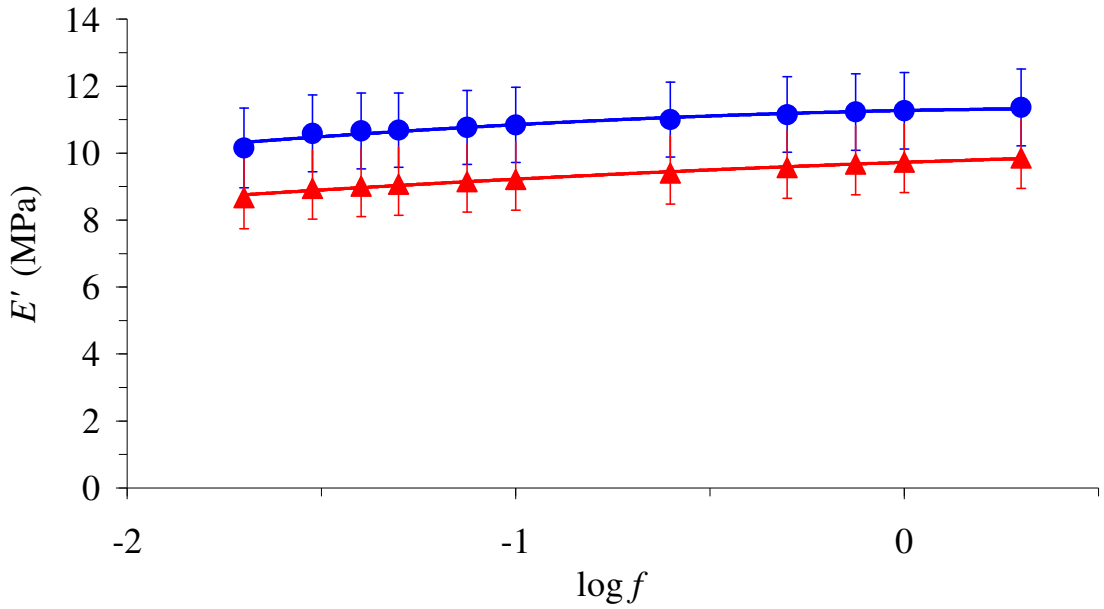

Figure H. 1: Mean values of E' plotted against the $\log_{10}f$, for cured (▲) and pre-treated (●) MED-4080 dumb-bells. Error bars represent the 95 % confidence intervals and the lines shown are second-order polynomials.

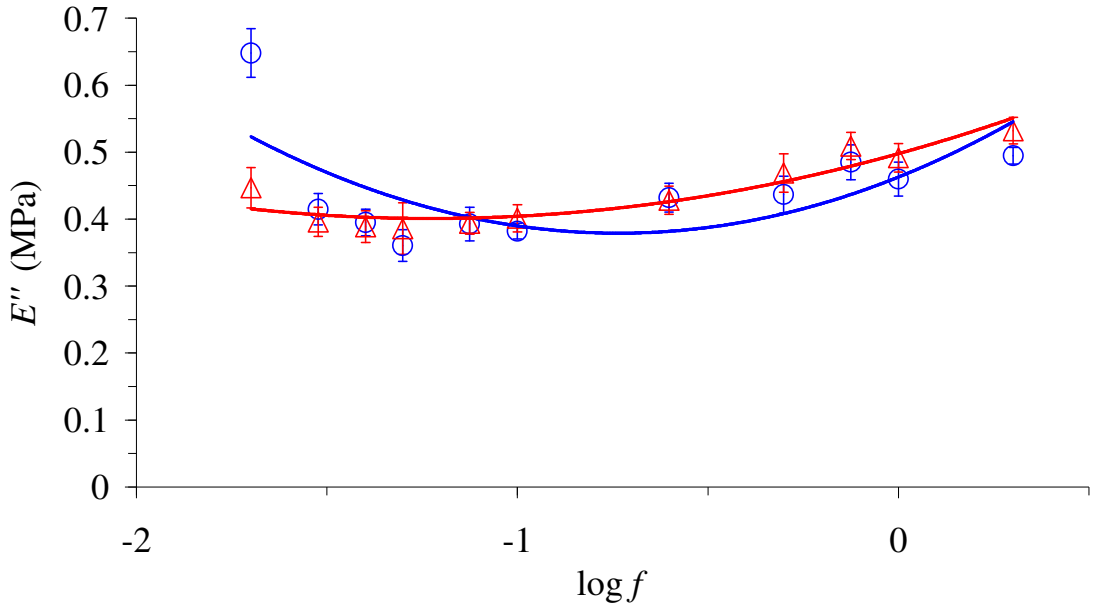

Figure H. 2: Mean values of E'' plotted against the $log_{10}f$, for cured (△) and pre-treated (○) MED-4080 dumb-bells. Error bars represent the 95 % confidence intervals and the lines shown are second-order polynomials.

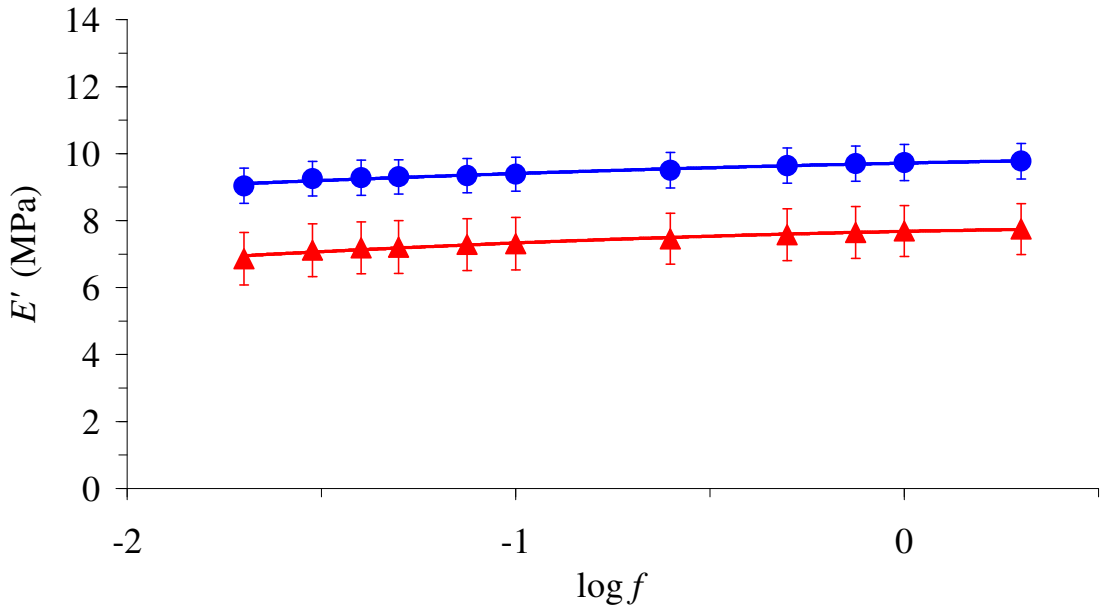

Figure H. 3: Mean values of E' plotted against the $log_{10}f$, for cured (▲) and pre-treated (●) C6-180 dumb-bells. Error bars represent the 95 % confidence intervals and the lines shown are second-order polynomials.

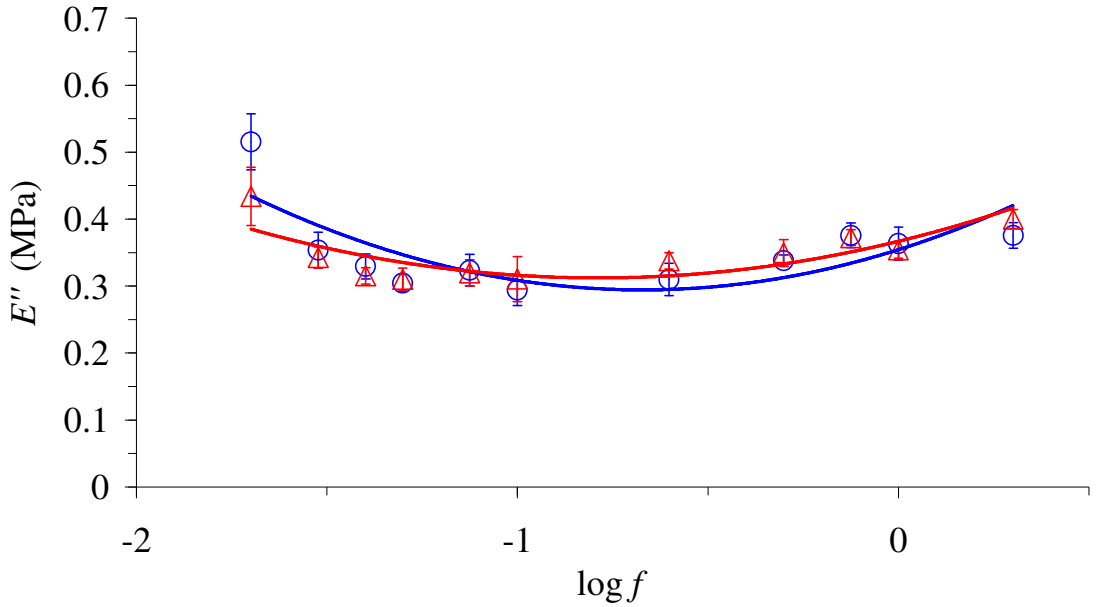

Figure H. 4: Mean values of E'' plotted against the $\log_{10}f$, for cured (△) and pre-treated (○) C6-180 dumb-bells. Error bars represent the 95 % confidence intervals and the lines shown are second-order polynomials.

The coefficients of the polynomials in Figure H. 1 and Figure H. 3 are given in Table H. 1. The coefficients given here enable the *E'* at a given frequency to be determined, as discussed in §3.8.

Table H. 1: Coefficients of the polynomials fitted to E' (cured and pre-treated dumb-bells) for each grade of silicone. R^2 is the square of the correlation coefficient and shows how well the polynomial curve fits the data. When R^2 = 1, there is a perfect correlation.

Grade	a_0'	a_1'	a_2'	R^2
C6-180	7.6776	0.2286	-0.1167	0.9759
MED-4080	9.725	0.4042	-0.0973	0.9876
C6-180	9.7181	0.2415	-0.0699	0.9771
MED-4080	11.273	0.2298	-0.1936	0.9557

The coefficients of the polynomials in Figure H. 2 and Figure H. 4 are given in Table 5.2. The coefficients given here enable the *E''* at a given frequency to be determined, as discussed in §3.8.

Table H. 2: Coefficients of the polynomials fitted to E'' (cured and pre-treated dumb-bells) for each grade of silicone. R^2 is the square of the correlation coefficient and shows how well the polynomial curve fits the data. When R^2 = 1, there is a perfect correlation.

Grade	a_0''	a_1''	a_2''	R^2
C6-180	0.3669	0.1387	0.088	0.6217
MED-4080	0.4978	0.1578	0.0643	0.8896
C6-180	0.3544	0.1788	0.133	0.5707
MED-4080	0.4628	0.228	0.1551	0.4439

APPENDIX I: ADDITIONAL RESULTS ON THE SWELLING MEASUREMENTS

I.1: Do different solvents have different swelling abilities?

As mentioned in §7.3, Table I. 1 lists the mean and standard deviation values of swelling (as a percentage of the original mass) of the medical grade silicones after swelling in solvents.

Table I. 1: Mean and standard deviation values of swelling (as a percentage of the original mass) of the medical grade silicones after swelling in cyclohexane, toluene, ethyl acetate, ethyl methyl ketone and n-butanol.

Solvent	**Grades**	**Mean swelling (as a percentage of the original mass)**	**Standard deviation**
cyclohexane			
	C6-165	127	4
	C6-180	93	3
	MED82-5010-80	140	5
	MED-4080	86	4
toluene			
	C6-165	117	5
	C6-180	88	1
	MED82-5010-80	131	2
	MED-4080	81	1
ethyl acetate			
	C6-165	71	1
	C6-180	52	1
	MED82-5010-80	80	1
	MED-4080	50	1
ethyl methyl ketone			
	C6-165	52	4
	C6-180	40	4
	MED82-5010-80	59	5
	MED-4080	37	3
n-butanol			
	C6-165	16	2
	C6-180	14	2
	MED82-5010-80	18	1
	MED-4080	15	2

I.2: Is it possible to calculate ϕ_P and the corresponding χ and υ_c from the swelling measurements using the swelling equilibrium method (equations 2.7, 2.8 and 2.9)?

As mentioned in §7.5, the mean and standard deviation values of ϕ_P and χ for the samples swollen in ethyl acetate, ethyl methyl ketone and n-butanol, are shown here in Table I. 2.

When the swelling equilibrium method was used to calculate χ (described in §2.5.4.6), this method seemed to work particularly well. Precise values in the range $0.765 \leq \chi \leq 0.874$, $0.810 \leq \chi \leq 0.938$ and $1.256 \leq \chi \leq 1.328$ were obtained when the silicone samples were swollen in ethyl acetate, ethyl methyl ketone and n-butanol respectively. These range of values obtained for χ appeared to be reasonable and are consistent with a previous study (Favre, 1996) which obtained values of 0.820, 0.869 and 1.277 after swelling the silicones in the same respective solvents. A study (Andreopoulos *et al.*, 1993) on silicones for maxillofacial applications obtained χ values of 0.667, 0.695 and 1.252 in ethyl acetate, ethyl methyl ketone and n-butanol, respectively. In particular, the χ values obtained by Andreopoulous *et al.* (1993) in n-butanol are similar to those obtained here.

However, as discussed previously in §2.5.4.6, substitution of these ϕ_P and χ values into the cross-link density equation (equation 2.9), gives a value of $\upsilon_c = 0$, which is not physically possible. Note that the values in Table I. 2 have been rounded off, hence if any non-zero υ_c values are obtained with these ϕ_P and χ values, this is because of a rounding off error.

Table I. 2: Mean and standard deviation values of ϕ_P and χ obtained for the medical grade silicones using the swelling equilibrium method (see §2.5.4.5 and §2.5.4.6). The swelling measurements were substituted into equation 2.8 (to calculate ϕ_P) and equation 2.9 (to calculate χ). The values for ρ_p and ρ_s, which are required in the calculations, are given in Table 3.2 (§3.2.1) and Table 3.5 (§3.9.1) respectively.

Solvent	**Grades**	**Mean ϕ_P**	**Standard deviation ϕ_P**	**Mean χ**	**Standard deviation χ**
ethyl acetate					
	C6-165	0.512	0.004	0.783	0.004
	C6-180	0.587	0.005	0.862	0.006
	MED82-5010-80	0.492	0.004	0.765	0.004
	MED-4080	0.597	0.007	0.874	0.008
ethyl methyl ketone					
	C6-165	0.563	0.022	0.835	0.024
	C6-180	0.627	0.022	0.914	0.029
	MED82-5010-80	0.539	0.021	0.810	0.021
	MED-4080	0.644	0.019	0.938	0.028
n-butanol					
	C6-165	0.807	0.023	1.292	0.076
	C6-180	0.825	0.022	1.293	0.131
	MED82-5010-80	0.818	0.014	1.256	0.044
	MED-4080	0.797	0.019	1.328	0.068

I.3: Swelling silicones in solvents with varying δ_S

As mentioned in §7.6, the plots obtained when all four silicone grades were swollen in the eleven solvents listed in Table 3.5 (§3.9.1), are shown here in Figure I. 1, Figure I. 2, Figure I. 3 and Figure I. 6. Also shown here are additional swelling plots for grades C6-165 and MED-4080 in Figure I. 4, Figure I. 5, Figure I. 7 and Figure I. 8.

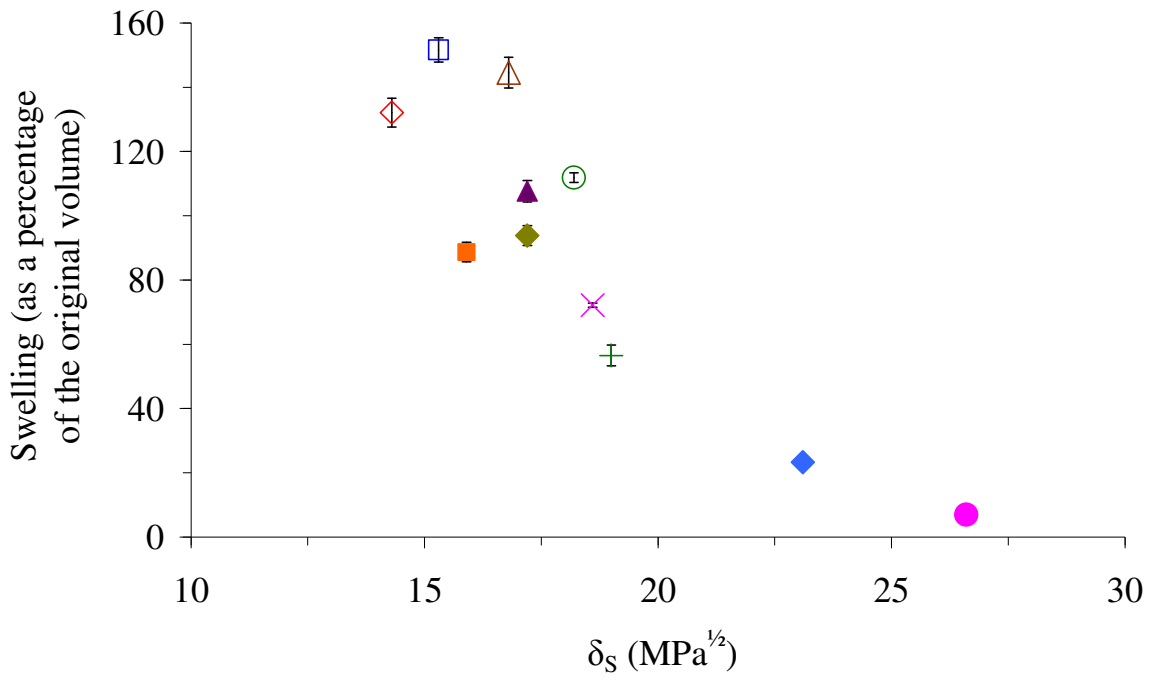

Figure I. 1: Mean values of swelling (as a percentage of the original volume) plotted against δ_S for C6-180. Error bars represent the standard deviations. The solvents shown are: 2,2,4-trimethylpentane (◇); n-heptane (□); diisobutyl ketone (■); cyclohexane (△); isopropyl acetate (▲); methyl isobutyl ketone (◆); toluene (○);ethyl acetate (×); ethyl methyl ketone (+); n-butanol (◆) and ethanol (●). Further information on these solvents, including values for ρ_s, which are required in the calculations, are available in Table 3.5 (§3.9.1). Error bars that are not visible have been obscured by the data point.

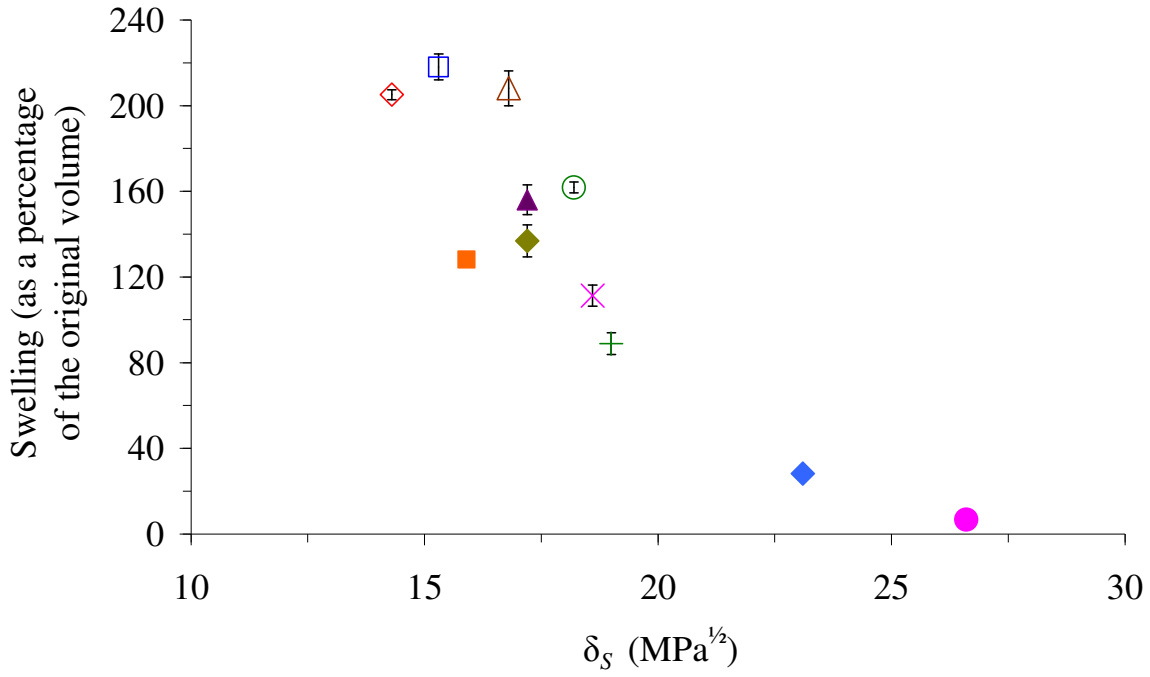

Figure I. 2: Mean values of swelling (as a percentage of the original volume) plotted against δ_S for MED-82-5010-80. Error bars represent the standard deviations. The solvents shown are: 2,2,4-trimethylpentane (◇); n-heptane (□); diisobutyl ketone (■); cyclohexane (△); isopropyl acetate (▲); methyl isobutyl ketone (◆); toluene (○);ethyl acetate (×); ethyl methyl ketone (+); n-butanol (◆) and ethanol (●). Further information on these solvents, including values for ρ_s, which are required in the calculations, are available in Table 3.5 (§3.9.1). Error bars that are not visible have been obscured by the data point.

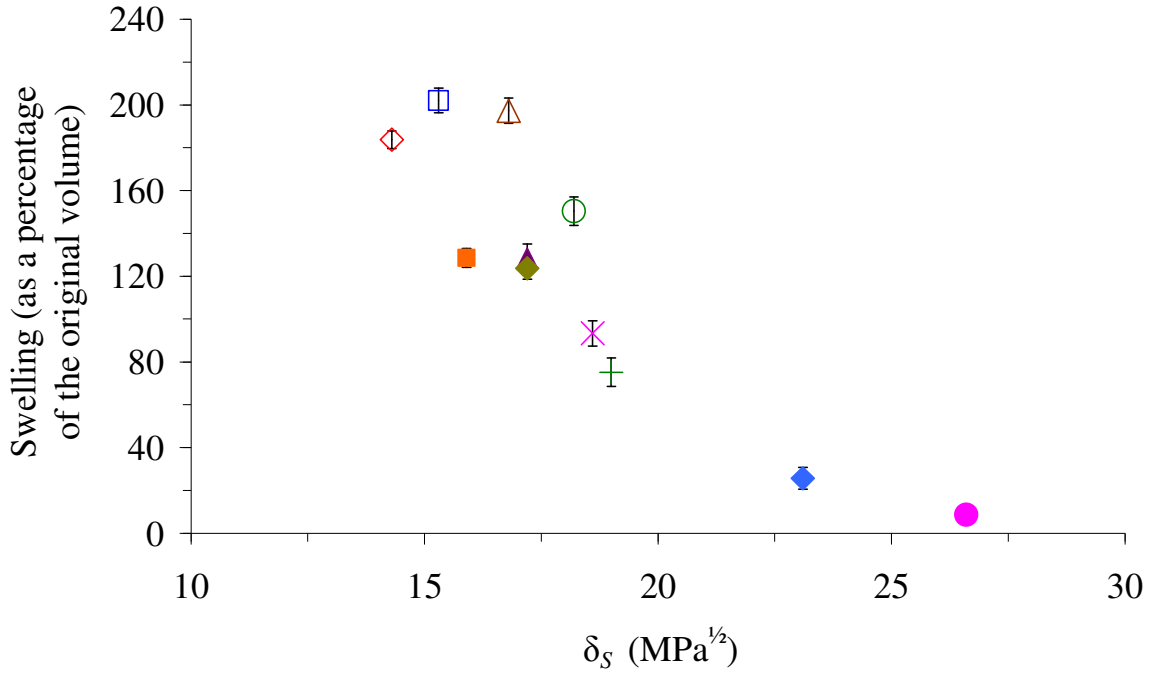

Figure I. 3: Mean values of swelling (as a percentage of the original volume) plotted against δ_S for C6-165. Error bars represent the standard deviations. The solvents shown are: 2,2,4-trimethylpentane (◇); n-heptane (□); diisobutyl ketone (■); cyclohexane (△); isopropyl acetate (▲); methyl isobutyl ketone (◆); toluene (○);ethyl acetate (×); ethyl methyl ketone (+); n-butanol (◆) and ethanol (●). Further information on these solvents, including values for ρ_s, which are required in the calculations, are available in Table 3.5 (§3.9.1). Error bars that are not visible have been obscured by the data point.

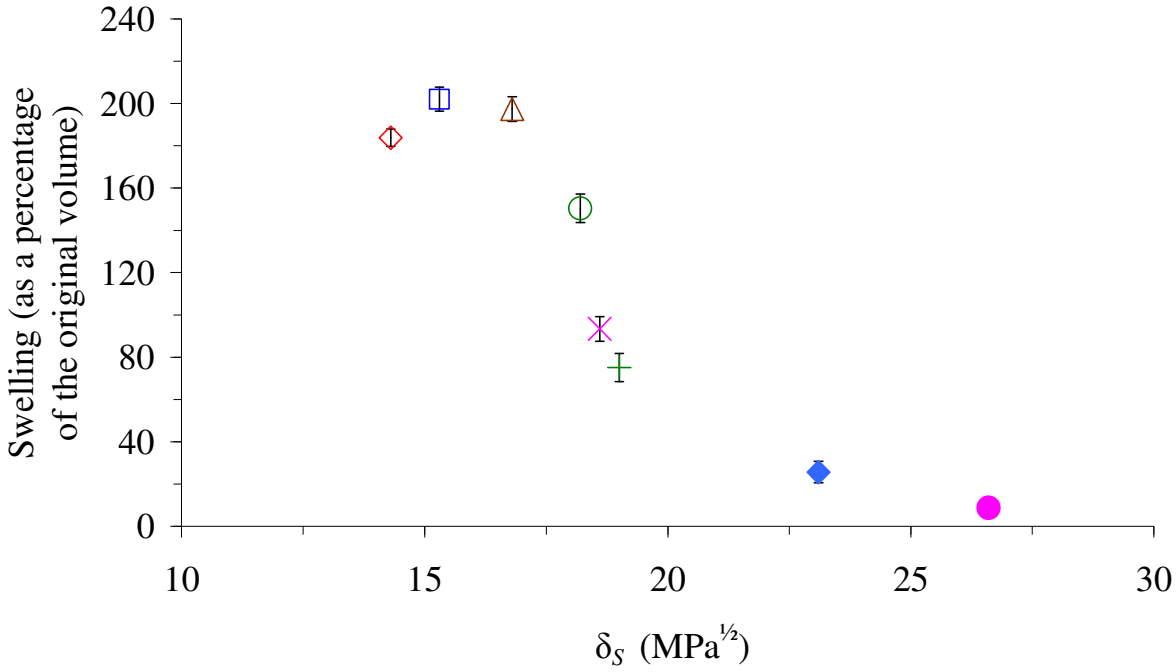

Figure I. 4: Mean values of swelling (as a percentage of the original volume) plotted against δ_S for C6-165. Error bars represent the standard deviations. The solvents shown are: 2,2,4-trimethylpentane (◇); n-heptane (□); cyclohexane (△); toluene (○); ethyl acetate (×); ethyl methyl ketone (+); n-butanol (◆) and ethanol (●). Further information on these solvents, including values for ρ_s, which are required in the calculations, are available in Table 3.5 (§3.9.1). Error bars that are not visible have been obscured by the data point.

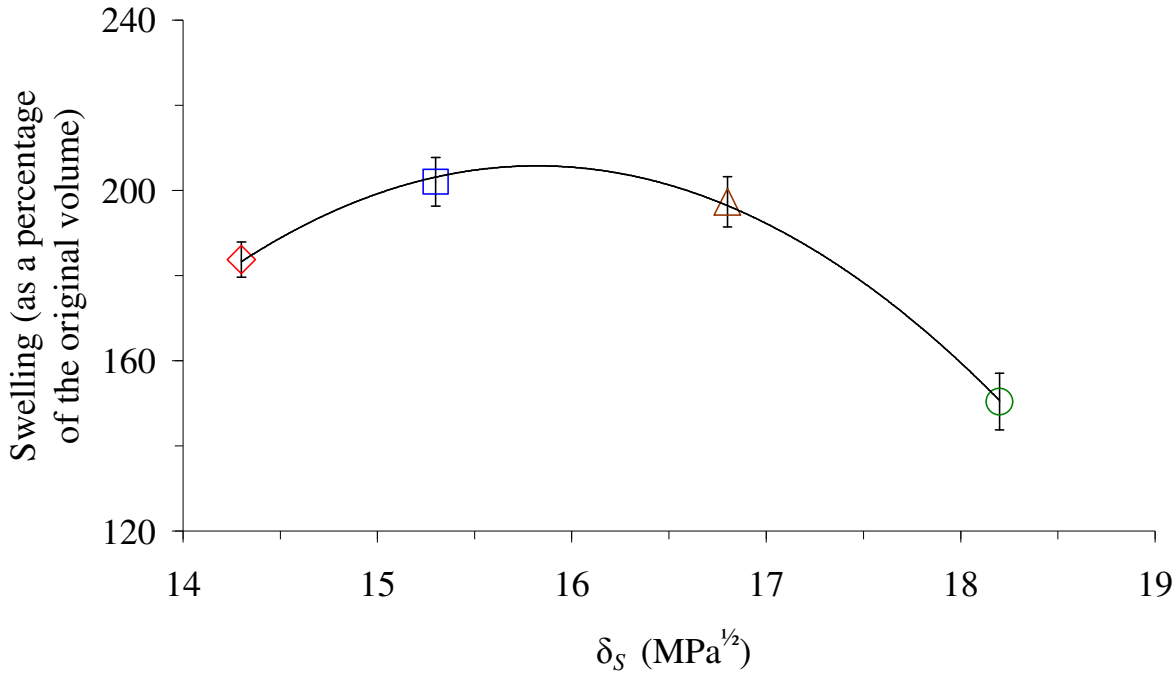

Figure I. 5: Mean values of swelling (as a percentage of the original volume) plotted against δ_S of the solvents with the greatest swelling ability, for C6-165. Error bars represent the standard deviations. The line shown is the second-order polynomial that gave the best fit to the data. (The equation of the line is $y = -9.729 x^2 + 307.83x - 2229.2$ and $R^2 = 0.99$). The solvents shown are: 2,2,4-trimethylpentane (◇); n-heptane (□); cyclohexane (△) and toluene (○). Further information on these solvents, including values for ρ_s, which are required in the calculations, are available in Table 3.5 (§3.9.1).

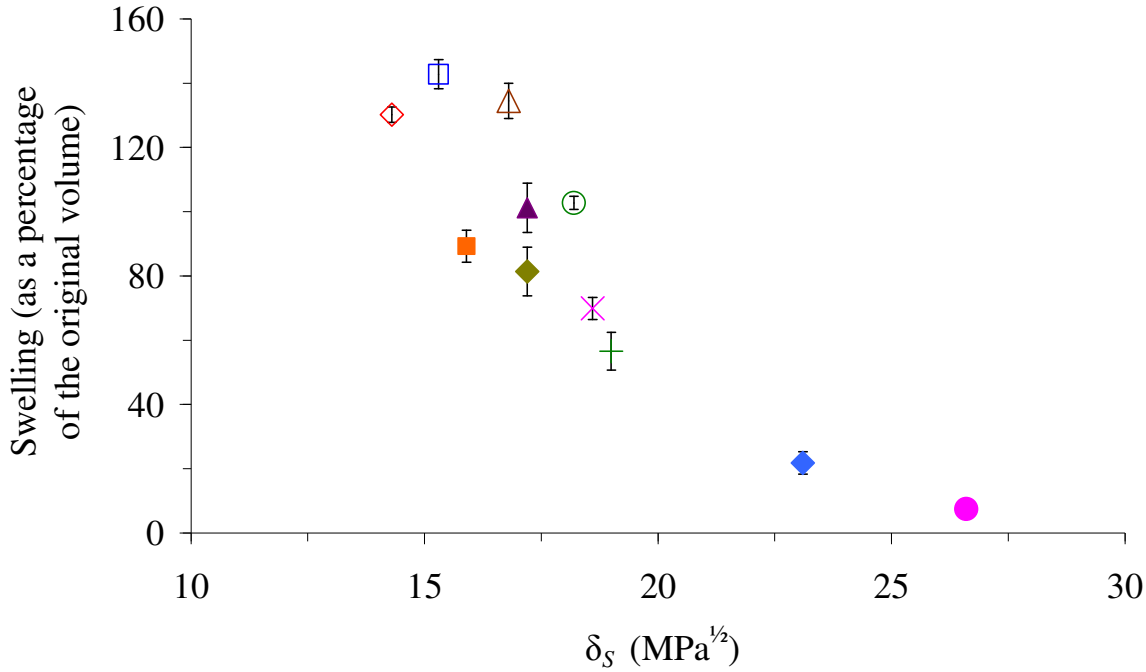

Figure I. 6: Mean values of swelling (as a percentage of the original volume) plotted against δ_S for MED-4080. Error bars represent the standard deviations. The solvents shown are: 2,2,4-trimethylpentane (◇); n-heptane (□); diisobutyl ketone (■); cyclohexane (△); isopropyl acetate (▲); methyl isobutyl ketone (◆); toluene (○);ethyl acetate (×); ethyl methyl ketone (+); n-butanol (◆) and ethanol (●). Further information on these solvents, including values for ρ_s, which are required in the calculations, are available in Table 3.5 (§3.9.1). Error bars that are not visible have been obscured by the data point.

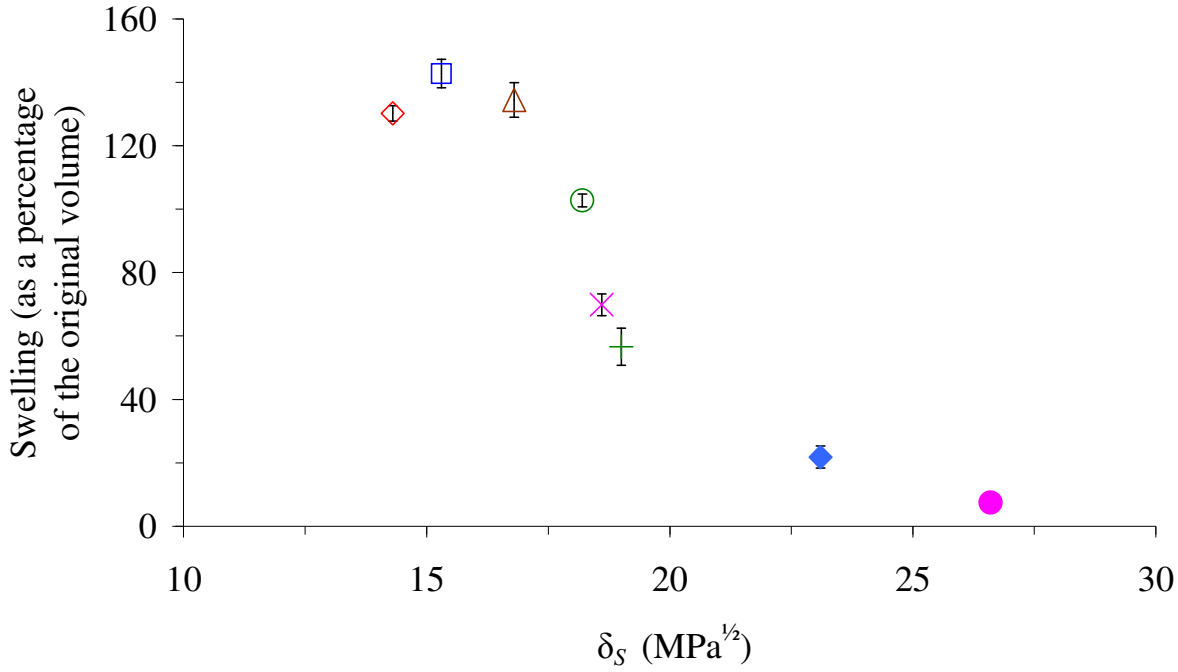

Figure I. 7: Mean values of swelling (as a percentage of the original volume) plotted against δ_S for MED-4080. Error bars represent the standard deviations. The solvents shown are: 2,2,4-trimethylpentane (◇); n-heptane (□); cyclohexane (△); toluene (○); ethyl acetate (×); ethyl methyl ketone (+); n-butanol (◆) and ethanol (●). Further information on these solvents, including values for ρ_s, which are required in the calculations, are available in Table 3.5 (§3.9.1). Error bars that are not visible have been obscured by the data point.

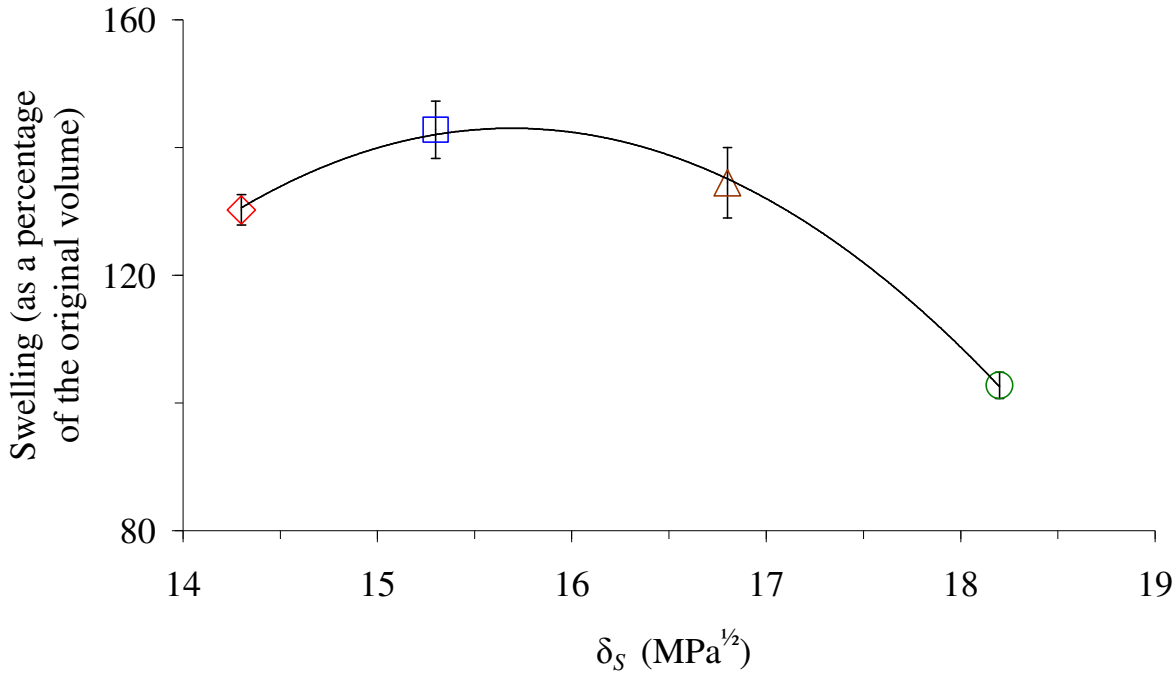

Figure I. 8: Mean values of swelling (as a percentage of the original volume) plotted against δ_S of the solvents with the greatest swelling ability, for MED-4080. Error bars represent the standard deviations. The line shown is the second-order polynomial that gave the best fit to the data. (The equation of the line is. $y = -6.4262\ x^2 + 201.67x - 1439.2$ and $R^2 = 0.99$). The solvents shown are: 2,2,4-trimethylpentane (◇); n-heptane (□); cyclohexane (△) and toluene (○). Further information on these solvents, including values for ρ_s, which are required in the calculations, are available in Table 3.5 (§3.9.1).

I.4: Using the δ_P value obtained in § 7.6, is it possible to calculate χ using Hildebrand's solubility parameter theory (equation 2.12) and then calculate the corresponding υ_c (equation 2.7)?

As mentioned in §7.7, the mean and standard deviation values of ϕ_P, χ and υ_c for the samples swollen in ethyl acetate, ethyl methyl ketone and n-butanol, are shown here in Table I. 3 and Table I. 4. Figure I. 9 compare the υ_c values obtained, as mentioned in §7.7.

The Hildebrand's solubility parameter theory (equation 2.12), described in § 2.5.4.6, was also used to calculate χ. The results in §7.7 and §7.8 showed that χ is dependent on the choice of K, χ_s and δ_P, the parameters used in equation 2.12. In particular, comparing the results in Table I. 3 and Table I. 4 showed that χ is sensitive to the value of δ_P, because when δ_P increased slightly, χ decreased considerably. For example, δ_P values in the range 15.6 $MPa^{½}$ - 15.9 $MPa^{½}$, produced reasonable and precise χ values in the range $0.628 \leq \chi \leq 0.695$, $0.688 \leq \chi \leq 0.758$ and $2.26 \leq \chi \leq 2.42$ when the silicone samples were swollen in ethyl acetate, ethyl methyl ketone and n-butanol, respectively. While, when δ_P = 15.3 $MPa^{½}$ was used, χ increased slightly to 0.771, 0.835 and 2.588, in the same respective solvents. As discussed previously in §I.2, these χ values are consistent with those obtained in previous studies.

Table I. 3: Mean values of χ and υ_c obtained for the medical grade silicones using Hildebrand's solubility parameter theory, when a constant δ_P value of 15.3 $MPa^{1/2}$ is used (assuming K=1, χ_s =0.34, R=8.31 J/Kmol and T=298K). As the value of χ does not alter for each grade, standard deviation values are only shown for υ_c. Standard deviation values for ϕ_P have previously been shown in Table 7.2. The values for V_S, δ_S, ρ_p and ρ_s, which are required in the calculations, are given in Table 3.2 (§3.2.1) and Table 3.5 (§3.9.1).

Solvent	**Grades**	ϕ_P	χ	υ_c (x 10^{-5} mol/cm^3)	**Standard deviation υ_c (x 10^{-5})**
ethyl acetate					
	C6-165	0.512	0.771	6.2	1.8
	C6-180	0.587	0.771	59.4	4.9
	MED82-5010-80	0.492	0.771	-2.5	1.6
	MED-4080	0.597	0.771	69.5	7.3
ethyl methyl ketone					
	C6-165	0.563	0.835	1.4	17.2
	C6-180	0.627	0.835	65.5	28.0
	MED82-5010-80	0.539	0.835	-14.1	11.4
	MED-4080	0.644	0.835	88.9	28.8
n-butanol					
	C6-165	0.807	2.588	-1746	7.6
	C6-180	0.825	2.588	-1744	0.0002
	MED82-5010-80	0.818	2.588	-1747	6.6
	MED-4080	0.797	2.588	-1750	6.5

Table I. 4: Mean values of χ and υ_c obtained for the medical grade silicones using Hildebrand's solubility parameter theory, when δ_P varies between 15.6-15.9 $MPa^{1/2}$ (assuming K=1, χ_s =0.34, R=8.31J/Kmol and T=298K). As the value of χ does not alter for each grade, standard deviation values are only shown for υ_c. Standard deviation values for ϕ_P have previously been shown in Table 7.2. The values for V_S, δ_S, ρ_p and ρ_s, which are required in the calculations, are given in Table 3.2 (§3.2.1) and Table 3.5 (§3.9.1).

Solvent	**Grades**	**δ_P $MPa^{1/2}$**	ϕ_P	χ	**υ_c (x 10^{-4} mol/cm^3)**	**Standard deviation υ_c (x 10^{-4})**
ethyl acetate						
	C6-165	15.8	0.512	0.650	6.6	0.3
	C6-180	15.9	0.587	0.628	15.2	0.7
	MED82-5010-80	15.6	0.492	0.695	3.2	0.2
	MED-4080	15.7	0.597	0.672	13.6	0.9
ethyl methyl ketone						
	C6-165	15.8	0.563	0.711	8.2	2.4
	C6-180	15.9	0.627	0.688	18.5	3.6
	MED82-5010-80	15.6	0.539	0.758	3.2	1.5
	MED-4080	15.7	0.644	0.734	17.5	3.4
n-butanol						
	C6-165	15.8	0.807	2.31	-137	1.1
	C6-180	15.9	0.825	2.26	-127	5.1
	MED82-5010-80	15.6	0.818	2.42	-129	0.02
	MED-4080	15.7	0.797	2.36	-144	1.2

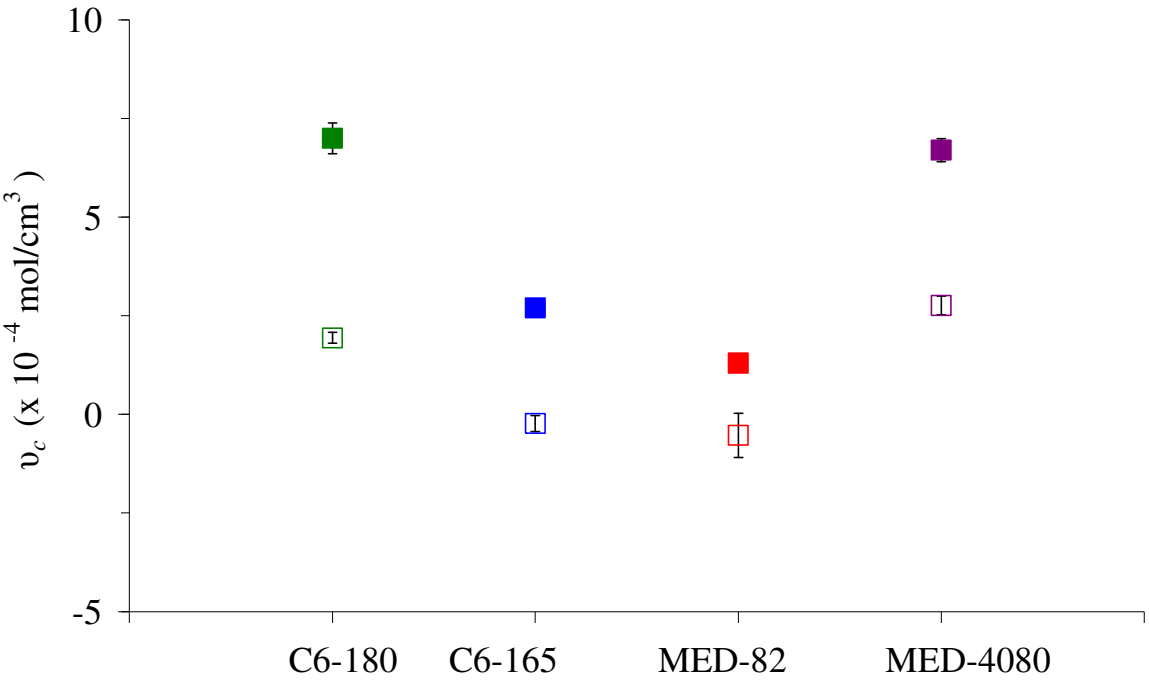

Figure I. 9: Mean value of υ_c plotted against the silicone grades: C6-180 (□■); C6-165 (□■); MED-82-5010-80 ((□■) abbreviated to MED-82 on the figure) and MED-4080 (□■). The values were obtained from Table 7.4 (in toluene; shown as (filled squares)), and from Table 7.3 (in toluene; shown as (unfilled squares)). Both values of υ_c were calculated using Hildebrand's solubility parameter theory. The error bars shown represent the 95% confidence intervals. Error bars that are not visible have been obscured by the data point.

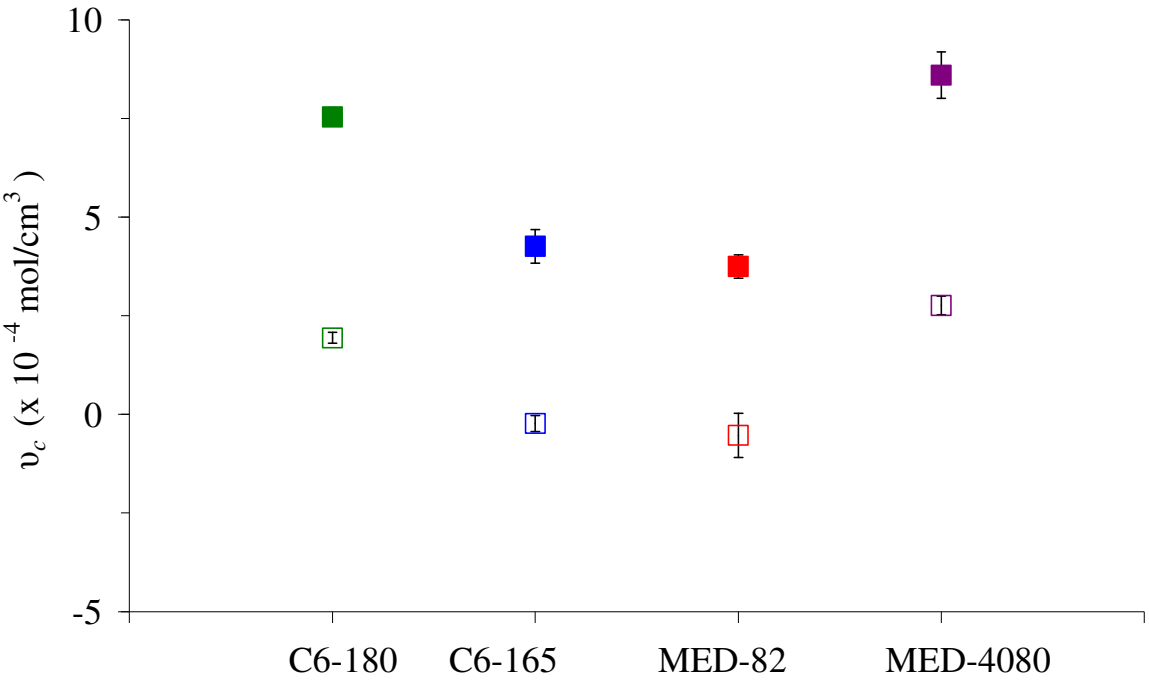

Figure I. 10: Mean values of υ_c plotted against the silicone grades: C6-180 (□■); C6-165 (□■); MED-82-5010-80 ((□■) abbreviated to MED-82 on the figure) and MED-4080 (□■). The values were obtained from Table 7.3 and are shown for samples swollen in cyclohexane (filled squares) and toluene (unfilled squares). The error bars shown represent the 95% confidence intervals. Error bars not shown have been obscured by the data point.

I.5: The effect that pre-treatment has on the cross-link density and how this relates to the modulus of pre-treated silicones

As discussed in §3.9.2 and §7.1, the cross-link density measurements before and after pre-treatment are shown here for samples that were swollen in toluene, ethyl acetate and ethyl methyl ketone. These are only preliminary results and therefore no general conclusion can be drawn, unless further measurements are carried out.

Table I. 5: Swelling (as a percentage of the original volume) and ϕ_P before and after pre-treating (in physiological saline solution at 37°C for five months) of samples swollen in toluene, ethyl acetate and ethyl methyl ketone. The values for ρ_p and ρ_s, which are required in the calculations, are given in Table 3.2 (§3.2.1).

Solvent	**Grades**	**Swelling (as a percentage of the original volume) before pre-treatment**	**Swelling (as a percentage of the original volume) after pre-treatment**	**ϕ_P before pre-treatment**	**ϕ_P after pre-treatment**
toluene	C6-165	151	141	0.398	0.415
	C6-180	113	113	0.475	0.469
	MED82-5010-80	162	162	0.382	0.381
	MED-4080	102	101	0.493	0.497
ethyl acetate	C6-165	95.6	112.8	0.512	0.470
	C6-180	70.6	69.2	0.587	0.591
	MED82-5010-80	103.4	105.0	0.492	0.488
	MED-4080	67.7	64.2	0.597	0.609
ethyl methyl ketone	C6-165	78.0	72.3	0.563	0.580
	C6-180	59.7	54.9	0.627	0.645
	MED82-5010-80	85.9	83.7	0.539	0.544
	MED-4080	55.5	53.0	0.644	0.654

Table I. 6: χ and v_c of medical grade silicone samples before and after pre-treatment (in physiological saline solution at 37 °C for five months). χ were calculated after the samples were swollen in toluene ethyl acetate and ethyl methyl ketone, using the swelling equilibrium method. The values for V_S, δ_S, ρ_p and ρ_s, which are required in the calculations, are given in Table 3.2 (§3.2.1) and Table 3.5 (§3.9.1).

Solvent	**Grades**	**χ before pre-treatment**	**χ after pre-treatment**
toluene	C6-165	0.691	0.703
	C6-180	0.750	0.746
	MED82-5010-80	0.68	0.68
	MED-4080	0.766	0.769
ethyl acetate			
	C6-165	0.783	0.746
	C6-180	0.862	0.868
	MED82-5010-80	0.765	0.762
	MED-4080	0.874	0.890
ethyl methyl ketone			
	C6-165	0.835	0.854
	C6-180	0.914	0.939
	MED82-5010-80	0.810	0.815
	MED-4080	0.938	0.952

Table I. 7: υ_c of medical grade silicone samples before and after pre-treatment (in physiological saline solution at 37 °C for five months). υ_c was calculated after the samples were swollen in toluene, ethyl acetate and ethyl methyl ketone, using Hildebrand's solubility parameter theory (assuming K=1, χ_s =0.34 δ_P =15.3 $MPa^{1/2}$, R=8.31 J/Kmol, T=298 K). χ did not change before (see Table 7.3) and after pre-treatment. The values for V_S, δ_S, ρ_p and ρ_s, which are required in the calculations, are given in Table 3.2 (§3.2.1) and Table 3.5 (§3.9.1).

Solvent	**Grades**	υ_c **(x 10^{-5} mol/cm^3) before pre-treatment**	υ_c **(x 10^{-5} mol/cm^3) after pre-treatment**
toluene	C6-165	-2.23	0.7
	C6-180	19.41	17.4
	MED82-5010-80	-5.29	-5.3
	MED-4080	27.61	29.4
ethyl acetate	C6-165	6.12	-10.16
	C6-180	59.44	63.57
	MED82-5010-80	-2.62	-4.00
	MED-4080	69.51	83.13
ethyl methyl ketone	C6-165	1.35	13.55
	C6-180	65.47	89.13
	MED82-5010-80	-14.14	-11.98
	MED-4080	88.92	103.48

Table I. 8: υ_c of medical grade silicone samples before and after pre-treatment (in physiological saline solution at 37 °C for five months). υ_c was calculated after the samples were swollen in toluene, ethyl acetate and ethyl methyl ketone, using Hildebrand's solubility parameter theory (assuming K=1, χ_s =0.34, R=8.31 J/Kmol, T=298 K, δ_P varied between 15.6 and 15.9 $MPa^{1/2}$ as shown in Table 7.4). χ did not change before and after pre-treatment. The values for V_S, δ_S, ρ_p and ρ_s, which are required in the calculations, are given in Table 3.2 (§3.2.1) and Table 3.5 (§3.9.1).

Solvent	**Grades**	υ_c **(x 10^{-4} mol/cm^3) before pre-treatment**	υ_c **(x 10^{-4} mol/cm^3) after pre-treatment**
toluene	C6-165	2.7	3.2
	C6-180	7.0	6.8
	MED82-5010-80	1.3	1.3
	MED-4080	6.7	6.9
ethyl acetate	C6-165	6.58	4.03
	C6-180	15.21	15.74
	MED82-5010-80	3.17	2.98
	MED-4080	13.57	15.20
ethyl methyl ketone	C6-165	8.22	9.95
	C6-180	18.47	21.15
	MED82-5010-80	3.15	3.46
	MED-4080	17.51	19.26

Table I. 5, Table I. 6, Table I. 7 and Table I. 8 show the swelling (as a percentage of the original volume), ϕ_P, χ and υ_c of non pre-treated and pre-treated silicone samples, which were swollen in toluene, ethyl acetate and ethyl methyl ketone. For the toluene measurements, Table I. 5 shows that after pre-treating the silicones, the swelling (as a percentage of the original volume) remained fairly constant for three of the grades (C6-180, MED-82-5010-10 and MED-4080) and increased very slightly for grade C6-165. It also shows that after pre-treatment, ϕ_P either increased (grade C6-165 and MED-4080) or decreased (grade C6-180 and MED-82-5010-10) very slightly.

Table I. 6 shows that pre-treatment slightly increased the χ of two grades (C6-165 and MED-4080) but slightly decreased the χ of grade C6-180. It also showed that the υ_c of three grades (C6-180, C6-165 and MED-4080) increased after pre-treatment but the υ_c of grade MED-82-5010-80 decreased. Table I. 7 shows that pre-treating the silicones slightly increased the υ_c for two of the grades (C6-165 and MED-4080). However, the υ_c of grade MED-82-5010-80 remained fairly constant and that of grade C6-180 decreased slightly. Table I. 8 shows that pre-treating the silicones slightly increased the υ_c of two of the grades (C6-165 and MED-4080) but slightly decreased the υ_c of the other two grades.

The preliminary testing showed that pre-treating (in physiological saline solution at 37°C) the short-term implant silicone grades (C6-165, C8-180 and MED-4080) for five months, does not seem to greatly affect the swelling (as a percentage of the original volume), ϕ_P and χ. The preliminary results indicate that when the swelling equilibrium method is used to calculate χ, pre-treatment substantially affects the cross-link density, υ_c. On the other hand, if Hildebrand's solubility parameter theory is used to calculate χ, the preliminary results indicate that the υ_c is only substantially affected if the solubility parameter of the silicone, δ_P is simply equated to the solubility parameter of the solvent ,δ_S, in which the silicones swell the most (discussed in §2.5.4.6, §3.9.4 and §8.5). These results are not unexpected, as it has been discussed in §8.5 and in Chapter 7, that it is difficult to obtain reliable and precise υ_c values for the non pre-treated samples (results reported in Chapter 7) when the swelling equilibrium method and Hildebrand's solubility parameter theory (when δ_P is simply equated to δ_S in which the silicone swells the most) are used to calculate χ.

Hence, it is not clear whether these substantial effects on υ_c are real effects or whether it is because the υ_c equation (equation 2.7) is sensitive to the combination of ϕ_P and χ values used, as discussed in §8.5.

Since, the υ_c values obtained after pre-treatment do not appear to be substantially affected when Hildebrand's solubility parameter theory is used to calculate χ (provided that a suitable method is used to estimate δ_P), the results indicate that precise υ_c values can be obtained with this method. Recall that this method also produces reliable but not absolute υ_c values for the non pre-treated samples as discussed in §8.5. However, the pre-treated results are only preliminary and no general conclusions can be drawn, without taking a reasonable number of swelling measurements. Therefore it is suggested that, further swelling measurements of pre-treated silicone pieces should be carried out. A statistical analysis, particularly on the ϕ_P and χ values of these additional measurements would be useful, before any further conclusions can be drawn. Interestingly, as summarised in §8.3, the results in Chapter 4 show that pre-treating the same grades for 29 days (in physiological saline solution at 37°C) does not significantly affect the moduli of grade MED-4080, except for the *E'* at frequencies above about 30 Hz. However, as discussed in §7.2, it has been reported (Doležel et al., 1989b; Vondráček and Doležel, 1984) that the cross-link density and consequently the modulus of silicone rubber pacemakers increased initially and then decreased, after being implanted in the human body for a year. Another study (Polyzois, 2000) (discussed in §4.2), on silicones for maxillofacial applications, also suggested that the cross-link density and consequently the modulus may increase after storage in water at 37°C. It would be interesting to measure the cross-link density and modulus before and after implantation of a silicone implant, as no such study has been published.

I.6: Swelling Elast-Eon™ 3 in solvents

No previous study has measured the cross-link density of Elast-Eon™ 3 using the swelling technique. Therefore, as part of the experiments for this project, samples of Elast-Eon™ 3 were swollen in toluene, ethyl acetate, ethyl methyl ketone, n-butanol, cyclohexane and cyclohexanone. It was found that, the Elast-Eon™ 3 dissolved in ethyl acetate, ethyl methyl ketone and cyclohexanone. Appreciable swelling occurred in toluene but not in cyclohexane; good solvents for silicone (see §7.4). Although, appreciable swelling occurred in n-butanol (a bad solvent for silicone; see §7.4), the sample became extremely sticky and split into smaller pieces.

It has been suggested (Grulke, 1989) that, generally $(\delta_S - \delta_P)^2$ must be small for the components to be miscible or mix in all proportions. It has also been suggested (Sperling, 1997) that, if $(\delta_S - \delta_P)^{½} < 1$ (cal/cm^3)^{½} the polymer may dissolve in the solvent (where 1 (cal/cm^3)^{½} ≈ 2.046 MPa^{½}). Elast-Eon™ 3 did not dissolve or become sticky in toluene; according to Sperling (1997), this suggests that if toluene has a value of δ_S = 8.9 (cal/cm^3)^{½}, then the Elast-Eon™ 3 does not dissolve in toluene, because δ_P < 7.9 (cal/cm^3)^{½} (≈ 16.1 MPa^{½}). On the other hand, Elast-Eon™ 3 did dissolve in ethyl methyl ketone; according to Sperling (1997), this suggests that if ethyl methyl ketone has a value of δ_S = 9.3 (cal/cm^3)^{½}, then the Elast-Eon™ 3 dissolves in ethyl methyl ketone because δ_P > 8.3 (cal/cm^3)^{½} (≈ 17.0 MPa^{½}). However, this seems to contradict the results obtained earlier for toluene, which suggested that since Elast-Eon™ 3 did not dissolve in toluene, then δ_P < 7.9 (cal/cm^3)^{½} for Elast-Eon™ 3.

Hence, according to the results obtained from the toluene swelling measurements, it was not expected that the Elast-Eon^{TM} 3 would dissolve in ethyl methyl ketone (and similarly in ethyl acetate and cyclohexanone), because the toluene measurements suggested that δ_P < 7.9 $(cal/cm^3)^{½}$. Although, it is not possible to make any general conclusions, as no previous study has measured the δ_P of Elast-Eon^{TM} 3. Furthermore, these are only preliminary results and therefore no general conclusions can be drawn, unless further measurements are carried out.

REFERENCES

AKLONIS, J. J. & MACKNIGHT, W. J. (1983a) *Introduction to Polymer Viscoelasticity*. pp. 36-84. 2nd edition. New York; Chichester: John Wiley & Sons.

AKLONIS, J. J. & MACKNIGHT, W. J. (1983b) *Introduction to Polymer Viscoelasticity*. pp. 1-35. 2nd edition. New York; Chichester: John Wiley & Sons.

ALDERMAN, A. K., CHUNG, K. C., DEMONNER, S., SPILSON, S. V. & HAYWARD, R. A. (2002) The rheumatoid hand: A predictable disease with unpredictable surgical practice patterns. *Arthritis & Rheumatism-Arthritis Care & Research,* 47**,** 537-542.

ALDERMAN, A. K., UBEL, P. A., KIM, H. M., FOX, D. A. & CHUNG, K. C. (2003) Surgical management of the rheumatoid hand: Consensus and controversy among rheumatologists and hand surgeons. *Journal of Rheumatology,* 30**,** 1464-1472.

ANDREOPOULOS, A. G., POLYZOIS, G. L. & EVANGELATOU, M. (1993) Swelling properties of cross-linked maxillofacial elastomers. *Journal of Applied Polymer Science,* 50**,** 729-733.

ASTM D2240-00: *Standard test method for rubber property- Durometer hardness*. American Society for Testing and Materials.

ASTM WK4863: *Standard practice/guide for the mechanical characterization of lumbar nucleus devices. Draft standard edition (2005).* American Society for Testing and Materials.

AZIZ, T., WATERS, M. & JAGGER, R. (2003) Analysis of the properties of silicone rubber maxillofacial prosthetic materials. *Journal of Dentistry,* 31**,** 67-74.

BAGLEY, E. B., NELSON, T. P., BARLOW, J. W. & CHEN, S. A. (1970) Internal pressure measurements and liquid-state energies. *Industrial and Engineering Chemistry Fundamentals,* 9**,** 93-97.

BARTON, A. F. M. (1975) Solubility parameters. *Chemical Reviews,* 75**,** 731-753.

BARTON, A. F. M. (1983) *CRC Handbook of solubility parameters and other cohesion parameters,* Boca Raton: CRC Press, Inc.

BECKENBAUGH, R. D., DOBYNS, J. H., LINSCHEID, R. L. & BRYAN, R. S. (1976) Review and analysis of silicone-rubber metacarpophalangeal implants. *Jounal of Bone and Joint Surgery-American Volume,* 58**,** 483-487.

BEEVERS, D. J. & SEEDHOM, B. B. (1993) Metacarpophalangeal joint prostheses: a review of past and current designs. . *Proceedings of the Institution of Mechanical Engineers Part H-Journal of Engineering in Medicine,* 207**,** 195-206.

BEEVERS, D. J. & SEEDHOM, B. B. (1995) Metacarpophalangeal joint prostheses. A review of the clinical results of past and current designs. *The Journal of Hand Surgery-British and European Volume,* 20**,** 125-136.

BENHAM, P. P., CRAWFORD, R. J. & ARMSTRONG, C. G. (1996) *Mechanics of Engineering Materials*. pp. 514-543. 2nd edition. Harlow: Longman.

BIDDIS, E. A., BOGOCH, E. R. & MEGUID, S. A. (2004) Three-dimensional finite element analysis of prosthetic finger joint implants. *International Journal of Mechanics and Materials in Design,* 1**,** 317.

BIEBER, E. J., WEILAND, A. J. & VOLENEC-DOWLING, S. (1986) Silicone-rubber implant arthroplasty of the metacarpophalangeal joints for rheumatoid arthritis. *Journal of Bone and Joint Surgery-American Volume,* 68**,** 206-209.

BIRKEFELD, A. B., ECKERT, H. & PFLEIDERER, B. (2004) A study of the aging of silicone breast implants using 29Si, 1H relaxation and DSC measurements. *Biomaterials,* 25**,** 4405-4413.

BLAIR, W. F., SHURR, D. G. & BUCKWALTER, J. A. (1984) Metacarpophalangeal joint implant arthroplasty with a Silastic spacer. *Journal of Bone and Joint Surgery-American,* 66**,** 365-370.

BLAND, M. (2000) *An introduction to medical statistics*. pp. 185-209. 3rd edition. Oxford; New York: Oxford University Press.

BLANKS, R. F. & PRAUSNITZ, J. M. (1964) Thermodynamics of polymer solubility in polar and nonpolar systems. *Industrial and Engineering Chemistry Fundamentals,* 3**,** 1-8.

BOONSTRA, B. B. (1979) Role of particulate fillers in elastomer reinforcement: A review. *Polymer,* 20**,** 691-704.

BOONSTRA, B. B., COCHRANE, H. & DANNENBERG, E. M. (1975) Reinforcement of silicone-rubber by particulate silica. *Rubber Chemistry and Technology,* 48**,** 558-576.

BOYER, R. F. & SPENCER, R. S. (1948) Some thermodynamic properties of slightly cross-linked styrene-divinylbenzene gels. *Journal of Polymer Science,* 3**,** 97-127.

BRALEY, S. (1970) Chemistry and properties of medical-grade silicones. *Journal of Macromolecular Science-Chemistry,* A4**,** 529-544.

BRANDON, H. J., JERINA, K. L., WOLF, C. J. & YOUNG, V. L. (2003) Biodurability of retrieved silicone gel breast implants. *Plastic & Reconstructive Surgery,* 111**,** 2295-2306.

BRANDON, H. J., YOUNG, V. L., JERINA, K. L. & WOLF, C. J. (2001) Variability in the properties of silicone gel breast implants. *Plastic & Reconstructive Surgery* 108**,** 647-655.

BRIQUET, F., COLAS, A. & THOMAS, X. (1996) Silicones for medical use. *XIIIth Technical Congress: Polymers for Biomedical Use.* Le Mans, France.

BRISTOW, G. M. & WATSON, W. F. (1958) Cohesive energy densities of polymers. Part 1.- Cohesive energy densities of rubbers by swelling measurements. *Transactions of the Faraday Society,* 54**,** 1731 - 1741.

BRYDSON, J. A. (1988) *Rubbery materials & their compounds*. pp. 254-270. London: Elsevier Applied Science.

BRYDSON, J. A. (1999) *Plastic materials*. pp. 814-852. 7th edition. Oxford: Butterworth-Heinemann.

BS 903-A2:1995; ISO 37:1994: *Physical testing of rubber — Part A2: Method for determination of tensile stress-strain properties*. British Standards Institution

BS 903-A6:1992; ISO 815:1991: *Physical testing of rubber-Part A6: Method for determination of compression set at ambient, elevated or low temperatures*. British Standards Institution.

BS EN ISO 868:2003: *Plastics and ebonite —Determination of indentation hardness by means of a durometer (Shore hardness).* British Standards Institution.

BS ISO 7619-1:2004: *Rubber, vulcanized or thermoplastic —Determination of indentation hardness — Part 1: Durometer method (Shore hardness).* British Standards Institution.

BUECHE, A. M. (1955a) The curing of silicone rubber with benzoyl peroxide. *Journal of Polymer Science,* 15**,** 105-120.

BUECHE, A. M. (1955b) Interaction of polydimethylsiloxanes with swelling agents. *Journal of Polymer Science,* 15**,** 97-103.

CARPENTER, D. W. (1990) Solution Properties. In: *Concise Encyclopaedia of Polymer Science and Engineering*, edited by: KROSCHWITZ, J. I. pp 1070-1071. New York: John Wiley & Sons, Inc.

CHEREMISINOFF, N. P., BOYKO, R. & LEIDY, L. (1993) Analytical test methods for polymer characterization. In: *Elastomer Technology Handbook*, edited by: CHEREMISINOFF, N. P. pp 9-16. Boca Raton; Ann Arbor; London; Tokyo: CRC Press, Inc.

CLARSON, S. J., DODGSON, K. & SEMLYEN, J. A. (1985) Studies of cyclic and linear poly(dimethylsiloxanes): 19. Glass transition temperatures and crystallization behaviour. *Polymer,* 26**,** 930-934.

COLAS, A. (1990) Silicones: Preparation, properties and performance. *Chimie Nouvelle, The Journal of the "Société Royale de Chimie" (Belgium),* 8**,** 847.

COLAS, A. & CURTIS, J. (2004a) Medical application of silicones In: *Biomaterials Science: An Introduction to Materials in Medicine*, edited by: RATNER, B. D., HOFFMAN, A. S., SCHOEN, F. J. & LEMMONS, J. E. pp 697-707. California; London: Elsevier Academic Press.

COLAS, A. & CURTIS, J. (2004b) Silicone biomaterials: History and chemistry. In: *Biomaterials Science: An Introduction to Materials in Medicine*, edited by: RATNER, B. D., HOFFMAN, A. S., SCHOEN, F. J. & LEMMONS, J. E. pp 80-86. California; London: Elsevier Academic Press.

COLEMAN, M. M., SERMAN, C. J., BHAGWAGAR, D. E. & PAINTER, P. C. (1990) A practical guide to polymer miscibility. *Polymer,* 31**,** 1187-1203.

COWIE, J. M. G. (1994) *Polymers : Chemistry & physics of modern materials*. pp. 157-186 and 274-320. 2nd edition. London: Blackie Academic & Professional (Chapman & Hall).

CRAIG, R. G., KORAN, A. & YU, R. (1980) Elastomers for maxillofacial applications. *Biomaterials,* 1**,** 112-117.

DELANEY, R., TRAIL, I. A. & NUTTALL, D. (2005) A comparative study of outcome between the NeuFlex and Swanson metacarpophalangeal joint replacements. *The Journal of Hand Surgery-Journal of the British Society for Surgery of the Hand,* 30**,** 3-7.

DIAMANT, Y. & FOLMAN, M. (1979) Influence of dewetting on the damping properties of a filled polymer system: 1. Static characterization. *Polymer,* 20**,** 1025-1033.

DOI, K., KUWATA, N. & KAWAI, S. (1984) Alumina ceramic finger implants - A preliminary biomaterial and clinical-evaluation. *The Journal of Hand Surgery-American Volume,* 9**,** 740-749.

DOLEŽEL, B., ADAMÍROVÁ, L., NÁPRSTEK, Z. & VONDRÁČEK, P. (1989a) In vivo degradation of polymers .I. Change of mechanical-properties in polyethylene pacemaker lead insulations during long-term implantation in the human-body. *Biomaterials,* 10**,** 96-100.

DOLEŽEL, B., ADAMÍROVÁ, L., VONDRÁČEK, P. & NÁPRSTEK, Z. (1989b) In vivo degradation of polymers : II. Change of mechanical properties and cross-link density in silicone rubber pacemaker lead insulations during long-term implantation in the human body. *Biomaterials,* 10**,** 387-392.

DOOTZ, E. R., KORAN, A. & CRAIG, R. G. (1993) Physical property comparison of 11 soft denture lining materials as a function of accelerated aging. *The Journal of Prosthetic Dentistry,* 69**,** 114-119.

DOOTZ, E. R., KORAN, A. & CRAIG, R. G. (1994) Physical-properties of 3 maxillofacial materials as a function of accelerated aging. *The Journal of Prosthetic Dentistry,* 71**,** 379-383.

DOTY, P. & ZABLE, H. S. (1946) Determination of polymer-liquid interaction by swelling measurements. *Journal of Polymer Science,* 1**,** 90-101.

DUDEK, T. & BUECHE, F. (1964) Polymer-solvent interaction parameter and creep of ethylene-propylene rubber. *Rubber Chemistry and Technology,* 37**,** 894-903.

DVORNIC, P. R. & LENZ, R. W. (1990) *High temperature siloxane elastomers,* Heidelberg; New York: Huthig & Wepf Verlag Basel.

FAVRE, E. (1996) Swelling of crosslinked polydimethylsiloxane networks by pure solvents: Influence of temperature. *European Polymer Journal,* 32**,** 1183-1188.

FAVRE, E., NGUYEN, Q. T., CLEMENT, R. & NEEL, J. (1996) Application of Flory-Huggins theory to ternary polymer-solvents equilibria: A case study. *European Polymer Journal,* 32**,** 303-309.

FERRY, J. D. (1961a) *Viscoelastic properties of polymers*. pp. 201-319. New York; London: John Wiley & Sons, Inc.

FERRY, J. D. (1961b) *Viscoelastic properties of polymers*. pp. 1-40. New York; London: John Wiley & Sons, Inc.

FLEMING, S. G. & HAY, E. L. (1984) Metacarpophalangeal joint arthroplasty 11 year follow-up study. *The Journal of Hand Surgery-British and European Volume,* 9**,** 300-302.

FLORY, P. J. (1942) Thermodynamics of high polymer solutions. *The Journal of Chemical Physics,* 10**,** 51-61.

FLORY, P. J. (1950) Statistical mechanics of swelling of network structures. *The Journal of Chemical Physics,* 18**,** 108-111.

FLORY, P. J. (1953) *Principles of polymer chemistry*. pp. 495-540. Ithaca, New York: Cornell University Press.

FLORY, P. J. (1970) Fifteenth Spiers memorial lecture. Thermodynamics of polymer solutions. *Discussions of the Faraday Society,* 49**,** 7-29.

FLORY, P. J. & REHNER, J. J. (1943) Statistical mechanics of cross-linked polymer networks. 2. Swelling. *The Journal of Chemical Physics,* 11**,** 521-526.

FOLIART, D. E. (1995) Swanson silicone finger joint implants: A review of the literature regarding long-term complications. *Journal of Hand Surgery-American Volume,* 20**,** 445-449.

GELLMAN, H., STETSON, W., BRUMFIELD, R. H., COSTIGAN, W. & KUSCHNER, S. H. (1997) Silastic metacarpophalangeal joint arthroplasty in patients with rheumatoid arthritis. *Clinical Orthopaedics and Related Research,* 342**,** 16-21.

GHANBARI-SIAHKALI, A., MITRA, S., KINGSHOTT, P., ALMDAL, K., BLOCH, C. & REHMEIER, H. K. (2005) Investigation of the hydrothermal stability of cross-linked liquid silicone rubber (LSR). *Polymer Degradation and Stability,* 90**,** 471-480.

GILLESPIE, T. E., FLATT, A. E., YOUM, Y. & SPRAGUE, B. L. (1979) Biomechanical evaluation of metacarpophalangeal joint prosthesis designs. *Journal of Hand Surgery-American Volume,* 4**,** 508-521.

GOLD, R. H., BASSETT, L. W. & SEEGER, L. L. (1988) The other arthritides - roentgenologic features of osteo-arthritis, erosive osteo-arthritis, ankylosing-spondylitis, psoriatic-arthritis, reiters disease, multicentric reticulohistiocytosis, and progressive systemic-sclerosis. *Radiologic Clinics of North America,* 26**,** 1195-1212.

GOLDBERG, A. J., CRAIG, R. G. & FILISKO, F. E. (1978) Polyurethane elastomers as maxillofacial prosthetic materials. *Journal of Dental Research,* 57**,** 563-569.

GOLDFARB, C. A. & STERN, P. J. (2003) Metacarpophalangeal joint arthroplasty in rheumatoid arthritis - A long-term assessment. *Journal of Bone and Joint Surgery-American Volume,* 85**,** 1869-1878.

GRULKE, E. A. (1989) Solubility Parameter Values. In: *Polymer Handbook*, edited by: BRANDRUP, J. & IMMERGUT, E. H. pp VII/519-VII/559. Chichester; New York: John Wiley & Sons, Inc.

GUNATILLAKE, P. A., MARTIN, D. J., MEIJS, G. F., MCCARTHY, S. J. & ADHIKARI, R. (2003) Designing biostable polyurethane elastomers for biomedical implants. *Australian Journal of Chemistry,* 56**,** 545-557.

GUNATILLAKE, P. A., MEIJS, G. F., MCCARTHY, S. J. & ADHIKARI, R. (2000) Poly(dimethylsiloxane)/poly(hexamethylene oxide) mixed macrodiol based polyurethane elastomers. I. Synthesis and properties. *Journal of Applied Polymer Science,* 76**,** 2026-2040.

HAGERT, C. G. (1975) Metacarpophalangeal joint implants .2. Roentgenographic study of Niebauer-Sutter metacarpophalangeal joint prosthesis. *Scandinavian Journal of Plastic and Reconstructive Surgery and Hand Surgery,* 9**,** 158-164.

HAGERT, C. G., EIKEN, O., OHLSSON, N. M., ASCHAN, W. & MOVIN, A. (1975) Metacarpophalangeal joint implants .1. Roentgenographic study on Silastic finger joint implant, Swanson design. *Scandinavian Journal of Plastic and Reconstructive Surgery and Hand Surgery,* 9**,** 147-157.

HANSRAJ, K. K., ASHWORTH, C. R., EBRAMZADEH, E., TODD, A. O., GRIFFIN, M. D., ASHLEY, E. M. & CARDILLI, A. M. (1997) Swanson metacarpophalangeal joint arthroplasty in patients with rheumatoid arthritis. *Clinical Orthopaedics and Related Research,* 342**,** 11-15.

HAUSER, R. L., WALKER, C. & KILBOURNE, F. L. (1956) Swelling of silicone elastomers. *Industrial and Engineering Chemistry,* 48**,** 1202-1208.

HAYES, R. A. (1986) A new look at measurements of network density. *Rubber Chemistry and Technology,* 59**,** 138-141.

HAZDAT-CHEMICAL-HAZARDS-DATABASE *University of Birmingham*.

HELMER, J. D. & POLMANTEER, K. E. (1969) Supercooling of polydimethylsiloxane. *Journal of Applied Polymer Science,* 13**,** 2113-2118.

HEMMERICH, K. J. (1998) Accelerated aging. General aging theory and simplified protocol for accelerated aging of medical devices. *Medical Plastics and Biomaterials***,** 16-23.

HERNANDEZ, R., WEKSLER, J., PADSALGIKAR, A. & RUNT, J. (2008) In vitro oxidation of high polydimethylsiloxane content biomedical polyurethanes: Correlation with the microstructure. *Journal of Biomedical Materials Research Part A,* 87A**,** 546-556.

HILDEBRAND, J. H. & SCOTT, R. L. (1950) *The solubility of nonelectrolytes* New York: Reinhold.

HUBA, A. & MOLNÁR, L. (2001) Measurement of dynamic properties of silicone rubbers. *Periodica Polytechnica Mechanical Engineering,* 45**,** 87-94.

HUBA, A., MOLNÁR, L., CZMERK, A. & FISCHL, T. (2005) Dynamic analysis of silicone elastomers. *Materials Science, Testing and Informatics II; Materials Science Forum,* 473-474**,** 85-89.

HUGGINS, M. L. (1942a) Some properties of solutions of long-chain compounds. *Journal of Physical Chemistry,* 46**,** 151-158.

HUGGINS, M. L. (1942b) Theory of Solutions of High Polymers. *Journal of the American Chemical Society,* 64**,** 1712-1719.

HUGGINS, M. L. (1943) Properties of Rubber Solutions and Gels. *Industrial and Engineering Chemistry,* 35**,** 216-220.

HUKINS, D. W. L. (1990) Clinical signs and dynamics of segmental instability In: *Back Pain: Classification of symptoms*, edited by: FAIRBANK, J. C. T. & PYNSENT, P. B. pp 139 -144. Manchester: Manchester University Press.

HUKINS, D. W. L., MAHOMED, A. & KUKUREKA, S. N. (2008) Accelerated aging for testing polymeric biomaterials and medical devices. *Medical Engineering & Physics,* 30**,** 1270-1274.

HUTCHINSON, D. T., SAVORY, K. M. & BACHUS, K. N. (1997) Crack-growth properties of various elastomers with potential application in small joint prostheses. *Journal of Biomedical Materials Research,* 37**,** 94-99.

JACQUES, C. H. M. & WYZGOSKI, M. G. (1979) Prediction of environmental-stress cracking of polycarbonate from solubility considerations. *Journal of Applied Polymer Science,* 23**,** 1153-1166.

JAMES, G. (1993a) *Advanced modern engineering mathematics*. pp. 778-788. Wokingham: Addison-Wesley Publishing Company.

JAMES, G. (1993b) *Advanced modern engineering mathematics*. pp. 675-779. Wokingham: Addison-Wesley Publishing Company.

JAMES, G., BURLEY, D., CLEMENTS, D., DYKE, P., SEARL, J. & WRIGHT, J. (1996) *Modern engineering mathematics*. pp. 588-589 2nd edition. Harlow: Addison-Wesley Publishing Company.

JENSEN, C. M., BOECKSTYNS, M. E. H. & KRISTIANSEN, B. (1986) Silastic arthroplasty in rheumatoid MCP-joints. *Acta Orthopaedica Scandinavica,* 57**,** 138-140.

JEPSON, N. J. A., MCCABE, J. F. & STORER, R. (1993) Age changes in the viscoelasticity of permanent soft lining materials. *Journal of Dentistry,* 21**,** 171-178.

JOSÉ, N. M., PRADO, L. A. S. A. & YOSHIDA, I. V. P. (2004) Synthesis, characterization, and permeability evaluation of hybrid organic-inorganic films. *Journal of Polymer Science Part B: Polymer Physics,* 42**,** 4281-4292.

JOYCE, T. J. (2003) Snapping the fingers. *Journal of Hand Surgery-British and European Volume,* 28B**,** 566-567.

JOYCE, T. J. (2004) Currently available metacarpophalangeal prostheses: their designs and prospective considerations. *Expert Review of Medical Devices,* 1**,** 193-204.

JOYCE, T. J., MILNER, R. H. & UNSWORTH, A. (2003) A comparison of ex vivo and in vitro sutter metacarpophalangeal prostheses. *Journal of Hand Surgery-British and European Volume,* 28B**,** 86-91.

JOYCE, T. J. & UNSWORTH, A. (2000) The design of a finger wear simulator and preliminary results. *Proceedings of the Institution of Mechanical Engineers Part H-Journal of Engineering in Medicine,* 214**,** 519-526.

JOYCE, T. J. & UNSWORTH, A. (2002a) A literature review of "failures" of the Swanson finger prosthesis in the metacarpophalangeal joint. *Hand Surgery,* 7**,** 139-146.

JOYCE, T. J. & UNSWORTH, A. (2002b) A test procedure for artificial finger joints. *Proceedings of the Institution of Mechanical Engineers Part H-Journal of Engineering in Medicine,* 216**,** 105-110.

KATZ, P. P. (1995) The impact of rheumatoid arthritis on life activities. *Arthritis Care & Research,* 8**,** 272-278.

KAY, A. G., JEFFS, J. V. & SCOTT, J. T. (1978) Experience with Silastic prostheses in the rheumatoid hand. A 5-year follow-up. *Annals of the Rheumatic Diseases,* 37**,** 255-258.

KENNAN, J. J., PETERS, Y. A., SWARTHOUT, D. E., OWEN, M. J., NAMKANISORN, A. & CHAUDHURY, M. K. (1997) Effect of saline exposure on the surface and bulk

properties of medical grade silicone elastomers. *Journal of Biomedical Materials Research,* 36**,** 487-497.

KIMANI, B. M., TRAIL, I. A., HEARNDEN, A., DELANEY, R. & NUTTALL, D. (2009) Survivorship of the NeuFlex silicone implant in MCP joint replacement. *The Journal of Hand Surgery- European Volume,* 34**,** 25-28.

KIRSCHENBAUM, D., SCHNEIDER, L. H., ADAMS, D. C. & CODY, R. P. (1993) Arthroplasty of the metacarpophalangeal joints with use of silicone-rubber implants in patients who have rheumatoid arthritis. Long-term results. *Journal of Bone and Joint Surgery-American Volume,* 75**,** 3-12.

KNAUB, P., CAMBERLIN, Y. & GERARD, J.-F. (1988) New reactive polymer blends based on poly(urethane-ureas) (PUR) and polydisperse polydimethylsiloxane (PDMS): control of morphology using a PUR-b-PDMS block copolymer. *Polymer,* 29**,** 1365-1377.

KREYSZIG, E. (2006) *Advanced Engineering Mathematics*. pp. 1049-1057. 9th edition. Hoboken, N.J: John Wiley & Sons Inc.

LAMBERT, J., M. (2006) The nature of platinum in silicones for biomedical and healthcare use. *Journal of Biomedical Materials Research Part B: Applied Biomaterials,* 78B**,** 167-180.

LESLIE, L., KUKUREKA, S. & SHEPHERD, D. E. T. (2008a) Crack growth of medical-grade silicone using pure shear tests. *Proceedings of the Institution of Mechanical Engineers Part H, Journal of Engineering in Medicine,* 222**,** 977-982.

LESLIE, L. J., JENKINS, M. J., SHEPHERD, D. E. T. & KUKUREKA, S. N. (2008b) The effect of the environment on the mechanical properties of medical grade silicones. *Journal of Biomedical Materials Research Part B: Applied Biomaterials,* 86B**,** 460-465.

LEVIER, R. R., HARRISON, M. C., COOK, R. R. & LANE, T. H. (1995) What is silicone? (Reprinted from Plastic and Reconstructive Surgery, Vol 92, Pg 163-167, 1993). *Journal of Clinical Epidemiology,* 48**,** 513-517.

LEWIS, F. (1962) Science and technology of silicone rubber. *Rubber Chemistry and Technology Rubber Reviews,* 35**,** 1222-1275.

LINSCHEID, R. L. (2000) Implant arthroplasty of the hand: Retrospective and prospective considerations. *The Journal of Hand Surgery-American Volume,* 25**,** 796-816.

MAHOMED, A., CHIDI, N. M., HUKINS, D. W. L., KUKUREKA, S. N. & SHEPHERD, D. E. T. (2009) Frequency dependence of viscoelastic properties of medical grade silicones. *Journal of Biomedical Materials Research Part B: Applied Biomaterials,* 89B**,** 210-216.

MALCZEWSKI, R. M., JAHN, D. A. & SCHOENHERR, W. J. (2003) Peroxide or platinum? Cure system considerations for silicone tubing applications. Dow Corning Healthcare.

MANDL, L. A., GALVIN, D. H., BOSCH, J. P., GEORGE, C. C., SIMMONS, B. P., AXT, T. S., FOSSEL, A. H. & KATZ, J. N. (2002) Metacarpophalangeal arthroplasty in rheumatoid arthritis: What determines satisfaction with surgery? *Journal of Rheumatology,* 29**,** 2488-2491.

MARTIN, D. J., WARREN, L. A. P., GUNATILLAKE, P. A., MCCARTHY, S. J., MEIJS, G. F. & SCHINDHELM, K. (2000) Polydimethylsiloxane/polyether-mixed macrodiol-based polyurethane elastomers: biostability. *Biomaterials,* 21**,** 1021-1029.

MAS (2004) Pyrocarbon Finger Joint Implant. Health Technology Scientific Literature and Policy Review. *Medical Advisory Secretariat (MAS), Ontario Ministry of Health and Long Term Care for the Ontario Health Technology Advisory Committee***,** 1-34.

MCMASTER, M. (1972) The natural history of the rheumatoid metacarpophalangeal joint *Journal of Bone and Joint Surgery-British Volume,* 54B**,** 687-697.

MEAKIN, J. R., HUKINS, D. W. L., ASPDEN, R. M. & IMRIE, C. T. (2003) Rheological properties of poly(2-hydroxyethyl methacrylate) (pHEMA) as a function of water content and deformation frequency. *Journal of Materials Science-Materials in Medicine,* 14**,** 783-787.

MENARD, K. (1999) *Dynamic mechanical analysis: A practical introduction*. pp. 91-123. Boca Raton; London; New York; Washington, D.C.: CRC Press Inc

MILLER, T. M., ZHAO, L. C. & BRENNAN, A. B. (1998) Rubber-elasticity of hybrid organic-inorganic composites evaluated using dynamic mechanical spectroscopy and equilibrium swelling. *Journal of Applied Polymer Science,* 68**,** 947-957.

MINAMIKAWA, Y., PEIMER, C. A., OGAWA, R., FUJIMOTO, K., SHERWIN, F. S. & HOWARD, C. (1994) In-vivo experimental-analysis of silicone implants used with titanium grommets. *The Journal of Hand Surgery-American Volume,* 19**,** 567-574.

MULDER, M. H. V. & SMOLDERS, C. A. (1984) On the mechanism of separation of ethanol/water mixtures by pervaporation I. Calculations of concentration profiles. *Journal of Membrane Science,* 17**,** 289-307.

MURAMOTO, A. (1982) Dependence of interaction parameter on molecular-weight and concentration for solutions of poly(dimethylsiloxane) in methylethylketone. *Polymer,* 23**,** 1311-1316.

MURATA, H., HONG, G., HAMADA, T. & POLYZOIS, G. L. (2003) Dynamic mechanical properties of silicone maxillofacial prosthetic materials and the influence of frequency and temperature on their properties. *International Journal of Prosthodontics,* 16**,** 369-374.

MURATA, H., TAGUCHI, N., HAMADA, T., KAWAMURA, M. & MCCABE, J. F. (2002) Dynamic viscoelasticity of soft liners and masticatory function. *Journal of Dental Research,* 81**,** 123-128.

MURATA, H., TAGUCHI, N., HAMADA, T. & MCCABE, J. F. (2000) Dynamic viscoelastic properties and the age changes of long-term soft denture liners. *Biomaterials,* 21**,** 1421-1427.

MURAYAMA, T. (1978) *Dynamic mechanical analysis of polymeric material,* Amsterdam; Oxford; New York: Elsevier Scientific Publishing Company

NAIDU, S. H. (2007) Oxidation of silicone elastomer finger joints. *The Journal of Hand Surgery-American Volume,* 32**,** 190-193.

NAIDU, S. H., GRAHAM, J. & LAIRD, C. (1997) Pre- and postimplantation dynamic mechanical properties of silastic HP-100 finger joints. *The Journal of Hand Surgery-American Volume,* 22**,** 299-301.

NETSCHER, D., ELADOUMIKDACHI, F. & GAO, Y. H. (2000) Resurfacing arthroplasty for metacarpophalangeal joint osteoarthritis: A good option using either perichondrium or extensor retinaculum. *Plastic and Reconstructive Surgery,* 106**,** 1430-1433.

NIELSEN, L. E. (1974) *Mechanical properties of polymers and composites,* New York: Marcel Dekker, INC.

NIJHUIS, H. H., MULDER, M. H. V. & SMOLDERS, C. A. (1993) Selection of elastomeric membranes for the removal of volatile organics from water. *Journal of Applied Polymer Science,* 47**,** 2227-2243.

NUNEZ, V. A. & CITRON, N. D. (2005) Short-term results of the Ascension pyrolytic carbon metacarpophalangeal joint replacement arthroplasty for osteoarthritis. *Chirugie de la main,* 24**,** 161-164.

O'SULLIVAN, S., NAGLE, R., MCEWEN, J. A. & CASEY, V. (2003) Elastomer rubbers as deflection elements in pressure sensors: investigation of properties using a custom designed programmable elastomer test rig. *Journal of Physics D: Applied Physics,* 36**,** 1910-1916.

ORWOLL, R. (1990) Solubility of Polymers. In: *Concise Encyclopaedia of Polymer Science and Engineering*, edited by: KROSCHWITZ, J. I. pp 1066-1068. New York: John Wiley & Sons, Inc.

ORWOLL, R. A. (1977) Polymer-solvent interaction parameter chi. *Rubber Chemistry and Technology,* 50**,** 451-479.

PARKKILA, T., BELT, E. A., HAKALA, M., KAUTIAINEN, H. & LEPPILAHTI, J. (2005) Comparison of Swanson and Sutter metacarpophalangeal arthroplasties in patients with rheumatoid arthritis: A prospective and randomized trial. *The Journal of Hand Surgery-American Volume,* 30**,** 1276-1281.

PARKKILA, T. J., BELT, E. A., HAKALA, M., KAUTIAINEN, H. J. & LEPPILAHTI, J. (2006) Survival and complications are similar after Swanson and Sutter implant replacement of metacarpophalangeal joints in patients with rheumatoid arthritis. *Scandinavian Journal of Plastic and Reconstructive Surgery and Hand Surgery,* 40**,** 49-53.

PENROSE, J. M. T., WILLIAMS, N. W., HOSE, D. R. & TROWBRIDGE, E. A. (1997) In-situ simulation of one-piece metacarpophalangeal joint implants using finite element analysis. *Medical Engineering & Physics,* 19**,** 303-307.

PETTERSSON, K., WAGNSJO, P. & HULIN, E. (2006) NeuFlex compared with Sutter prostheses: A blind, prospective, randomised comparison of Silastic metacarpophalangeal joint prostheses. *Scandinavian Journal of Plastic and Reconstructive Surgery and Hand Surgery,* 40**,** 284-290.

PINCUS, T., CALLAHAN, L. F., SALE, W. G., BROOKS, A. L., PAYNE, L. E. & VAUGHN, W. K. (1984) Severe functional declines, work disability, and increased mortality in seventy-five rheumatoid arthritis patients studied over nine years. *Arthritis & Rheumatism,* 27**,** 864-872.

PODNOS, E., BECKER, E., KLAWITTER, J. & STRZEPA, P. (2006) FEA analysis of silicone MCP implant. *Journal of Biomechanics,* 39**,** 1217-1226.

POLYZOIS, G. L., HENSTENPETTERSEN, A. & KULLMANN, A. (1994) An assessment of the physical-properties and biocompatibility of 3 silicone elastomers. *Journal of Prosthetic Dentistry,* 71**,** 500-504.

POLYZOIS, G. L., TARANTILI, P.A., FRANGOU, M.J., ANDREOPOULOS, A.G. (2000) Physical properties of a silicone prosthetic elastomer stored in simulated skin secretions. *The Journal of Prosthetic Dentistry,* 83**,** 572-577.

PYLIOS, T. & SHEPHERD, D. E. T. (2007) Biomechanics of the normal and diseased metacarpophalangeal joint: implications on the design of joint replacement implants. *Journal of Mechanics in Medicine and Biology,* 7**,** 163-174.

PYLIOS, T. & SHEPHERD, D. E. T. (2008a) Soft layered concept in the design of metacarpophalangeal joint replacement implants. *Bio-Medical Materials and Engineering,* 18**,** 73-82.

PYLIOS, T. & SHEPHERD, D. E. T. (2008b) Wear of medical grade silicone rubber against titanium and ultrahigh molecular weight polyethylene. *Journal of Biomedical Materials Research Part B: Applied Biomaterials,* 84**,** 520-523.

QUINN, K. J. & COURTNEY, J. M. (1988) Silicones as biomaterials. *British Polymer Journal,* 20**,** 25-32.

RAO, J. S. & GUPTA, K. (1984) *Introductory course on theory and practice of mechanical vibrations* New Delhi; Bangalore; Bombay; Calcutta; Madras; Hyderabad: Wiley Eastern Limited.

RETTIG, L. A., LUCA, L. & MURPHY, M. S. (2005) Silicone implant arthroplasty in patients with idiopathic osteoarthritis of the metacarpophalangeal joint. *The Journal of Hand Surgery-American Volume,* 30**,** 667-672.

RICKLES, R. N. (1966) Molecular transport in membranes. *Industrial and Engineering Chemistry,* 58**,** 18-35.

RIOS, S., CHICUREL, R. & DEL CASTILLO, L. F. (2001) Potential of particle and fibre reinforcement of tyre tread elastomers. *Materials & Design,* 22**,** 369-374.

ROGERS, G. & MAYHEW, Y. (1994) *Engineering thermodynamics work and heat transfer*: Longman.

SABER-SHEIKH, K., CLARKE, R. L. & BRADEN, M. (1999a) Viscoelastic properties of some soft lining materials II-ageing characteristics. *Biomaterials,* 20**,** 2055-2062.

SABER-SHEIKH, K., CLARKE, R. L. & BRADEN, M. (1999b) Viscoelastic properties of some soft lining materials: I-effect of temperature. *Biomaterials,* 20**,** 817-822.

SAVORY, K. M., HUTCHINSON, D. T. & BLOEBAUM, R. (1994) Materials testing protocol for small joint prostheses. *Journal of Biomedical Materials Research,* 28**,** 1209-1219.

SCHERBAKOV, M. & GURVICH, M. R. (2005) Probabilistic modelling of hysteretic behavior of elastomers under 3-D cyclic loading. *Journal of Elastomers and Plastics* 37**,** 123-147.

SCHMIDT, K., WILLBURGER, R., OSSOWSKI, A. & MIEHLKE, R. K. (1999a) The effect of the additional use of grommets in silicone implant arthroplasty of the metacarpophalangeal joints. *The Journal of Hand Surgery: Journal of the British Society for Surgery of the Hand,* 24**,** 561-564.

SCHMIDT, K., WILLBURGER, R. E., MIEHLKE, R. K. & WITT, K. (1999b) Ten-year follow-up of silicone arthroplasty of the metacarpophalangeal joints in rheumatoid hands. *Scandinavian Journal of Plastic and Reconstructive Surgery and Hand Surgery,* 33**,** 433-438.

SCOTT, R. L. (1945) The thermodynamics of high-polymer solutions: II. The solubility and fractionation of a polymer of heterogeneous distribution. *The Journal of Chemical Physics,* 13**,** 178-187.

SCOTT, R. L. & MAGAT, M. (1945) The thermodynamics of high-polymer solutions: I.The free energy of mixing of solvents and polymers of heterogeneous distribution. *The Journal of Chemical Physics,* 13**,** 172-177.

SCOTT, R. L. & MAGAT, M. (1949) Thermodynamics of high-polymer solutions .3. Swelling of cross-linked rubber. *Journal of Polymer Science,* 4**,** 555-571.

SERINA, E. R., MOTE, C. D. & REMPEL, D. (1997) Force response of the fingertip pulp to repeated compression - effects of loading rate, loading angle and anthropometry. *Journal of Biomechanics,* 30**,** 1035-1040.

SHAW, M. T. & MACKNIGHT, W. J. (2005) *Introduction to polymer viscoelasticity* Hoboken, New Jersey: John Wiley & Sons Inc

SHEEHAN, C. & BISIO, A. (1966) Polymer/solvent interaction parameters. *Rubber Chemistry and Technology,* 39**,** 149-192.

SHEPHERD, D. E. T. & JOHNSTONE, A. J. (2002) Design considerations for a wrist implant. *Medical Engineering & Physics,* 24**,** 641-650.

SHEPHERD, D. E. T. & JOHNSTONE, A. J. (2005) A new design concept for wrist arthroplasty. *Proceedings of the Institution of Mechanical Engineers Part H: Journal of Engineering in Medicine,* 219**,** 43-52.

SIMMONS, A., HYVARINEN, J., ODELL, R. A., MARTIN, D. J., GUNATILLAKE, P. A., NOBLE, K. R. & POOLE-WARREN, L. A. (2004) Long-term in vivo biostability of poly(dimethylsiloxane)/poly(hexamethylene oxide) mixed macrodiol-based polyurethane elastomers. *Biomaterials,* 25**,** 4887-4900.

SIMMONS, A., HYVARINEN, J. & POOLE-WARREN, L. (2006) The effect of sterilisation on a poly(dimethylsiloxane)/poly(hexamethylene oxide) mixed macrodiol-based polyurethane elastomer. *Biomaterials,* 27**,** 4484-4497.

SIMMONS, A., PADSALGIKAR, A. D., FERRIS, L. M. & POOLE-WARREN, L. A. (2008) Biostability and biological performance of a PDMS-based polyurethane for controlled drug release. *Biomaterials,* 29**,** 2987-2995.

SPERLING, L. H. (1997) *Polymeric multicomponent materials : an introduction,* New York ; Chichester: John Wiley & Sons, Inc.

STANLEY, J. K. (1992) Conservative surgery in the management of rheumatoid disease of the hand and wrist. *The Journal of Hand Surgery: Journal of the British Society for Surgery of the Hand,* 17**,** 339-342.

STARCH, M. (2002) New developments in silicone elastomers for skin care. *Associate Industry Scientist, Life Sciences Industries, Dow Corning Corporation.*

STOKES, K., MCVENES, R. & ANDERSON, J. M. (1995) Polyurethane elastomer biostability. *Journal of Biomaterials Applications,* 9**,** 321-354.

STOKOE, S. M., UNSWORTH, A., VIVA, C. & HASLOCK, I. (1990) A finger function simulator and the laboratory testing of joint replacements. *Proceedings of The Institution of Mechanical Engineers Part H-Journal of Engineering in Medicine,* 204**,** 233-240.

SUMMERS, W. R., TEWARI, Y. B. & SCHREIBER, H. P. (1972) Thermodynamic interaction in polydimethylsiloxane-hydrocarbon systems from gas-liquid chromatography. *Macromolecules,* 5**,** 12-16.

SWANSON, A. B. (1968) Silicone rubber implants for replacement of arthritic or destroyed joints in hand. *Surgical Clinics of North America,* 48**,** 1113-1127.

SWANSON, A. B. (1969) Finger joint replacement by silicone rubber implants and concept of implant fixation by encapsulation. *Annals of the Rheumatic Diseases,* 28**,** 47-55.

SWANSON, A. B. (1972) Flexible implant arthroplasty for arthritic finger joints - rationale, technique, and results of treatment. *Journal of Bone and Joint Surgery-American Volume,* A 54**,** 435-544.

SWANSON, A. B., MEESTER, W. D., SWANSON, G. D., RANGASWAMY, L. & SCHUT, G. E. D. (1973) Durability of silicone implants- an in vivo study. *Orthopaedic Clinics of North America,* 4**,** 1097-1112.

SWANSON, A. B. & SWANSON, G. D. (1985) Osteoarthritis in the hand. *Clinics in Rheumatic Diseases,* 11**,** 393-420.

SWANSON, A. B., SWANSON, G. D. & ISHIKAWA, H. (1997) Use of grommets for flexible implant resection arthroplasty of the metacarpophalangeal joint. *Clinical Orthopaedics and Related Research,* 342**,** 22-33.

SWANSON, J. W. & LEBEAU, J. E. (1974) Effect of implantation on physical-properties of silicone-rubber. *Journal of Biomedical Materials Research,* 8**,** 357-367.

SWEENEY, W. T., FISCHER, T. E., CASTLEBERRY, D. J. & COWPERTHWAITE, G. F. (1972) Evaluation of improved maxillofacial prosthetic materials. *The Journal of Prosthetic Dentistry,* 27**,** 297-305.

TAKAHASHI, S. (1983) Determination of cohesive energy densities of unsaturated polyester resins from swelling measurements. *Journal of Applied Polymer Science,* 28**,** 2847-2866.

TAKIGAWA, S., MELETIOU, S., SAUERBIER, M. & COONEY, W. P. (2004) Long-term assessment of Swanson implant arthroplasty in the proximal interphalangeal joint of the hand. *The Journal of Hand Surgery-American Volume,* 29**,** 785-795.

THOMSON, W. T. (1964) *Mechanical vibrations* London: George Allen & Unwin Ltd.

THOMSON, W. T. (1965) *Vibration theory and applications,* London: George Allen & Unwin Ltd.

TOMPA, H. (1956) *Polymer Solutions*. pp. 55-121. London: Butterworth Scientific Publications.

TONGUE, B. H. (1996) *Principles of vibration,* New York; Oxford: Oxford University Press, Inc.

TRAIL, I. A., MARTIN, J. A., NUTTALL, D. & STANLEY, J. K. (2004) Seventeen-year survivorship analysis of silastic metacarpophalangeal joint replacement. *Journal of Bone and Joint Surgery-British Volume,* 86B**,** 1002-1006.

TRELOAR, L. R. G. (1958) *The physics of rubber elasticity* pp. 123-150. 2nd edition.: London : Oxford University Press.

VONDRÁČEK, P. & DOLEŽEL, B. (1984) Biostability of medical elastomers: a review. *Biomaterials,* 5**,** 209-214.

WAGNER, W. C., KAWANO, F., DOOTZ, E. R. & KORAN, A. (1995a) Dynamic viscoelastic properties of processed soft denture liners: Part 1-Initial properties. *The Journal of Prosthetic Dentistry,* 73**,** 471-477.

WAGNER, W. C., KAWANO, F., DOOTZ, E. R. & KORAN, A. (1995b) Dynamic viscoelastic properties of processed soft denture liners: Part 2-Effect of aging. *The Journal of Prosthetic Dentistry,* 74 299-304.

WARD, I. M. (1990a) *Mechanical properties of solid polymers*. pp. 15-26. 2nd edition. Chichester: John Wiley & Sons

WARD, I. M. (1990b) *Mechanical properties of solid polymers*. pp. 79-193. 2nd edition. Chichester: John Wiley & Sons.

WARD, I. M. & SWEENEY, J. (2004) *An Introduction to the mechanical properties of solid polymers,* Chichester: John Wiley & Sons.

WARD, T. C. & PERRY, J. T. (1981) Dynamic mechanical properties of medical grade silicone elastomer stored in simulated body fluids. *Journal of Biomedical Materials Research,* 15**,** 511-525.

WARRICK, E., PIERCE, O., POLMANTEER, K., SAAM, J. & (1979) Silicone elastomer developments 1967-1977. *Rubber Chemistry and Technology,* 52**,** 437-525.

WATANABE, H. & MIYAUCHI, T. (1973) Determination of solubility parameter for siloxane segment the solubility of iodine in liquid polydimethylsiloxane. *Journal of Chemical Engineering of Japan* 6 109-114.

WATERS, M., JAGGER, R., WILLIAMS, K. & JEROLIMOV, V. (1996) Dynamic mechanical thermal analysis of denture soft lining materials. *Biomaterials,* 17**,** 1627-1630.

WEI, Y. T., NASDALA, L., ROTHERT, H. & XIE, Z. (2004) Experimental investigations on the dynamic mechanical properties of aged rubbers. *Polymer Testing,* 23**,** 447-453.

WEIGHTMAN, B., SIMON, S., ROSE, R., RADIN, E. & PAUL, I. (1972) Environmental fatigue testing of Silastic finger joint prostheses. *Journal of Biomedical Materials Research,* 6**,** 15-24.

WEIR, C. E., LESER, W. H. & WOOD, L. A. (1950) Crystallization and 2nd-Order transitions in silicone rubbers. *Journal of Research of the National Bureau of Standards,* 44**,** 367-372.

WEISS, A. P. C., MOORE, D. C., INFANTOLINO, C., CRISCO, J. J., AKELMAN, E. & MCGOVERN, R. D. (2004) Metacarpophalangeal joint mechanics after 3 different silicone arthroplasties. *The Journal of Hand Surgery-American Volume,* 29**,** 796-803.

WILLIAMS, M. L., LANDEL, R. F. & FERRY, J. D. (1955) Mechanical properties of substances of high molecular weight. The temperature dependence of relaxation mechanisms in amorphous polymers and other glass-forming liquids. *Journal of the American Chemical Society,* 77**,** 3701-3707.

WILSON, H. J. & TOMLIN, H. R. (1969) Soft lining materials: Some relevant properties and their determination. *The Journal of Prosthetic Dentistry,* 21**,** 244-250.

WILSON, R. L. & CARLBLOM, E. R. (1989) The rheumatoid metacarpophalangeal joint. *Hand Clinics,* 5**,** 223-237.

WILSON, Y. G., SYKES, P. J. & NIRANJAN, N. S. (1993) Long-term follow-up of Swanson Silastic arthroplasty of the metacarpophalangeal joints in rheumatoid arthritis. *The Journal of Hand Surgery-British and European Volume,* 18**,** 81-91.

WRIGHT, P. S. (1976) Soft lining materials: Their status and prospects. *Journal of Dentistry,* 4**,** 247-256.

XIE, Z. M., WEI, Y. T., LIU, Y. Y. & DU, X. W. (2004) Dynamic mechanical properties of aged filled rubbers. *Journal of Macromolecular Science-Physics,* B43**,** 805-817.

XUE-HAI, Y., NAGARAJAN, M. R., GRASEL, T. G., GIBSON, P. E. & COOPER, S. L. (1985) Polydimethylsiloxane-polyurethane elastomers: Synthesis and properties of segmented copolymers and related zwitterionomers. *Journal of Polymer Science: Polymer Physics Edition,* 23**,** 2319-2338.

YANG, C. Z., LI, C. & COOPER, S. L. (1991) Synthesis and characterization of polydimethylsiloxane polyurea-urethanes and related zwitterionomers. *Journal of Polymer Science Part B-Polymer Physics,* 29**,** 75-86.

YELIN, E., MEENAN, R., NEVITT, M. & EPSTEIN, W. (1980) Work disability in rheumatoid arthritis - effects of disease, social, and work factors. *Annals of Internal Medicine,* 93**,** 551-556.

YERRICK, K. & BECK, H. (1964) Solvent resistance of silicone elastomers: solvent-polymer interactions *Rubber Chemistry and Technology,* 37**,** 261-267.

YU, R., KORAN, A., 3RD & CRAIG, R. G. (1980) Physical properties of maxillofacial elastomers under conditions of accelerated aging. *Journal of Dental Research,* 59**,** 1041-1047.

ZELLERS, E. T. (1993) Three-dimensional solubility parameters and chemical protective clothing permeation. 1. Modelling the solubility of organic solvents in Viton® gloves. *Journal of Applied Polymer Science,* 50**,** 513-530.

ZHANG, H., CHEN, Y., ZHANG, Y., SUN, X., YE, H. & LI, W. (2008) Synthesis and characterization of polyurethane elastomers *The Journal of Elastomers and Plastics,* 40**,** 161-178.